Role of Peptidoglycan Deacetylase in *Staphylococcus aureus* Virulence and Survival

Jamal A. Alorabi

Thesis submitted in accordance with the requirements of the University of Liverpool for the degree of Doctor in Philosophy

April 2016

UNIVERSITY OF LIVERPOOL

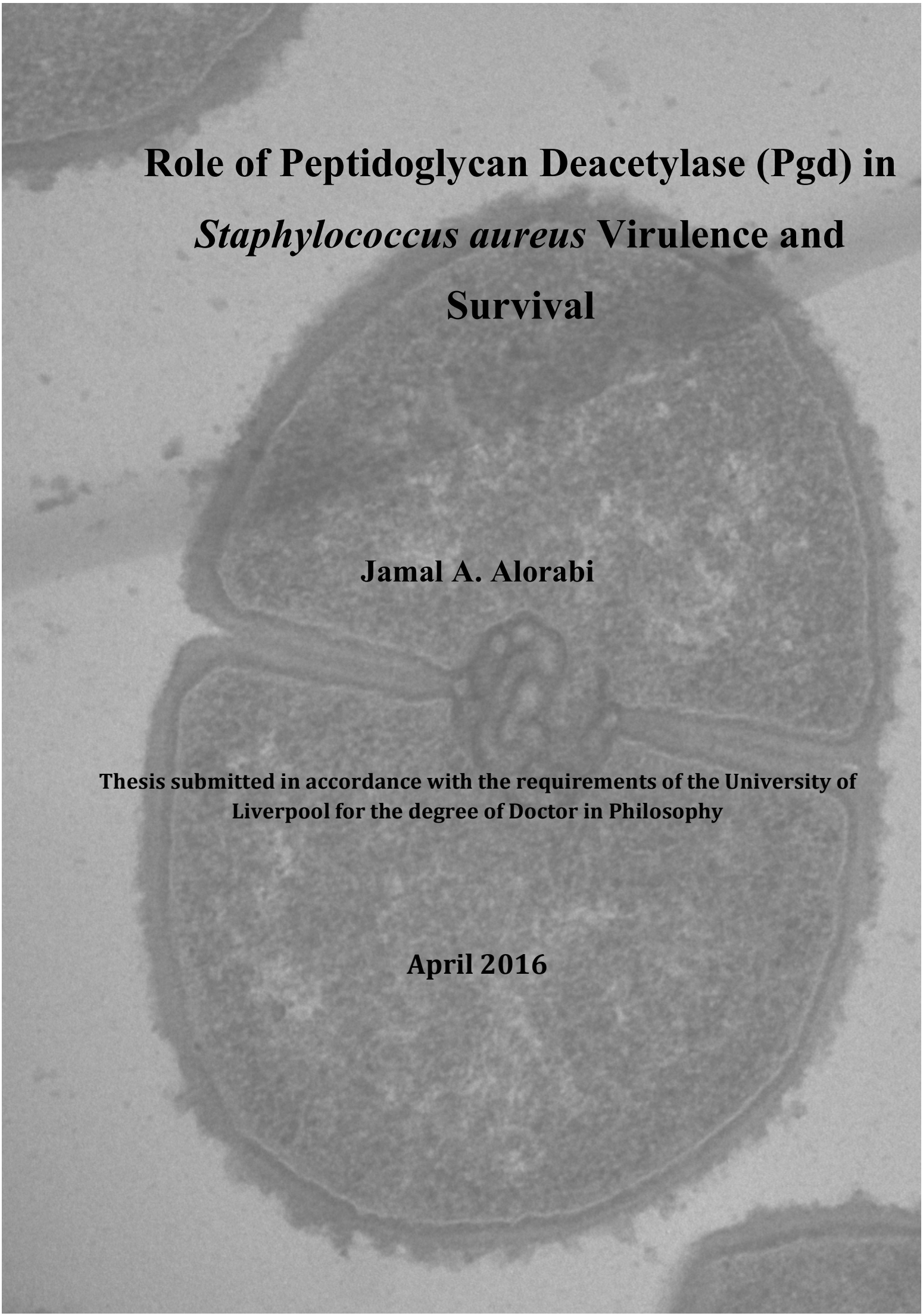

Role of Peptidoglycan Deacetylase (Pgd) in *Staphylococcus aureus* Virulence and Survival

Jamal A. Alorabi

Thesis submitted in accordance with the requirements of the University of Liverpool for the degree of Doctor in Philosophy

April 2016

Acknowledgement

First and foremost, I thank Allah for making this work possible and giving me the ability and patience to complete my research at wonderful Institute of Integrative Biology, Department Functional and Comparative Genomics, Liverpool University.

I would like to thank my supervisors Dr. Mal Horsburgh and Dr. Dan Rigden for their advice and support throughout my PhD study. In addition, I would like to thank my two advisors Professor Alan McCarthy and Dr. P. G. Miller for their guidance and support during my research stage.

I would like to thank those who gave me training course: Alison Beckett for Transmission electron microscopy (TEM) training, Dr. Joanna Wnetrzak and Dr. Marco Marcello for confocal Microscopy training, Dr Elaine Waters for Pneumonia and bacteraemia infection models, Dr Nikki Black for BioFlux and Suzan Rooijakkers for neutrophils and complement deposition assays.

I would like to thank all my friends and also those who have helped me in the lab, especially Paul Loughnane and Jean Wood for helping me to get through all what I want in my work.

I owe thanks to my wife and kids who shared the life with me and makes the success and happiness during my study is possible.

Specifically, I would like to acknowledge financial support from the Royal Saudi Government and Taif University during my studies.

Abstract

Staphylococcus aureus is an opportunist human pathogen that colonises the anterior nares and is shed onto skin. The bacterium is most frequently a cause of skin and soft-tissue infections, yet is also a major cause of respiratory, urinary tract, bone, eye and brain infections. Evolution of the bacterium has selected strains that are more antibiotic resistant, particularly in the hospital environment and more recently in the community. The pathogen has the capacity for secreting a wide range of proteins that contribute to survival from host immunity and competing microflora.

The bacterial cell wall is a vital structural polymer serving mechanical roles to protect bacteria from osmotic challenges and it serves as a scaffold for the attachment of many anchored proteins and anionic polymers for interaction with extracellular components. Peptidoglycan of *S. aureus* is modified by enzyme catalysed decoration of *N*-acetyl muramic acid with teichoic acid and O-acetylation which promotes lysozyme resistance. Further modification of teichoic acid engenders properties linked to colonisation and survival during the life-cycle.

This research study sought to assign roles of *S. aureus* secreted proteins of unknown function using bioinformatics. From this approach the study identified a peptidoglycan deacetylase (Pgd) and this enzyme catalyses a reduction in acetylation of N-acetyl glucosamine in biosynthesis of the cell wall. An allelic replacement mutant revealed altered muropeptide composition that was consistent with its proposed N-deacetylase activity, and transmission electron microscopy (TEM) revealed a reduction in cell wall thickness.

S. aureus pgd exhibited increased surface charge to influence a range of phenotypes, including autolysis, resistance and biofilm formation. Resistance was increased to lysozyme, and most notably there was rescue of the lysozyme sensitivity phenotype of an *oatA* mutant (lacking peptidoglycan O-acetyltransferase [oatA] activity). Hydrodynamic flow biofilm assay revealed that both *S. aureus pgd* and *oatA* mutants exhibited negligible biofilm formation on a glass surface; treatment of the surface with plasma fluid increased biofilm capability. Biofilms of *S. aureus pgd* cultured in static conditions revealed an opposite phenotype with a thicker, but loosely adherent biofilm. Confocal laser scanning microscopy (CSLM) combined with viability staining it was revealed that in the biofilm, there were increased dead cells compared with wild-type.

An increased lag phase of growth of *S. aureus pgd* was identified, and quantitative label free proteomics was used to determine that multiple metabolism and cell wall proteins were differentially expressed, compared with the wild-type strain. The proteome analysis revealed that the *pgd* mutant expressed increased levels of the lytic transglycosylase, IsaA and this might explain the biofilm phenotype. Further contributions to the biofilm phenotype could be due to decreased expression of protein A and reduced pyruvate metabolism enzymes.

S. aureus pgd was killed more rapidly in an opsonophagocytosis assay compared with its isogenic parent but showed equivalent levels of complement deposition and serum survival. Infection models of pneumonia and bacteraemia were tested and revealed reduced bacterial loads for lung and kidney, respectively.

The S. aureus pgd mutant phenotype requires further study and it should provide insights into cell wall structure and function. Pgd could represent a future candidate vaccine antigen due to its likely cell surface exposure and contribution to key cellular processes.

Abbreviations

APS	Ammonium persulphate
BHI	Brain heart infusion
BLAST	Basic local alignment search tool
CWS	Cell wall sorting
DNA	Deoxyribonucleic acid
EDTA	Ethylenediaminetetraacetic acid
et al.	*Et alia* (and others)
Fig.	Figure
Glu	Glucose
GlcNAC	N-acetylglucosamine
IPTG	Isopropylthiogalactopyranoside
LTA	Lipoteichoic acid
LC-MS/MS	Liquid chromatography tandem mass spectrometry
LSM	Laser scanning microscopy
NMR	Nuclear magnetic resonance spectroscopy
MurNAC	N acetylmuramic acid
PAGE	Polyacrylamide gel electrophoresis
Pbp	Penicillin binding protein
PBS	Phosphate buffered saline
PCR	Polymerase chain reaction
PGT	Peptidoglycan glycosyl transferase
PMN	Polymorphonuclear neutrophils
RT	Room temperature
SDTE	SDS, DTT, Tris-HCl, EDTA buffer
SDS	Sodium dodecylsulphate
TAE	Tris-HCl, acetate EDTA buffer
TEM	Transmission electron microscopy
TSB	Tryptone soy broth
ATP	Adenosine triphosphate
UDP	Uridine diphosphate
UV	Ultraviolet

WTA	Wall-teichoic acid
3D	Three dimensional

Measurement and Units

bp	Base pair
ºC	Degree Celsius
cfu	Colony forming units
Da	Dalton
G	Gram
H	Hour
kDa	Kilo dalton
kV	Kilovolt
L	Litre
M	Molar
mg	Milligram
min	Minute
ml	Millilitre
mM	Millimolar
Mw	Molecular weight
µg	Microgram
µl	Micro litre
µM	Micro molar
µF	Micro faraday
ng	Nanogram
nm	Nanometre
rcf	Relative centrifugal force
rpm	Revolutions per minute
sec	Second
V	Volt
v/v	Volume per volume

Table of Contents

List of Figure

List of tables

CHAPTER 1

1.1. Introduction

1.1.1. Overview of *Staphylococcus aureus* and its clinical importance

Staphylococcus aureus is a Gram-positive bacterium that belongs to the *Staphylococcaceae* family. The species is found as part of microbial flora of the human body as commensal organism; it persistently colonises around 20-30% of the general population asymptomatically, especially in nostrils, pharynx, axillae, vagina, and it is shed onto the skin surface. Notably, it has the capacity to be a harmful pathogen and causes several infections as an opportunist (Lazarevic *et al.*, 2011a; Sibbald *et al.*, 2006)

As an opportunistic pathogen, the invasion of *S. aureus* can lead to a wide range of infections across the human body, ranging from superficial skin and soft tissue infections to systemic or chronic infections in different organs. The diversity of disease ranges in severity from the most frequent presenting pathology of skin and soft tissue infections (impetigo, furuncles, folliculitis, fasciitis, and abscesses),to invasive infections of the bloodstream (bacteraemia), heart (endocarditis) and respiratory system (pneumonia) disease, bone (septic arthritis and osteomyelitis) and brain (meningitis) infection. The mechanisms involved with the switch between carriage of commensal *S. aureus* to life-threatening infections are only partly known. In most cases this switch follows the breakage of a key barrier of skin or mucosa, for example from a wound, intravascular device or surgery (Rasmussen *et al.*, 2011).

This access opportunity allows bacteria to establish locally by adherence and/or spread to tissues from access to the bloodstream. Infection severity and patient outcomes are dependent on the balance between bacterial virulence properties and the immune response efficiency (Lowy, 1998).

This ability of *S. aureus* to infect organs under different environmental conditions such as, supply of blood, immune defences, oxygen, local pH, is a key challenge in the study of this bacterium. This must be combined with a rigorous understanding of the physiology of the bacteria combined with informed use of experimental models. *S. aureus* is frequently described as being multifaceted, versatile, flexible and adaptable as commentary to reflect its environmental interactions and responses to changes (Archer, 1998). *S. aureus* isolates variably encode a wide range of toxins that contribute to the diversity and severity of diseases. (Francois *et al.*, 2010; Gittelman *et al.*, 1991; Lazarevic *et al.*, 2011b; Lew and Waldvogel, 2004; Sibbald *et al.*, 2006). The majority of these toxins will be discussed later.

A clinically-relevant feature of *S. aureus* is its capability to adhere to and colonise different synthetic materials to form structured biofilms. These structures are important in the lifestyle of bacterial communities and develop from a coordinated sequence of events, including initial attachment, microcolony formation, maturation and detachment. Biofilm formation provides significant protection from defences from host responses and antibiotics during colonisation and infection. Most common infections due to biofilm-associated infection are reported to be nosocomial infections arising from medical devices such as, heart valves, bone prostheses, or implanted catheters (Otto, 2013).

Although adequate and prolonged antibiotic therapy can be successfully used against this bacterium, many infections can be difficult to eliminate and often relapse, suggesting *S. aureus* adapts itself to environmental changes by producing effective survival responses (Lazarevic *et al.*, 2011b; Powers *et al.*, 1990). The continued emergence of *S. aureus* resistance thwarts the effectiveness of antimicrobial drugs. The emergence of antibiotic resistance in *S. aureus* was reported first in the mid-1940s when bacteria became resistant to penicillin by producing beta-lactamase to degrade penicillin antibiotic. Subsequently, a semi-synthetic penicillin (called methicillin) was developed to overcome the resistance. This antibiotic was effective against penicillin-resistant *S. aureus,* since it was not affected by beta-lactamase. However, shortly after the introduction of methicillin, the first reports in 1961 indicated that *S. aureus* had evolved resistance. 20 years later, it was found that certain *S. aureus* strains harboured the specific gene, *mecA* that encodes the low affinity penicillin binding protein (called PBP2a) responsible for the methicillin-resistance and this was rapidly horizontally transferred reducing its clinical effectiveness for treatment (Chambers and Deleo, 2009).

In recent years, there have been reports of MRSA isolates with reduced susceptibility to vancomycin and isolated instances of vancomycin resistant strains. MRSA strains have spread worldwide and are now endemic in hospitals of most countries. The strains that are known causes of nosocomial infections are described as hospital-acquired MRSA (HA-MRSA) and are characteristically multiply resistant to a range of antibiotics. The recent emergence of community-associated MRSA (CA-MRSA) has seen the rise of successful clonal groups that remain susceptible to many antibiotics classes, but have apparently increased virulence and frequently encode

different toxins such as, exfoliatin A, and Panton-Valentine leukocidin (PVL) (Lazarevic *et al.*, 2011b). Genetically, it is possible to distinguish between these two groups of strains by the variability in many genetic regions. For example, HA-MRSA strains generally carry a large cassette *mec* element (SCC*mec*) in their chromosome accounting for their resistance, including to several non-β-lactam antimicrobials, while CA-MRSA carries a smaller SCC*mec* element resulting in resistance to fewer non-β-lactam classes (David and Daum, 2010). Whether MRSA strains are more virulent than methicillin- susceptible strain (MSSA) is still debated. Nevertheless, HA-MRSA are reported to cause bacteremias with high mortality rate. In recent years, CA-MRSA and particularly the clonal group of isolates named as USA300 were reported to be spread outside of hospitals causing infections especially in close contact between people such as in schools, sports teams and military recruits (David and Daum, 2010; DeLeo *et al.*, 2010). Typically CA-MRSA, especially USA300 isolates, carry important previously infrequently identified genes *lukS*/*lukF*-PV, encoding the PVL toxin and causing serious necrotising pneumonias and many skin infections. The specific role of PVL toxin in pathogenicity of CA-MRSA is still the subject of much debate, but CA-MRSA strains are reported without this toxin (DeLeo *et al.*, 2010). A general upregulation of toxin synthesis and numerous uncharacterised genome SNPs are likely to explain the emergence and alternative virulence and pathology of these strains. These strains are now circulating in hospitals leading to blurred distinctions between CA-MRSA and HA-MRSA in the USA (DeLeo *et al.*, 2010). Taken together, this rapid evolution combined with an expanded virulence determinant repertoire highlights *S. aureus* as a versatile and problematic opportunist pathogen that will remain a challenge for clinical teams and researchers.

1.1.2 Virulence of *S. aureus*

This ability of *S. aureus* to cause several infections is due largely to secreted virulence factors that engender specific virulence strategies. These proteins are collectively named the exoproteome or secretome (Lazarevic *et al.*, 2011b; Sibbald *et al.*, 2006). To be able to cause disease in host niches, *S. aureus* needs to differentially express virulence factors; some of these are displayed at the bacterial surface inserted into the membrane or either covalently or ionically attached to the cell wall, while others are released from the cell to cause pathology or inhibit host processes (Sibbald *et al.*, 2006).

Infection by *S. aureus* is frequently described to follow from sequential steps: adherence to host (either cell surfaces or host components), evasion from immune defence, and finally spreading and tissue invasion (Fournier, 2008; Holbrook and Lowy, 1998). Each step requires coordinated expression of virulence factors, therefore, these factors are often divided into different classes based on their role during the process of infection. A proportion are anchored to the cell wall of bacteria as adherence factors (e.g. protein A and fibronectin binding protein, Fnb), whereas others are secreted as extracellular proteins (e.g. alpha toxin and PVL) required for the cell damage, dissemination and spreading (Arvidson and Tegmark, 2001). Many membrane-anchored and surface-located secreted proteins are most highly expressed early during infection when cell density is low. This initial expression phase is followed by secreted toxins and enzymes being most highly expressed later in infection, when cell surface-attached proteins are downregulated (Arvidson and Tegmark, 2001; Cheung *et al.*, 2008), (Fig 1.1). This pattern of protein expression is under the control of the quorum-sensing system, *agr*, the master regulator of

virulence gene expression. The *agr* density signalling mechanism is activated by the accumulation of extracellularly secreted auto-inducing peptide during exponential growth phase (Novick, 2003). This system is discussed in more detail later.

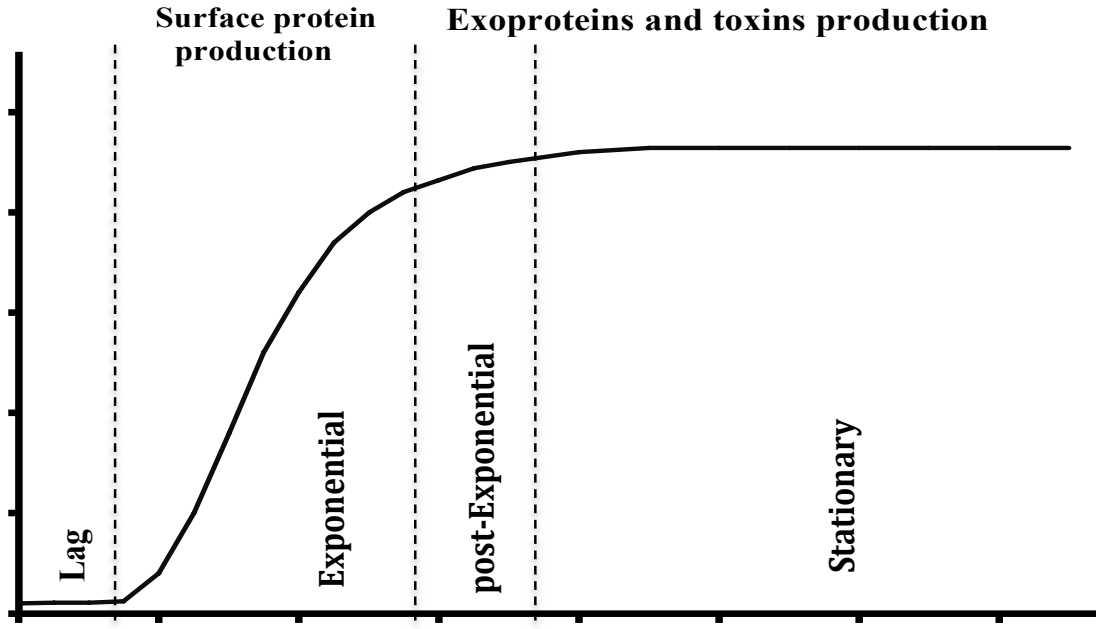

Fig. 1.1 Schematic of growth and secreted protein production of *S. aureus*. Initial adaptation of bacteria occurs during the lag phase, followed by cells multiplying and synthesising necessary surface proteins for growth, adhesion and cell division during exponential phase. The majority of *S. aureus* exoproteins including toxins are produced during late exponential phase due to activation of density-dependent signalling via Agr. Adapted from (Harris *et al.*, 2002).

Virulence factors can be divided into groups based on their functions; (i) proteins participating in invasion and adhesion of host cells, (ii) secreted proteins and toxins and (iii) proteins that circumvent host immune defence (Hecker *et al.*, 2010; Sibbald *et al.*, 2006). In addition to these groups, there are many proteins required for nutrient acquisition from the host, which are not discussed further here. However,

there is not always a clear distinction between many virulence factors that reveal overlapping functions that can act individually or together (Dinges *et al.*, 2000; Foster and Hook, 1998; Lowy, 1998). A subset of key virulence proteins is listed in (Table 1.1).

1.1.2.1. Surface proteins participating in adhesion to host cells.

A key group of proteins required for host adhesion belong to the family of Microbial Surface Components Recognising Adhesive Matrix Molecules (MSCRAMMs) proteins. *S. aureus* isolates express up to twenty different MSCRAMMs which are directed to the cell surface after secretion during the exponential growth phase (Fig. 1.1). MSCRAMMs are covalently attached to peptidoglycan via their C-terminal sorting signal catalysed by the specific transpeptidase enzymes, sortase (SrtA and B). These adhesins assist with the initiation of infection by adhering to, or interacting with host matrix components, including collagen, fibronectin, vitronectin, fibrinogen and bone sialoprotein. Adhesion is mediated by among others, clumping factors A and B, collagen adhesion (Cna), fibronectin-binding proteins (FnbA and B), serine-aspartate repeat proteins (SdrC-E) and the iron-regulated adhesin IsdA (Dreisbach *et al.*, 2011; Foster and Hook, 1998; Fournier, 2008). In addition to adherence functions, MSCRAMMs have roles in colonisation, prevention of opsonophagocytosis, and several mediate uptake into host cells (Massey *et al.*, 2001; Palmqvist *et al.*, 2004). Development of vaccines against this family of MSCRAMMS proteins has been actively pursued (Rivas *et al.*, 2004).

Table 1.1. Selected virulence factors produced by *S. aureus.*

Secretome	Description	Virulence Role	Functions
FnbA, FnbB, IsdA, SdrC-E, ClfA, ClfB	Surface protein adhesin	Colonise host tissues	Adhesion, fibrinogen- or fibronectin- binding proteins
Coa, ClfA, ClfB, Spa,	Surface protein	Immunological modulation and disguise	Coagulase, clumping factors A and B, protein A
Staphyloxanthin, KatA	Biochemical compounds	Survival inside phagocytes	Antioxidant pigments, Catalase production
Hla, b, HlgA-C, Geh, HysA, LukD to F, LukS, Lip, Nuc	Toxins, invasins, damaging membrane	To lysis cell membrane of host and spread bacteria	Leukotoxin, lipases, emolysine, hyaluronidase
Spa, Efb,	Surface-factors	To inhibit phagocytosis	Protein A, Efb blocks the C3 and C5 convertases
SEA to G, TSST-1, Eta, Etb	Exotoxins	Lead to cause signs of septic shock	Cytotoxicity
VanA, MecA, BlaZ	Resistance	As resistance factors used to antimicrobial agents	Resistance to both Vancomycin and Methicillin.
This data was adapted from [Hecker *et al.*, 2010; Sibbald *et al.*, 2006].			

1.1.2.2. Exoproteins

The excreted group of proteins includes those able to cause pathology and promote the spreading of this bacterium through host tissues, including leukocidins and hyaluronidase. *S. aureus* isolates secrete multiple enzymes such as proteases, coagulase, hemolysins and lipases that act upon tissue of the host. The α-hemolysin (alpha-toxin) can lyse both leucocytes and erythrocytes (Verdon *et al.*, 2009).

Leucocidins act to form holes in the membrane of target cells. The Panton-Valentine leucocidin (PVL) toxin, consisting of two components encoded by *lukF*-PV and *lukS*-PV, is able to lyse monocytes and neutrophils. PVL was first identified many years ago, but recently was reported associated with *S. aureus* CA-MRSA isolates, particularly those with SCCmec type IV, and was reported to cause several dermatological diseases such as, necrotising of skin and abscesses, and also involved in pneumonia infections (DeLeo *et al.*, 2010). Moreover, *S. aureus* can express superantigens such as exfoliatin A and B toxins, toxic shock syndrome toxin-1 (TSST-1) and several enterotoxins are responsible for food poisoning (Schlievert, 1993).

1.1.2.3. Immune evasion proteins

This group of secreted proteins includes a diverse set of structures and modes of action. These proteins range from Protein A and Sbi, which are surface attached and facilitate antibody and complement evasion, to OatA and TagO which catalyse the addition of acetyl groups and teichoic acids to peptidoglycan. These diverse proteins act collectively as virulence factors that enable the bacterium to limit opsonophagocytosis (Hecker *et al.*, 2010; Sibbald *et al.*, 2006; Smith *et al.*, 2011b).

1.1.2.4. Peptidoglycan modification for immune escape

Lysozyme is a cationic enzyme produced in various locations of human and animal hosts as part of their innate immunity, where it acts as a key antimicrobial peptide activity against invading bacteria. The enzyme catalyses cleavage of *β*-1,4 glycosidic bounds between disaccharides units, *N*-acetylmuramic acid (NAM) and *N*-

acetylglucosamine (NAG), of peptidoglycan (PG) leading to membrane damage and cell lysis. *S. aureus* isolates are highly resistant to lysozyme which mainly arises from two enzyme catalysed PG modifications: O-acetylation and teichoic acid (TA) addition. Both surface changes protect the bacterial surface from lysozyme binding by steric inhibition of its active site to the sugar backbone. The O-acetylation of PG promotes resistance against the bacteriolytic activity of lysozyme with the teichoic acid acting in concert. Mediated by the products of the *dlt* operon, teichoic acid can also be modified structurally with D-alanine, which increases positive charge to further limit interaction with cationic lysozyme (Neuhaus and Baddiley, 2003).

1.1.2.5. Protein A (Spa) and Immunoglobulin-binding Protein (Sbi)

Both Spa and Sbi have domains for immunoglobulin G (IgG)-binding and have roles in the virulence of *S. aureus*. These proteins bind the Fc region of IgG to prevent complement fixation and thus recognition by the neutrophil FcγR receptor which limits opsonophagocytosis (Smith *et al.*, 2011b), (see section: 6. 3. 5.).

1.1.2.6. Staphylococci avoidance from complement attacks.

The innate immune system is a primary defence against all microbes. This system comprises three effector mechanisms that allow rapid and efficient killing. First, diverse antimicrobial peptides recognise bacterial structures and lyse the membrane of bacteria, leading to rapid killing provided the concentration of peptides is effective and granules of neutrophils contain a high concentration of these peptides.

Second, the complement system promotes killing upon its activation by multiple foreign microbial molecules that differ in their interaction. Each stimulus leads to the cleavage of C3 and generation of a C3 convertase that generates chemoattractant and opsonin components, C3a and C3b (Fig. 1.2.). The C3b acts as a surface-

targetting opsonin that increases neutrophil phagocytosis through enhanced recognition.

Third, phagocytic cells, mostly neutrophils and macrophages, ingest and kill microbes within a few seconds. Bacterial infection produces several chemoattractants including chemokine interleukin-8 (IL-8) and complement C5a. These chemoattractants are sensed by neutrophils, leading to induced cellular activity and receptor expression. Nearby endothelial cells also express specific receptors to allow neutrophil egress across the endothelium guided by chemotactic gradients (e.g. IL-8) (Phillipson and Kubes, 2011). Neutrophils migrate towards the site of infection by detecting the activated complement and chemokines and upon phagocytosis their cytosol activates granules that contain neutrophil serine proteases (NSPs), myeloperoxidase, and antimicrobial peptides, that direct killing of bacteria (Rooijakkers *et al.*, 2005).

Once at the site of infection, neutrophils kill bacteria using multiple mechanisms. After phagocytosis the neutrophils engulf opsonised bacteria once they recognise either C3b- or IgG-bound bacteria. Once the plasma membrane of the neutrophil surrounds the bacterium to complete the uptake process the release of antimicrobial peptides from granules promotes lysis (van Kessel *et al.*, 2014); This process is called degranulation (Korkmaz *et al.*, 2010), which also releases NADPH oxidase that catalyses production of superoxide, leading to production of further reactive oxygen plus nitrogen intermediates and the generation of hypochlorous acid. A final mechanism of neutrophil killing targets extracellular bacteria via the extrusion of chromatin loaded with histones, and the proteases cathepsin and elastase, all of which are antimicrobial. These neutrophil extracellular traps (NETs) trap and kill bacteria (Remijsen *et al.*, 2011).

In addition to capsule proteins, Sbi and MSCRAMMS including Spa, there is a suite of secreted proteins that are important for inhibiting complement activation and opsonisation of the bacterial surface. These proteins include staphylokinase (SAK), Extracellular fibrinogen-binding (Efb), and staphylococcal complement inhibitor

(SCIN) proteins. The latter protein (SCIN) is able to block C3 convertase activities (C3bBb and C4b2A) that cleave of C3 protein into C3a and C3b. The C3b fragment functions as a surface-bound opsonin, increasing neutrophil phagocytosis when bound to the surface of *S. aureus* and SCIN prevents C3b formation (Fig.1.2.), (Rooijakkers *et al.*, 2005). *S. aureus* surface proteins act as plasminogen (PLG) receptors that enable PLG to become activated by SAK which releases plasmin (PL). PL functions to proteolyse several activating molecules of the complement cascade, particularly C3b, and IgG via removal of the Fc region (required for C1q-mediated activation via the classical pathway). Extracellular fibrinogen-binding (Efb) of *S. aureus* binds to C3 and this blocks cleavage by C3 convertases to limit generation of C3b; Efb targets a central point of the cascade, blocking each form of activation, classical, alternative and lectin (Fig.1.2), (Foster, 2009; Rooijakkers *et al.*, 2006). Chemotaxis inhibitory protein of staphylococci (CHIPS) binds to the neutrophil C5a receptor to block its recognition of the proteolysed C5 protein, an activity that limits neutrophil recruitment (Rooijakkers *et al.*, 2006; Rooijakkers *et al.*, 2005). Staphylococcal superantigen-like-protein 7 (SSL-7) binds IgA1-2 and C5, to control the immune response during infections (Fig.1.2) (Foster, 2009; Fournier, 2008).

Furthermore, *S. aureus* has microcapsular polysaccharides, particularly serotype 5 and 8 involved in several infections, allowing bacteria to escape from immune response such as, activation of complement systems (Watts *et al.*, 2005). Most *S. aureus* strains can produce polysaccharide intercellular adhesin (PIA) encoded by the *ica* operon, which directs cell-cell adhesion and biofilm formation, making networks able to stabilize cells and reducing phagocytosis (section 5.3.6.) (Cramton *et al.*, 1999).

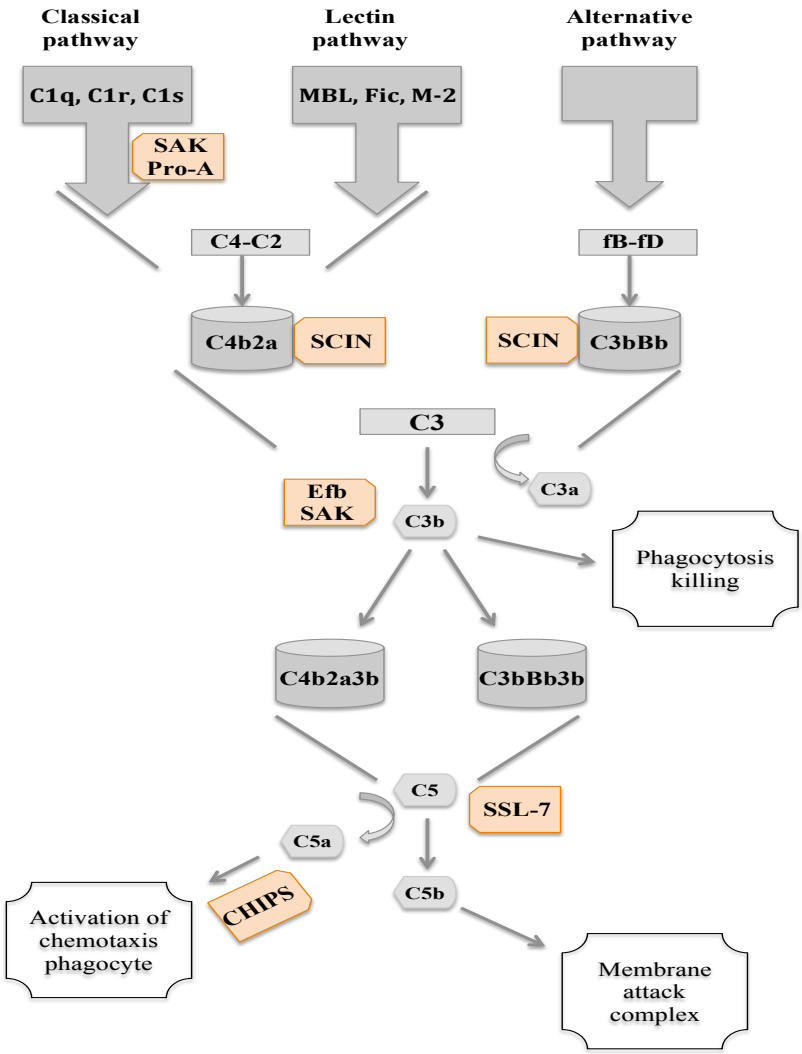

Fig. 1.2 *S. aureus* inhibition of complement activation. The complement system has three pathways directing formation of surface-bound C3 convertases that cleave C3 to release C3b for surface deposition and formation of C5 convertases. The surface-detecting activators [C1q, Fic (ficolins), MBL (mannose-binding lectin)] and protease components [M-2 (MASP-2), C1r and C1s] of the classical and lectin pathway are indicated. Several complement components (C2 and C4) and factors (fB and fD) form, respectively, the C3 convertases C4b2a and C3bBb that cleave C3 protein resulting in microbe-bound C3b. As opsonisation with C3b increases there is formation of C5 convertases (C4b2a3b and C3bBb3b) leading to C5b-9-mediated lysis and release of the chemoattractant C5a. Secreted *S. aureus* factors (orange) help to evade complement system: staphylokinase (Sak), extracellular fibrinogen-binding (Efb), staphylococcal complement inhibitor (SCIN), protein A (pro-A), chemotaxis inhibitory protein of staphylococci (CHIPS) and staphylococcal superantigen-like-protein 7 (SSL-7) are indicated at the stage they interfere with the complement cascade. (Adapted from (Rooijakkers *et al.*, 2005).

1.1.3. The cell wall and peptidoglycan structure

Peptidoglycan (PG) is a polymer serving mechanical roles to protect bacteria from osmotic challenges and surrounds *S. aureus* with a thickness of around 30 nm. PG is a scaffold that provides sites for the attachment of anchored-surface proteins and anionic polymers for interaction with extracellular matrices. PG has key roles in bacterial growth, morphogenesis and separation, pathogenesis, interaction with the environment, biofilm formation and homeostasis (Sharif *et al.*, 2009; Typas *et al.*, 2012). Teichoic acids are anionic polymers, which are covalently anchored to the PG layer in the cell wall, as wall teichoic acid (WTA), or attached to the lipid of the cytoplasmic membrane as lipoteichoic acid (LTA), (Fig. 1.3.) (Madigan *et al.*, 2003).

1.1.3.1. Peptidoglycan synthesis

Peptidoglycan is composed of disaccharide glycan units cross-linked by short stem peptides producing a structure that surrounds the inner or cytoplasmic membrane in Gram-negative or Gram-positive bacteria, respectively (Frankel and Schneewind, 2012; Typas *et al.*, 2012). The disaccharide units *N*-acetylmuramic acid and *N*-acetylglucosamine are conserved in the PG of all bacteria (Fig. 1.4), however, both bridge and stem differ in their structures between organisms. In *S. aureus*, there is a pentaglycyl (L-Gly)$_5$ cross-linking bridge, while the stem peptide is a pentapeptide comprising L-Ala-D-Gln-L-lys-D-Ala-D-Ala (Sharif *et al.*, 2009). The structure of peptidoglycan is shown in Fig. 1.3.

The synthesis of PG occurs through three main steps (Fig.1.4). Firstly, there is a soluble biosynthetic step in the cytoplasm where the precursor UDP-*N*-

acetylmuramyl and UDP-*N*-acetylglucosamine pentapeptides are synthesised. These precursors are next linked with undecaprenyl phosphate (carrier bactoprenol) at the inner membrane, producing a lipid II subunit (lipid-anchored-disaccharide-pentapeptide-monomer), which are then are flipped within the membrane to become outward-facing. The third step occurs when the lipid II subunit is polymerised by a transglycosylation reaction to release undecaprenyl pyrophosphate and disaccharide glycan chains are inserted into PG the growing structure (Frankel and Schneewind, 2012; Typas *et al.*, 2012). Final assembly of the PG structure requires transpeptidation activity, including two essential enzymes located at the cytoplasmic membrane, DD-transpeptidase (TPase) and glycosyltransferase (GTase). The GTase catalyses the formation of a β−1,4 glycosidic bond between the glycan units, resulting in a polymerised glycan chain. TPase (also called penicillin-binding protein) acts in the creation of a cross-linking bridge, a peptide bond between glycine of the pentaglycyl segment $(L\text{-}Gly)_5$ and a neighbouring stem pentapeptide L-Ala. The final three-dimensional PG structure serves as a lattice, which encapsulates the whole surface of the bacterium (Sharif *et al.*, 2009; Typas *et al.*, 2012).

PG polymerisation, therefore, is achieved by the coordinated activities of two types of enzymatic reactions: transglycosylation (the formation of linear disaccharide glycan chains), and transpeptidation (the formation of peptide cross bridges between glycan strands. There are five different PBPs (PBP1-5) of *S. aureus* and these membrane-bound enzymes catalyse both transpeptidase and carboxypeptidase reactions. β-lactam antibiotics block cell wall synthesis by binding to enzymatic sites of PBP proteins (Chambers and Miick, 1992; Waxman and Strominger, 1983). The resulting growth inhibition is circumvented in *S. aureus* MRSA isolates, whereby an

alternative penicillin-binding protein (PBP2a) is expressed from the *mec*A gene, and this has reduced affinity for binding β-lactam antibiotics (Baek *et al.*, 2014). All PBPs possess transpeptidase activity, however PBP2 possesses an additional transglycosylation activity. Two monofunctional transglycosylases (MGT), SgtA and SgtB identified in *S. aureus* have been confirmed to have transglycosylase activity in vitro. Curiously these proteins are not essential in *S. aureus* but, in the absence of PBP2 activity, SgtB is essential for bacterial viability, suggesting the bacteria need a single transglycosylases, either SgtB or PBP2 for their survival (Kuroda *et al.*, 2003; Reed *et al.*, 2011).

Supplementing those activities outlined, in *S. aureus* there are additional genes for peptidoglycan synthesis including *murA* and *murZ* (also called *murAB* or *murA2*). MurA is a UDP-GlcNAc enolpyruvyl transferase enzyme that catalyses reaction of UDP-GlcNAc (UDP-N-acetylglucosamine) with phosphoenolpyruvate (PEP) as a committed stage for peptidoglycan biosynthesis. The key reaction product, UDP-GlcNAc enolpyruvate is subsequently reduced to UDP-MurNAc (UDP-N-acetylmuramic acid) as a PG biosynthesis precursor. The *murA* gene is conserved across the bacteria but Gram-positive bacteria harbour a *murZ* gene encoding UDP-GlcNAc enolpyruvyl transferase enzyme (MurZ). The specific role of MurZ is unknown, though its expression was observed to increased when *S.aureus* was exposed to inhibitors of PG biosynthesis, indicating a potential contributory role in PG synthesis.

Purification and characterisation has indicated that both MurA and MurZ enzymes are very similar biochemically. Both are essential genes in *S. aureus,* but during the

exponential phase, the expression level of MurA was observed to be higher than MurZ expression (Blake *et al.*, 2009). Both PBP2 and MurZ expressions are controlled by the signal transduction system VraSR (Depardieu *et al.*, 2007), which is discussed later.

1.1.3.2 Peptidoglycan (PG) hydrolases

The activity of hydrolases is required to attach new peptides transferred by transpeptidases into the layers of PG. The PG requires cleavage of covalent bonds during its growth to allow newly attached peptide to insert between glycan layers without affecting its thickness. In addition, cleavage of PG is required for reductive cell separation. From studies of bacteria it is known that the hydrolases are necessary during cell division for separation of the daughter cells, and after this is completed, they sculpt the shape, thickness of PG and determine bacterial size (Typas *et al.*, 2012). The majority of PG synthesis takes place at the cross-wall peptidoglycan (mid-cell) that separates daughter cells during cell division (Frankel and Schneewind, 2012). Cell autolysis is directed by proteins with PG hydrolysis activity that are located at the cell wall of Gram-positive bacteria like *S. aureus*, including muramidase, endopeptidase, amidase and glucosaminidase activities (Fig. 1.3) Amidases have an important role in septum cleavage, and lytic endopeptidases and transglycosylases also contribute to cell separation (Typas *et al.*, 2012). Three autolysins were identified in staphylococci that are responsible for hydrolysis of the cross-wall for separation of the daughter cells; Atl, Sle1 and LytN genes (Frankel and Schneewind, 2012).

Autolysin activity must be controlled to prevent cell lysis. Covalent modifications of the PG control the activities of autolysins. In a wide range of bacterial species, de-*N*-acetylation, *O*-acetylation and *N*-acetylation of peptidoglycan are described as important for conferring intrinsic resistance to PG hydrolysis (Dupont and Clarke, 1991; Raymond *et al.*, 2005; Vollmer and Tomasz, 2000).

1.1.4. Biofilm formation

Biofilm formation protects bacteria from disruptive environmental conditions including antimicrobial compounds and clearance mechanisms of host immune defence. The development of a biofilm structure is a complex process including three steps: initial attachment, accumulation (maturation) and dispersal (detachment). The initial bacterial attachment to a surface of metal (e.g. indwelling medical device) or plastic is dependent on bacterial surface components and the physicochemical properties of the surfaces. For example, initial attachment of *S. aureus* to these abiotic surfaces is governed by surface proteins; including autolysins (AtlA and AtlB), accumulation-associated protein (Aap) and teichoic acids (WTA and LTA) (Speziale *et al.*, 2014). Contrastingly, attachment to a biotic surface or synthetic surface coated with host plasma proteins (e.g. fibrinogen, fibronectin) are controlled by cell wall-anchored (CWA) proteins of *S. aureus* (section: 5.3.6.). Bacterial communities in a biofilm structure (matrix) produce or release a wide range of contributory factors, including extracellular DNA (eDNA), proteins, and exopolysaccharides or other polymers. Clumping factor (ClfA), surface proteins SasC and SasG and serine aspartate repeat protein SdrC all contribute to biofilm formation either individually or together (Speziale *et al.*, 2014).

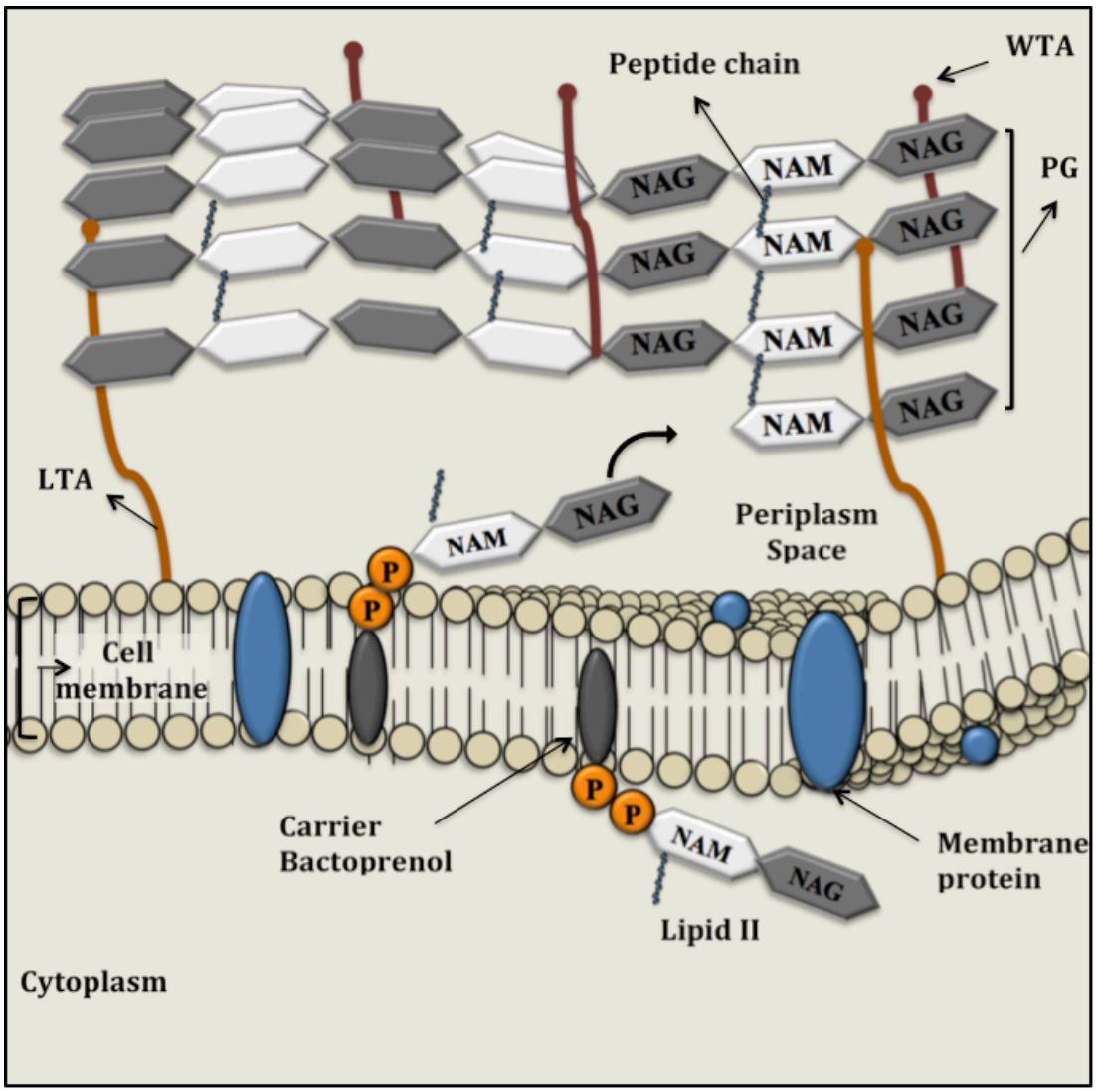

Fig. 1.3. Cell wall structure of *S. aureus* and other Gram-positive bacteria. The major structural components; peptidoglycan (PG), periplasmic space, cell membrane and cytoplasm are indicated, except the polysaccharide layer above the PG. Both teichoic acids (LTA, WTA) are indicated. Synthesis of a new peptidoglycan strand begins when a precursor is synthesised in the cytoplasm, linked to the transport lipid (bactoprenol phosphate), and then flipped across the cell membrane. A lipid II subunit is polymerised by glycosyltransferase (GTase) to release undecaprenyl pyrophosphate and disaccharide glycan chains and attachment of a new chain of PG by a DD-transpeptidase (TPase). Adapted from (Madigan *et al.*, 2003; Typas *et al.*, 2012).

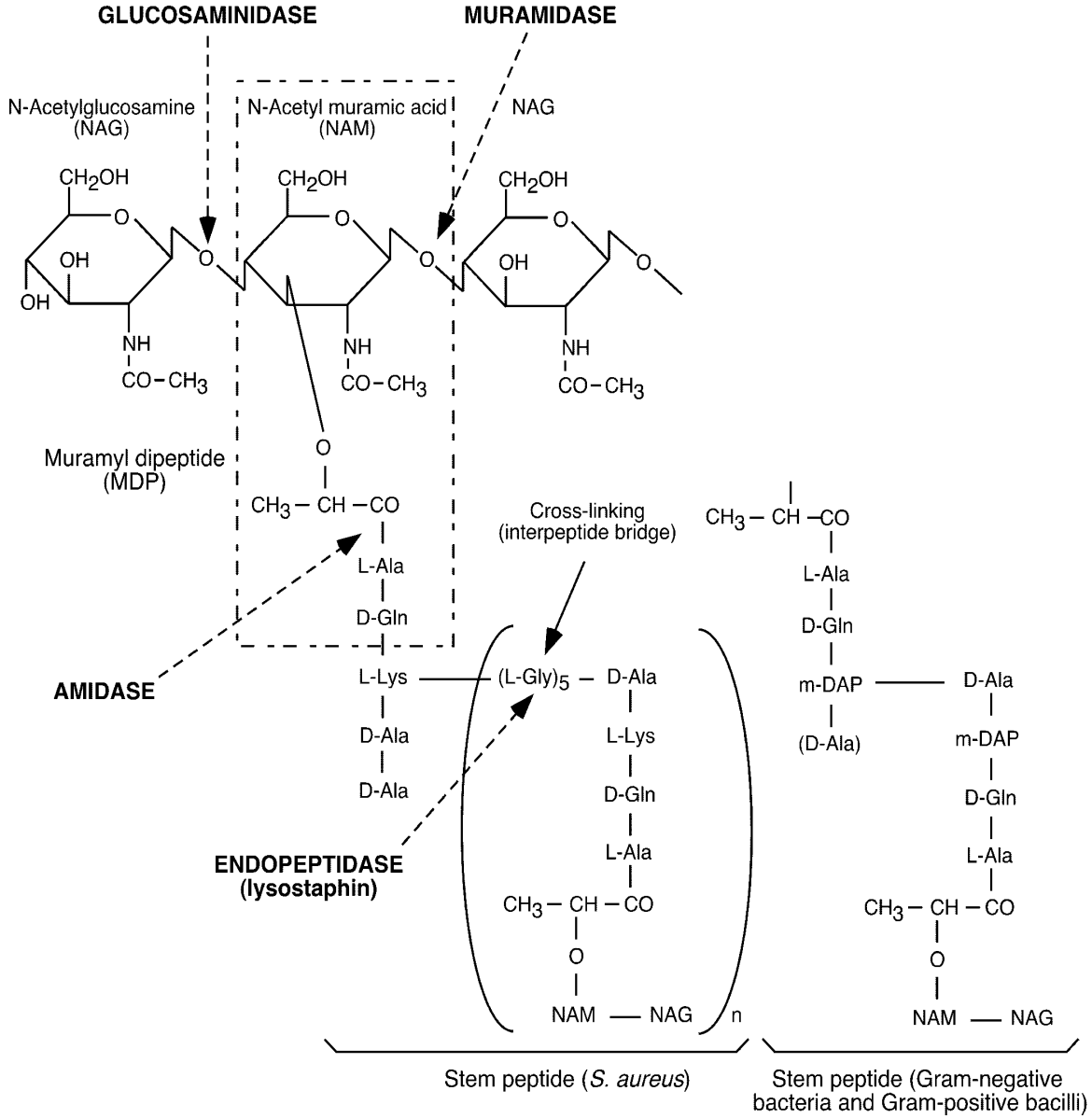

Fig. 1.4. Schematic of peptidoglycan (PG) structure of *S. aureus* (left) and other bacteria, Gram-positive bacilli and Gram-negative bacteria (right). The activity of each enzyme (muramidase, endopeptidase, amidase and glucosaminidase) is indicated by a dashed arrow (Fournier and Philpott, 2005).

1.1.5. Regulation of virulence genes

Host infections reflect the coordinated expression of virulence genes. How *S. aureus* achieves this is only partly understood. Research has identified multiple global regulators that that hierarchically control *S. aureus* virulence factor expression, however a limitation of the experiments means it remains to be discovered exactly how all the regulatory proteins control specific responses to multiple environmental and nutrient conditions. Many genes that encode virulence proteins are regulated by multiple global regulators producing a response to the different signals that arise from the extra- and intracellular conditions (Dunman *et al.*, 2001). Two major response networks most intensively studied to date coordinate expression of many virulence factors; the two-component signal transduction system (TCSTS) accessory gene regulator (*agr*) and staphylococcal accessory regulator (*sarA*) (Cheung *et al.*, 2008). These major regulatory pathways and the others that interactively control virulence are described in detail below.

1.1.6. Quorum-sensing system (QS)

Bacterial communication is achieved by two types of signals; signals sensed by bacteria that are produced in adaptation to the environment, and signals directed by some bacteria for conjugation. In *S. aureus*, the small, secreted auto-inducing peptide (AIP) is used for signaling and communication is coordinated by the TCST system collectively called Agr.

1.1.6.1. The agrBDCA locus and its regulation

As previously described, in *S. aureus* there is growth phase-dependent expression of virulence factors (Arvidson and Tegmark, 2001; Cheung *et al.*, 2008; Novick and Geisinger, 2008). The *agr* system is a TCSTS that enables *S. aureus* to adapt to its own population size then increase and decrease subsets of virulence proteins, in response to density governed by sensing the extracellular level of auto-inducing peptide (AIP), a small thiolactone ring peptide (Dunman *et al.*, 2001; Lyon and Novick, 2004).

The unique specificity of this QS system in staphylococci is that the major effector is RNAIII, a complex regulatory RNA, instead of the transcription factor response typically observed with other genera. This *agr*/RNAIII mechanism up-regulates secreted virulence proteins and toxins while concomitantly it down-regulates many virulence factors associated with the cell surface (Arvidson and Tegmark, 2001; Dunman *et al.*, 2001; Novick and Geisinger, 2008; Recsei *et al.*, 1986).

The *agr* locus is a four gene operon, *agrBDCA,* with two divergent promoters, P2 and P3 (Fig.1.5). The P2 promoter drives expression of the *agrBDCA* transcript (RNAII) and the P3 promoter is responsible for the RNAIII transcript. AgrD is a propeptide whereby the N-terminus is used for membrane attachment and the C-terminus interacts with AgrB, a transporter endopeptidase. The AgrD propeptide is processed by AgrB into a thiolactone peptide (AIP) and secreted (the mechanism of secretion still unknown). The increasing concentration of AIP in the environment due to cell number will eventually stimulate the activation of the AgrC sensor by autophosphorylation on the membrane surface. The AgrC sensor transfers the

phosphate to AgrA enabling AgrA to bind to the intergenic region of *agr* P2-P3. AgrA thus produces upregulation of *agrBDCA* and RNAIII transcripts. The P2 promoter acts in an autoactivation circuit so the RNAIII molecule serves as a regulatory effector of *agr* system via the P2 promoter (Dunman *et al.*, 2001; Novick and Geisinger, 2008). This process will lead to amplifying AIP production. RNAIII is responsible for the major upregulation and downregulation of exoprotein production and surface proteins transcription respectively, during postexponential and stationary growth phases.

1.1.6.2. RNAIII

RNAII is a 514 nucleotide riboregulator acting as the *agr* regulon effector. RNAIII folds as a stable, complex structure with regulatory RNA function; it also encodes a peptide of 24 amino acids (delta-hemolysin). The general structure of RNAIII is conserved across staphylococcal species. Functional analysis of the structure revealed that the 3' end of RNAIII is required and essential for repressing the transcription of cell wall protein genes, such as protein A gene (*spa*), while both sub-regions, 5' and 3' are active-independently and able to stimulate alpha-hemolysin gene (*hla*) transcription (Novick and Geisinger, 2008). Mechanistically, RNAIII binding to protein A (Spa) transcript sequence creates a substrate for RNase III to accelerate *spa* mRNA digestion (Morrison *et al.*, 2012). RNAIII directs upregulated expression of alpha-hemolysin by interaction with secondary structure in the *hla* mRNA. Activation of the *agr* system also leads to stimulate and repress another TCST called SaeRS as well as the SarA-like repressor, Rot, by the same mechanism of its RNAIII interaction. At least two loops in the RNAIII structure is predicted to

interact with the *rot* mRNA transcript to prevent ribosome binding and translation (Cheung *et al.*, 2004; Novick and Geisinger, 2008).

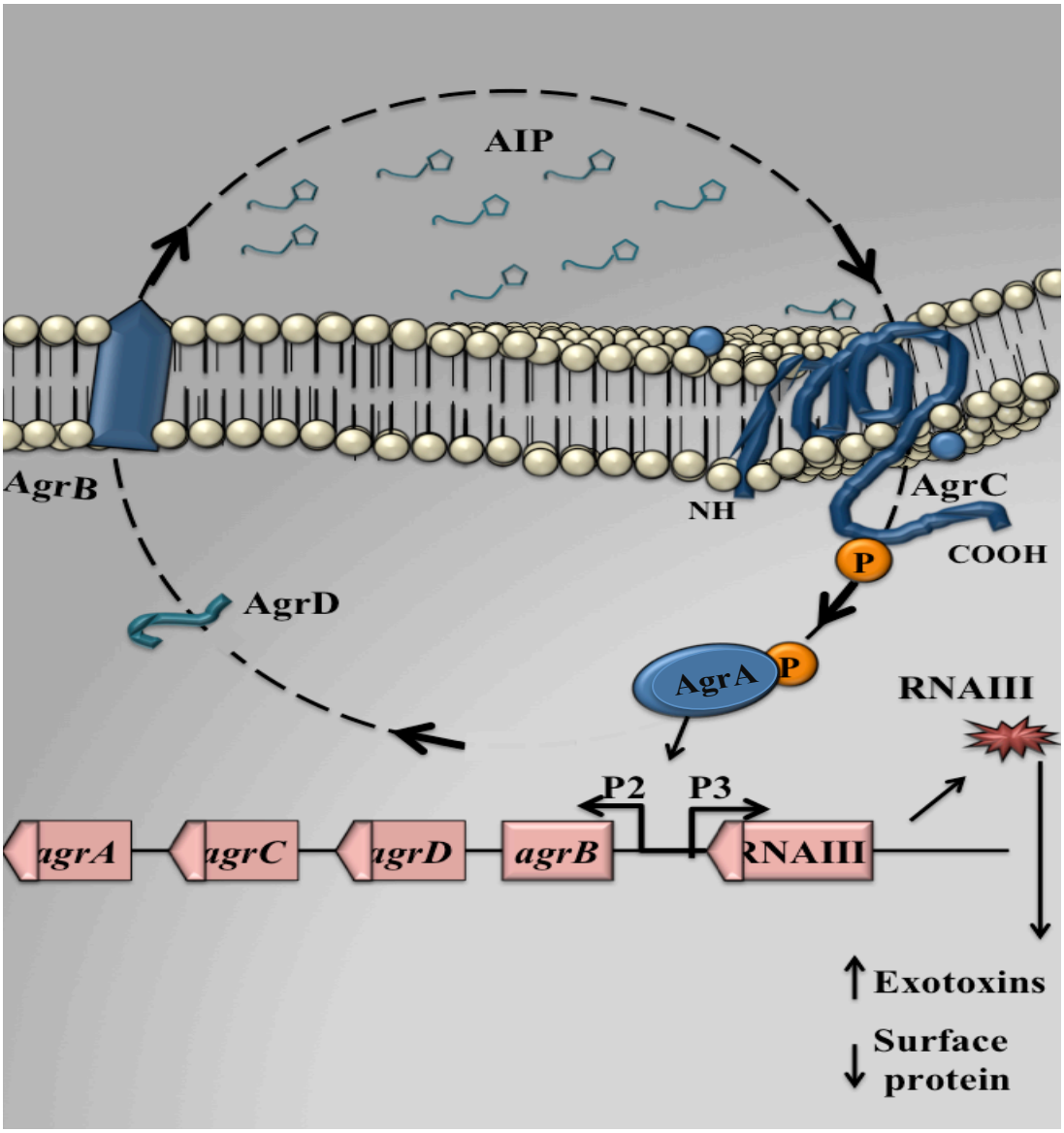

Fig 1.5. The *S. aureus agr* system. The products of the Agr system: AgrA (response regulator), AgrD, AgrB and AgrC (sensor kinase) are indicated. Thiolactone peptide (AIP) induces a surface signal via the AgrC sensor, leading to transfer of a phosphoryl group to AgrA which activates *agr* system. The P3 promoter acts on an autoactivation circuit for transcription of RNAIII, which serves as the regulatory effector of *agr* system. Partially adapted from Novic and Geisinger (2008).

1.1.7. Accessory sigma factor B (σ^B)

The alternative σ factors of *S. aureus* include σ^H, σ^B and σ^S (Bischoff *et al.*, 2004). Of these, σ^B has the best-understood role in cell biology of the organism. A total of 198 genes are regulated by activity of σ^B, including several adherence and virulence-associated genes that are up-regulated, whereas transcription of multiple toxins and exoproteins are repressed. This identified that σ^B can act conversely to the *agr* operon effector, RNAIII. σ^B activates upregulated expression of genes associated with peptidoglycan synthesis and hydrolysis activity together with genes for cell surface proteins such as, clumping factor (*clfA*), fibronectin-binding protein (*fnbA*), UDP-N-acetylglucosamine transferase (*murA*), holin-like proteins (*lrgA* and *IrgB*) and peptidoglycan hydrolase (*lytM*). In addition, the virulence regulator genes *sarA*, *sarS* and RNAIII are up-regulated by σ^B (Bischoff *et al.*, 2004). Regulation of the *S. aureus* crtOPQMN operon encoding enzymes for biosynthesis of the C_{30} triterpenoid carotenoid that is the characteristic golden pigment of the species occurs solely by σ^B-dependent transcription (Lan *et al.*, 2010).

1.1.8. Rot

The transcription factor Rot (repressor of toxins), has an opposite role to RNAIII by down-regulating expression of secreted proteins, as when repressed by RNAIII, and up-regulating the expression of the cell surface proteins such as protein A (Spa). (Morfeldt *et al.*, 1995; Novick and Geisinger, 2008).

1.1.9. SarA family of transcriptional regulators

In additional to the *agr* system, *S. aureus* expresses various other regulatory proteins to control virulence factor production during growth and infection. The *sarA* family of proteins is involved with the regulation of many virulence proteins either directly or in coordination with *agr*.

The 1.2 kb *sarA* locus, is transcribed as three overlapping transcripts: *sar*P1 (0.58 kb), *sar*P3 (0.84 kb) and *sar*P2 (1.15 kb) that are under temporal control during the growth cycle. The 3' end sequences of these transcripts are identical, but driven by three independent promoters (P1, P3 and P2) overlapping transcripts are produced, each of which encodes the main 372-bp *sarA* gene that yields a 14.5-kDa SarA protein (Bayer *et al.*, 1996; Manna and Cheung, 2001). The prototypic member of the SarA family is central for the regulation of virulence factors productions (Cheung *et al.*, 2008; Liu *et al.*, 2006). In contrast to RNAIII, SarA is constitutively expressed during *S. aureus* growth phases, however, the complement of *sar*A transcripts differs during growth phases. Both *sarP1* and *sarP3* are initially transcribed within exponential growth phase, while *sarP2* is expressed throughout stationary growth phase (Manna *et al.*, 1998; Morrison *et al.*, 2012).

In contrast with the *agr* locus, SarA activates the expression of exoproteins (e.g. α, β and δ toxins, proteases) and cell surface proteins (e.g. Spa, FnbA), either directly or via upregulation of the *agr* locus. SarA binds to the promoters of a range of genes, including *spa*, *hla, fnbA*, *agr, cna* (collagen adhesin) and the *ica* operon (for biofilm), (Cheung *et al.*, 2004; Didier *et al.*, 2010; Manna and Cheung, 2001) (Table 1.2). Studies indicated that SarA regulates expression of its target genes by directly

binding to promoters of target genes, or by stabilising mRNA, or indirectly through downstream effectors (e.g. SarA binds *agr* promoter to modulate RNAIII) (Cheung *et al.*, 2008; Manna and Cheung, 2001). In addition, SarA binds to the promoters of further SarA-like regulators such as *sarS* and *sarV* (Didier *et al.*, 2010). Valle and colleagues discovered that SarA was able to bind to the *ica* operon, responsible for expression of polysaccharide intercellular adhesin PIA, and improved biofilm formation (Ruch *et al.*, 2003). Biofilm formation and related effects are described in (section 5.3.6).

From Table 1.2, it is clear that SarA has regulatory activities to repress and stimulate its target genes. In vitro, the maximum level of the separate *sarA* transcripts was observed during postexponential growth phase. Each transcript in the *sarA* locus is repressed multiply; by the SarR protein (generally binding *sar*P1 transcript promoter), by SigmaB (binding central of P3), and by its product, the SarA protein (binding to P1 and P3) (Cheung *et al.*, 2008; Manna *et al.*, 1998). Whether total SarA production alters during growth cycle and the significance of this amount on bacterial physiology is debatable (Manna and Cheung, 2001). Didier and co-workers found that phosphorylation of SarA was the key effected upon its capacity to bind DNA. Phosphorylation of SarA was observed *in vivo*, as a step of post-translation modification, but it was not reported *in vitro* (Didier *et al.*, 2010) and may be related to environmental cues.

Table 1.2 Virulence factors regulated by *agr* and *sarA* up to 2004. Adapted from (Cheung *et al.*, 2004)

Virulence factors	**Strains**	
	agr	*sarA*
Aureolysin (Metalloprotease)	+	-
Enterotoxin B	+	+
Enterotoxin C	+	Unknown
K-hemolysin	+	+
L-hemolysin	+	+
N-hemolysin	+	+
Q-hemolysin	+	+
exfoliatins A and B	+	Unknown
Fatty acid modifying enzyme FemA	+	+
FemA	Unknown	+
FemB	+	Unknown
HysA (hyaluronate lyase)	+	Unknown
Lipase	+	-
Phospholipase C	+	Unknown
Set8 (exotoxin)	+	Unknown
Set9 (exotoxin)	Unknown	+
SplA, B, D and F (proteases)	+	+
SspB (cysteine protease)	Unknown	-
Staphylokinase	+	Unknown
TSST-1	+	+
V8 protease (SspA)	+	-
Clumping factor A	No effect	Unknown
Clumping factor B	No effect	+
Coagulase	-	+
Collagen-binding protein	±	-
Capsular polysaccharide (type 5)	+	+
Fibronectin-binding protein A	-	+
Fibronectin-binding protein B	-	+
GyrA	-	Unknown
LrgAB	+	+
PBP3	Unknown	-
Protein A	-	-
SdrC	Unknown	+
Vitronectin-binding protein	-	Unknown

* (+) Up-regulated and (-) Down-regulated (±) in certain strain up-regulated while others down-regulated

Although SarA is the best studied member of the SarA family, there are ten SarA-like proteins reported, six of which are partially described: SarS, R, T, U, V, and

MgrA (Rat) (Liu *et al.*, 2006). Several of these SarA homology proteins are described briefly as they are outside the scope of this study (Cheung *et al.*, 2004; Cheung *et al.*, 2008; Manna and Cheung, 2001).

1.1.10. SarA homologues

1.1.10.1 SarS and SarT

Activation of the requlatory systems *agr*, SaeRS, and Rot, leads to downregulation of two gene products, SarS and SarT. The SarT protein is a single domain SarA homologue (118 amino acids) that is usually repressed by Agr and SarA. The expression of *sarT* leads to upregulated production of SarS (250 amino acids) that in turn upregulates *spa* expression and down-regulates alpha toxin (*hla*) (Cheung *et al.*, 2004; Cheung *et al.*, 2008). It was proposed RNAIII may repress the expression of the *spa* gene indirectly by downregulation of *sarT* production that would reduce *sarS* production. SarA represses *sarT* to upregulate alpha-toxin production (Cheung *et al.*, 2004; Cheung *et al.*, 2008). SarT can act as repressor of both RNAIII and *hla* transcription highlighting a complex network (Schmidt *et al.*, 2001).

1.1.10.2. SarU

The expression of *sarU* (247 amino acids) is controlled by SarT production. It was observed that SarU can regulate RNAIII and contributes to the expression of the majority of virulence factors that are controlled as part of the *agr* regulon (Cheung *et al.*, 2008; Manna *et al.*, 2004).

1.1.10.3. SarV

sarV encodes a 116-residue transcription factor of the SarA family that is expressed at a low level under *in vitro* conditions; *sarV* is expressed significantly more highly in both *sarA and mgrA* mutants (Cheung *et al.*, 2004; Novick, 2003), with both gene products being determined to be *sarV* gene repressors. Similar to those genes involved in virulence and autolysis controlled by *sarA* and *mgrA* (Table 1.2) SarV regulates the same virulence factors, and additional genes for autolysis (*atl*, *scdA*, *irgB*) and protease (*splA*) (Cheung *et al.*, 2004; Novick, 2003). In contrast to the effect with *sarA and mgrA* mutations, the inactivation of *sarV* led to increased resistance to both penicillin-and Triton X-100-induced lysis, compared with its parent strain; Overexpression of *sarV* decreased autolysis, suggesting that SarV acts to control selective genes concerned with lysis (Manna *et al.*, 2004).

1.1.11. MgrA

MgrA (also named Rat) is a global regulatory member of the SarA protein family. MgrA is a key regulator of autolytic activity in *S. aureus* (section 5.3.4) and inactivation of *mgrA* produced a growth defect and also increased penicillin and Triton X-100-induced autolysis (Ingavale *et al.*, 2003). MgrA modulates expression of virulence genes and mutation also increased expression of both *sarS* and *spa*, with downregulation of *agr*, RNAIII and *hla*. Despite both *agr* and SarA upregulating *hla* and downregulating *spa* transcription, *sarA* transcription was unaffected by *mgrA* mutation, indicating a direct role for MgrA in regulation of both *spa* and *hla* genes in a SarA-independent manner. MgrA binds promoters of both *sarS* and *hla* to modulate expression, highlighting the complex interaction between MgrA and other

regulators, SarS, SarT and *agr* as an interconnected virulence regulatory network (Ingavale *et al.*, 2005). *S. aureus* resistance to methicillin and vancomycin. are reported to be associated with oxacillin, ciprofloxacin and vancomycin resistance, particularly in MRSA isolates (Didier *et al.*, 2010).

1.1.12. SarR

SarR is a further SarA family DNA-binding protein (115 amino acids) that can repress expression of *sarA* gene. Inactivation of *sarR* affects regulatory gene expression (e.g. *agr* system) (Cheung *et al.*, 2008). In addition inactivation of both sarR and sarA together revealed that during early growth phase both genes contributed to regulating expression of *agr*. SarR has potential to bind the same region as SarA on the *agr* promoter meaning they work together as key regulators of *agr* activity. (Manna and Cheung, 2006). SarR has a key role in regulating virulence genes, such as *sspA* (V8 serine protease) and *aur* (metalloprotease aureolysin) (Gustafsson and Oscarsson, 2008). Tamber and colleagues identified a repressor of SarR transcription called the *rsr* locus (Tamber *et al.*, 2010).

1.1.13. Two-component signal transduction systems (TCSTS)

The TCSTS play an essential role in bacterial adaption, virulence and survival by sensing external environmental changes and modulating expression of genes in response to a wide range of stimuli (Zhu *et al.*, 2010). TCSTS pathways comprise a phosphotransfer reaction that occurs between two conserved components, a histidine kinase (HK) and a response regulator (RR) (Gao and Stock, 2009). The HK is characteristically the input element of the signal pathway, which is designed to sense

the external stimulus to input into the signalling pathway. The RR is characteristically the output of the system, controlled by the HK component to effect the cellular response. The HK component auto-phosphorylates at a coserved histidine generating a phosphoryl group that is subsequently transferred onto aspartate of the RR, which activates it to obtain a response. This activation of the RR component will lead to regulated expression of the target regulon (Gao and Stock, 2009).

TCSTS systems are involved with most biological networks of the microbe, including regulation of virulence factors (Martin *et al.*, 1999). Several fundamental TCSTS have been described among bacterial species involved in key bacterial processes. For example, in the bacterium *Caulobacter crescentus*, the *ctrA* gene encodes a RR required for restriction of DNA replication and regulation of membrane protein expression, whereas the *resDE* system genes regulate expression associated with respiration and oxygen availability (Martin *et al.*, 1999). The genome of *S. aureus* includes sixteen TCSTS systems and one additional system located on the island SCC*mec* (staphylococcal cassette chromosome *mec*). The *agr* system (previously described) contains a TCS in its locus encoded by *agrCA* genes (Fig.1.4.). Other relevant systems for this study include those encoded by *saeRS*, *srrAB*, *arlSR, yycFG* and *lytSR* (Kuroda *et al.*, 2003; Martin *et al.*, 1999; Novick, 2003).

1.1.13.1. SaeRS TCSTS

Staphylococcal accessory element (Sae) locus is central to the regulation of many secreted virulence factors upregulating *hla*, *coa* and *hld* genes and downregulating *spa* and *sspA* genes (Giraudo *et al.*, 1999; Giraudo *et al.*, 1997). The *sae* locus

contains *saeR* and *saeS* genes, encoding the two-component system RR and HK, respectively. Inactivation of *sae* leads to reduced levels of alpha -and beta-hemolysin, coagulase and DNase with it having a cntral role for expression of exoproteins (Giraudo *et al.*, 1999). SaeRS is proposed to be concerned with coordinating the environmental signalling via the quorum-sensing *agr* system (Novick, 2003). Of note, the wild-type strain Newman, commonly used for virulence assays, has a proline (Pro18) instead of leucine (Leu18) in its SaeS domain compared with other staphylococcal strains. This single change in SaeS is responsible for increasing the phosphorylation level of SaeR, leading to increased expression of some virulence proteins. It is believed that the expression of target genes is dependent on the extent of SaeR phosphorylation. For example, a high level of SaeR phosphorylation is necessary for expression of class1 genes, including *sbi* (IgG biding protein, Sbi), *fnbA* (fibronectin binding protein A), *fib* (fibrinogen binding protein Fib), *efb* (fibrinogen binding protein Efb), *coa* (coagulase), *eap* (extracellular adherence protein, EAP), *sae* genes. A low level of SaeR phosphorylation, occurring independent of sensory SaeS, is sufficient to express the class II genes, including *hla* and *hlb* genes. Finally, in some strains the transcription of the *sae* locus is activated by the *agr* system, while *sigB* and *rot* contribute to repression (Mainiero *et al.*, 2010).

1.1.13.2. SrrAB

The staphylococcal respiratory response system (SrrAB) is a TCSTS that regulates energy transduction based on the oxygen levels (Pragman *et al.*, 2007; Pragman *et al.*, 2004). SrrA is a 28-kDa response regulator located in the cytoplasm of *S. aureus*, whereas, SrrB is a 66-kDa histidine kinase located to the membrane (Pragman *et al.*,

2004). SrrAB is required for expression of *spa, icaR* (transcriptional repressor of *icaADBC*) and *tst* genes by binding to region of promoters under aerobic condition. Thus, SrrA can act to increase production of both Spa and TSST-1, to enhance virulence factor expression in an environment supplemented with oxygen, whereas modukating the IcaR level alters the *ica* locus expression for biofilm formation. Overexpression of SrrAB was reported to decrease virulence in an animal model of infection and reduce biofilm formation in microtitre plates. SrrAB regulates genes controlling metabolism including enzymes such as, aconitase and fumarase (Throup *et al.*, 2001).

1.1.13.3. ArlSR

Autolysis-related locus (ArlSR) is a TCSTS involved in cell wall regulation together with several virulence genes. Inactivation of either *arlS* or *arlR* increased the production of Spa, V8 serine protease, Coa, Hla, and lipase, indicating that *arlSR* down-regulates the transcription of their cognate genes (Fournier *et al.*, 2001). In addition, inactivation of *arlSR* causes decreased *sarA* transcription, but increases the level of RNAII and RNAIII transcripts. Finally, this system was not reported to be auto-regulated however, the expression of *arlSR* locus was stimulated by *sarA* and *agr* systems, indicating their interaction (Fournier *et al.*, 2001). Its role in regulation of virulence factors expression remains to be investigated including its mechanisms. ArlRS was reported to be involved in biofilm formation of *S. aureus* on a polystyrene plate (Zhu *et al.*, 2010).

1.1.13.4. VraSR

The exposure of *S. aureus* to inhibitors of cell wall synthesis immediately affects the transcription of many genes associated with cell wall biosynthesis, such as *pbp2, sgtB, murZ* and *vraSR*; these genes are part of a cell wall stimulon (Gardete *et al.*, 2006). In this study, transcription of 139 genes was upregulated by vancomycin challenge, with 46 of these not induced in a *vraSR* mutant indicating a TCSTS regulon associated with peptidoglycan synthesis: pencillin-binding protein 2 (PBP2), UDP-N-acetylglucosamine enolpyruvyl transferase (MurZ) and monofunctional glycosyltransferase (SgtB). The VraS HK responds to fragments of damaged peptidoglycan when cell wall synthesis is inhibited. VraSR is an important positive regulator in the biosynthesis of peptidoglycan and significantly increases bacterial resistance to antibiotics such as glycopeptides and β-lactams (Kuroda *et al.*, 2003). Research has proposed that peptidoglycan damage is the main source activating this TCSTS from responses of the VraS phosphorylation state. This system therefore appears to serve as a sentinel with the capability of sensing damages in the cell wall peptidoglycan to rapidly coordinate responses to generate a resistance phenotype in *S. aureus* (Belcheva and Golemi-Kotra, 2008).

1.1.13.5. LytSR

In *S. aureus,* cells of a *lytS* mutant form aggregates in liquid culture and display an increased rate of autolysis when challenged with either penicillin or Triton X-100 inducers. On this basis it was proposed that the LytSR TCSTS participates in either modulation of murein hydrolase activities or gene expression. A *lytS* mutant also exhibited greater biofilm formation in a microtitre plate assay (Zhu *et al.*, 2010).

The expression of two genes *lrgA* and *lrgB* regulated by LytSR, together with Agr and SarA in *S. aureus* in particular is involved in blocking murein hydrolases in peptidoglycan (Groicher *et al.*, 2000; Zhu *et al.*, 2010). The LytSR TCSTS serves to sense damage in cell peptidoglycan and induce the expression of *lrgAB* operon to limit damage. A *lytSR* mutation limits *lrgAB* expression and induces autolysis by increasing susceptibility to Triton X-100, supporting this TCSTS having an important role in the regulation of hydrolase activity (Lehman *et al.*, 2015; Zhu *et al.*, 2010). Overexpression of LytR (RR) increased *lrgAB* promoter activity during growth and changed morphology of biofilm (Lehman *et al.*, 2015).

1.1.13.6. WalKR

The WalKR (also called YycG/YycF) two-component system was first identified in *Bacillus subtilis* as encoding an essential TCSTS. This system (WalKR) is conserved among Gram-positive bacteria, including *Streptococcus pneumoniae* and *S. aureus*. The auto-phosphorylation of WalK (HK) leads to transfer of its phosphoryl group to the cytoplasmic WalR protein (RR) (Dubrac and Msadek, 2004). WalR regulates transcription of multiple genes associated with peptidoglycan biosynthesis and modification that accounts for the essential requirement of this TCSTS in the viability of many Gram-positive bacteria, including *S. aureus* (Dubrac and Msadek, 2004; Martin *et al.*, 1999). The *walkR* locus is expressed during the exponential phase and then turned off at the beginning of stationary phase, indicating that this TCSTS has its important role during the exponential growth phase (Dubrac and Msadek, 2004). Dubrac and colleagues examined the essential role of WalKR in *S. aureus* strain ST1000, constructed as an IPTG-dependent inducible *walkR*

expression. Fluorescence microscopy combined with viability stains indicated that in the absence of IPTG >90% of bacterial cells were dead and had tended to aggregate but no cells lysis was detected. The presence of IPTG maintained 100% viability (Dubrac *et al.*, 2007). Cells become more resistant to lysostaphin under WalkR depletion (Dubrac *et al.*, 2007), indicating its role in cell wall structure and function. Initial study by the same group indicated that WalkR regulates the expression of genes associated with cell wall hydrolysis, including *lytM* (Dubrac and Msadek, 2004). Subsequent study confirmed that nine cell wall function genes, *lytM, ssaA, isaA, atlA, sceD* and four *ssaA*-homologous genes involved in different steps of bacterial cell wall homeostasis were regulated by WalKR. LytM and AtlA comprise the major autolysin activities of *S. aureus.*

When peptidoglycan structure was analysed under conditions of WalkR depletion the length of the glycan chain and cross-linking of peptidoglycan were significantly increased. The observed increase in length of glycans could result from a lack of SceD and IsaA muramidase activities. The disaccharide *N*- acetylglucosamine-*β*-(1,4)-*N*-acetylmuramic acid disappeared when WalkR transcription was limited implying an arrest of peptidoglycan synthesis and indicating this system is required for the turnover of cell wall by regulating both degradation and biosynthesis of peptidoglycan (Dubrac *et al.*, 2007). Strains producing high levels of the WalR response regulator, exhibited reduced virulence and this was proposed to be due to increased levels of released peptidoglycan fragments being recognised early by the host immune system, and implying this system controls autolytic activity *in vivo* (Delaune *et al.*, 2012).

Peptidoglycan integrity is critical for the cell viability and cell wall metabolism genes are tightly regulated. WalKR is a TCSTS identified as positively regulating peptidoglycan hydrolase synthesis, with three regulatory systems acting to repress peptidoglycan hydrolytic activities: LytSR ArlSR, and MgrA, all described above (Brunskill and Bayles, 1996; Fournier *et al.*, 2001; Ingavale *et al.*, 2003). Cell wall metabolism contributes to many phenotypes including sensitivity to many compounds that target the bacterial cell wall, especially antibiotics. A defect in autolysins leads to the tendency of single cell suspension to aggregate, notably observed with an *atlA* mutant (Dubrac *et al.*, 2007). The WalKR TCSTS is indirectly involved in biofilm formation of *S. aureus*. Depletion of this TCSTS causes a defect in primary adherence and impairs biofilm formation (Dubrac *et al.*, 2007).

The dynamics of peptidoglycan play an important role in pathogenicity of *S. aureus*; specifically, the anchored display of cell-wall-anchored molecules (e.g. WTA, Sbi, Spa, FnbA), the maintenance of cell shape, and the controlled degradation of peptidoglycan to limit release fragments of muropeptides, which are powerful virulence effectors and immune alarmones.

1.2.Thesis aims

S. aureus is responsible for a wide variety of infections and can survive in multiple niches. The success of this bacterium is attributed to its capacity to secrete many surface proteins that modify, protect and maintain cell wall structure from environmental pressures. *S. aureus* is often described as being multifaceted, flexible and adaptable in its interactions, especially in its response to environmental changes. In this context, there remain secreted proteins that have unknown function and a

description of their roles will help to better understand the lifecycle of this opportunist pathogen and the potential opportunities for design of new therapies.

The main aim of this study was to use bioinformatics methods to investigate *S. aureus* secreted proteins of unknown function to determine potential functions from their primary sequences by comparison with described motifs and homologous structures. These studies would inform potential biochemical functions of the proteins that would be tested experimentally.

From the bioinformatics predictions, laboratory investigations were planned to use a variety of molecular and biochemical studies of the purified proteins and inactivation of the cognate genes in *S. aureus*. It was anticipated that results from these studies may shed light on the molecular mechanisms that the target proteins had in specific infection and survival pathways such as immune evasion, metabolism, antimicrobial resistance or survival on the host.

CHAPTER 2

2. Bioinformatics analysis

2.1. Introduction

Significant changes in *S. aureus* epidemiology reported in recent years demonstrate that *S. aureus*, and most remarked its methicillin-resistant form, is evolving as a global pathogen causing both hospital and community-acquired infections (Vandenesch *et al.*, 2003; Voyich *et al.*, 2005). Since the first genome sequences of two *S. aureus* strains (N315 and Mu50) were published (Kuroda *et al.*, 2001), many additional virulence factors have been demonstrated. In one study, analysis of the proteome using 2D gels and mass spectrometry revealed that nearly 1000 out of 2600 proteins were still of unknown function [Hecker *et al*., 2010]. This study also demonstrated that particular secreted proteins of unknown functions were expressed in specific conditions. The experimental characterisation for each protein is expensive and time consuming {Watson and Thornton, 2009}, resulting in large gaps in our understanding of staphylococcal biology.

2.1.1. Signal peptide mediated protein secretion

Investigations of secreted protein functions and their cognate secretion systems in Gram-positive bacteria are increasingly important with some, e.g. bacilli, staphylococcal streptococci, of medical interest and high commercial value. The study of different protein secretion systems and their functions directly contribute to

increasing the knowledge required to facilitate the rational design of novel drugs (Oudega, 2003).

In eukaryotic and prokaryotic cells, most proteins destined to be exported from the cytosol (the exoproteome), to become part of the cell surface interface or the extracellular milieu contain a specific targeting signal sequence within the protein sequence, called the signal peptide (SP) (Sibbald *et al.*, 2006; Vonheijne, 1990). Most exoproteins are synthesized as preproteins (precursors) with an N-terminal signal peptide (SP) and these precursors are initially recognized by soluble factors that target them into the translocation system at the cell membrane. Subsequently, the preprotein is transported via a proteinaceous channel that acts as a translocation motor. The SP is then removed which releases the final protein from the membrane and immediately the mature protein folds into its native conformation (Tjalsma *et al.*, 2004)

Although signal peptides play an important role in directing proteins to their correct cellular compartments, they share no sequence homology (Paetzel *et al.*, 2002). In general, each SP consists of three distinct domains: a positively charged amino-terminal region (N-region); a hydrophobic region (H-region); and a carboxy-terminal domain (C-region) that is polar (Vonheijne, 1990). In bacteria, the N-region typically contains positively charged arginine (R) or lysine (K) amino acids that are proposed to interact with both the negatively charged phospholipids of the lipid bilayer and the translocation system (Akita *et al.*, 1990; Vonheijne, 1990). The H-region formed by hydrophobic residues can adopt an α-helical structure in the membrane. In the centre of the hydrophobic region, helix-breaking proline or glycine residues are usually

present to allow the formation of a hairpin-like structure that has ability to insert into the cell membrane (Tjalsma *et al.*, 2004). Following this region, the C-domain has a small sequence motif at the end, in forms Ala-X-Ala. This motif acts as a recognition sequence for the enzyme signal peptidase (SPase) that cleaves this SP immediately after translocation (Wooldridge, 2009)

Prokaryotic SPs are categorised by the modification and transport pathways into which SPs direct proteins. Currently, four distinct types of SP are known that share a common structure but differ in other details (Fig. 2.1.). Two SP types target the Sec pathway: the secretory signal peptide (Sec-type) and lipoprotein signal peptide. The other two SPs, the type IV (pseudopilin) SP and twin-arginine SP, use different pathways, namely the pseudopilin export and tat pathways, respectively. All preproteins with these SPs are processed by various signal peptidases (SPases) and are directed to various cellular destinations (Sibbald *et al.*, 2006). In general, preproteins with a twin-arginine SP are processed by type I SPase and directed to the cell wall or released extracellularly(Tjalsma *et al.*, 2004). Preproteins with a type IV SP are processed by type IV pseudopilin SPase (ComC) and are proposed to localise to the membrane or cell wall. However, these proteins represent the smallest group of secreted proteins compared with the majority of secreted proteins labelled with either lipoprotein or sec-type SPs (Antelmann *et al.*, 2001; Tjalsma *et al.*, 2000)

Similarly in *S. aureus,* preproteins that contain sec-type SPs are processed by type I SPase (SpsB) and are targeted to the cell wall or extracellular milieu. However, preproteins containing a lipoprotein SP are firstly lipid modified by phosphatidyl glycerol diacylglyceryl transferase (Lgt) then processed by the type II SPase (LspA).

Prolipoproteins originally thought to be retained to the cell membrane for interacting with the milieu (Antelmann *et al.*, 2001; Sibbald *et al.*, 2006).

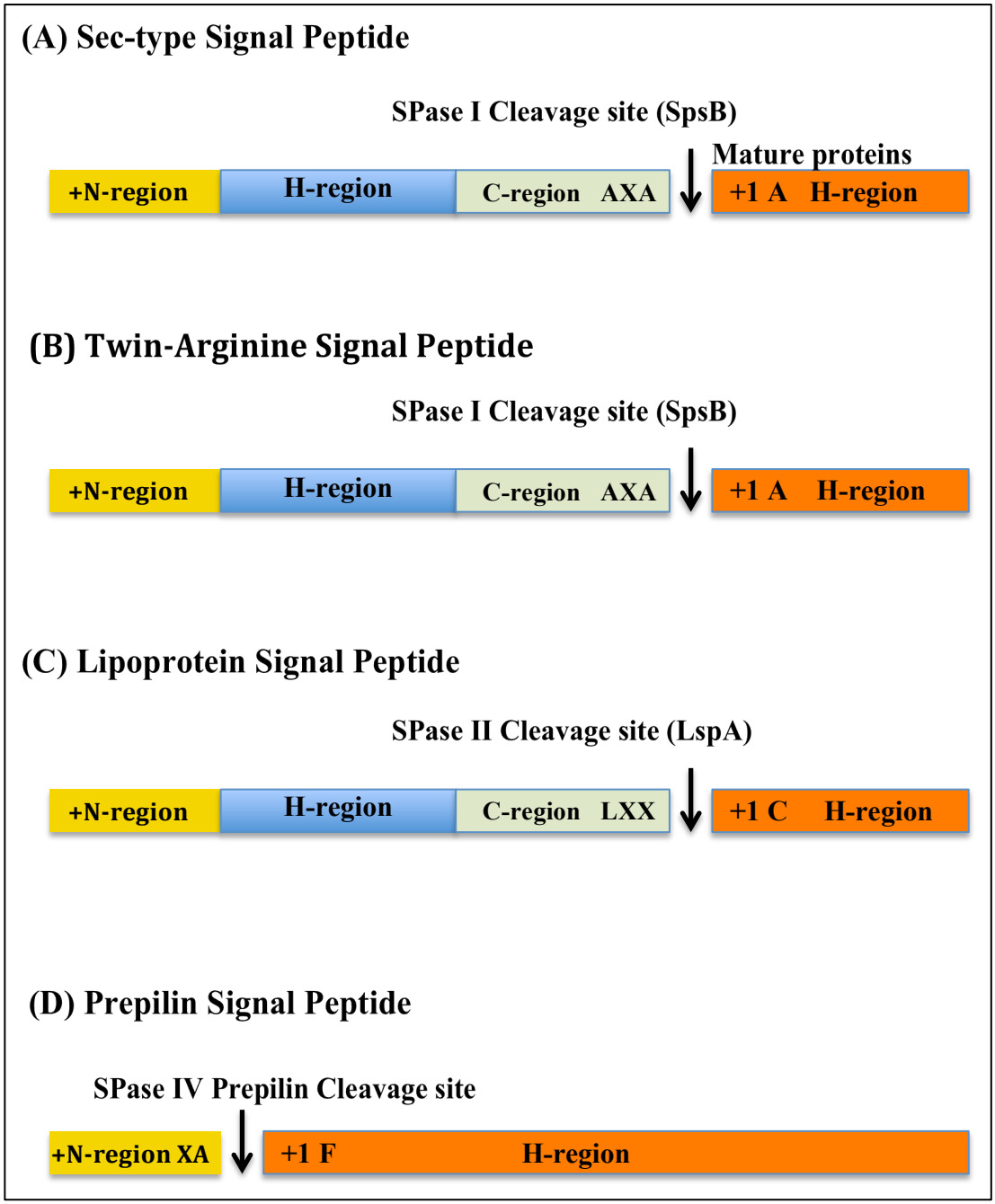

Fig. 2.1. General properties and classification of signal peptides of *S. aureus*. The four described SP features: sec-type (A), twin-arginine (B), lipoprotein (C) and prepilin (D). Figure modified from (Paetzel *et al.*, 2002; Sibbald *et al.*, 2006).

2.1.2. Predicted protein function

Despite infections with *S. aureus* being common worldwide, the key processes causing the different disease stages of colonization, invasion of host cell and persistence in tissues or other environments of host are not fully understood (Francois *et al.*, 2010). During the last decade, advancing methods led to sequencing of entire genomes of numerous pathogenic bacteria. The sequencing of *S. aureus* genomes revealed a high heterogeneity among different strains within the accessory genome, with around 75% of the sequences being conserved and thus representing the core genome. The studies also revealed several virulence factor-associated genes belong to this core part of the sequence in addition to housekeeping genes (Lindsay, 2008; Peacock *et al.*, 2002).

From the first genome sequences of *S. aureus* (strains N315 and Mu50) (Kuroda *et al.*, 2001), it was found that *S. aureus* codes for 2600 - 2700 proteins. Rapidly this revealed ~1000 of these proteins were of unknown function (Hecker *et al.*, 2010). Although the primary protein sequence presents valuable information, predicting function is known as one of the difficulties in biology. More recently functions have been predicted from distant homologies with bioinformatics tools such as HHpred (based on HHsearch and HHblits) together with predicted structures generated by homology modelling to infer a general function for a target protein (Rigden, 2009). In the study of bacterial pathogenesis proteins of unknown function that contain a SP make obvious targets for initial study since they have the greatest potential for host interaction (Lazarevic *et al.*, 2011b; Sibbald *et al.*, 2006).

Several bioinformatics tools have been developed for protein function prediction

with different degrees of success. Since molecular experimental study to characterise protein function is expensive and time-consuming, bioinformatics methods help address the prediction of protein function from sequence and structure data (Watson and Thornton, 2009). Combining the signatures of active site, catalytic site and motifs can be used predict the function from the primary sequence of a protein (unknown function). This approach, using database of several protein families, including homologues domain and motifs to predict a function for a unknown protein function (Whisstock and Lesk, 2003). In addition, the meta-PPISP server was used for predicting possible protein-protein interaction sites (Qin and Zhou, 2007).

2.2. Chapter aims

To identify potential functions in the exoproteome of *S. aureus* bioinformatic methods will be applied to determine the proteins with signal peptides to direct them through sec-pathway. This dataset will be refined by analysing the sequences of these proteins with bioinformatics approaches together with their metadata to separate unknown function proteins for further investigation. Finally, advanced bioinformatics will be used on a small subset of 3-4 proteins to predict function, which could involve modelling template structures with the query proteins.

2.3. Bioinformatics Methods

2.3.1 Determining the exoproteome of *S. aureus*

2.3.1.1 Identification of proteins with a signal peptide (SP)

To identify the signal peptide-bearing proteins of *S. aureus* Newman, the complete annotated proteome sequence comprising 2583 proteins was obtained from the UniProtKB database (Magrane and Consortium, 2011), (http://www.uniprot.org/). This dataset was interpreted locally using the prediction program SignalP 4.0 (Petersen *et al.*, 2011) to determine the secreted protein fraction. This program is a convenient tool to distinguish between non-signal peptides and signal peptides and identify cleavage sites (Petersen *et al.*, 2011). Additionaly, PRED-LIPO method (Bagos *et al.*, 2008), was used in this study for prediction of lipoprotein signal peptide of *S. aureus* proteins.

2.3.1.2. Predicting function of uncharacterised proteins

Multiple Sequence Alignment (MSAs) and homology detection are basic elements of bioinformatics methods and, with many applications, can be used to predict function, three-dimensional structure of a protein. Highly sensitive tools can identify and align distantly similar sequences that may provide information about a predicted protein, such as function, type of structure or evolution. Many programs have been developed to predict function this way, such as the HH-suite methods that are sensitive and accurate because of their ability to identify evolutionary relatives between different protein families; this is done by distinguishing between non-conserved and

conserved positions of residues among members of the family (Soding *et al.*, 2005). HH-suite methods were used in this study.

The HH-suite software package was used locally in this project. The open source software is used for sensitive sequence searching based on the pairwise alignment of Hidden Markov Models (HMMs); it contains rapid iterative protein sequence and search tools (Remmert *et al.*, 2012). HHblits is a faster and more sensitive tool compared with methods such as HMMER3 and PSI-BLAST. A build of multiple sequence alignments (MSAs) is converted to a HMM by adding pseudocounts of amino acids that are similar to the amino acids in the query sequence. HHsearch is used as a powerful implementation of the HMM comparison to find regions of uncharacterised proteins that match either known domains (e.g. in Pfam) or structures (in PDB) (Berman *et al.*, 2000; Punta *et al.*, 2012).

2.3.1.3 Modelling structure

This study predicted the potential structure for a subset of target proteins. Depending on whether homologous proteins having been identified, prediction methods that can be used for protein structure are divided into two types. First, if the target protein is similar to the structure of a matched protein (template), the model is built by copying the framework of this template; this is called template-based modelling (TBM) or homology modelling. Second, if there are not available templates, modelling of structure is used to build 3-dimensional structures from scratch; this procedure is called '*ab initio* modelling' and is only applicable to small protein < 150 residues (Rigden, 2009).

2.4 Bioinformatics results and analyses methods

2.4.1. Identifying sec-dependent secreted proteins of *S. aureus*.

The described bioinformatics methods were used to analyse the encoded 2583 proteins of *S. aureus* Newman strain. Each of the proteins that harboured an N-terminal sequence signal peptide (SP) motif was identified and collated. The analysis using SignalP 4.0 and PRED-LIPO programs indicated that the *S. aureus* Newman encodes 169 proteins that are apparently secreted through the sec pathway. Based upon bioinformatics methods, including HHpred and an analysis of metadata and information collected from databases and literature sources, it was determined that 56 (33%) of these secreted proteins were still regarded as hypothetical or being of unknown function. Of these unknown function proteins, 24 (43%) harboured the feature sequence of lipoproteins or lipobox sequence, with many containing motifs associated with enzymatic functions (Table 2. 1.).

Table 2. 1. SignalP 4.0 and HHpred analysis of *S. aureus* Newman proteins of uncertain function. Protein sequence matches to databases are listed with > 80% probability**.**

	Gene ID	Protein sequence		HHpred-homologous		Note
		Protein ID	Length (aa)	SP Type	Functional information	
1	NWMN_0022	A6QD62	772	Sig.	5'-nucleotidase; metallophosphatase	
2	NWMN_0181	A6QDM1	92	Sig.	PTS system, galactitol-specific IIB component; *Escherichia coli*	
3	NWMN_1863	A6QIF3	280	Sig.	DUF4097: Domain of unknown function	
4	NWMN_1649	A6QHT9	2186	Sig.	Hypothetical protein	
5	NWMN_0161	A6QDK1	322	Lipo.	Putative iron-uptake ABC transport	
6	NWMN_0087	A6QDC7	514	Sig.	Family: ThuA (PF06283)	
7	NWMN_0078	A6QDB8	241	Sig.	Receptor tyrosine kinase	
8	NWMN_2392	A6QJY2	1501	Sig.	PF07501- G5: G5 domain	
9	NWMN_0152	A6QDJ2	423	Lipo.	Solute-binding protein; various sugars.	
10	NWMN_0245	A6QDT5	124	Lipo.	Type II secretory pathway pseudopilin	
11	NWMN_2356	A6QJU6	151	Lipo.	DUF1307: Protein of unknown function	
12	NWMN_2270	A6QJL0	209	Lipo.	(PF12262) Lipase_bact_N	
13	NWMN_0724	A6QF64	279	Sig.	CHAP domain protein.	*
14	NWMN_0753	A6QF93	242	Lipo.	Uncharacterised protein	
15	NWMN_0925	A6QFR5	405	Sig.	LytR_cpsA_psr: Cell envelope-related transcriptional attenuator domain	*
16	NWMN_0931	A6QFS1	105	Sig.	Bacillolysin; solution structure, cell wall hydrolase, peptidoglycan-anchor; NMR; *Bacillus cereus*	
17	NWMN_1066	A6QG56	109	Sig.	Efb-homologous protein	*
18	NWMN_1690	A6QHY0	208	Lipo.	PF13670) PepSY_2: Peptidase propeptide	
19	NWMN_0336	A6QE26	284	Lipo.	Peptidase_M75: Imelysin or Algp7; Alginate-binding protein or EfeO, involved in iron uptake.	
20	NWMN_0368	A6QE58	130		Uncharacterised protein	
21	NWMN_2538	A6QKC8	152	Sig.	Uncharacterised protein	
22	NWMN_0402	A6QE92	105	Sig.	Staphylococcal complement inhibitor SCIN	*
23	NWMN_1077	A6QG67	241	Sig.	Staphylococcal toxin SSL5	*
24	NWMN_1396	A6QH36	305	Lipo.	Protein of unknown function (DUF1672)	
25	NWMN_2579	A6QKG9	374	Lipo.	Polysacc_deac_1: Polysaccharide deacetylase.	
26	NWMN_0369	A6QE59	208	Lipo.	Uncharacterised protein	
27	NWMN_0646	A6QEY6	131	Lipo.	Uncharacterised protein	
28	NWMN_1435	A6QH75	193	Lipo.	YkyA: Putative cell-wall binding	

	Gene ID	Protein sequence		HHpred-homologous		Note
		Protein ID	Length	SP Type	Functionally informative	
29	NWMN_0546	A6QEN6	122	Sig.	Protein of unknown function (DUF423)	
30	NWMN_0043	A6QD83	256	Lipo.	DUF576: Protein of unknown function	
31	NWMN_2372	A6QJW2	139	Sig.	DUF1310: Protein of unknown function	
32	NWMN_0759	A6QF99	156	Sig.	Efb-homologous protein	*
33	NWMN_1070	A6QG60	116	Sig.	SCIN-B, fibrinogen-binding protein	*
34	NWMN_0791	A6QFD1	346	Sig.	Magnesium and cobalt efflux protein	
35	NWMN_0585	A6QES5	168	Sig.	Uncharacterised protein	
36	NWMN_1252	A6QGP2	77	Sig.	Uncharacterised protein	
37	NWMN_0709	A6QF49	292	Lipo.	FadA: Fusobacterium adhesin A	
38	NWMN_1398	A6QH38	309	Lipo.	Protein of unknown function (DUF1672	
39	NWMN_0401	A6QE91	502	Sig.	Sugar binding protein	
40	NWMN_0958	A6QFU8	208	Lipo.	YkyA: Putative cell-wall binding lipoprotein.	
41	NWMN_1203	A6QGJ3	163	Sig.	ThiW: Thiamine-precursor transporter protein or thiamine-binding protein.	
42	NWMN_0908	A6QFP8	319	Lipo.	Ferrichrome ABC transporter lipoprotein: siderophore iron, receptor.	
43	NWMN_0364	A6QE54	190	Lipo.	YPMB protein; APC1927	
44	NWMN_1076	A6QG66	241	Sig.	(PF02876), Stap_Strp_toxin_C	*
45	NWMN_1123	A6QGB3	317	Lipo.	Uncharacterised protein	
46	NWMN_0601	A6QEU1	309	Lipo.	Metal ABC transporter substrate-binding lipoprotein cell membrane, copper transport, iron	
47	NWMN_0677	A6QF17	146	Lipo.	Domain of unknown function	
48	NWMN_0751	A6QF91	64	Sig.	Membrane translocase	
49	NWMN_0764	A6QFA4	189	Sig.	Cysteine peptidase	
50	NWMN_0665	A6QF05	150	Sig.	Uncharacterised protein	
51	NWMN_0292	A6QDY2	109	Sig.	Uncharacterised protein	
52	NWMN_1924	A6QIL4	154	Lipo.	Uncharacterised protein	
53	NWMN_1475	A6QHB5	232	Sig.	Uncharacterised protein	
54	NWMN_0338	A6QE28	571	Sig.	Iron permease FTR1	
55	NWMN_2545	A6QKD5	635	Sig.	Uncharacterised protein	
56	NWMN_1394	A6QH34	304	Lipo.	Protein of unknown function (DUF1672)	

*** Interpreted function but not recorded on NCBI and PDB and pfam database. (Sig.) protein with signal peptide motif, and (Lipo.) protein with lipobox sequence motif.**

From analysis of the various bioinformatics predictions methods it was determined that three of the 56 proteins of unknown function (A6QKG9, A6QD62 and A6QE26) were of particular interest. Each of these proteins matched the database significantly, with more than 99% probability and having identity ≥ 27% with another described protein. These three query proteins were selected, as they seemed to have interesting functions, for further characterisation based on these strong similarities of primary sequence, motifs, domains and amino acid conservation with homologous protein sequences of the pfam and/or PDB databases.

The available homology structure template was used to compare with modelling structure of queries proteins in order to visualize the position of active sites, motifs, conserved amino acids, plus charge and hydrophobicity of the target surface. Each of the three query proteins possessed features of an enzyme catalytic site, making them attractive to investigate by further study using more advanced bioinformatics methods to investigate their biological roles in *S. aureus*.

2.4.2. Analysis of predicted protein A6QE26 sequence.

The full-length protein sequence A6QE26 contains 284 residues. The PRED-LIPO server predicted a SP, with the N-terminal region containing a lipobox motif (IAAC) bearing a cleavage site between residues 17 and 18 (MKKLTTLLLASTLLIAA-C). This motif matched the lipoprotein signal peptide signature of Gram-positive bacteria that typically comprises one or more positively charged amino acids, followed by a region of hydrophobic amino acids and the lipobox motif including an invariant cysteine (C). Generally, the first position after the cysteine (C) residue, in the protein, is glycine (G) (Juncker *et al.*, 2003).

Analysis with HH-suite revealed that the A6QE26 sequence matched one Pfam domain, PF09375, present in the peptidase family M75 (Imelysin). A6QE26 resembled the homologous structures of four proteins: 1) protein 3at7 (39%), the AlgP7 protein of a *Sphingomonas sp*, 2) protein 3oyv (21%), imelysin from *Bacteroides ovatus* (PIBO), 3) protein 4ecg (24%), a putative iron-regulated protein from *Parabacteroides distasonis*, and 4) protein 3pf0 (12%), an imelysin-like protein from *Psychrobacter arcticus*. The sequence of these proteins, including A6QE26 sequence, presented a HXXE motif that was reported to be a metal binding, as a Zn-binding site. However, while the query proteins each harboured a HXXE motif, they had different reported functional annotation. For example, LruB protein from *Leptospira interrogans* is homologous to imelysin protein and, although it has the motif HXXE, it has a confirmed role in iron uptake (Xu *et al.*, 2011a). A HXXE motif is present in the EfeO protein sequence of *E. coli* O157:H7 and in the Algp7 protein sequence of *Sphingomonas sp* (Maruyama *et al.*, 2011). EfeO functions in iron uptake, while Algp7 functions as a concentrator of polysaccharide in a cell-surface pit (Maruyama *et al.*, 2011). Thus, this study suggests that A6QE26 protein maybe has direct or indirect role in iron uptake since the HXXE motif of LruB and EfeO is involved in iron uptake, or in polysaccharide binding as a homologue of AlgP7.

2.4.2.1. T-coffee alignments

To investigate function further, the T-coffee tool (Notredame *et al.*, 2000), was used, which is known to be an accurate method for making multiple sequence alignments (Poirot *et al.*, 2003). Using the data that was collected from using the HH-Suite

together with the literature-based information, all homologous proteins were aligned with the A6QE26 sequence again to compare their similarities so any conserved or related motifs aid with predicting function. The A6QE26 sequence contains conserved His126 and Glu129 residues that occur associated with the motif HKIE (as HxxE) that is located centrally in the sequence (Fig 2. 2.). The motif is present in two protein families, M75 and M14 (Marchler-Bauer *et al.*, 2015). The peptidase family M75 contains metallopeptidase activity, while peptidase family M14 contains metallocarboxypeptidase. Imelysin or 'insulin-cleaving membrane peptidase' from *P. aeruginosa* is a member of the M75 peptidase family, which harbours the motif HxxE, and is located at the outer membrane. Alignment of the sequences revealed the HxxE motif is located in the middle and relative position in the sequence of proteins A6QE26, EfeO and LurB, but this motif appears towards the C-terminus of PIBO protein sequence (Fig 2.2). The A6QE26 protein shares 14% sequence identity with LurB and 22% with Efe0.

The EfeUOB is an iron-transporter system, which is involved in Fe^{2+} transport at lower pH. It was reported that the EfeO is an essential component in this system but, its biochemical function is not clear yet. EfeO sequence contains N-terminal cupredoxin (CUP) domain, probably for binding iron, and C-terminal M75-like imelysin domain containing the GxHxxE motif (Xu *et al.*, 2011a). In general, this motif (HxxE) is known to be metal-binding, as a Zn-binding site for metallopeptidase M75. The sequence is also highly conserved among the EfeUOB family, suggesting this motif in EfeO might be acting as part of a metal (Fe^{2+})-binding site enabling iron transfer to the EfeU protein to transport iron as part of the iron uptake process (Rajasekaran *et al.*, 2010). In contrast, the CUP domain is not

fully conserved among members of the EfeO family or essential for function, despite its role in ferrous ion transport (Xu *et al.*, 2011a).

Based upon the current annotation of the *S. aureus* strain Newman genome in THE SEED and NCBI databases, the gene (ID: NWMN_0336) encoding A6QE26 protein is located in an operon similar to that of *E. coli EfeUOB*. This operon encodes a ferrous ion uptake transporter (data not shown), supporting a role in iron import.

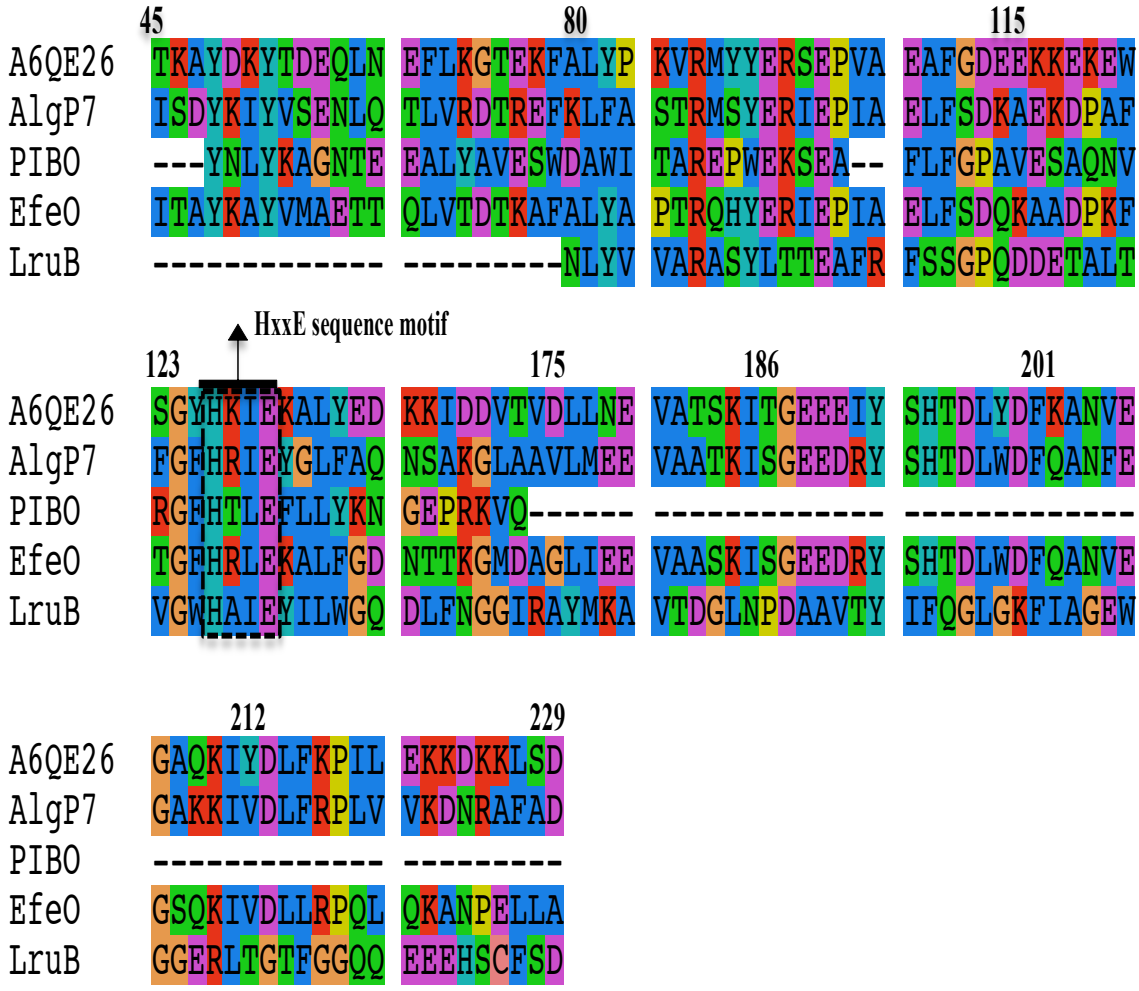

Fig. 2.2. Possible functional site in A6QE26. The most highly conserved region within a multiple sequence alignments (represented by different colours) of A6QE26 and several partially characterised homologues. The residue numbering for A6QE26 is shown at the top. Each of the proteins (AlgP7, PIBO, EfeO and LurB) have positionally-conserved amino acids, including a HxxE motif (black box with arrow).

2.4.2.2. Modeling the structure of A6QE26

No EfeO protein structure was available in the PDB database for comparison. A model structure of the query A6QE26 was constructed based on homologous structures of AlgP7, which is available from PDB, using the Modeller program on the HHpred server (Soding, 2005; Soding *et al.*, 2005). The A6QE26 model structure was loaded to the Pymol program locally (PyMOL Molecular Graphics System, Version 1.8 Schrödinger, LLC.), and was aligned with the AlgP7 structure available from PDB (Fig. 3.3.)

2.4.2.3. Overall structure and comparison

The modelled structure of A6QE26, based on AlgP7, (Fig. 2. 3.) indicates that A6QE26 consists of two bundles, each of which includes four major alpha-helices. Bundle one (B1) comprises four major ∝- helices (H1, residues 32-66; H2, 69-92; H3a, 95-101; H3c, 118-129, with a (HKIE) metal-binding motif region (red colour), and H4, 135-156). The helix (H3) divided into three helices (H3a, b and c), with loop regions inserted between them. Bundle two includes four major ∝- helices (H5, residues 161-179; H6, 190-215; H7, 218-238; H9, 253-277). The helix H8 (248-250) is included in bundle B2. From the A6QE26 model structure, 75% of all amino acids are appeared in alpha- helices, while the others were found in the turns and coils, revealing similarity with Algp7, which might extend to function.

2.4.2.4. Location of metal-binding motif (HxxE)

The model structure of A6QE26 (Fig. 2.4.) contains a metal-binding motif ^{120}HxxE^{123}, which is situated in H3c of bundle B1. By comparing the same side (Side 1) of both A6QE26 and Algp7 structures, there is a loop containing hydrogen bond and electrostatic networks that is in front of the metal-binding motif of Algp7 (Maruyama *et al.*, 2011) but, this loop is not in front of the metal-binding motif in the A6QE26 model, where the motif is present on the surface of A6QE26 to potentially bind metal. Similarly, the other side of both structures (side 2), a motif is present with the same arrangement (Fig. 2.4.). These observations support that A6QE26 may harbour peptidase activity, using binding zinc or this motif involved in binding a metal ion, such as iron that could be exchanged with another protein e.g. EfeU for iron utilisation.

2.4.2.5. Analysis using ConSurf and Meta-PPISP tools

As a further bioinformatics analysis the consurf tool (Glaser *et al.*, 2003), was used, since it is effective for estimating the evolutionary conservation of amino acid positions in a protein in relation to phylogenetic distance between homologous sequences. The model structure of A6QE26 was analysed by ConSurf server (Fig. 2. 5.) and revealed that most of the conserved amino acids are presented on one side of structure (side 1), with fewer on side 2, which were clustered around the motif, and possibly indicating a binding site (Fig. 2. 5A). The meta-PPISP server provided further support for interaction with another protein via side 1 (Fig. 2. 5C), possibly relevant to an interaction with another protein during iron uptake.

During the course of cloning work carried out in the lab (gene deletion, insertion for complementation and gene expression), a paper was published describing a function role for protein A6QE26, and was named FepA (Turlin *et al.*, 2013). The protein was shown to be involved in heme iron utilisation confirming the predictions from bioinformatics methods in this study, but making it less interesting for further study.

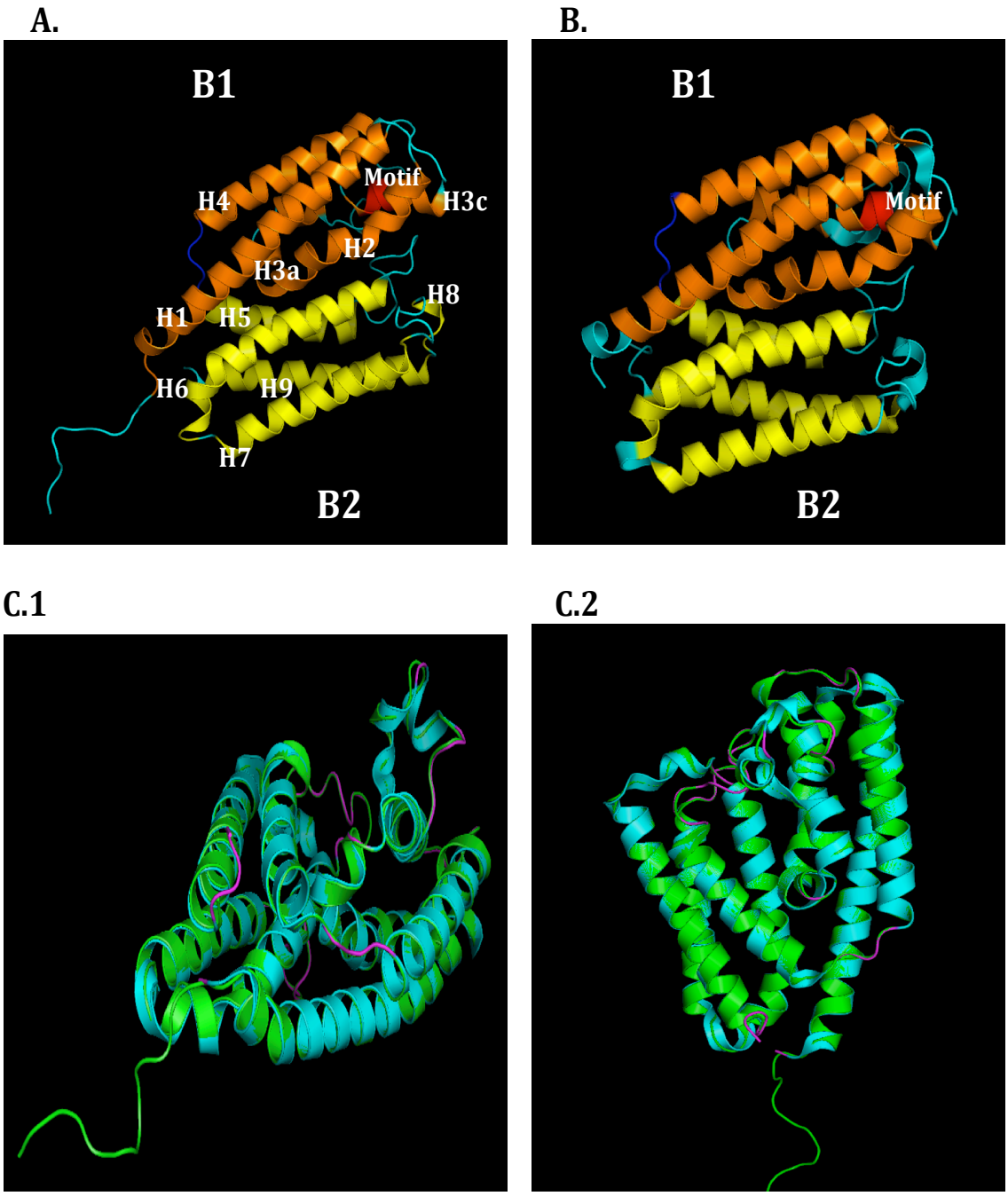

Fig. 2. 3. Structural fold prediction visualised using Pymol. **A, B**: overall structure of A6QE26 template and AlgP7 (PDB ID: 3AT7) respectively. The two bundles **B.1 and B.2** are coloured orange and yellow, respectively. Homology loops between structures is coloured in pink. Metal-binding motif HxxE is coloured red. **C1, C2,** structural alignment of A6QE26 (green) with AlgP7 (cyan).

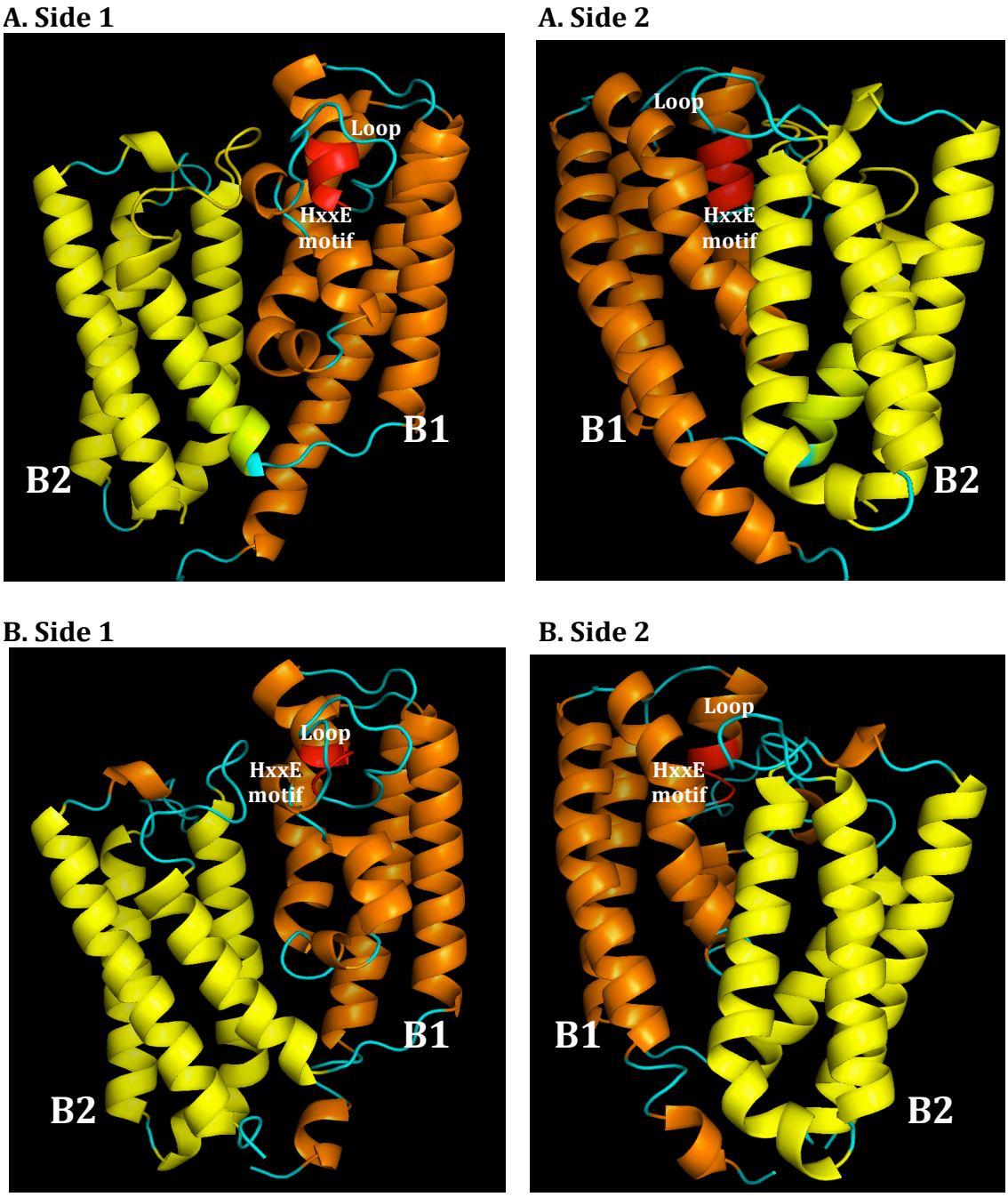

Fig. 2. 4. Comparing HxxE motif locations. The HxxE motif (red) is present on the surface of (A) A6QE26 and (B) Algp7. A loop (yellow) sits in front of the motif of Algp7, viewed from both sides (1 and 2); (B1) bundle 1 and (B2) bundle 2.

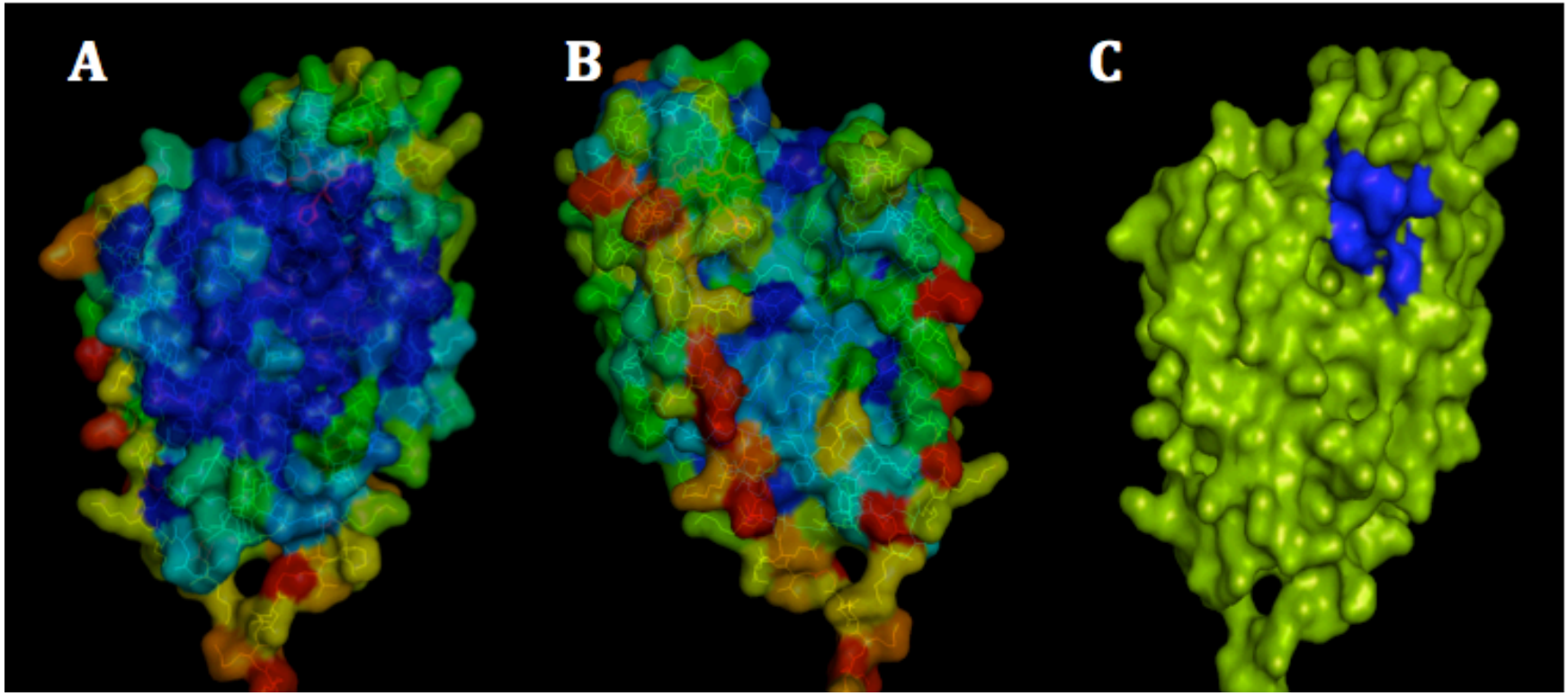

Fig. 2. 5. Evolutionary conservation of amino acids in a model of A6QE26 using ConSurf. (A) A predicted functional region in side 1 of A6QE26, which is highly conserved (residue coloured blue). (B) Fewer conserved amino acids in side 2, but the groove is strongly conserved (residues blue) beside the HxxE motif. (C) Side 1 shows the interface area of seven conserved amino acids, possibly serving as protein-protein interaction site, were detected using meta-PPISP.

2.4.3. Bioinformatics analysis of predicted protein A6QD62

A second protein investigated, A6QD62, has a sequence length of 772 amino acids bearing an N-terminal signal peptide (SP) with a likely cleavage site between SNA_{27} and $_{28}$AE residues, as determined by using the SignalP 4.0 program. The A6QD62 protein does not contain a lipoprotein motif, however an LPxTG motif was detected, which is located in the C-terminus between residues 739 and 752 (Fig. 2.6.). This motif is used for sortase-directed covalent attachment to the peptidoglycan, an activity detected in most Gram-positive bacteria (Sibbald *et al.*, 2006).

The HH-Suite program revealed that A6QD62 was homologous to structures of 5'-nucleotidases (5'-NTs). Three homologous structures from PDB with different shared % sequence identities were found: 5'-nucleotidase from CD73 protein of human 29% (code 4h1s), 5'-nucleotidase from *Thermus thermophilus* 31% (code 2z1a), and UshA protein from *E. coli* 28% (code 1hp1), as well as a Pfam domain match to 5'-nucleotidase with 39% identity (code PF02872). Thus, these data indicated that A6QD62 could harbour the same activity of 5'-nucleotidase.

2.4.3.1. T-coffee alignments

The T-coffee was used to align three sequences, query A6QD62, bacterial 5'-nucleotidase (*E.coli,* UshA protein) and human 5'-nucleotidase (5'NT protein), which were obtained from UniProtKB database. Alignment shows that the primary sequences of both A6QD62 and UshA share low (~15%) overall sequence identity with human 5'NT but revealed several clusters of highly conserved amino acids (Fig. 2. 6.). This observation was similarly reported by other alignment study between

human 5'-nucleotidase (5'NT protein) and bacterial 5'-nucleotidase (5'-NTs), including *E. coli* UshA protein (Knofel and Strater, 1999). However, the clusters in these sequences, includes A6QD62, (Fig. 2. 6.) contain typically active-site residues such as, Histidine (His) and aspartic acids (Asp). It was reported that the main requirements for catalysis are dimetal clusters with its ligands and catalytic Asp-His dyad. For example, in UshA sequence, the catalytic His117 and Asp120 dyad is an essential player in the catalytic mechanism of 5'-nucleotidase activity (Knofel and Strater, 1999).

T-coffee alignments revealed two signature motifs that occur as HxxD, and are conserved between all sequences (Fig. 2. 6.), indicating possible similarity function between these proteins. For example, these motifs consist of His93-Asp96 and His164-Asp167 in A6QD62 sequence,. These motifs also conserved across the *Haemophilus influenza, Archaeoglobus fulgidus* and *Boophilus microplus* sequences (Knofel and Strater, 1999). However, only the A6QD62 sequence presented a motif LPXTG in the end of C-terminal, indicating this protein is surface-attached at the cell wall membrane.

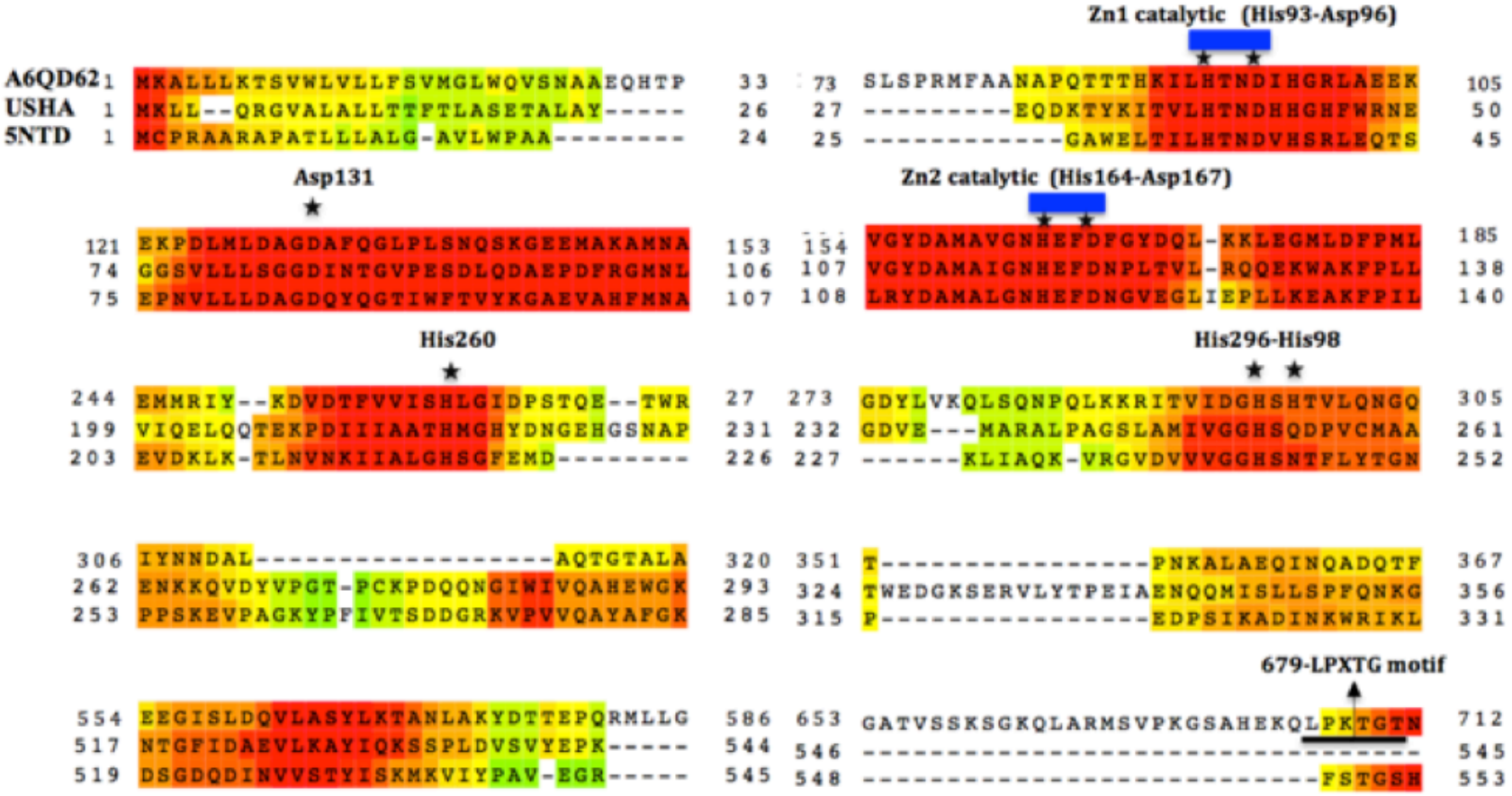

Fig. 2. 6. Sequence alignment of A6QD62, UshA (*E. coli*) and 5NTD (Ecto-5'-nucleotidase of human). Stronger sequence similarity is indicated in red. Two catalytic motifs, Zn1 and Zn2, are labelled with a star and blue line in the top. Other catalytic residues indicated by star in the top. This figure was generated by the T-coffee programme.

2.4.3.2 Modelling structure of A6QD62

2.4.3.2.1 Overall structure and comparison

The model structure of A6QD62 (Fig. 2.7. A,B,C) contains two domains linked by loops. The overall query structure conformation is similar to the 5'NTs fold of *E. coli* UshA (Fig. 2.7. D&E), and CD73 of human. The N-terminal domain (residues 27-352) consists of a mixture of eleven strands and seven helices, whereas the C-terminal domain (residues 385-753) contains 9-helices and 7-sheets, bordered by a large signal peptide and the LPxTG motif.

Compared with the *E. coli* 5'NT (UshA) the C-terminal domain of A6QD62 also contains additional residues (Phe479 and Phe563), which were reported to be involved for the catalytic step of N-terminal domain by binding substrate, such as the adenosine group (Knofel and Strater, 1999).

2.4.3.2.2. Location of catalytic residues on structure

The catalytic Asp-His dyad and di-metal centre that are known as important for the catalytic step are located at the interface in the cleft and between the two domains in the model structure of query protein. Moreover, these catalytic sites or residues are present in the N-terminal domain sequence (Fig. 2.7. A, B, C)

2.4.3.2.3. Consurf and Metal-PPISP tools

The catalytic site is located in a region that has a positive electrostatic potential, which potentially attracts the negatively charged substrate, such as phosphoesters (Knofel and Strater, 1999). The PPISP output indicates that 5 conserved residues between the query and 5'NTs of human might participate in protein-protein interactions (data not shown) however, these amino acids are present after the LPxTG motif (Fig. 2. 6), and may be important for other interactions.

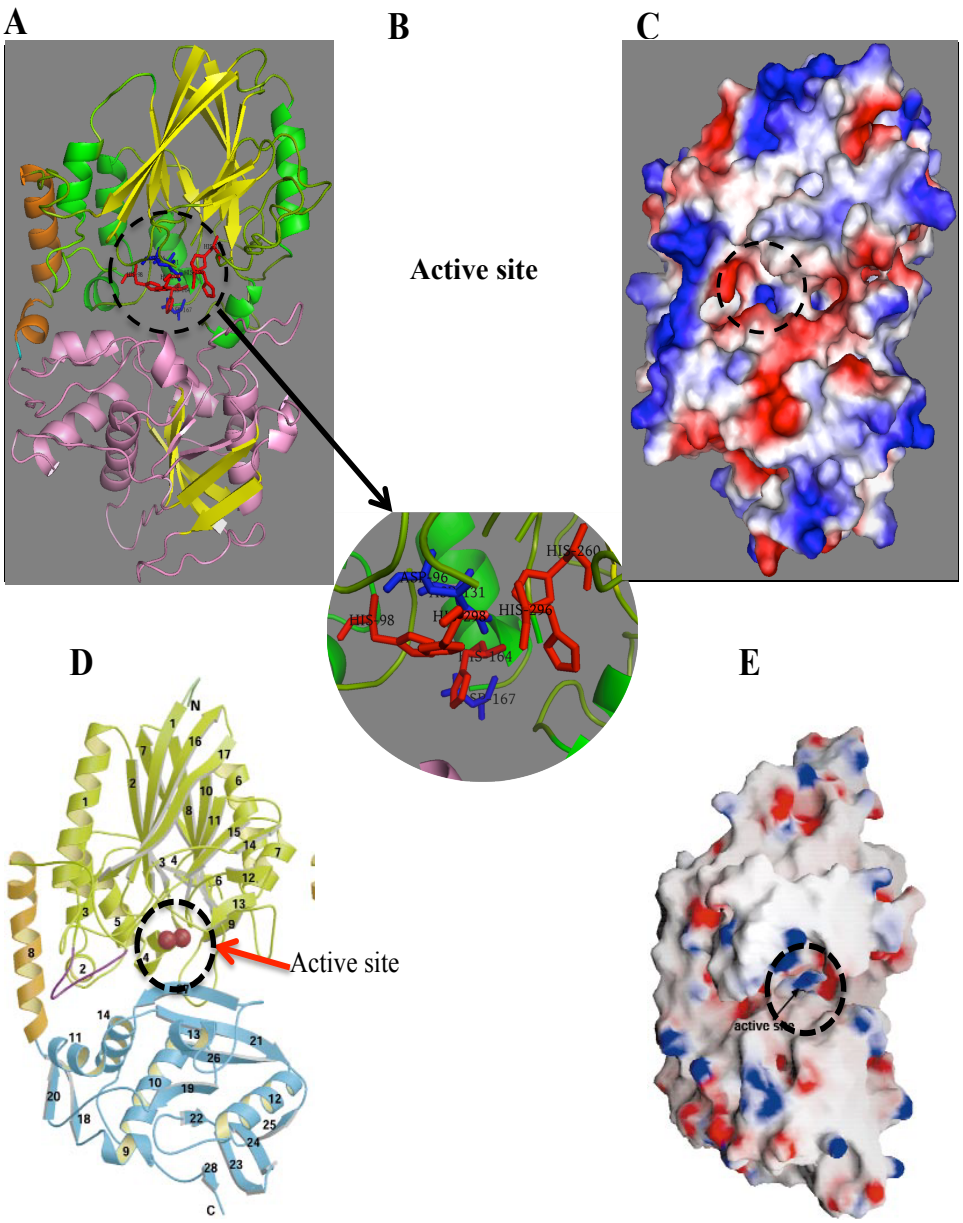

Fig. 2. 7. Modelled structure of A6QD62 showing a catalytic site similar to 5'NT of *E. coli*. **A**, N-terminal and C-terminal domains are coloured in green and light pink, respectively, with yellow sheets in both domains. Both domains are linked together by a loop mediated by alpha helix (orange). **B**, Active-site region that contains core catalytic His164-Asp167 and other catalytic residues. **C**, the surface of A6QD62 model was coloured using pymol for its electrostatic potential (deep cleft with positively-charged residues at the catalytic region). Surface with positively charged residues in blue, and with negatively charged residues in red colour. **D**, structure of 5'NT of *E. coli* shows a deep cleft for the di-zinc centre. **E**,display of active site region within the surface electrostatic potential, as described by (Knofel and Strater, 1999).

Numerous phosphotransferases and phosphatases use a 'two-metal-ion' mechanism to catalyse phosphoryl transfer. The 5'nucleotidases (5'-NTs) contain di-metal sites, and are members of a large superfamily of metallophosphatases. This superfamily includes phosphatases with various substrate specificities, e.g. protein phosphatases, nucleases and nucleotidases (Knofel and Strater, 1999).

5'-nucleotidases have also described to be involved in UDP-sugar hydrolase activity (Knofel and Strater, 1999). 5'NT of animal cells, which is located at the cell surface, can play an important role in the hydrolysis of extracellular nucleotides, such as ATP, ADP, UTP or the diadenosine polyphosphates that were identified to act as extracellular messengers. Membrane bound extracellular nucleotidases (ectonucleotidases), including 5'nucleotidase (5'-NTs), apyrases, and ATPase can degrade ATP, for example to dephosphorylate ATP to ADP, AMP and adenosine. This enzymatic function was found to terminate the ATP actions of neurotransmitter in the brain and periphery (Knofel and Strater, 1999; Zimmermann, 1996), and 5'NTs were implicated in cell-cell and cell-matrix interactions and trans-membrane signalling (Knofel and Strater, 1999).

Bacterial 5'nucleotidases (5'-NTs) are found to be highly homologous to 5'-NT proteins of animals. For example, the gene *ushA* from *E. coli* encodes an enzyme with zinc-binding sites, and is reported to possess activities of 5'-nucleotidase and UDP-sugar hydrolase (Knofel and Strater, 2001). This secreted enzyme is located in the periplasmic space and can degrade the imported UDP-glucose to uridine, phosphate and glucose 1-phosphate (via an unknown mechanism) for utilisation by the cell (Burns and Beacham, 1986; Knofel and Strater, 1999).

2.4.3.3. Annotation of the gene cluster

The Seed server (data not shown) and NCBI databases reveal that the gene (ID: NWMN_0022 and size 2319bp) encoding A6QD62 is conserved across strains of *S. aureus* but there is no gene colocalisation with other genes across different genera. The *S. aureus* protein is annotated as a virulence-associated cell wall-anchored protein (surface associated staphylococcal protein H, SasH). During this work, a paper was found, in which it was described as adenosine synthase, renamed AdsA, an enzyme converting adenosine monophosphate into adenosine that is used to escape phagocytic clearance (Thammavongsa *et al.*, 2009).

Despite this finding, which considerably reduced interest in continued study, there was no activity study of the protein for hydrolysis of extracellular UDP-glucose to serve as a carbon source, an activity regulated by oxygen levels (Burns and Beacham, 1986). The *adsA* gene may be involved in increasing bacterial survival, similar to the AdsA homologue NudP of *Streptococcus agalactiae,* which contributes to survival in blood (Firon *et al.*, 2014). From bioinformatics analysis, this protein could harbour multiple functions that would be achieved by the active site located on the surface.

In summary, the SasH/AdsA protein potentially contains a di-zinc centre that might hydrolyse UDP-sugar, as described in *Salmonella* and *E. coli* (Knofel and Strater, 2001). In addition to the nucleotidase activity reported recently. The protein could be involved in degrading UDP-glucose to extra uridine, phosphate and glucose 1-phosphate in order to be used as an important carbon source as indicated by (Glaser *et al.*, 1967).

2.4.4. Bioinformatic analysis of predicted protein A6QKG9

A third exoprotein investigated was A6QKG9, which contains 374 amino acids bearing an N-terminal signal peptide (SP) with a likely cleavage site between $EKA_{\mathbf{28}}$ and $_{\mathbf{29}}QN$ residues, determined with the SignalP 4.0 program. In addition, A6QKG9 sequence contains a lipobox motif for sorting. The motif cleavage site was predicted to be $S_{20}/_{21}CSK$, using the PRED-LIPO server (Fig 2. 8). Thus, this protein can be recognized, during translocation, by both signal peptidases for cleaving its sites (SPase1 and SPase2), meaning that its location needs confirming during investigations.

HH-Suite results indicated that A6QKG9 contained a domain that matched polysaccharide deacetylase (PF01522) in the pfam database, with 27% identity (Table 2. 2.). This domain is found in a family of polysaccharide deacetylases. This family includes the nodulation protein B (NodB) from *Rhizobium* sp., which is a chitooligosaccharide deacetylase, and the family includes yeast chitin deacetylases. Chitin deacetylases sit within a family of 4-carbohydrate esterases (CE4) in the Carbohydrate-Active Enzymes (CAZY) database, which is specialized in enzymes that breakdown and/or build complex glycoconjugates and carbohydrates (Cantarel *et al.*, 2009)

Numerous bacterial members of the CE4 family are involved in evading lysis by host glycosidases, by catalysing the N- or O-deacetylation of substrates, for example, de-*N*-acetylating sugar amino acids on cell wall peptidoglycan (Urch *et al.*, 2009). This

action allows degradation and remodelling of the surface of bacteria, which avoids recognition by mammalian host enzymes like lysozyme (Oberbarnscheidt *et al.*, 2007).

With further investigation using HHpred server, it was found that the sequence of A6QKG9 matched four structures from PDB with different identities: (1) SpPgdA 20% from *Streptococcus pneumoniae* (PDB code 2c1i), which is a peptidoglycan deacetylase; (2) SmPgdA 16% from *Streptococcus mutans* (PDB code 2W3Z, which is polysaccharide deacetylase; (3) PgaB from *E. coli*, strain K12, (codes 3VUS and 4F9D), which catalyses the N-deacetylation of poly-beta-1,6-N-acetyl-D-glucosamine (PGA) that is required for a biofilm adhesion; and (4) BaCE4, carbohydrate esterase from *Bacillus anthracis* (PDB code 2J13), which is a putative peptidoglycan deacetylase. These homologous proteins are representatives of the esterase family CE4 (Blair *et al.*, 2005a; Deng *et al.*, 2009).

2.4.4.1. T-Coffee alignments

These homologous proteins above (SpPgdA, SmPgdA, PgaB and BaCE4) were aligned with query A6QKG9 protein sequence to determine if query sequence conserved that unique arrangement of the CE4 motifs (MT1-MT5). These motifs form the active site for enzymatic activity (Little *et al.*, 2012). Superposition of the A6QKG9 and other proteins, especially SpPgdA, active sites (Fig. 2.8.) reveal that the sequence of A6QKG9 has elements from each of the five motifs with seven significant differences compared with SpPgdA. A6QKG9 has the canonical motifs (MT1 and MT2) similar to other CE4 members (Fig. 2.8.). MT1 includes two

aspartic acids, the catalytic base (Asp-139) and the metal-coordinating residue (Asp-140), whereas, MT2 contains two histidines, the metal-coordinating residues. His-251 and His-255. Interestingly the MT1 of BaCE4 lacks the second aspartic acid, which is replaced with asparagine (N), whereas the MT2 of PgaB has extra residues between its two histidines, as opposed to a three residues spacer as presented in other CE4 members, including A6QKG9 (Fig. 2.8.). The MT3 is also well conserved with exception that the arginine (Arg) is replaced by histidine (His-291). However, Arg-333 found later in the sequence could be an alternative, since it appears in the cleft of the model structure of A6QKG9 close by the catalytic base, Asp-139 (Fig. 2.10A). Similarly, MT3 of PgaB lacks its arginine. MT4 and MT5 have the most significant differences. The tryptophan (Trp) and aspartic acid (Asp) residues are absent in MT4 of A6QKG9. However, Trp-85 and Asp-337 respectively could be alternatives, since both are located on the side of the active site cleft of A6QKG9 model structure, close by His-62 (Fig. 2.10A). Both leucine (Leu) and histidine (His) are missing in MT5 of both A6QKG9 and PgaB. However, Leu-208 and His-62/ His-291 presented in the sequence of A6QKG9 and very well located in active site could be alternatives. The differences in MT4 and MT5 were previously reported in CE4 members, PgaB and SmPgdA (Deng *et al.*, 2009; Little *et al.*, 2012). Finally, a lipobox motif, responsible for anchoring the protein to the bacterial surface, is located in the N-terminal of A6QKG9 sequence but is not found in the sequences of other CE4 members (Fig. 2.8).

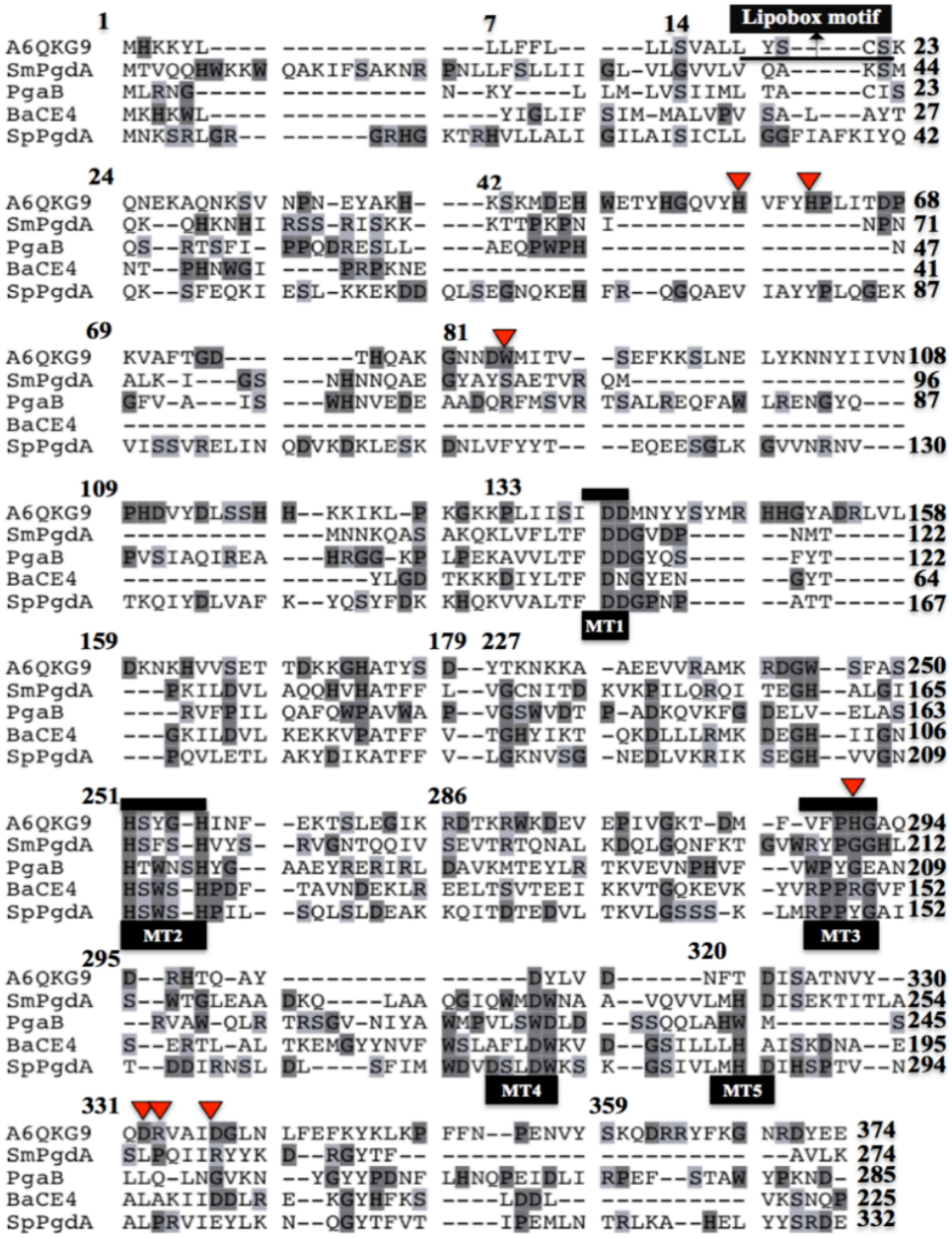

Fig. 2.8. *S. aureus* A6QKG9 aligned with three described de-N-acetylases. Proteins, SmPgdA, PgaB, BaCE4 and SpPgdA are compared with A6QKG9. The number located in the top of alignment is referred to A6QKG9 sequence. The important metalloenzyme catalytic site of two metal-binding residues; His-251 and His-255 in motif (MT2) plus Asp-139 and Asp-140 in motif (MT1) are conserved in the A6QKG9 sequence and other homologues, which indicated (black line) in the top of the alignment. Other residues, His-58, His-62, His-291; Asp-332, Asp-337, Arg-333 and Trp-84 are conserved (red triangle), and expected to be contributed for enzymatic activity. These catalytic residues assemble on the cleft of A6QKG9 model structure (Fig. 2.9). The alignment was performed using the T-coffee programme.

2.4.4.2 Modeling the structure of A6QKG9- overall structure and comparison

Although significant motifs and residues were detected in the A6QKG9 sequence, no structural data exist. Therefore, Modeller was used to make a model structure for A6QKG9; using the *Streptococcus pneumonia* PgdA protein (SpPgdA) structure as template structure and its sequence identity ≥ 27%. The quality of a model structure can be approximately predicted from the sequence similarity between the target and template. A comparison with the pneumococcal SpPgdA structure revealed that the metalloenzyme catalytic site was conserved, whereby a His-His-Asp zinc- binding triad with a nearby Asp and His forms the catalytic site. This metalloenzyme mechanism is shared throughout the carbohydrate esterase family CE4 (Blair *et al.*, 2005b). The model structural data in combination with alignments reveal that A6QKG9 enzyme consists of a single domain, which uses a His251-His255- Asp140 zinc- binding triad associated with the conserved catalytic acid (histidine; His-62/His-291) and base (aspartic acid; Asp139) to carry out base/acid catalysis as explained by other study such as, PgdA protein (SpPgdA) of *S. pneumonia* PgdA protein (SpPgdA) (Blair *et al.*, 2005a).

The first structure of a carbohydrate esterase family CE4 member, that of the *Bacillus subtilis* peptidoglycan (PG) deacetylase (PdaA, also named as BaPdaA or BaCE4), visualised a substrate-binding cleft, used for binding PG *N*-acetyl muramic acid residues. A more recent structure study of SpPgdA indicates that its catalytic domain exhibits the same conserved cleft but with a zinc ion coordinated by zinc-binding triad comprising of His-His-Asp (Blair *et al.*, 2006; Blair *et al.*, 2005a). The active site of A6QKG9 displays a conserved metal-binding triad. The catalytic

subsite contains a zinc-binding triad (as His-His-Asp) comprising of two-histidine (His251, His255) from motif 2 and one aspartic acid (Asp140) from motif 1. This metal-binding triad (His-His-Asp) is generally conserved throughout the CE4 family members such as CICDA and SpPgdA, but exceptions include BaCE4, which only has two metal histidine (motif 2) coordinating residues but no aspartic acid from motif 1 as explained by (Blair *et al.*, 2006; Blair *et al.*, 2005a), and (Fig. 2.8.) The model structure of A6QKG9 also contains Asp139, from motif 1 in a position similar to that observed in structure of SpPgdA, which server as an acetate ion as discussed by (Blair *et al.*, 2006). The authors concluded that the zinc ion is coordinated by two-histidine (motif 2), an aspartic acid (from motif 1), and a water (H_2O), which interacted with the acetate molecule. One of acetate oxygen interacts with an aspartic acid (Asp from motif 1), which in turn is linked by a buried arginine (Arg from motif 3). The same oxygen also binds Histidine (His, from motif 5) and interact with aspartic acid (Asp from motif 4) (Blair *et al.*, 2006). Thus, from alignments and model structure, A6QGK9 has three motifs (MT1, MT2 and MT3), while other missing residues from MT4 and MT5 were observed in different location on A6QKG9, but they are in the right place at the cleft of its model structure, possibly participating in enzymatic activity (Fig. 2.9 & 2.10). Thus, A6QKG9 protein is a member of carbohydrate esterase family CE4 and shares a number of sequence motifs, including conserved aspartic acid and histidine residues that possibly indicate a function as deacetylase such as, de-*N*-acetylation of GlcNAc sugars in peptidoglycan of *S. aureus*, similar to SpPgdA enzyme activity. It would be useful to determine a A6QKG9 crystal structure for further analysis and in order to determine the reaction mechanism.

2.4.4.3. Meta-PPISP.

Meta-PPISP was used to analyse the template structure and indicated that 48 residues (data not shown) located to in to the top an area of a cleft (Fig. 2.9C), suggesting these amino acids might participate in protein-protein interactions. In addition, electrostatics of A6QGK9 model structure was generated by PyMOL programme to analyse the surface and indicated that the catalytic site is located in a region that has a negative electrostatic potential (Fig. 2.9A), which potentially functions to interact with a positively charged substrate.

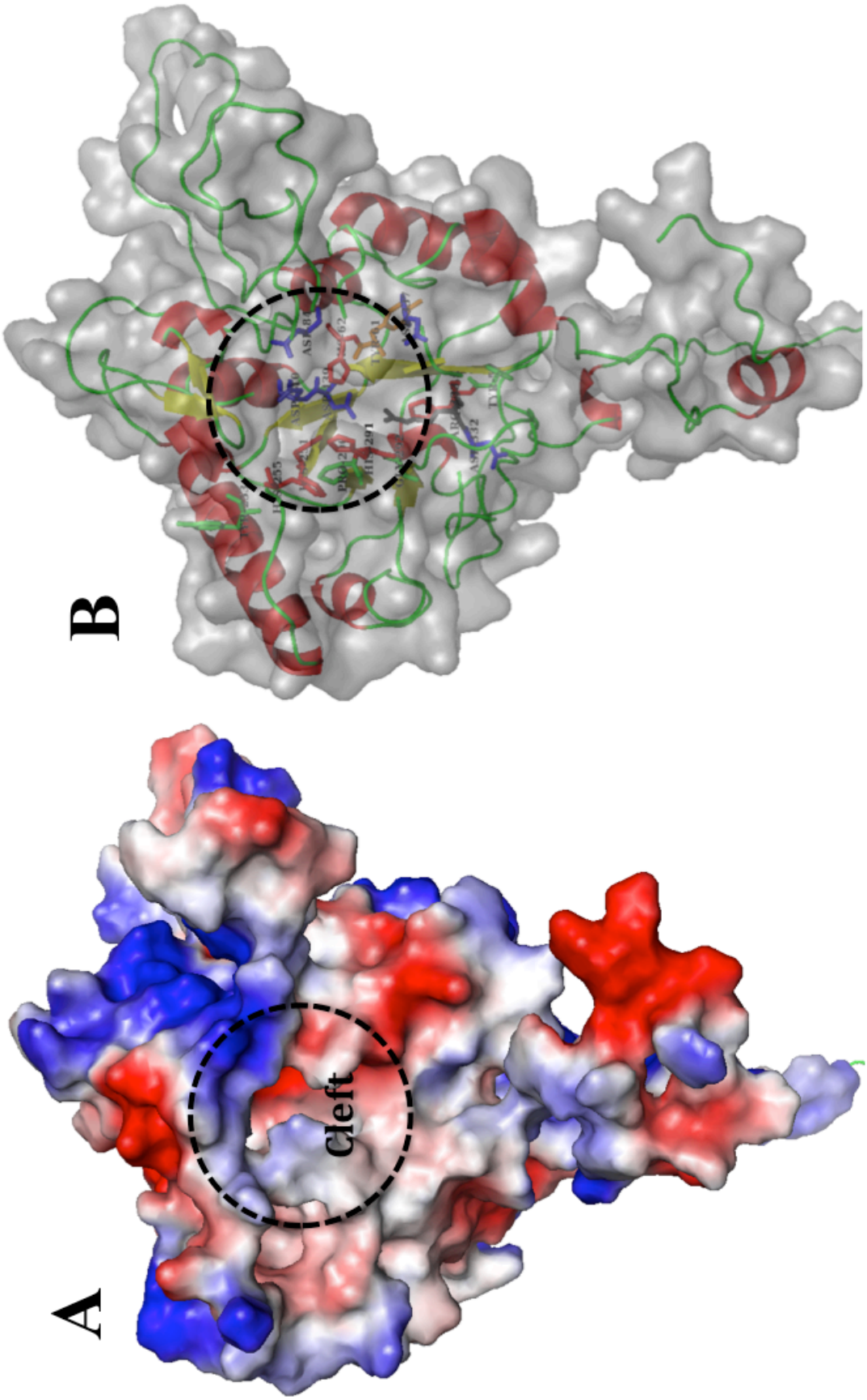
B
A
Cleft

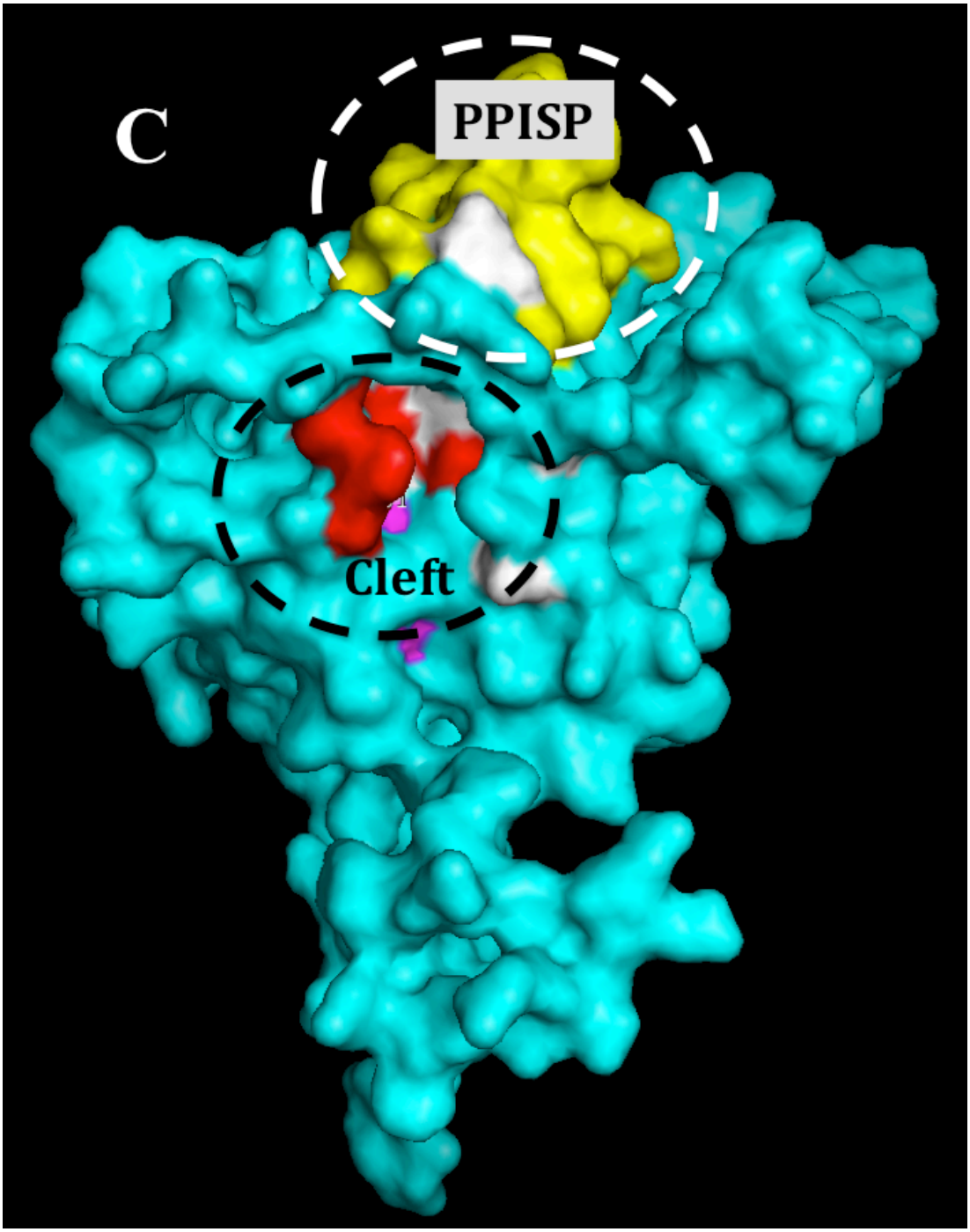

Fig.2.9. Visualisation of modelling structure of A6QKG9, using PyMol methods. A, B shows the cleft on the surface. This cleft (circled in black) shows a negative charge (A) and harbours the proposed catalytic residues of the CE-4 family of esterases, including five His, four Asp and and Arg on the surface of the cleft (B). Forty-eight residues identified using Meta-PPISP form an area at the top of the cleft (yellow colour), and might participate in protein-protein interactions.

Conclusion

A comparison of the *S. aureus* secreted protein A6QKG9 model structure with the SpPgdA and SmPgdA structures revealed that the metalloenzyme catalytic site was conserved in A6QKG9, whereby a His-His-Asp zinc-binding triad with nearby Asp and His residues collectively forms the catalytic site. This metalloenzyme mechanism is shared with the carbohydrate esterase family CE4 (Blair *et al.*, 2005a; Deng *et al.*, 2009), and was located together with known catalytic residues belonging to CE4 family in the *S. aureus* A6QKG9 query sequence.

Deletion of the gene *pgdA* encoding SpPgdA protein in *Streptococcus pneumoniae* produced hypersensitivity to lysozyme and reduced virulence in a mouse model of infection (Blair *et al.*, 2005a). This SpPgdA protein is a member of the CE-4 family and its crystal structure indicates all of the catalytic residues also present in the A6QKG9 sequence.

SmPgdA shares homology with a described polysaccharide deacetylase domain and catalytic domains of peptidoglycan GlcNAc de-N-acetylase of *Listeria monocytogenes* and *Streptococcus pneumoniae.* Inactivation of the gene encoding SmPgdA protein in *Strep. mutans* led to altered colony texture and a slightly increased cell surface hydrophobicity (Deng *et al.*, 2009). The crystal structure of *S. mutans* smPgdA protein shows the characteristic carbohydrate esterase fold, described above, but no peptidoglycan-specific activity was observed. Instead, it might act on a polysaccharide at the bacterial cell surface where the mutant has significantly increased aggregation/agglutination with salivary agglutinin (SAG) (Deng *et al.*, 2009).

From this analysis data, it appears that A6QKG9 protein contains all catalytic residues required for peptidoglycan deacetylase of an unknown substrate yet. From the comparative analysis with the other proteins described here it was determined that A6QKG9 protein is a Pgd-like protein and will be named as such going forward in this study.

2.4.5. Further proteins of unknown function

During this research study the catalytic functions of two of the three chosen proteins were described or identified. Consequently, as insurance moving forward, two further proteins were targeted for functional studies as possible replacement targets. These proteins, named in the Uniprot database as AOAOH3K682 and SA2061, were analyzed during this study (Some data is not shown below, as it was not fully completed). Both *AOAOH3K682* and *Sa2061* genes were inactivated, but not investigated further. SA2061 protein is still at unknown function, especially in *S. aureus*. However, by analysis its sequence, this protein was not matched homologous protein, and therefore it needs more investigation in future work.

The most interesting is the function of AOAOH3K682 protein in *S. aureus,* which had not yet been determined. However, HH-Suite analysis revealed that its sequence had around 30% identity with another protein from *Streptococcus pyogenes* called myosin-cross-reactive antigen (McrA) with size 67 kDa. A McrA of *Strep. pyogenes* was reported to be a fatty acid hydratase, acting on the double bound of an unsaturated fatty acid to generate a saturated fatty acid. The protein activity is achieved by a motif sequence GXGXXGX, which detoxifies antimicrobial fatty

acids (AFAs), such as linoleic and oleic acids (Volkov *et al.*, 2010). The active site residues (motif) of McrA were observed in the *S. aureus* AOAOH3K682 sequence as well as other motifs contributing to activity against AFAs. This study suggests that AOAOH3K682 may act as McrA of *Strep. pyogenes*, and therefore this protein needs more investigation.

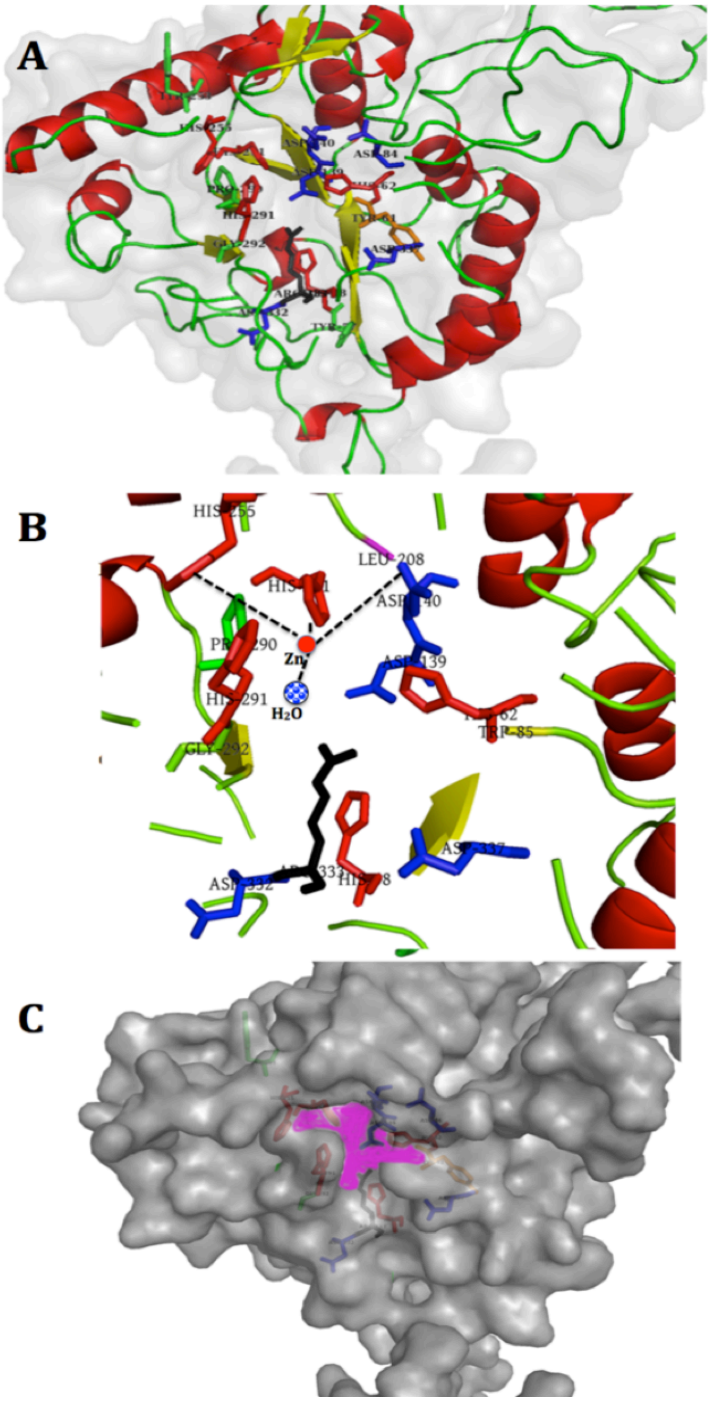

Fig. 2.10. Overview of the S. *aureus* Pgd (A6QKG9) model structure. (A) a zoom of Fig.2.9B to show active site and its residues. (B) Scheme for the possibly active site residues on A6QKG9 of *S. aureus*. It is expected that the Zinc ion (red circle) bind residues (H-251 and H-255) and an aspartic acid (D-140) in this area. Other residues; histidine (H-58, H-62, 291), aspartic acids (D-139, D-332 and D-337) and arginine (R-333) are indicated and may be involved in this active site. (C) A6QKG9 surface shows the cleft and the location of residues that are indicated in (A). The model structure of pgd compared with overall structure of the spPgd and smPgd structures (Deng *et al.*, 2009).

2.4.6. Future focus of this study

The identification of a *S. aureus* protein with homology to N-deacetylases using homology searching and structural prediction/modeling produced a focus for future research to determine whether this predicted function was correct. Given the potential importance of the protein in cell wall surface regulation, the study focused intensively to study its role using a molecular genetic and functional genomics approach.

CHAPTER 3

3. Materials and Methods

3. 1. Materials

3.1.1. Reagents.

All chemical reagents were obtained from Bioline (Meridian Life Science, UK), Fisher Scientific (Germany) and Sigma-Aldrich, unless otherwise stated. The preparation and storage of reagents was performed according to manufacturer's instructions. Water (ddH_2O) was deionised using a reverse osmosis purification system.

3.1.2. Bacterial strains and plasmids

Bacteria, plasmids and antibiotics that were used for this study are listed in Table 3.2. *E. coli* Top10 was used as a general cloning host via the production of competent cells for transformation with plasmids constructed by ligation of PCR-amplified genes. The pMUTIN4 vector was used for creating *S. aureus* mutants by allelic replacement, following resolution of integrated plasmid intermediates by using phage transduction. The low copy number pSK5632 plasmid was used for complementation of gene mutants in *S. aureus* strains. *S. aureus* strain RN4220, a methylation-positive, restriction-negative host strain, was used as a cloning intermediate for construction of desired strains. The plasmids PTB361 and PET 24d+ were used as vectors to clone genes for overexpression studies and both contain a T7 promoter for expression by induction of T7 RNA polymerase.

Table 3.1. Genes included in this study to determine their functions.

Gene name	***ID gene**	**Size (bp.)**	***ID Protein**	**Size (a.a)**	**Mass (Da)**	**Bioinformatics analysis results**
a6qe24	NWMN_0336	855	A6QE26	284	32.24	Iron uptake
a6qd62	NWMN_0022	2319	A6QD62	772	83.42	Nucleotidase activity or hydrolysis of UDP-sugar.
pgd	NWMN_2579	1125	A6QKG9	374	43.55	Deacetylase of peptidoglycan or polysaccharide.
mcrA	NWMN_0050	1776	A6QD90	591	67.64	Detoxification of oleaic acid, hydratase.
SA2061	SA2061	1212	Q7A443	403	43.92	MFS transporter capable of transporting small solutes in response to chemiosmotic ion gradients

***Sequences and data were obtained from NCBI and Uniprot databases.**

Table 3.2. Bacterial strains and plasmids used in this study. Antibiotics (Sigma) are as follows: ampicillin (Ap), 100 μg ml^{-1}; kanamycin (Kan), 50 μg ml^{-1}; erythromycin (Ery), 25 μg ml^{-1}; chloramphenicol (Cm), 10 μg ml^{-1}; tetracycline (Tet), 12.5 μg ml^{-1} with *E. coli* strains and 5 μg ml^{-1} with *S. aureus* strains.

Strains	**Description**	**Lab ID**	**Reference/Source**
S. aureus			
Newman	Wild-type	LIV028	(Duthie and Lorenz, 1952)
SH1000	Wild-type strain, *rsbU* repaired strain of *S. aureus* 8325-4	LIV023	(Horsburgh *et al.*, 2002a)
SF8300	Clinical isolate (USA300)	LIV1138	(Montgomery *et al.*, 2009)
BHICC	MRSA clinical isolate. SCCmec type II, Biofilm positive.	LIV1175	(O'Neill *et al.*, 2007)
RN4220	Intermediate cloning host restriction negative, methylation-positive	LIV124	(Novick, 1991)
Newman *atl*	*atl* insertional inactivation mutant, Ery	LIV232	(Foster, 1995)
SA113	Wild-type strain	LIV1142	(Bera *et al.*, 2005)
SA113 *oatA*	Single-deletion mutant (*oatA*:: kan), lacks MurNac O-acetylation	LIV1144	(Bera *et al.*, 2005)
SA113 *tagO*	Single-deletion mutant (*tagO*::*ermB*), lacks MurNac WTA	LIV1143	(Bera *et al.*, 2007)
SA113 *oatA*, *tagO*.	Double-deletion mutant (*oatA*:: kan *tagO*::ermB), lacks both MurNac WTA and O-acetylation	LIV1145	(Bera *et al.*, 2007)
Escherichia coli and plasmids used in this study			
Top10	Chemically competent cell, cloning host.	LIV131	Lab stock
pMutin4	Suicide vector for allelic replacements containing *lacZ*. Ap, *E. coli*; Ery, *S. aureus*.	LIV697	(Vagner *et al.*, 1998)
pET24d+	Vector for overexpressing proteins with His_6 tag. T7 promoter. Kan, *E. coli*.	LIV849	Lab stock
pTB361	Vector for overexpressing proteins. Tet, *E. coli*.	LIV713	Lab stock
pSK5632	Shuttle vector used for complementation. Ap, *E. coli*; Cm, *S. aureus*	LIV711	(Grkovic *et al.*, 2003)
pLysS	*E. coli* BL21 (DE3)	LIV036	Lab stock
pDG1513	pMTL22 derivative, containing the tetracycline resistance cassette		(Guerout-Fleury *et al.*, 1995)
pDG792	Plasmid pML22, containing the kanamycin resistance cassette		(Guerout-Fleury *et al.*, 1995)

***S. aureus* strains (created during in this study)**

Newman *pgd*	*Newman pgd*::*tet*. Tet.	LIV3005	This study
Newman pJAL-*pgd*	*Newman* containing pSK5632+*pgd.* Cm.	LIV3018	This study
Newman *pgd* pJAL-*pgd*	Complemented strain. Newman *pgd* containing pSK5632+*pgd.* Cm.	LIV3021	This study
SF8300 *pgd*	SF8300 *pgd*::*tet*. Tet.	LIV3017	This study
SF8300 pJAL-*pgd*	SF8300 containing pSK5632+*pgd.* Cm.	LIV3020	This study
SF8300 *pgd* pJAL-*pgd*	Complemented strain. SF8300 *pgd* containing pSK5632+*pgd.* Cm.	LIV3023	This study
SH1000 *pgd*	SH1000 *pgd*::*tet*. Tet.	LIV3000	This study
SH1000 pJAL-*pgd*	SH1000 containing pSK5632+*pgd.* Cm.	LIV3019	This study
SH1000 *pgd* pJAL-*pgd*	Complemented strain. SH1000 *pgd* containing pSK5632+*pgd.* Cm.	LIV3022	This study
BH1CC *pgd*	BHICC *pgd*::*tet*. Tet.	LIV3043	This study
BH1CC pJAL-*pgd*	BHICC containing pSK5632+*pgd.* Cm.	LIV3045	This study
BH1CC *pgd* pJAL-*pgd*	Complemented strain. BHICC *pgd* containing pSK5632+*pgd.* Cm.	LIV3044	This study
Newman *oatA*	*Newman oatA*::*kan*. Kan	LIV1187	This study
Newman *tagO*	*Newman tagO*::*erm*.	LIV1189	This study
Newman *oatA tagO*	*Newman oatA*::*kan tagO*::*erm*. Kan	LIV1205	This study
Newman *pgd oatA*	*Newman pgd*::*tet oatA*::*kan*. Tet,Kan	LIV1190	This study
Newman *pgd tagO*	*Newman pgd*::*tet tagO*::*erm*. Tet, Erm	LIV1203	This study
SA113 *pgd*	SA113 *pgd*::*tet*. Tet	LIV1184	This study
SA113 *pgd oatA*	SA113 *pgd*::*tet oatA*::*kan*. Tet, Kan	LIV1186	This study
SA113 *pgd oatA tagO*	SA113 *pgd*::*tet oatA*::*kan tagO*::*erm*	LIV1207	This study
SF8300 *oatA*	SF8300 *oatA*::*kan*. Kan	LIV1192	This study
SF8300 *pgd oatA*	SF8300 *pgd*::*tet oatA*::*kan*. Tet, Kan	LIV1180	This study
Newman *mcrA*	Newman *mcrA*::*tet.* Tet.	LIV3004	This study
SH1000 *mcrA*	SH1000 *mcrA*::*tet.* Tet.	LIV2002	This study
Newman *a6qd62*	Newman *a6qd62*::*tet.* Tet.	LIV2995	This study
SH1000 *a6qd62*	SH1000 *a6qd62*::*tet.* Tet.	LIV2992	This study
Newman *SA2061*	Newman *SA2061*::*tet.* Tet.	LIV3012	This study
SH1000 *SA2061*	SH1000 *SA2061*::*tet.* Tet.	LIV3015	This study
RN4220 *mcrA* pSK5632-*mcrA*	RN4220 *mcrA* containing PSK5632+ *mcrA.* Cm.	LIV1162	This study

Plasmids generated in this study for the complementation			
pJAL	pSK5632 containing cloned *pgd* gene plus *tet* cassette	LIV1141	This study
pMcrA	pSK5632 containing *mcrA* plus *cm* cassette	LIV1142	This study
pSA2061	pSK5632 containing *sa2061*plus *cm* cassette	LIV1170	This study
pA6QD62	pSK5632 containing *a6qd62* plus *cm* cassette	LIV1171	This study
Plasmids generated in this study for overexpression			
PJamal-PCR2	PET24d + *pgd.* Kan	LIV1132	This study
PJamal-PCR2	*E. coli* BL21 (DE3) pLysS with pET24d + *pgd.* Kan	LIV1132-A	This study
EX-A6QD62	PET24d + *a6qd62.* Kan	LIV1131	This study
EX-MCRA	PET24d + *mcrA.* Kan	LIV1134	This study
EX-SA2061	PET24d + *SA2061.* Kan	LIV1147	This study

Table 3.3. Oligonucleotide primers designed for PCR amplification. The sequence of the restriction enzyme (RE) site is underlined.

Gene ID	Purpose		DNA Primer Sequence 5' → 3'	RE
a6qe26 (NWMN_0336)	**Knock out (KO)**	**F1**	ACATGAATTCTGCAACTGAGCAACCATCAG	*Eco*RI
		R1	CCGGTACCTGCTTCTGCAACTGGTTCAG	*Kpn*I
		F2	ATAACTGCGGCCGCGTGATGATATCCAAATGAAC	*Not*I
		R2	CGACGGATCCAACGGTGCACCACTATGTCGT	*Bam*HI
	Complementation (CO)	**F**	CGACGGATCCGAGAAGGTATGTTACGTGAC	*Bam*HI
		R	TTATAAAGCTTGGCACCGCCAATACCTAACA	*Hind*III
	Overexpression (EX)	**F**	GTATACCATGGGCATCAACGTTATTAATTGCT	*Nco*I
		R	TTATACTCGAGTTCAGTAATCACAGCCAT	*Xho*I
a6qd62 (NWMN_0022)	**Knock out (KO)**	**F1**	ACAT GAATTC TTG CAC TGA TGT ATA TTG CA	*Eco*RI
		R1	CC GGTACC GAT GGT GCG TTG GAT GTT AC	*Kpn*I
		F2	ATAACT GCGGCCGC ACT GTA TCA AGC AAG AGT GG	*Not*I
		R2	CGAC GGATCC TCT TAT ATA TTG AAT GAA CG	*Bam*HI
	Complementation (CO)	**F**	TTAC AGATCT ACG CCA ATA TAT ACA ATA TAA	*Bgl*II
		R	TTAC GTCGAC TTA TCA ACG GTT ATC GCT	*Sa*ll
	Overexpression (EX)	**F**	GTATA CATATG ACA AGT GTA TGG CTC GTT	*Nde*l
		R	TTATA CTCGAG GCT AGC TTT TCT ACG TCG TAC	*Xho*I

Gene ID	Purpose		DNA Primer Sequence 5' → 3'	RE
pgd (NWMN_2579)	**Knock out (KO)**	**F1**	ACAT GAATTC GTA CTG CTA TGG AGT TAA GAC	*Eco*RI
		R1	CC GGTACC TAC AGT AAT CAT CCA ATC AT	*Kpn*I
		F2	ATAACT GCGGCCGC TAC AGA TAT ATC AGC AAC GA	*Not*I
		R2	CGAC GGATCC TGG CTG CGC AGT AAT ATC TAA	*Bam*HI
	Complementation (CO)	**F**	CGAC GGATCC GAC GAT ACT ATG GAC GAC ATT	*Bam*HI
		R	TTATA AAGCTT CTT GCA CAT ATT GTC CTT GCC	*Hind*III
	Overexpression (EX)	**F**	ATT CCATGG AAAATAAATCTGTTAATCCA	*Nco*I
		R	TTATA CTCGAG TTC TTC ATA ATC CCG ATT CC	*Xho*I
mcrA (NWMN_0050)	**Knock out (KO)**	**F1**	ACATGAATTCGGAATTGGTTAAGTTCACTC	*Eco*RI
		R1	CCGGTACCAGAACTCATCTAATA CAGAC	*Kpn*I
		F2	ATAACTGCGGCCGCTGTATCACTTAGGTGTATCA	*Not*I
		R2	CGACGGATCCTCCAGCTGTTACCAGTCCGA	*Bam*HI
	Complementation (CO)	**F**	TTACGGATCCTTAAGTAACTTCTTTCAA	*Bam*HI
		R	TTATAAAGCTTACATCATTTCTGTCCCAG	*Hind*III
	Overexpression (EX)	**F**	GTATACATATGTATTACAGTTATGGAAAT	*Nde*l
		R	TTATACTCGAGTAACAATTTGTGTTCTTT	*Xho*I

Gene ID	Purpose		DNA Primer Sequence 5' → 3'	RE
SA2061	Knock out (KO)	F1	ACATGAATTCTTGAGTACGCATGGAATCACTT	*Eco*RI
		R1	CCGGTACCGATCAACTGCAGTTGCGATAC	*Kpn*I
		F2	ATAACTGCGGCCGCACTGTTGGTCTAGATG	*Not*I
		R2	CGACGGATCCTCTCAACACAGAAGCTGACA	*Bam*HI
	Complementation (CO)	F	TTACAGATCTACGCACATAGACGTGCAATTG	*Bgl*II
		R	TTACGTCGACTTG TGCCAATCAGTACATCA	*Sal*I
Tetracycline (*tetB*)	Amplify *tet* from pDG1513	F	ATAACTGCGGCCGCGGCGGATTTTATGACCGAT GAAG	*Not*I
		R	CCGGTACCTTAGAAATCCCTTTGAGAATGTTT	*Kpn*I
Kanamycin (*kan*)	Isolate *kan* from pDG792	F	ACAGGTACCGAAAACCCAGGACAATAACC	*Kpn*I
			ACAGGTACCCTCGGGACCCCTATCTAG	*Kpn*I
	M13	F	GTAAAACGACGGCCAG	
		R	CAGGAAACAGCTATGAC	

3.1.3. Protein purification buffers

Lysis buffer (for 1 litre)

50mM NaH_2PO_4

300mM NaCl

10mM imidazole

Adjust pH to 8.0

Washing buffer (for 1 litre)

50mM NaH_2PO_4

300mM NaCl

20-60mM imidazole (the concentration of imidazole required for elution is protein dependent)

Adjust pH to 8.0

Elution buffer (for 1 litre)

50mM NaH_2PO_4

300mM NaCl

250mM imidazole

Adjust pH to 8.0

(A) Separating gel 10% (for one gel)

dH_2O	1.75 ml
30% acrylamide	2.5 ml
3M Tris-HCl/SDS, pH 8.45	2.5 ml
Glycerol	0.75 ml
30% APS (Ammonium persulfate)	7µL
TEMED	7µL

(B) Separating gel 4% (for one gel)

dH_2O	1.95 ml
30% acrylamide	0.4 ml
3M Tris-HCl/SDS, pH 8.45	0.775 ml
30% APS (Ammonium persulfate)	7µL
TEMED	7µL

SOC media for 1 litre

20 g	Tryptone
5 g	Yeast extract
0.186 g	KCl
0.5 g	NaCl
2.4 g	MgSO4, anhydrous
4 g	Glucose

3.2. Methods

3.2.1. Bacterial culture

Broth and agar media were prepared according to the manufacturer's instructions using distilled water and sterilised by autoclaving at 121^{o}C for 15 min. *E. coli* strains were routinely grown overnight in Luria-Bertani (LB) medium (LAB M, Quest Park, Lancashire, UK) at 37^{o}C with shaking at 250 rpm and supplemented, as appropriate, with antibiotics: 12.5 μg ml^{-1} tetracycline (Tet), 50 μg ml^{-1} kanamycin (Kan) and 100 μg ml^{-1} ampicillin (Amp).

S. aureus strains (Newman, SF8300, SH1000 and BHICC) including their mutants and their complemented counterparts were typically cultured in brain heart infusion (BHI) (LAB M, Quest Park, Lancashire, UK) at 37^{o}C with shaking at 250 rpm. The supplementation of media with antibiotics is listed for relevant strains in Tables 3.1 and 3.2.

3.2.2. Preparation of competent cells

3.2.2.1. Chemically competent cells of *E. coli* Top10.

Chemically competent *E. coli* Top10 were prepared according to the Hanahan method (Hanahan *et al.*, 1991). A frozen stock of *E. coli* Top10 (LIV131; Table 3. 2.) was streaked onto an LB plate and incubated overnight at 37^{o}C. Next, several colonies were aseptically transferred to a 500 ml flask containing 100 ml of SOB media and incubated at 37^{o}C, with shaking at 225 rpm until the OD600 nm reached

0.5. The culture was chilled on ice for 20 min and then cells were harvested by centrifugation at 3,220 rcf for 10 min. The pellet was resuspended gently in 25 ml of cold FSB buffer and incubated on ice for 15 min. Next, the cells were harvested again as described and resuspended in 8 ml of cold FSB buffer. Subsequently, 280 µl of DMSO (99.7 % dimethyl sulphoxide, Fisher Scientific) was added to the mixture and incubated for a further 10 min on ice. Finally, the cells were aliquoted and frozen using dry ice with 100% ethanol, prior to storage at -80^{o}C until use. A 200µl aliquot of the competent cells was assessed for its effectiveness by transformation with 100 ng of pMUTIN4 to ensure numbers of colonies yielded on an LB ampicillin plate were greater than 10^{8} colonies per µg DNA.

3.2.2.2. Electrocompetent cells of *S. aureus* RN4220.

The strain *S. aureus* RN4220 (LIV124) was used as an intermediate cloning host and electrocompetent cells were prepared according to a commonly used method (Schenk and Laddaga, 1992). Strain RN4220 was grown overnight in 10 ml B2 broth at 37^{o}C. Following this, 2 ml of overnight culture was added to 1 litre of fresh B2 and cultured under the same conditions until growth reached mid-log phase (OD600 nm ~ 0.8). Cells were harvested by centrifugation at 1500 rcf for 10 min at 4^{o}C. The pellet was washed three times by resuspension in 300 ml sterile cold-water and harvested by centrifugation at 1500 rcf for 10 min, followed by three washes with 100 ml, 50 ml and 25 ml of 10 % (v/v) ice-cold glycerol, respectively. Cells were harvested and resuspended in 1.25 ml of ice-cold glycerol, then aliquoted in 200 µl batches in sterile 2 ml eppendorfs and frozen using dry ice with 100% ethanol and then stored at -80^{o}C until use.

3.2.3. Bacterial storage

All bacterial strains used in this project were stored as resuspended cells in LB medium containing 15% (v/v) glycerol, and stored at -80 ^{O}C.

3.2.4. Genomic DNA extraction

Genomic DNA from *S. aureus* was extracted with a DNeasy Blood & Tissue kit (QIAGEN) using a modified protocol. One or several colonies were transferred to 10 ml BHI media with culture overnight at 37^{o}C, shaking at 225 rpm. Cells were harvested from overnight culture by centrifuging for 10 min at 1500 rcf. Subsequently, supernatant was discarded and the cells were completely resuspended in 180 µl enzymatic lysis buffer (180 µl ELB buffer plus 2 µl lysostaphin [5 µg ml^{-1}] and 20 µl lysozyme [1 mg ml^{-1}]). After mixing, the cells were incubated for 1 h at 37^{o}C to ensure lysis then 25 µl proteinase K and 200 µl AL buffer were added consecutively, with mixing between, to the lysed cells and mixed before incubating at 56^{o}C for 30 min. Next, 200 µl of 99% (v/v) ethanol was added to the mixture and vortexed before pipetting onto the Mini spin column, which was centrifuged at 6030 rcf for 1 the min. The flow-through was discarded from the collection tube and 500 µl AW1 buffer was added onto the spin column, followed by centrifuging at 6030 rcf for 1 min and again discarding the flow-through. AW2 buffer (500 µl) was added to the column and centrifuged at 6030 rcf for 1 min, followed by discarding the flow-through and replacing the collection tube. A 2 min centrifuge cycle was used to dry the membrane of the column. Finally, the DNA was collected into a sterile 1.5 ml tube by pipetting 50µl ddH_2O directly onto the spin column membrane followed by centrifugation at 18400 rcf for 1 min. The DNA quality and concentration was

measured using a NanoDrop-1000 (Thermo Scientific) then stored at -20 ^{o}C until use.

3.2.5. Plasmid extraction from bacteria

Plasmids and their respective host *E. coli* strains used during this study are listed in (Table 3. 2.). *E. coli* strains containing the desired plasmid were grown in LB broth with selective concentrations of antibiotic (Table 3. 2) at 37 ^{o}C with shaking at 200 rpm for overnight. Plasmids from the host cells were harvested with the Isolate II Plasmid Mini Kit (BioLine). Briefly, 10 ml of overnight culture was centrifuged at 18400 rcf for 10 min and the supernatant discarded. The pellet was resuspended in 250 µl resuspension buffer P1 (containing RNase A) and mixed by pipetting up and down to fully resuspend clumps. Subsequently, 250 µl lysis buffer P2 was added to the mixture and mixed gently by inverting the tube 6-8 times, to avoid shearing genomic DNA and contaminating the plasmid, followed by incubating at room temperature for 5 min. Afterwards, 350 µl neutralization buffer P3 was added to the mixture to neutralise the NaOH present in buffer P2 and mixed gently prior to centrifuging at 21200 rcf for 10 min. The clarified supernatant phase was transferred to a spin column, placed in a 2 ml collection tube and then centrifuged at 13500 rcf for 1 min. The filtrate was discarded each time and the collection tube reused. Next, 500 µl wash buffer PW1 was added directly onto the membrane column then centrifuged at 13500 rcf for 1 min prior to adding 600 µl wash buffer PW2 and centrifuging again at 13500 rcf for 1 min. The filtrate was discarded and the silica membrane dried by centrifuging the spin column once more at 13500 rcf for 2 min. Finally, the DNA was collected into a sterile 1.5 ml tube by pipetting 50 µl ddH_2O

directly onto the spin column membrane then centrifuging at 18400 rcf for 1 min. 5 µl of the plasmid DNA was tested using a single restriction enzyme digest followed by agarose gel electrophoresis to confirm the size of plasmid. The quality and concentration of extracted plasmid was determined by NanoDrop-1000 (Thermo Scientific) and DNA was stored at -20 ^{o}C until use.

3.2.6. DNA manipulations.

3.2.6.1. Oligonucleotide primers.

Oligonucleotide primers for amplification of each gene of interest are outlined in Table 3.3. Custom oligonucleotide primers were designed with the following criteria; each primer was typically between 18 to 26 bases. The 5' end of each primer for cloning consisted of a specific restriction site for ligation; all primers were selected with a GC content of approximately 50%; the calculation of annealing temperature (Tm) of these primers was between 55^{o}C and 65^{o}C. All primers were purchased from Eurofins Genomics, Germany and were dissolved in Milli-Q water and stored at -20^{o}C.

3.2.6.2. Polymerase Chain reaction (PCR)

Dependent on their purpose, three different groups of primers were designed in this study (Table 3.3).

Group one were designed for creating gene mutants: four primers were designed and used to amplify two flanking regions of the target gene [left arm (LA) and right arm (RA)] from the genome of *S. aureus* Newman. These LA and RA regions, around 1

kb in length, were amplified from the genome of *S. aureus* and coligated with *tet* or *kan* resistance cassettes to generate disrupted alleles in shuttle vector pMUTIN4. This pMUTIN4 construct was used as a suicide vector for the allelic replacement of the target gene (Fig. 3. 1.). The tetracycline gene (*tet*) was isolated from the pDG1513 vector, while kanamycin (*kan*) was amplified from pDG782 vector (Guerout-Fleury *et al.*, 1995).

Group two primers were designed for gene complementation studies: a pair of primers were designed to amplify the full-length target gene (including potential promoter and terminator sequences upstream ~200bp and downstream ~50bp) from *S. aureus* Newman strain for cloning into the complementation vector pSK5632.

Group three primers were designed for generating overexpression plasmids: primers were synthesised to amplify the full-length sequence of a target gene (excluding the 5' N-terminal signal peptide and 3' stop codon sequences) from *S. aureus* Newman genomic DNA. The amplified and digested DNA was cloned into pET24d+, which was used for the overexpression of the target gene using the *E. coli* BL21 (DE3) strain. This is discussed further in (section 4.3.3.2). The PCR parameters, reaction mixture and quantities are outlined (Table 3.4-5).

Table 3.4. PCR amplification cycle parameters

Step	Cycle	TM	Time
1	Primary denaturation	95 ^{o}C	3 min
2	Denaturation	95 ^{o}C	20 s
3	Annealing	55 ^{o}C	30 s
4	Extension	72 ^{o}C	1 min per kb
	Step 2-4 repeated for 30 cycles		
5	Final Extension	72 ^{o}C	3-10 min
6	Hold sample	4 ^{o}C	As required

3.2.6.3. Agarose gel electrophoresis

Agarose gel electrophoresis is a common method used for separating and identifying DNA based upon its size from the rate of movement through an agarose gel with an applied potential difference. PCR amplicons and restriction enzyme digests were routinely separated on a 1% (w/v) agarose gel for up to 1 h at 90 V (or until DNA species resolution was optimal). Agarose gels were prepared by heating a mixture of 1x TAE buffer and agarose (Sigma Ultra). Next Midori green DNA Stain was added to the gel mixture (2µl/100ml) and mixed gently. Subsequently, the mixture was cooled to 50 ^{O}C and poured into the gel tray. After resolution, DNA bands were cut from gels visualised using a UV transilluminator set with a long wavelength, 365 nm (UV-P, USA), to minimise damage (Fig. 4.2). Finally, DNA was extracted using the manufacturer's protocol for the Isolate II PCR and Gel kit (Bioline, A Meridian Life Science, UK). Extracted DNA was measured by NanoDrop and stored at -20 ^{o}C until use.

Table 3. 5. **PCR mixture for a typical 50 µl reaction volume.**

Reagent	Volume	Final concentration
BioMix Red (Bioline)	25 µl	2X reaction mix (stable Taq polymerase, buffer and loading dye)
Template DNA	1.5 µL	~2.5 ng template DNA
Primer Forward	1.5 µl	100 pmol μL^{-1}
Primer Reverse	1.5 µl	100 pmol μL^{-1}
ddH_2O	20.5 µl	Up to 50 µL
Accuzyme (BIOLINE)	1 µl	2.5 U μL^{-1}
Final 50 µL		

3.2.6.4. DNA quantification

DNA concentration was routinely quantified prior to each cloning step. A NanoDrop -1000 system (Thermo Fisher scientific, Germany) was used for measuring the DNA concentration and quality. The sample in ddH_2O was applied to the instrument pedestal and the absorbance was read at 260 nm.

3.2.6.5. Restriction enzyme digests.

All restriction enzymes (Table 3.6) were obtained from Thermo Scientific and DNA digests were achieved as recommended in the manufacturer's guidance (Thermo Scientific). In general, both insert and plasmid DNAs were digested in 50 µl reactions including 2-8 units of restriction enzyme per 1 µg of DNA, 5 µl of appropriate 10x buffer (dependent on the recommendation) and water up to 50 µl.

DNA digestion was performed for 1-2 h at 37^{o}C. For verification of the digest and gel extraction of desired DNA portions, 5x loading buffer was mixed with the digest mixture followed by separation with electrophoresis on 1% (w/v) agarose for 1 h (or as required for resolution) at 90 V. DNA was extracted from agarose as described above and stored at –20 ^{o}C until required.

3.2.6.6. DNA Ligation.

Ligation of digested insert and plasmid DNA fragments using T4 DNA ligase with ligase buffer was achieved as recommended using manufacturer's instructions (Thermo Scientific). Briefly, the reactions occurred in a 20 µl volume, including 1 µl of T4 DNA ligase (~3 Weiss units), 2 µl of 10x buffer, made up with dH_2O. Insert and plasmid DNA were quantified to establish the volumes required for fragment to vector ratios of 4:1. The DNA ligation reaction was incubated overnight at 4^{O}C before transforming *E. coli* TOP10 competent cells.

Table 3. 6. Features of restriction enzyme (RE) digests and cloning purpose.

DNA amplicons and RE sites for each gene:		**Antibiotic cassette and RE sites**	**Plasmid and RE sites**	**Cloning Purpose**
Genes: *a6qe26, a6qd62 pgd mcrA SA2061*		*tet* cassette: *Not*I & *Kpn*I	pMUTIN4: *Eco*RI & *Bam*HI	For creating gene mutants by allelic replacement
LA fragment	*EcoR*I & *Kpn*I			
RA fragment	*Not*I & *Bam*HI			
Genes: *a6qd62 & SA2061*			pSK5632: *Bgl*II & *Sal*I	For gene complementation in mutant strains and control in wild-type
Target gene with 200 bp upstream and 50 bp downstream	*Bgl*II & *Sal*I			
Genes: *a6qe26 pgd mcrA*			pSK5632: *BamH*I & *Hind*III	
Target gene with 200 bp upstream and 50 bp downstream	*BamH*I & *Hind*III			
Gene name: *a6qd62* **Gene name: *mcrA***		None	PET24d+ with: *Nde*I & *Xho*I	For target gene overexpression in *E. coli* BL21 (DE3)
Target gene excluding the 5' signal peptide and 3' stop codon sequence	*Nde*I & *Xho*I			
Gene name: *a6qe26* **Gene name: *pgd***			*Nco*I & *Xho*I	
Target gene excluding the 5' signal peptide and 3' stop codon sequence	*Nco*I & *Xho*I			

3.2.7. *E. coli* transformation

Chemically competent cells of *E. coli* were prepared using the Hanahan method (Hanahan *et al.*, 1991) For transformation, 5µl of a ligation was mixed with 100 µl of competent cells in a 2 ml Eppendorf tube and then incubated on wet ice for 30 min. Next, the cells were subjected to heat shock by transferring the tube from wet ice to a 37 ^{O}C water bath with incubation for 90 s; this facilitates internalisation of DNA. Afterwards the transformation was returned to wet ice for 3 min. Next, 900 µl of LB medium was added to the cells and incubated at 37 ^{O}C with shaking for 1 h. Subsequently, 50-100 µl of cells were spread onto LB plates containing the appropriate antibiotics and incubated at 37 ^{O}C overnight or up to 48 h. Empty vector was used as the control for transformations. Features of the relevant plasmids are presented in Table 3.7.

Table 3. 7. Plasmid features relevant to cloning strategies

Constructed plasmid	Purpose	Resistant gene
pMUTIN4	Suicide vector for allelic replacement of target genes. Replication proficient in *E. coli* (Vagner *et al.*, 1998).	*amp* for *E. coli* *erm* for *S. aureus* *tet* insert in mutant alleles
pSK5632	*E. coli/S. aureus* low copy number shuttle vector suitable for gene complementation studies in *S. aureus* (Grkovic *et al*., 2003).	*amp* for *E. coli* *cm* for *S. aureus*
pET24d+	Vector for protein overexpression studies in *E. coli*. T7 promoter and His-tag sequences	*kan* for *E. coli*

3.2.8. Clone selection strategies following transformation

Following transformation of competent cells of *E. coli* TOP10 the resulting colonies were cultured on selective agar plates. Around 20 colonies were selected from each transformation and isolated on selective plates containing appropriate antibiotics, as described above, and incubated at 37 ^{O}C overnight. Subsequently, 10 ml of fresh LB broth with any selective supplements was inoculated with a chosen colony and incubated at 37^{O}C for overnight. The recombinant plasmids were extracted from overnight cultures using Isolate II Plasmid Mini Kit (BioLine), as described previously, followed by screening to ensure correct cloning using the appropriate restriction enzymes with discrimination of inserts after gel electrophoresis as described above (Fig. 4.3. and 4.4). Verified transformant clones were stored with 15% glycerol at - 80^{o}C until use.

3.2.9. Preparation of *S. aureus* for transformation

Transformation of *S. aureus* RN4220 strains was performed as described previously (Schenk and Laddaga, 1992). Prior to transformation of *S. aureus* plasmids were concentrated by precipitation. Typically, 200 μL of DNA sample was mixed with an equal volume of isopropanol plus 20 μL of 3M sodium acetate (pH 5.2). The mixture was incubated at room temperature for 1 min and centrifuged for 20 min at 21200 rcf to pellet the DNA. The DNA was washed with 500 μL of 70 % (v/v) ethanol then centrifuged at 21200 rcf for 5 min. The DNA pellet was vacuum-dried at 40^{o}C for 5 min, followed by adding up to 50 μL of ddH_2O then stored at -20 ^{o}C.

3.2.9.1 Transformation of *S. aureus* by electroporation

Aliquots (200 μL) of RN4220 competent cells were mixed gently with 2 μL (200 ng/μl) of plasmid DNA in chilled electroporation cuvettes, 0.1 cm gap (Cell projects, UK) and kept on wet ice for 20 min. Competent cells alone served as a plasmid negative control. For transformation the cells/DNA mixture was mixed again gently and using an electroporator (Gene Pulser^{TM} ,Bio-Rad) it was pulsed with the following parameters: capacitance 25 μF, resistance 100 Ω and 1.6 kV.

Immediately following electroporation the mixtures were replaced on ice for 3 min and the contents transferred to a chilled 1.5 ml Eppendorf tubes containing 800 μl of recovery media (SOC) and incubated at 37^{o}C for 1 h. Cells were plated onto selective agar containing either tetracycline for cells transformed with constructs of pMUTIN4 or chloramphenicol for cells transformed with constructs of pSK5632, with incubation overnight at 37^{o}C. Selected and culture isolated colonies of RN4220 were tested by PCR using the primer pair F-M13 and R-M13 (Table 3. 3) to identify the presence of cloned inserts.

3.2.9.3. Phage transduction

Of the target genes *a6qe62, pgd, mcrA and SA2061* each were selected as their cognate integrated pMutin4 and/or pSK5632 constructs in RN4220. From this intermediate cloning strain, bacteriophage Ø11 lysates were prepared to transduce desired alleles to strains SH1000, Newman, SF8300 and BH1CC, using SH1000 Ø11 mediated genetic transduction. RN4220 donor strains were infected with ϕ11 to obtain high titre (~10^{10} pfu ml) phage lysates. These strains were cultured in LK

medium at 37^{O}C overnight. A mixture comprised of 5 ml LK broth (1% w/v tryptone, 0.5% w/v yeast and 0.7% w/v KCl), 5ml phage buffer (1mM MgSO4, 4mM CaCl2, 50mM Tris-HCl pH7.8, 5.9 g/L NaCl and 1 g/L gelatin) and 200 µl ϕ11 phage was mixed with 300 µl of donor culture and incubated at room temperature overnight until completely lysed. Next, lysates were filtered by using sterile syringe filters (0.22 µm MILLEX®GP) and stored at 4 ^{O}C.

For transduction of *S. aureus* SH1000, Newman, SF8300 or BH1CC strains (recipient strains) cells were infected with ϕ11 lysates of the RN4220 donor strains. Recipient strains were grown in 20 ml LK broth at 37 ^{O}C overnight then centrifuged at 1500 rcf for 10 min. The pellet was resuspended in 1 ml LK broth, then 500 µl of the recipient cell suspension was added to 1 ml LK with 10 mM $CaCl_2$ plus 500 µl of ϕ11 lysate then incubated stationary at 37^{O}C for 25 min followed by 15 min with shaking at 250 rpm. Afterwards, 1 ml ice-cold 0.02 M sodium citrate was added to the mixture and incubated on ice for 5 min prior to centrifuging again. Next, the pellet was resuspended in 1 ml of 0.02 M Na citrate and incubating on ice for 1 h. Finally, cell suspensions were plated onto LK plates containing 0.05 % w/v Na citrate and incubated for 1 h at 37C. Cells were then overlaid with top agar containing appropriate selective antibiotics and incubated for 24-48 h at 37 ^{o}C.
Clones were picked and cultured on selective agar prior to colonies being screened by PCR. Correct clones were stored at -80 ^{O}C with 15% v/v/ glycerol.

CHAPTER 4

4. Molecular investigation of gene function of S. aureus

4.1. Introduction

Generally, the principles that support using genetic manipulation to characterise gene function in pathogenic bacteria are best summarised by Stanley Falkow's molecular update of Koch's Postulates (Falkow, 1988). More precisely, genetic manipulation of target genes that encode putative virulence proteins is used to produce inactivated or modified alleles that can subsequently be examined for loss of contribution to virulence, either *in vitro* or preferably *in vivo*. With this approach, it is important to demonstrate that gene complementation restores the virulence back to near wild-type levels.

Early studies of bacteriophages revealed that certain bacterial strains presented resistance for phage infection but were infected by phage when either the titer was greatly raised (Rountree, 1956) or the recipient strains were previously heat-shocked. This indicated that the infection barrier system could be overwhelmed by transient inactivation (Asheshov and Jevons, 1963). The majority of *Staphylococcus aureus* isolates have an effective, robust barrier which hinders DNA exchange. In the laboratory, this can be seen to prevent the transformation of plasmid vectors into the bacterial cell because by virtue of this system called a restriction-modification barrier (RM). Consequently, genetic researchers have focused on the use certain lab

strains of transformable *S. aureus*, particularly the strain RN4220 (Baba *et al.*, 2008; O'Neill, 2010; Voyich *et al.*, 2005).

Three out of four known types of R-M system are known in staphylococci and recently described in detail (Monk and Foster, 2012). A type I R-M system (SauI) includes genes encoding a host specificity of DNA (*hsd*) component, a modification protein (HsdM), a specifity protein (HsdS) and a restriction endonuclease protein (HsdR). These gene products combine to form a complex of either $HsdSHsdM_2$ or $HsdSHsdM_2HsdR_2$. The $HsdSHsdM_2$ complex protects target DNA sequences from restriction by catalysing the transfer of a methyl from S-adenosylmethionine to adenine residues within the target DNA sequence, while the complex of $HsdSHsdM_2HsdR_2$ functions as a restriction endonuclease, which can recognise and cleave unmethylated target DNA sequence. The *S. aureus* RN4220 strain that was obtained by UV and chemical mutagenesis of strain NCTC8325-4 carries a nonsense mutation in the *hsdR* gene, making this strain deficient for restriction and an important intermediate cloning host for *S. aureus* strain construction (Nair *et al.*, 2011; Waldron and Lindsay, 2006).

Certain type II R-M systems are widely used by molecular biologists, with their restriction endonuclease enzymes making for effective reagents for recombinant studies. Type II R-M systems are used for digesting nucleic acid at specific sequences for cloning. The cleavage of the target DNA sequence can be prevented by the DNA methylation status. In *S. aureus*, Sau3AI was the first type II R-M system that was described in detail, but this system is uncommon in isolates of *S. aureus* (Stobberingh *et al.*, 1977; Waldron and Lindsay, 2006).

Type IV R-M systems are known to be the simplest form of restriction system, which includes a single protein with the ability to detect the methylation status in order to hinder uptake of foreign DNA (Corvaglia *et al.*, 2010; Kelleher and Raleigh, 1991). The *SauUSI* gene was classified as a type IV R-M system in the majority of *S. aureus*, and it requires dATP or ATP for endonuclease activity of foreign DNA (Xu *et al.*, 2011b). The motif recognised by *SauUSI* is identified by cytosine methylation. The *E. coli* strains widely used for cloning, such as TOP10 and DH10B are able to methylate both cytosine and adenine. Consequently the plasmid isolated from these *E.coli* strains can be readily degraded by *SauUSI* (Monk and Foster, 2012). In order to avoid this restriction barrier of type IV in *S. aureus*, the plasmid should be isolated from an *E. coli* strain that is defective in methylation of cytosine (Monk and Foster, 2012). Analysis of the *SauUSI* gene in RN4220 revealed a nonsense mutation in the middle of the sequence, making it able to modify foreign DNA but not restrict it (Monk *et al.*, 2012).

4.1.1. Heterologous expression of proteins

The T7-directed protein expression system is one of the most commonly used for the overexpression of target DNA in *E. coli* and derives from T7 bacteriophage replication life-cycle components. The utility of the expression system arises from the high degree of specificity that the phage T7 RNA polymerase has for cognate promoter sequences. The polymerase recognises only the T7 bacteriophage promoter sequences and not those of *E. coli*, leading to selective transcription of large amounts of RNA. The pET24d+ plasmid is one of a series plasmid vectors designed for gene cloning and protein overexpression from target DNA sequences when ligated

downstream from the T7 promoter (Studier *et al.*, 1990). The *E. coli* lysogen BL21 (λDE3) strain was originally developed as a host for expressing genes and was engineered with the *lacUV5* promoter providing IPTG-inducible expression of the polymerase (Studier *et al.*, 1990). The pET24d+ plasmid contains a T7 promoter located 5' of a multiple cloning site, and there is a T7*lac* promoter controlling LacI repressor expression to modulate the IPTG-dependent regulation. In addition, this plasmid has a C-terminal hexa-histidine tag, which facilitates purification of the target protein, and an N-terminal T7 tag. This plasmid has a kanamycin resistance gene for selection during growth. Two host *E. coli* B strains are commonly used for the expression: BL21 (λDE3) and BL21 (λDE3) pLysS. The latter strain contains pLysS vector which has a T7 lysozyme gene. This phage lysozyme is a natural life-cycle antagonist of T7 RNA polymerase and is used to decrease the basal level expression of protein that might be toxic to the host cell (Moffatt and Studier, 1988).

4.2 Chapter Aims

In the previous chapter five genes were analysed variously using bioinformatics methods to establish predicted functions (Table 3.1). The aim of this chapter was therefore to generate strains to enable functional studies of each of the target genes (*a6qe26*, *a6qd62, pgd, mcrA* and *SA2061* genes). As a basis to study gene functions the production of three strains was attempted: an allelic replacement mutant; a complementation strain, and a protein overexpression strain.

Firstly, creating the mutant strain was based on allelic replacement using a suicide vector that when resolved will disrupt the target gene on the chromosome with a selectable marker cassette.. Secondly, creation of the complementation strain was made using the low copy shuttle vector PSK5632 carrying the target gene for subsequent transformation of the respective gene mutant strain (additionally the plasmid would be used to transform the isogenic wild-type as a control strain). Finally, attempts would be made to create an *E. coli* protein overexpression strain with a plasmid carrying the target gene. These aim being that these strains would aid subsequent studies of target gene function.

4.3. Results and Discussion

Inactivation and complementation strain construction

4.3.1. Creation of gene mutant strains by allelic replacement.

The process of allelic replacement for mutagenesis used the suicide vector pMUTIN4 vector followed by transductional outcross as presented in (Fig. 4. 1). Allelic replacement of *a6qe26*, *a6qd62, pgd, mcrA* and *SA2061* genes was carried out by amplifying two 1 kb flanking regions to the left and right of the target using primers pairs F1/R1 and F2/R2 respectively. A tetracycline cassette gene was amplified in addition; all primers are listed in (Table 3.3). These three fragments were digested with specific restriction enzymes *Eco*RI/*Kpn*I, *Not*I/*Bam*HI and *Not*I/*Kpn*I, respectively. Subsequently, these digested fragments were co-ligated into pMUTIN4 vector digested with *Eco*RI and *Bam*HI. The resulting recombinant plasmid ligations for each target gene were used to transform *E. coli* TOP10. Identification of tetracycline-resistant colonies was followed by extracting the plasmids confirm the presence of desired fragments.

4.3.1.1. Screening and confirming successful transformants

Prospective correctly cloned plasmids were extracted and digested with various combinations of restriction enzymes. Each plasmid was digested with separate enzyme combinations to release four fragments as following: *Bam*HI/*Kpn*I (~2600 bp includes right flank plus *tet*), *Not*I/*Eco*RI (~2600 bp includes left flank plus *tet*), *Bam*HI/*Eco*R1 (~3600 bp includes both flanks plus *tet*) and *Not*I/*Kpn*I (~1600 bp,

tet) (Fig. 4. 3.). Identification of each fragment indicated that the production of the recombinant suicide allelic replacement constructs was achieved successfully.

4.3.1.2. Transformation and transduction of *S. aureus* strains

The constructed plasmids were precipitated prior to electroporation of *S. aureus* RN4220 strains. Colonies growing on the selective media with tetracycline were confirmed with acid formation on mannitol agar and PCR using forward and reverse M13 primers. Next, phage ϕ11 lysates of the clones were prepared and used to infect *S. aureus* strains Newman, SF8300, SH1000 and BH1CC. Correct allelic replacement via transduction outcross was achieved with selection for tetracycline-resistant, erythromycin-sensitive clones (Section 3.2.8). Despite several attempts the mutant of *a6qe24* failed due to problems with transduction of *S. aureus* but importantly, a paper was published that described the function of protein A6QE26 as FepA (Turlin *et al.*, 2013), and involved in heme iron utilisation as predicted by bioinformatics methods in this study. Work on this gene was discontinued. Correct allelic replacements of the *a6qd62, pgd, mcrA and sa2061* genes were confirmed by PCR using the external primer pair (Table 3. 3.).

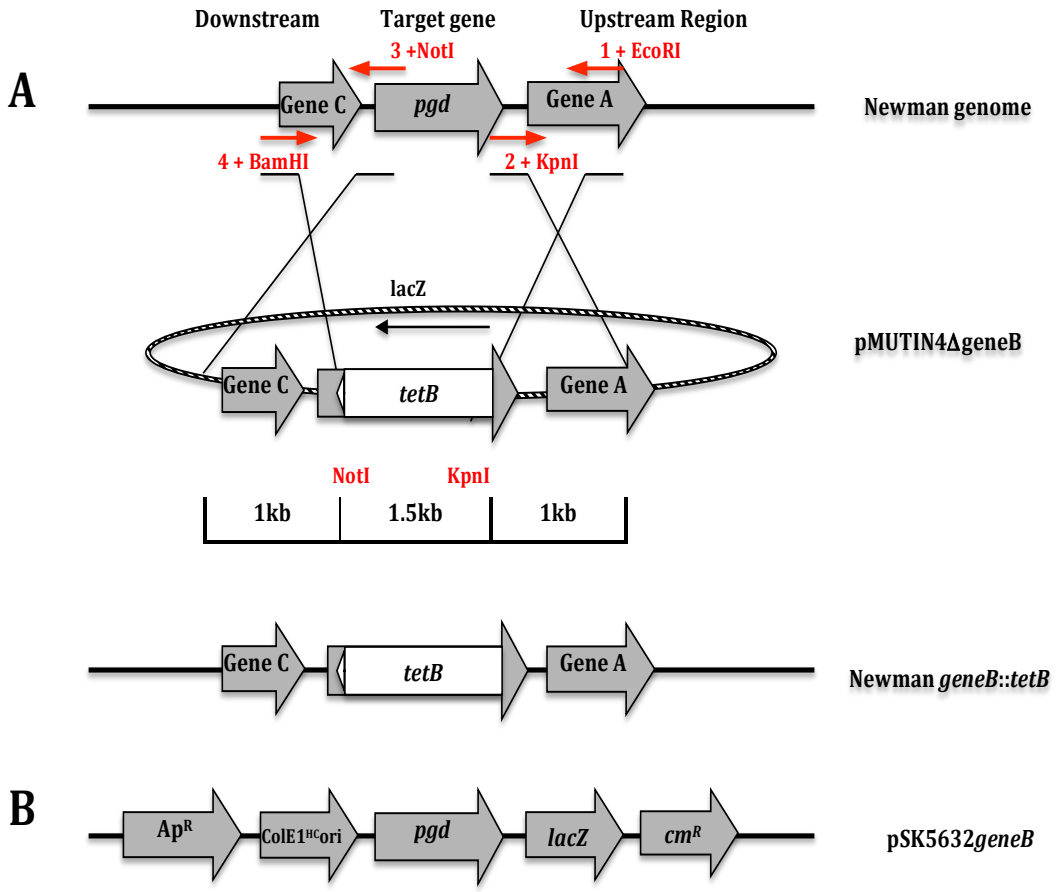

Fig. 4.1. Schematic of allelic replacement construction in *S. aureus*. (A) Allelic replacement of *pgd* gene in the genome of *S. aureus* using the suicide plasmid pMutin4 by homologous recombination of the cloned *pgd* gene regions where the *tetB* cassette replaces *pgd*. The left-hand flanking region upstream of *pgd* was amplified by primer 1 with an *Eco*RI sequence and primer 2 with *Kpn*I (red arrows), while the right-hand region downstream was amplified with primers 3 and 4 bearing a *Not*I and BamHI site respectively (red arrows). In the isogenic mutant *pgd*::*tetB,* the *tetB* contains its own promoter and is in the opposite orientation to *pgd* in wild type. (B) The map of the complementation vector PJAL (pSK5632-*pgd*). Only relevant part of the complementation vector pJAL is shown. The *pgd* gene with its translational signal sequence was cloned into the multiple cloning sitee of pSK5632 by using *Bgl*II and *Hind*III restriction sequences.

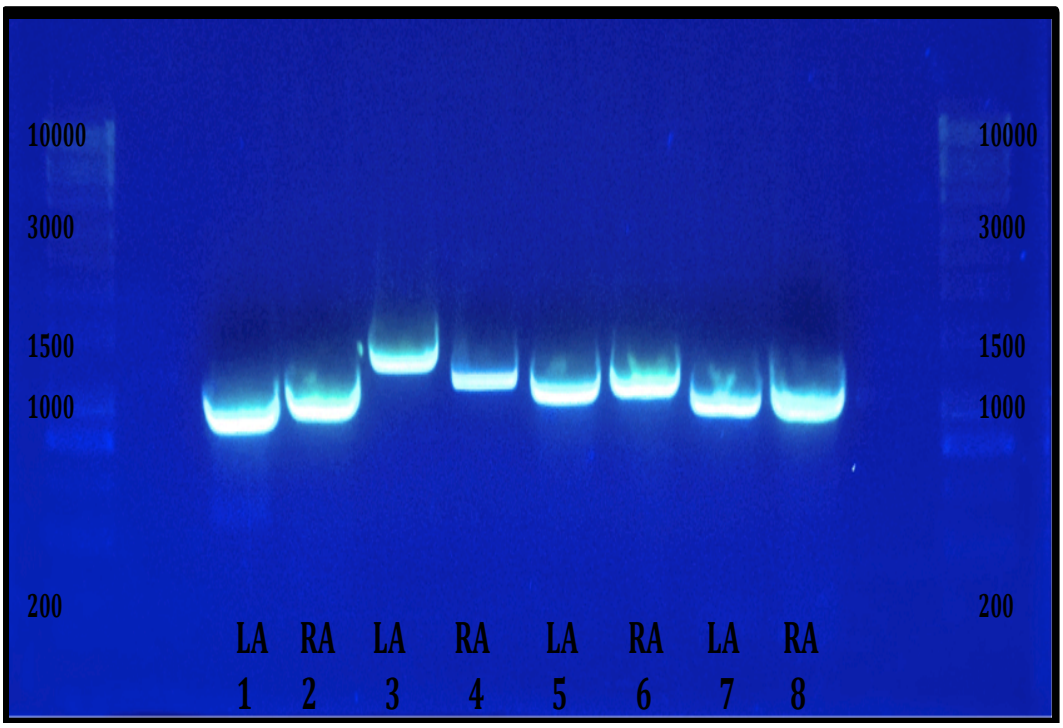

Fig. 4.2. PCR-amplified flanking sequence and *tet* cassette of gene mutants from mutant construction confirmation. Lanes 1,2: left (LA) and right (RA) sequences of *a6qe26* gene plus *tet* (~1000 bp and 1100 bp); Lanes 3,4: LHS and RHS flanking fragments of *a6qd62* gene plus *tet* (~1400 bp and 1200 bp); Lanes 5,6: left and right fragments of *pgd* gene plus *tet* (~1100 bp and 1200 bp) and lanes 7,8: left and right fragments of *mcrA* gene plus *tet* (~1000 bp) and 1000 bp). A DNA size marker is shown for reference.

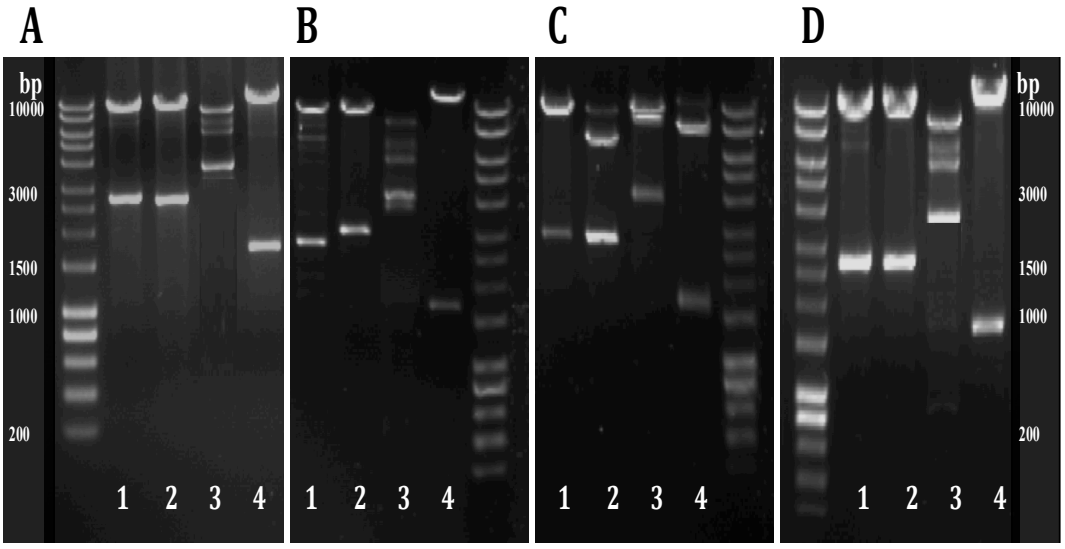

Fig. 4.3. Restriction digest analysis of allelic replacement construct plasmids. Purified pMUTIN4 vector constructs from transformants were digested to produce three fragments; RHS, *tet* and LHS. and separated by gel electrophoresis alongside a DNA size ladder. The corresponding digest fragments belonging to *a6qe26* gene (A), *a6qd62* (B), *pgd* gene (C) and *mcrA* gene (D). Restriction enzymes fragments of expected sizes as follows; Lane 1: *Bam*HI/*Kpn*I (RHS plus *tet*), (2) *Not*I/*Eco*RI (LHS plus *tet*), (3) *Bam*HI/*Eco*R1 (RHS plus *tet*) and (4) *Not*I/*Kpn*I LHS plus *tet*).

4.3.2. Construction of pSK5632 complementation plasmids

The low-copy number vector pSK5632 was used for complementation analysis, into which a copy of each target gene was cloned. The full length of each target gene (*a6qe26, a6qd62, pdg and mcrA*) plus a 200-bp sequence upstream and 50-bp downstream of the open frame was amplified using forward and reverse primers designed for each gene (Table 3.3). Next, the PCR fragment of each gene (*a6qe26,pgd and mcrA*) was digested and cloned as a *Bam*HI/*Hind*III fragment into pSK5632, while the fragments of *a6qd62* and *SA2061* genes were cloned after

*Bgl*II/*Sal*I digest. After *E. coli* transformation with ligations, colonies were grown on selective agar plate with ampicillin. Clones were selected and extracted plasmids were confirmed by enzyme digestion (Fig. 4.4.). The five resulting constructs produced were: pE26, pD62, pJAL-*pgd*, pMcrA, and pSA respectively. These correctly cloned complementation vectors, plus pSK5632 as a control, were used to transform *S. aureus* RN4220 then transduced using phage ϕ11 into strains Newman, SF8300, SH1000 and BH1CC.

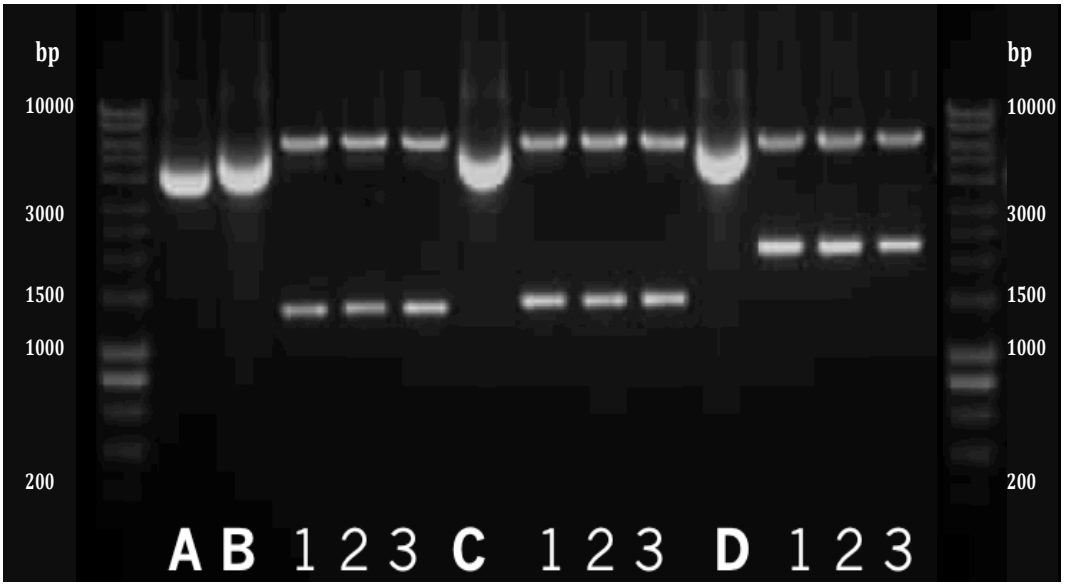

Fig. 4.4. Confirmatory restriction digestion analysis of pSK5632 plasmids bearing cloned fragments. Lanes (A), pSK5632 (undigested control); (B) *a6qe26* gene fragments: (C) *pgd* gene fragments; (D) *mcrA* gene *fragments.* The upper band represents plasmid with the insert gene below. Three constructed plasmids were digested for each transformants and indicated as (1, 2 & 3). The size of the *Bam*HI and *Hind*III cloned inserts are: *a6qe26*, 1162bp, *pgd*, 1384bp and *mcrA*, 2062bp.

4.3.3. Pgd Overexpression

4.3.3.1. Preparation of competent expression host cells

The host strains, *E. coli* BL21 (λDE3) and BL21 (λDE3) pLysS were made chemically-competent by using $CaCl_2$ standard treatment methods (Park and Batt, 2004). A single colony of each strain was cultured in 10 ml Luria-Bertani (LB) without antibiotic for *E. coli* BL21 (λDE3) or with 25 μg ml^{-1} chloramphenicol for BL21(λDE3) pLysS, and incubated at $37^{O}C$ overnight. Next, 2ml of culture was transferred into 200 ml fresh LB in a l l flask and cells grown at 37°C with shaking (250 rpm) until OD_{600} reached around 0.5 (~ 3 h). Subsequently, the culture was transferred into centrifuge tubes and chilled on wet ice for 20 min. After, the tubes were centrifuged at 3000 g for 10 min at $4^{O}C$, followed by discarding the supernatants prior to cell suspension in 100 mL of cold 0.1 M $CaCl_2$. The cells were then transferred into 50 ml polypropylene falcon tubes and incubated on wet ice for 30 min followed by repeat centrifugation. Next, the supernatants were discarded and cells resuspended gently in 4 mL cold 0.1M $CaCl_2$ contained 15% (v/v) glycerol. Finally, 200 μL cells were transferred into 1.5 mL Eppendorf tubes and the aliquots were stored at -80 ^{O}C until use.

4.3.3.2. Cloning of *S. aureus pgd* in pET24d+ expression plasmid

The plasmid pET24d+ was purified from *E. coli* (Table 3.2) using an Isolate II Plasmid Mini Kit (BioLine) (Section 3.8.). For gene amplification, the *pgd* specific forward (F) and reverse (R) primer sequences (Table 3.3) were designed by incorporating a *Nco*I restriction site (CCATGG) at the 5' end of the forward primer (F) and *Xho*I restriction site (CTCGAG) at the 5' end of the reverse primer (R) that

excluded the stop codon sequence from the 3' end of *pgd*. The gene was PCR-amplified in triplicate reactions from the genome of *S. aureus* Newman with these primers. This multiple amplification was done to limit subsequent cloning of *pgd* sequences containing PCR enzyme fidelity errors and thereby ensure at least one correct gene sequence for overexpression analysis. The three amplicons of the *pgd* gene were labelled as *pgd*PCR1, *pgd*PCR2 and *pgd*PCR3 and were cloned into vector pET24d+ at the multi-cloning site. For this, the purified DNAs, *pgd*PCR1, *pgd*PCR2 and *pgd*PCR3 and pET24d+ plasmid, were restriction digested with *Nco*I and *Xho*I as described previously (Section 3.2.6.5) and purified prior to their ligation as described previously (Section 3.2.6.6). The recombinant *pgd* plasmids created this cloning were named pJAMAL1, pJAMAL2 and pJAMAL3 (Table 3.2) for the three *pgd* amplicons from distinct PCR reactions, respectively.

4.3.3.3. Transformation of *E. coli* Top10 with pET24d+ ligations

Transformation of *E. coli* Top10 was achieved using the Hanahan method (Section 3.14) and colonies were grown on selective agar plates containing kanamycin. From the transformation plates, single colonies (5-12) were selected from each of the three independent ligation sets and transferred to fresh agar plates for subsequent analysis. The recombinant plasmids were isolated using the Isolate II Plasmid Mini Kit (BioLine) (Section 3.8.) and colony PCR was performed using forward (F) and reverse (R) primers for the overexpression PCR of *pgd* (Table 3. 2.) The presence of inserts was determined by separation of PCR products on 1% (w/v) agarose gels.

4.3.3.4. Analysis of plasmid clones by restriction enzyme digestion

For confirmation of DNA cloning, the extracted recombinant plasmids were digested with *Nco*I and *Xho*I restriction enzymes under the same conditions described above. The presence of both the 5.3 kb plasmid and ~1.1 kb *pgd* insert was confirmed for multiple clones (Fig. 4.5) indicating there was correct cloning.

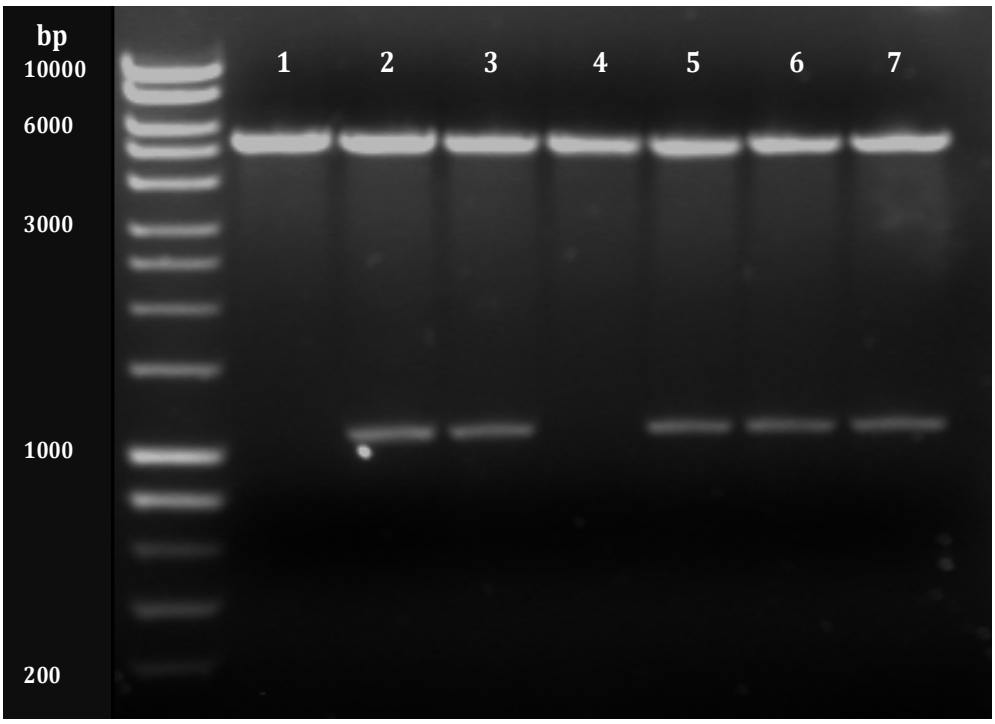

Fig. 4.5. Plasmid digestion of *pgd* clones in pET24d+. Double digestion of purified plasmids using *Nco*I and *Xho*I of clones from *pgd*PCR2 (lanes 1 to 3) and *pgd*PCR3 (lanes 4 to 7), indicating pET 24d(+) (~ 5300bp) and inserts (~ 1124bp).

4.3.3.5. DNA sequencing to confirm correct amplification

To verify that the cloned insert *pgd* sequences matched the original sequence of the *pgd* gene from *S. aureus* Newman, two constructed plasmids: pJAMAL2 and pJAMAL3 bearing *pgd*PCR2 and *pgd*PCR3 PCR products were sequenced. The plasmids were extracted, as described above, and sent for sequence determination by

GATC Biotech (Germany); specifically, 20 µl (~50ng) of each plasmid was sequenced with specific forward (F of *pgd;* (Table 3. 3.) and the plasmid-specific T7 reverse primers (M13). Analysis of sequence data indicated that the cloned *pgd*PCR2 sequence contained three errors resulting in three different amino acids. In contrast, the *pgd*PCR3 sequence was identical to the original *S. aureus* Newman *pgd* sequence (Fig. 4A); Appendix). Thus, pJAMAL3 plasmid has correct *pgd* sequence and was used for expression studies with pJAMAL2 plasmid included only as a comparator.

4.3.3.6. Transformation and overexpression of Pgd

With the aim of testing Pgd protein expression from the cloned gene copies, the *pgd* containing pET24d+ plasmids pJAMAL2 and pJAMAL3 were introduced into expression host strains. Transformation of *E. coli* BL21 (λDE3) and BL21 (λDE3) pLysS strains (Section 4.3.3.) was performed with the transformants used immediately for expression analysis, as described below.

A single colony from each of the transformation plates was used to inoculate 10 mL LB containing 10 µg ml^{-1} kanamycin. Cultures were grown overnight at 37°C with shaking at 225 rpm. Next, 1 mL of overnight culture was transferred into 50 mL LB in a 250 mL flask containing 50 µg ml^{-1} kanamycin, and incubated with the same conditions. Once the OD_{600} of cultures reached ~0.5, protein expression was induced by adding isopropyl- β-D-1-thiogalactopyranoside (filter-sterilised) to a final concentration of 1 mM, and the cells were grown for 3 h at 37°C with shaking at 225 rpm. Subsequently, cells were collected by centrifugation at 1500 rcf for 10 min at 4°C and used immediately or stored briefly at -20°C.

4.3.3.7. Optimisation of Pgd induction

For the optimisation of Pgd induction duration, the cells were grown, as described above, until the OD_{600} of cultures reached ~0.5 when the target protein was induced by the addition of 1 mM ITPG as final concentration. At defined time points (0, 1, 2, 3 and 4 h), samples were taken from cultures and measured their OD600. SDS sample buffer was used for disrupting cells and solubilising proteins at 80°C for 5 min. Proteins were separated by SDS-PAGE and the total cell proteins of each sample were compared with controls of both *E. coli* BL21 (λDE3) cells and *E. coli* BL21(λDE3) cells transformed with plasmid pET24d(+) to examine the effectiveness of overexpression conditions.

The Pgd target protein was clearly expressed after 2 h post-induction, but in only certain clones. From three independent experiments, it was evident that both clones tested that were transformed with pJAMAL3 plasmid did not express Pgd protein, whereas, the strains with pJAMAL2 expressed the target Pgd (Fig. 4.7.), with a protein band migrating to ~43 kDa (Fig. 4.8.). From these experiments and the sequencing it appeared that the *pgd*PCR3 gene copy, that has the correct sequence, might not be expressed due to toxicity to *E. coli*.

4.3.3.8. Purification of Pgd using His-Trap FF columns

Although the expressed Pgd protein did not have the correct primary sequence due to PCR errors, it was nonetheless expressed and purified for potential production of antibodies targeting the protein in future studies.

4.3.3.8.1. Cell lysis

The bacterial cells from induction with IPTG were lysed using sonication. First, the cells were resuspended in 10 mL lysis buffer per 500 ml of culture and incubated on wet-ice for 30 min. Next, the cells were sonicated 6 times with 10 s pulses at 200 W to disrupt the cells completely and samples of cell lysates from both the overexpression strain and control *E. coli* BL21 (lDE3) with empty vector were separated by 10 % SDS-PAGE and compared.

4.3.3.8.2. Purification of Pgd protein

Pgd protein was purified by two different methods, manually using Mastereflex Pumps and/or AKTA pure chromatography systems (Fig. 4. 6-8). In both methods, 1ml HisTrap FF columns (GE healthcare Life Sciences) were used. First, cells were lysed as mentioned above and subsequently the cells suspension (lysed) was centrifuged at 15900 rcf for 30 min at $4^{O}C$ and the supernatant or soluble protein was used. The target protein pgd was captured on 1 ml HisTrap FF columns (GE healthcare Life Sciences) and eluted with a linear gradient imidazole to determine the best concentration of imidazole. First, the HisTrap column was washed with 5 ml dH_2O to remove all 20% (v/v) ethanol, followed by two washes with 5 ml lysis buffer in 10 mM imidazole pH 8.0. Next, 10 mL of the supernatant lysate was added into the column to bind a target protein to the column and the unbound proteins were collected in the tube as washes. With the manual pump, the column was washed with 5 mL of increasing concentrations of imidazole (a stepped gradient of imidazole starting from 20, then 30, 50 and 60 mM imidazole PH 8.0) and followed by washing

with 5mL elution buffer (250 mM imidazole pH 8.0). Each wash was collected and the samples were tested by SDS-PAGE (Fig. 4.7).

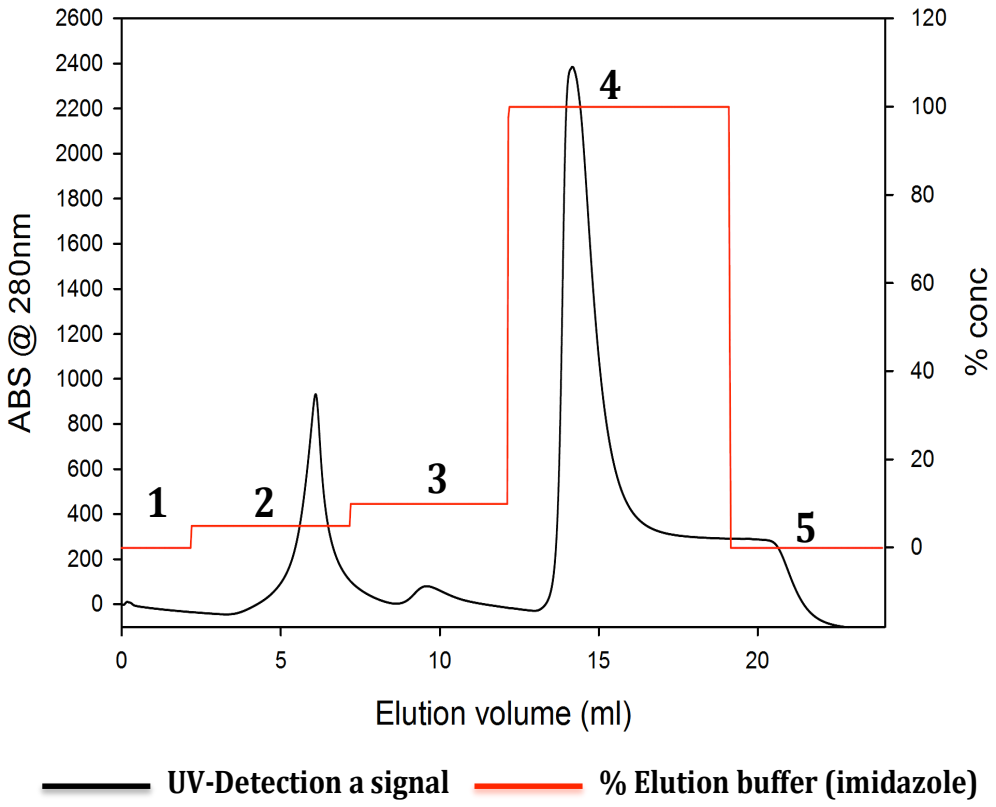

Fig. 4.6. Chromatogram of Pgd purification using the AKTA system. The different steps of the purification are indicated; (1) equilibration, (2) loading of sample, (3) washing column with imidazole, (4) elution of protein and (5) re-generation. 100 mM Imidazole, pH 8 was used as 100% eluting solution.

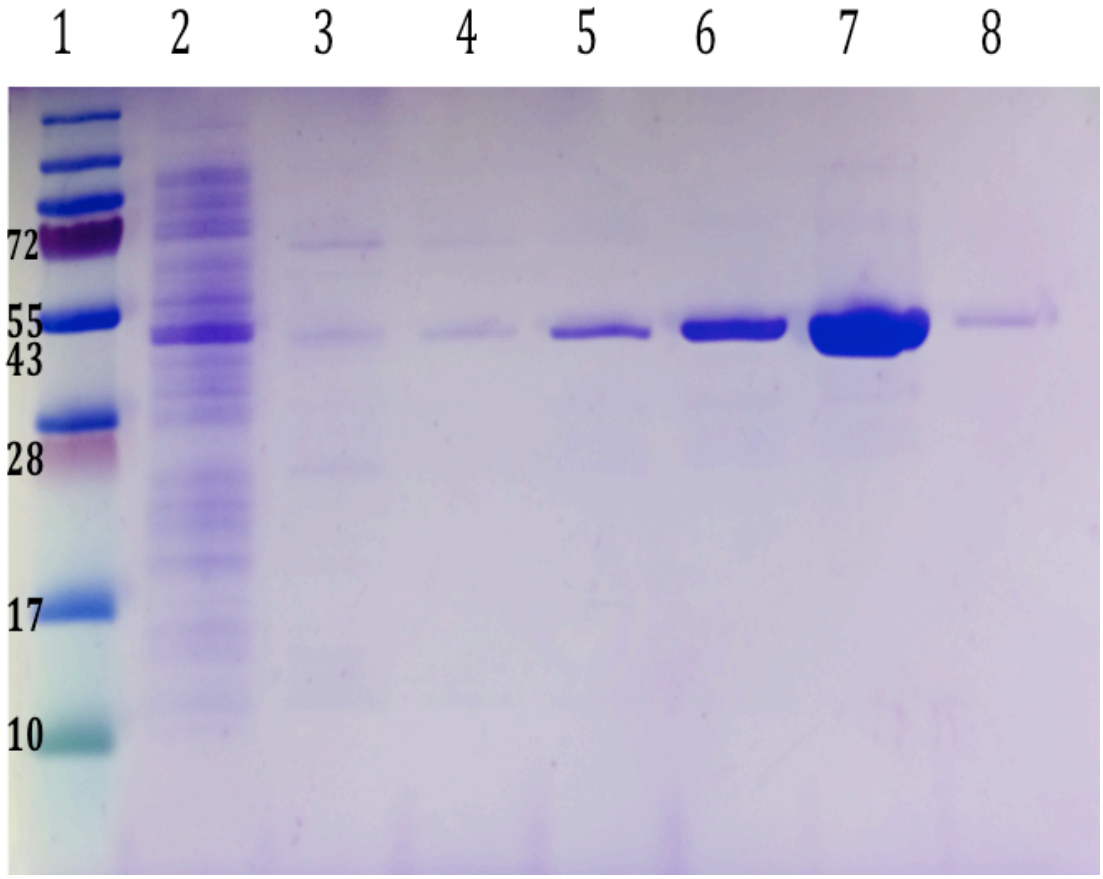

Fig. 4.7. 10% SDS PAGE of Pgd purification from *E. coli* BL21(DE3) pJAMAL2. Lanes: (1) Molecular weight marker (Fermentas), (2) cell lysate, (3) flow through, (4-8) column washes from a linear gradient of imidazole buffer starting from 20, 30, 50, 60 and 250 mM imidazole pH 8.0, respectively.

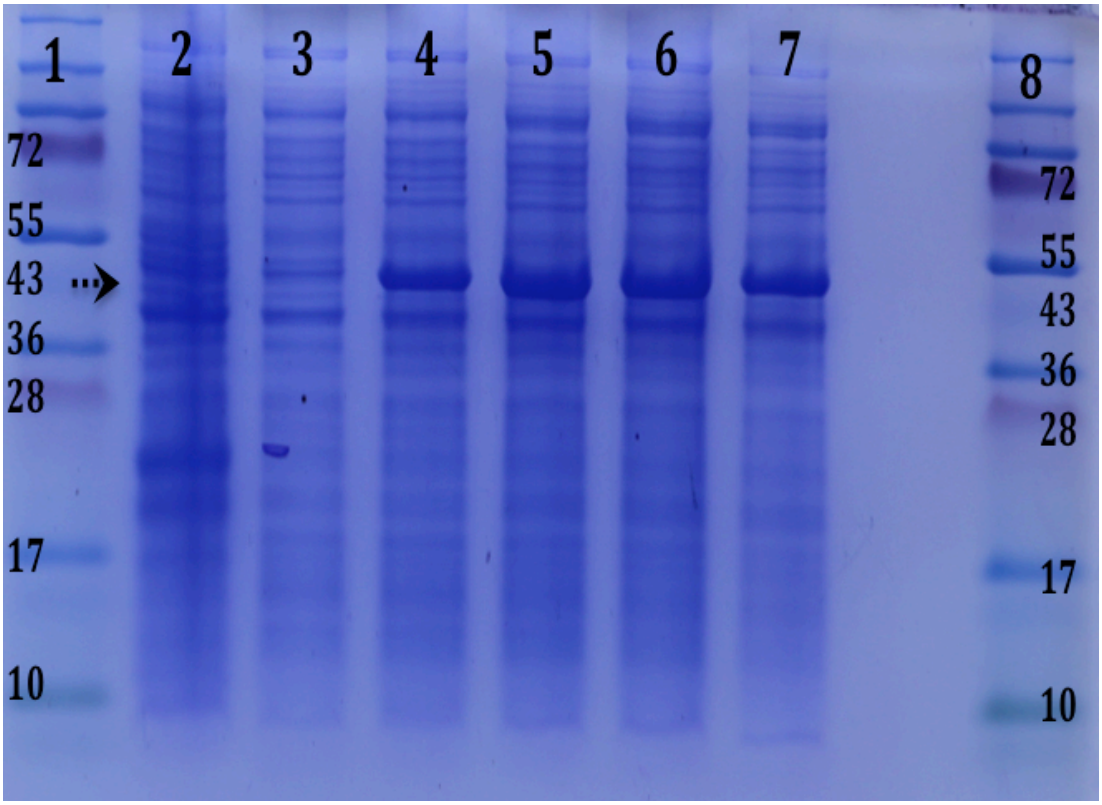

Fig. 4.8. SDS electrophoresis of Pgd protein expressed from pJAMAL2. The total cell proteins of strains are as follows: *E. coli* BL21 (λDE3) strain without pET24d^{+} as control (lane 2), or with pET 24d $^{+}$ with no insert as control (lane 3), or bearing pJAMAL2 (lanes 4 to 7), Lanes 4-7 represent samples after 1,2,3 and 4 h of induction with IPTG, respectively. Arrow indicates the location of the expressed Pgd protein. The size of Pgd protein is 43 KDa. Lane 1 and 8, Molecular weight marker kDa (Fermentas).

4.3.3.9. Protein toxicity assay

In order to assess whether the *pgd*PCR3 clone from pJAMAL3transformation, representing the correct *pgd* gene sequence, is cytotoxic to host *E. coli* BL21(λDE3), a previously described protocol was used (pET System Manual for toxicity assay -

8th ed, 1999, Novagen). The toxicity assay consists of plating the bacterial cells transformed with either constructed plasmid, pJAMAL2 or pJAMAL3, LB plates in the absence or presence of 1 mM IPTG and kanamycin, with LB plates with or without kanamycin serving as plating controls.

Based upon this protocol, it is expected that most cells can form colonies on LB-plates without supplementation. Toxic proteins will result in more than 2% colonies on plates containing 1mM IPTG and more than 0.01% on plates containing both kanamycin and IPTG. Toxicity of a target protein can cause the accumulation of cells in the culture, which no longer maintain or expression. This is because of the likely for loss of constructed plasmid in culture immediately before induction as described by manufacture of pET plasmid (pET System Manual for toxicity assay - 8th ed, 1999, Novagen). The experiment using the described protocol (Table 4.1) revealed that *E. coli* BL21 (λDE3) pJAMAL2 plated at 5% forming colonies on kanamycin plus IPTG or IPTG alone. In contrast, the pJAMAL3 bearing clone formed nil or ~0.1% colonies, respectively. From these results there is confirmation that Pgd is possibly cytotoxic via this expression system at the levels achieved in *E. coli* BL21 (λDE3).

Therefore, this study so far suggests that the *pgd* gene was not expressed because this gene encodes an enzyme activity that may be toxic to *E. coli.* The proposed peptidoglycan deacetylase function might interfere with the pathways of GlcNAc metabolism inside the cell and limit proliferation of the host cell causing growth limitations and a lower capability to form colonies (Rosano and Ceccarelli, 2014). For future work, this gene needs to be cloned into different plasmids and expressed

in different bacteria to obtain the result, which can confirm or reject the result of this study.

Table 4. 1. Plasmid stability-toxicity assay

E. coli BL21(λDE3) with plasmid:	**Colonies (%) on LB**	**Colonies (%) on LB, Km,**	**Colonies (%) on IPTG**	**Colonies (%) on Km, IPTG**
pJAMAL3	3014 (100%)	2838 (44%)	3 (0.09%)	Zero (0%)
pJAMAL3	1698 (100%)	760 (46%)	2 (0.11%)	Zero (0%)
pJAMAL2	3308 (100%)	2747 (83%)	160 (5%)	158 (5%)
pJAMAL2	1588 (100%)	660 (41%)	130 (8%)	106 (7%)

Experiments were performed in triplicate and the average is indicated for each strain.

Summary.

To conclude this chapter, the correct cloning of vector constructs for the genetic study of the *pgd, mcrA* and *a6qe26* genes was achieved by producing allelic replacement, complementation and overexpression constructs. However, only Pgd expression was achieved in this study and it was revealed that the T7 overexpression system was not optimal for production of the protein due to cytotoxicity, however a gene mutant, PCR2 *pgd* (pJAMAL2), that was inadvertently produced during amplification was overexpressed and could be used for future antibody production.

CHAPTER 5

5. Physiological analysis of *Staphylococcus aureus* mutants.

5. 1. Introduction

Bacterial lipoproteins are secreted and localised to the cell wall during exponential growth phase. These lipoproteins can play critical physiological roles at the cell surface, such as transport, ligand binding, resistance to antimicrobials, signaling and protein folding (Hutchings *et al.*, 2009; Sutcliffe and Russell, 1995). Roles have also been described in virulence including host invasion, immunomodulation and adhesion (Kovacs-Simon *et al.*, 2011; Nakayama *et al.*, 2012). *S. aureus* has the capability to adhere and colonise different synthetic materials by forming a biofilm. These structures are important in the lifestyle of bacterial communities and develop from a coordinated sequence of events, including initial attachment, microcolony formation, maturation and detachment. The formation of biofilm provides significant protection from host defences and antibiotics during colonisation and pathogenesis. Most commonly, *S. aureus* infections that are described as biofilm-associated include nosocomial infections arising from medical devices, such as heart valves, bone prostheses, or implanted catheters (Otto, 2013).

Peptidoglycan (PG) has key roles in bacterial growth, morphogenesis and separation, pathogenesis, interaction with the environment, biofilm formation and homeostasis (Sharif *et al.*, 2009; Typas *et al.*, 2012). Modification of the PG structure is important for its biosynthesis, maintenance and degradation and this is controlled by different sets of secreted enzymes, which are tethered or ionically attached to the PG. For

example, peptidoglycan deacetylases (Pgd) of *Listeria monocytogenes* and *Streptococcus pneumoniae,* which belong to the carbohydrate esterase family 4 enzymes (CE4), can modify peptidoglycan (PG) by removing *N*-acetyl groups from *N*-acetylglucosamine. This role is known to contribute to the bacterial defence from human and animal mucosal lysozyme (Blair *et al.*, 2005a; Popowska *et al.*, 2009).

This study identified that Pgd of *S. aureus* is a lipoprotein that harbours a catalytic domain that is predicted to function as a de-*N*-acetylase of *N*-acetylglucosamine or another acetyl group in peptidoglycan, similar to function of the homologous Pgd protein of *Streptococcus pneumoniae*. The research described in this chapter therefore aimed at examining *S. aureus pgd* mutants through a range of different assays to identify phenotypic differences compared with their parent strains.

5.2. Materials and Methods

5.2.1. Bacterial strains and their culture

For the study of Pgd function, the allelic replacement *pgd* mutation was transduced to a set of *S. aureus* host strains. The use of a single *S. aureus* strain to study the species is increasingly discredited, due to the possibility of revealing only strain-specific effects. Consequently, this study generated *pgd* mutants with complemented variants of the strains Newman, SF8300, SH1000, BH1CC and SA113. Some of these choices were also a consequence of the phenotypes observed for the mutation, where greater clarity of the observed phenotype was needed. For example, in addition to Newman *pgd*, SF8300 *pgd,* SH1000 *pgd,* BH1CC *pgd* and SA113 *pgd,* an *oat*A (MurNAc O-acetyl transferase) mutant was combined with the *pgd* mutation to

observe the phenotype of single compared with double mutants for the study of lysozyme resistance and biofilm formation. The full details of strains are listed in Table 3.1 and 3.2.

The genotypes of mutant strains after transduction were confirmed by PCR, with sequencing where necessary, as discussed in Chapter 3. Briefly, DNA was released from bacteria using lysis buffer and purified with a DNeasy Blood & Tissue kit (QIAGEN). Extracted DNA was used as template for PCR using primers specific to the downstream and upstream regions of the gene of interest (Table 3.3; 3.4: 3.5). Transduction of mutant alleles was confirmed after separating the PCR products with 1% (w/v) agarose gels to reveal that the size of the amplified insert matched the expected size for the modified allele.

Antibiotic resistance testing was also used to confirm the selectable phenotype of the marked allele moved by transduction. Plates were prepared with appropriate antibiotic concentrations and a single colony was inoculated and incubated overnight at 37 ^{O}C as described in Chapter 3.

5.2.2. Cell growth curve

Phenotypes of isogenic strain sets of *S. aureus* Newman, SH1000, SF8300, and BH1CC, comprising: wild-type; *pgd* mutant; wild-type plus pJAL-*pgd*; and *pgd* mutant plus pJAL-*pgd*, were compared by culture in defined conditions. Growth curves of each strain were determined with culture in 50 mL BHI broth, either alone or supplemented with sterile filtered 1% (w/v) glucose. Culture was performed in 250 mL conical flasks with triplicate assays and inoculation was performed using

overnight cultures (section 5.2.1) adjusted to OD_{600}=0.05 as the starting value. Cultures were incubated at 37 ^{O}C in a water bath with shaking at 250 rpm and the turbidity was measured hourly at OD_{600} nm.

5.2.3. Staphyloxanthin pigment assay

S. aureus strains were assayed for their production of the carotenoid pigment staphyloxanthin using a modified protocol from a previous study (Liu *et al.*, 2005). Overnight culture was used to inoculate 10 mL BHI broth in sterile 50 mL centrifuge tubes (Fisher Scientific) to OD_{600}=0.05. Cells were incubated to allow aeration at 37 ^{O}C with shaking at 250 rpm for 24 h. Next, cells were harvested by centrifugation at 1500 rcf for 10 min then washed twice with 1x PBS (pH 7.2). The cell pellet was suspended with 1 mL of 100% (v/v) methanol and mixed thoroughly before incubating stationary at 37^{O}C for 2 h. Subsequently, the mixture was centrifuged at 15900 rcf for 5 min and 200 µL of supernatant was transferred in triplicate into a polystyrene 96-well plate for measuring the absorbance spectrum between 350-550 nm using a FLUOstar Omega plate reader.

5.2.4. Hydrophobicity assay

The microbial adherence to hydrocarbon (MATH) assay was used to determine the relative ability of *S. aureus* strains to adhere to the surface of hexadecane. Hexadecane (Sigma) was stored in the dark at 25 ^{O}C until use and a previously described experimental protocol was modified for the assay (Beck *et al.*, 1988). A single *S. aureus* colony was inoculated into 10 mL BHI broth in a 50 mL falcon tube and incubated overnight at 37^{O}C with shaking at 250 rpm (section: 5.2.2.). The

overnight culture was then sub-cultured into 50 mL BHI broth to inoculate at OD_{600} of 0.05; cultures were incubated overnight at 37^{O}C with shaking at 250 rpm. After growth, the cells were harvested by centrifugation at 15900 rcf for 10 min and washed twice with PBS buffer, pH 7.2. Next, cells were suspended in PBS buffer (pH 7.2) and the OD_{450} of each sample was adjusted to between 0.9-1.0 (initial reading). A 3 mL portion of each cell suspension sample was transferred into 15 mL Falcon conical tubes (Sigma) and 300 µL of hexadecane was added. The mixture was vortexed for 2 min and then left at RT for phases to separate for exactly 2 min. Subsequently, the lower aqueous phase was collected and the turbidity was measured at OD_{450} (final reading). The difference between the turbidity of the initial and final readings was taken as a measure of cell hydrophobicity and calculated as a percentage. This experiment was repeated at least 3 times.

5.2.5. Autolysis assays

Autolysis rates were investigated after challenge with penicillin-G and triton X-100 (Sigma) as alternative inducers of autolysis. The protocol was modified from previous studies (Bose *et al.*, 2012; Ingavale *et al.*, 2003). Separate assays were performed with *S. aureus* strains Newman, SF8300, SH1000 and BHICC, including their isogenic *pgd* mutants, and plasmid complemented variants (section: 5.2.2.). An *atl* insertional inactivation strain served as an autolysis control with it having greatly reduced autolysis. Overnight cultures (section: 5.2.2.) were used to inoculate 50 ml TSB broth in a 250 mL flask to an OD_{600} of 0.05 for each strain. Cultures were incubated in a water bath at 37^{O}C with shaking at 250 rpm until cell OD_{600} reached ~0.5. Next, cells were harvested by centrifugation at 1500 rcf for 10 min, then washed with 10 ml sterile PBS (pH 7.2). Subsequently, cells were suspended in 50

mL sterile PBS, pH 7.2 containing either 0.1 mg ml^{-1} penicillin G (Sigma) or 0.1% (v/v) triton X-100 (Sigma) then incubated at 37 ^{O}C with shaking at 250 rpm. Lysis of cells was monitored by measuring half-hourly the OD_{600} turbidity changes.

5.2.6. Lysozyme survival assays.

5.2.6.1. Lysozyme disc diffusion assay

S. aureus strains were grown overnight in tryptic soy broth (TSB, LAB M) at 37^{O}C with shaking at 250 rpm, including selective concentrations of antibiotic as appropriate (Table 3.2). These cultures were diluted in molten soft TSB agar at 50 ^{O}C to final OD_{600} 0.05 and immediately poured onto TSA plates. After 10-15 min, a sterile 6 mm paper disc prepared with 20 mg mL^{-1} lysozyme (hen egg-white, Sigma) was placed gently on the agar surface; all plates were incubated at 37^{O}C overnight.

5.2.6.2. Cell lysis after lysozyme challenge

S. aureus strains were cultured in TSB overnight, as described above, then this was used to inoculate 50 mL TSB cells for around 5 h growth (until end of exponential phase) at 37^{O}C with shaking. This was followed by adding sterile lysozyme to a final concentration of 30 mg mL^{-1} and measuring optical density hourly at OD_{600} to monitor cell lysis.

5.2.7. Biofilm formation assays.

A range of diverse assays were used within this study to evaluate biofilm formation and development over time in BHI broth, with or without added 1% (w/v) glucose or

4% (w/v) NaCl. Various types and brands of polystyrene plates were tested to monitor biofilm formation, mostly polystyrene plates that were untreated (hydrophobic) or that had been plasma-treated ('tc-treated') to generate a hydrophilic surface. Static conditions for biofilm formation were used with overnight growth of cultures without movement across the surface. In contrast to this static assay, measurement of biofilm formation was examined using a Bioflux assay device whereby biofilms were formed in the presence of a hydrodynamic flow.

5.2.7.1. Static conditions for biofilm formation

5.2.7.1.1. Biofilm formation on untreated polystyrene plate surfaces

Biomass of individual biofilms formed by strains was quantified using the commonly used microtitre plate method (Christensen *et al.*, 1985), which was modified in this study. *S. aureus* strains were tested for biofilm formation on polystyrene with culture using BHI broth in the absence or presence of 1% (w/v) glucose. Experiments were performed using untreated 96-well polystyrene plates, which are deemed to have a hydrophobic surface presentation, as described by the manufacturer (greiner bio one, Germany).

After incubation the plates were washed three time in distilled water (dH_2O) to remove excess cells that were unattached, followed by incubation of the plate at $60^{O}C$ for 1 h to fix cells onto the surface of plate. Next, 200 µL of crystal violet was added into each well, including broth only controls, and incubated at RT for 20 min to stain cells in the biofilm. After this, the excess dye was removed using at least three washes with dH_2O and the plate was incubated at $37^{O}C$ for an hour to dry.

Subsequently, the crystal violet dye was solubilised by adding 160 µL of 33% (v/v) glacial acetic acid (Emsure, USA). The OD_{490} of each well was measured by using a FLUOstar Omega plate reader (BMG Labtech). At least three biological replicates of each sample with 3-8 technical replicates per plate were performed for each sample in an assay. The mean values were determined for each strain tested, together with their standard deviation and standard error. The statistical significance of differences between samples was analysed using student's *t*-test.

5.2.7.1.2. Biofilm formation on plasma-treated surfaces

Biofilm growth of *S. aureus* strains on plasma-treated (tc-treated) surfaces and its measurement with crystal violet dye was performed as described in the previous section, except that the plates were exchanged for Nunclon plastic. Plasma treatment produces a hydrophilic surface as indicated by the manufacturer.

5.2.7.2. Imaging of biofilm formation with confocal microscopy

Confocal laser scanning microscopy (CLSM) was used to visualise biofilm formation and cell viability in conjunction with vitality stains.

Overnight cultures of *S. aureus* strains were diluted with BHI broth to obtain OD_{600}=0.05. Sterile 12 mm diameter glass coverslips (coated with poly-D-lysine, positively charged, neuVitro, USA) were placed into 12-well polystyrene plates (untreated, Greiner bio-one, Germany) prior to adding 300 µL of culture. Biofilm was allowed to develop over 24 h of incubation at 37^{O}C. Biofilm production and cell viability were evaluated using a BacLight live/dead kit, which contains SYTO9 and propidium iodide stains (L-7007, Molecular Probes, Invitrogen), following the

manufacturer's instructions and a previously described method (Bauer *et al.*, 2013). The BacLight dye was prepared by mixing 5 µL of component A (1.67 mM propidium iodide) and 4 µL of component B (1.67 mM SYTO 9) into 1 mL of distilled water. At the end of the incubation time, excess culture was removed carefully from each well-contained coverslip which were then washed twice with dH_2O. Next, 300 µL of mixture dye was added into the well and the plate was incubated at RT for 30 min in the absence of light. Afterwards, wells were washed twice more to remove excess dye. The coverslips were removed and inverted upon a microscope slide, followed by direct observation using confocal scanning laser microscopy (CSLM) (LSM-510, Zeiss), with the excitation/emission measured at 480/500 nm for SYTO-9 dye and 490/635 nm for propidium iodide (a dual-band emission filter at 500-550 nm/598-660 nm). The imaging was detected by LSM software and presented by image J software.

5.2.7.3. Hydrodynamic flow biofilm formation

Hydrodynamic flow biofilm formation using a BioFlux system was done in collaboration with Nikki Black at the University of Galway, who performed the assay and supplied raw data. The method used was a modification of a published protocol [Moormeier and Bayles, 2014]. The BioFlux 1000z microfluidic system (Fluxion Biosciences Inc., San Francisco, CA) was used to evaluate biofilm formation under shear flow conditions using BHI as growth medium with or without the addition of 1% (w/v) glucose. For cell growth, 200 µl of media was added to the output wells of a 48-well plate and the channels were primed for 5 min at 5.0 dynes/cm^2. After priming, the media was aspirated from the output wells and replaced with a 50 µl media suspension of cells grown to early exponential growth

phase and adjusted to an OD_{600} = 0.8. A further 50 µl of media was added to the input wells and the channels were seeded by pumping from the output wells to the input wells for 3-5 seconds at a speed of 3 dynes/cm^2. Bacterial cells were allowed to attach to the surface of the plate for 1 h at 37°C. Excess inoculum solution was aspirated from the output wells and a further 1.2 ml of media was added to the input wells. The flow rate was set at 0.6 dyne/cm^2 for 18 h (equivalent to 64 µl/hour). Bright field images were captured every 5 min at 10X magnification. A total of 217 images were captured over 18 h. The gain and exposure settings remained constant over the 18-hour period for all images.

5.2.8. Alamar Blue assays.

Culture of strain and metabolism was examined with Alamar blue stain (Invitrogen); the stain substrate is a water-soluble tetrazolium salt that consists of both resorufin and resazurin as oxidation-reduction (redox) indicators that yield a fluorescent signal and colorimetric change in response to the metabolic activity of cells. A blue colour with non-fluorescence reports oxidation, while a pink colour with fluorescence reports reduction (Byth *et al.*, 2001). *S. aureus* strains were grown at 37^{O}C in BHI broth with shaking overnight, as described previously. Cells were harvested by centrifugation at 1500 rcf for 10 min and then suspended in 50 mL fresh BHI broth (pH7.2) until the OD_{600} reached 0.05. Cultures were incubated at 37^{O}C with shaking until the OD reached OD_{600} of 0.5. Following this, 10 mL BHI broth (pH 7.2) was inoculated and the OD was adjusted to 0.5 nm to ensure that the number of cells was closely matched based upon turbidity, prior to adding Alamar Blue; 200 µL of suspended cells were transferred into sterile 96-well polystyrene plates followed immediately by adding 20 µL (1/10) of Alamar Blue with stationary incubation at

37^{O}C in the dark, as recommended by the manufacturer. A negative control comprised BHI plus Alamar Blue. Changes in absorbance were measured at wavelengths 570 nm and 600 nm using a FLUOstar Omega plate reader. Experiments were repeated at least 3 times and the mean value was determined.

5.3. Results and Discussion

5.3.1. Growth analysis of a *S. aureus pgd* mutant

The growth rate and yield of the *pgd* mutant was examined by comparative culture with the wild-type strains. The aim was to determine the role of the *pgd* gene in *S. aureus* physiology with respect to whether it is required for normal growth of *S. aureus* by examining the mutant and its isogenic wild type strain with their respective complementation plasmid variants across all four strains backgrounds, SH1000, Newman, SF8300 and BH1CC.

Relative turbidity measurements indicated that the *pgd* mutants exhibited a delay during the lag phase. This delay was significantly observed in three strain backgrounds (Newman, SF8300 and SH1000), but was more clearly observed with the isogenic *pgd* mutant of SF8300, when cultured in both BHI and BHI supplemented with 1% (w/v) glucose (Fig. 5.1; 5.2). The growth rate of *pgd* mutants and plasmid complementation variants was unaffected during exponential growth phase, with each sharing similar growth rates (rate data not shown); strains also reached similar post-exponential growth phase yields, compared with their parent strains; an exception was strain SF8300 *pgd* with a reduced yield in stationary phase.

The reason for the elongated lag phase in *pgd* mutants is unclear, as is the variation between strain backgrounds (e.g. compare SF8300 with BH1CC). Since the proposed role of Pgd is associated with cell wall metabolism and synthesis, the deletion of *pgd* in several *S. aureus* strains has an impact on a particular growth phase that might relate to growth ability, but nothing more definite can be stated. The lag phase is important for synthesising and secreting essential surface proteins to be used for cell growth (Harris *et al.*, 2002). The observations of altered growth in *S. aureus* have some similarities with the growth of a *pgdA* mutant of *S. pneumoniae*, but for this species mutation reduces growth during exponential phase when compared with the parental strain (Vollmer and Tomasz, 2000).

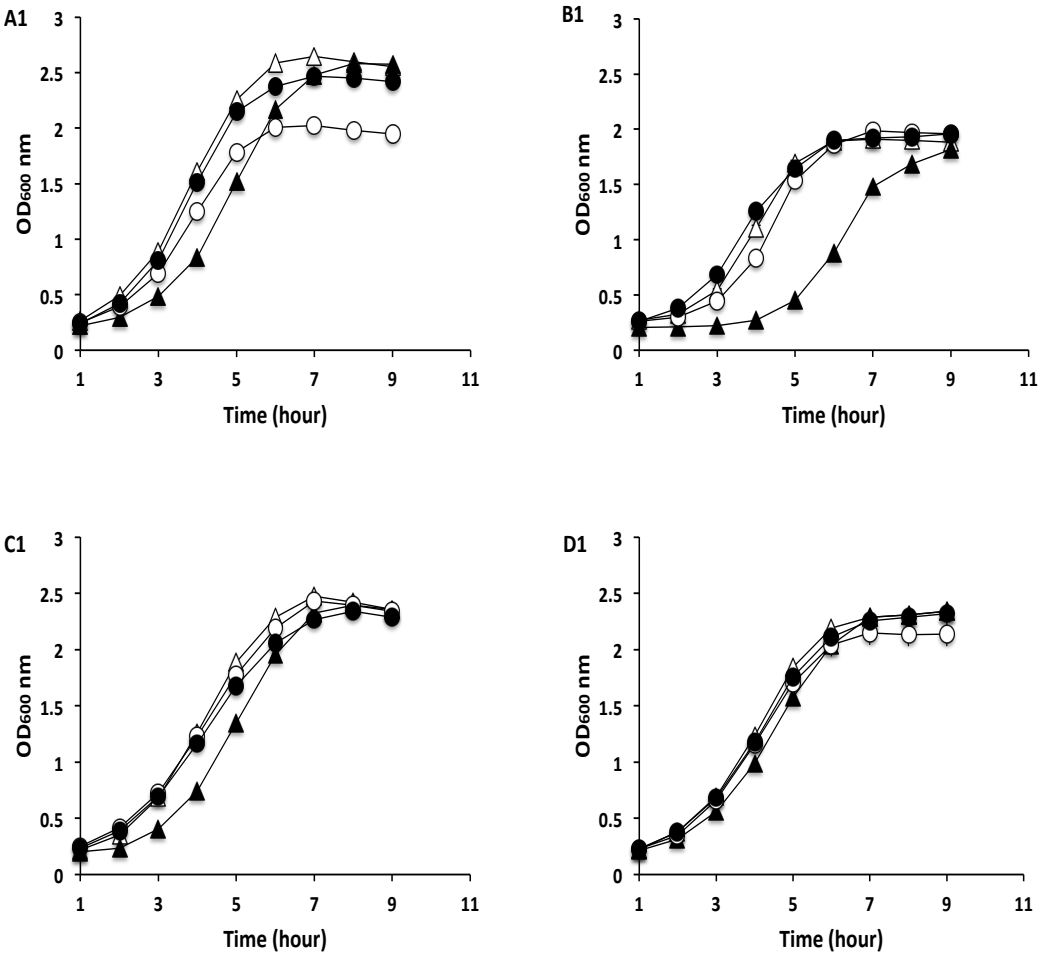

Fig. 5.1. **Growth curves of *S. aureus* strains cultured in BHI medium**. Growth of (A1) Newman, (B1) SF8300, (C1) SH1000 and (D1) BH1CC strains. Wild-type (empty triangle), *pgd* mutant (solid triangle), wild-type with pJAL-*pgd* plasmid (empty circle) and *pgd* mutant with *pgd* complementation plasmid (solid circle) at 37^{O}C. A minimum of triplicate experiments was performed. Standard errors were always within 0.70% of total mean.

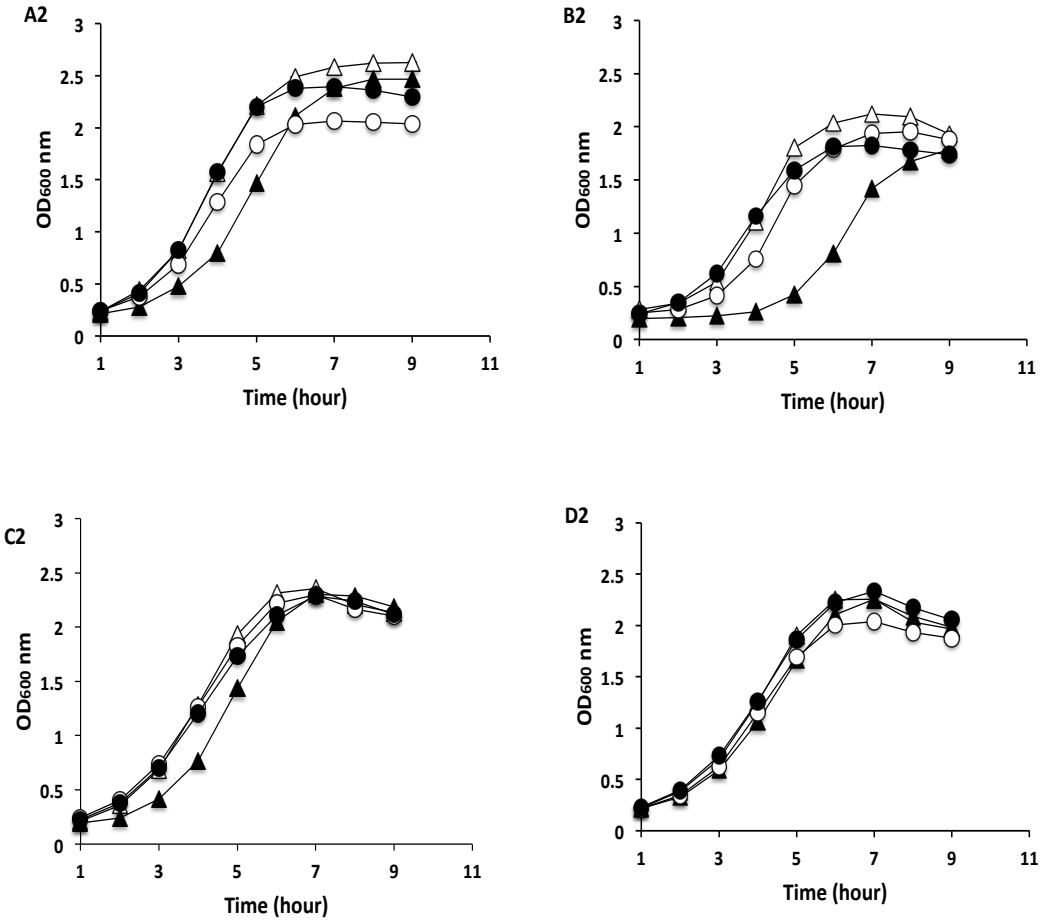

Fig. 5.2. **Growth curves of *S. aureus* strains cultured in BHI medium plus glucose**. Growth of (A2) Newman (B2) SF8300 (C2) SH1000 and (D2) BH1CC strains; Wild-type (empty triangle), *pgd* mutant (solid triangle), wild-type with pJAAL-*pgd* plasmid (empty circle) and *pgd* mutant with *pgd* complementation plasmid (solid circle) at 37^{O}C. A minimum of triplicate experiments was performed. Standard errors were always within 1.2 % of total mean.

5.3.2. Staphyloxanthin production

Since altered growth of the *pgd* mutant was observed across several strain backgrounds, together with visual differences in colony appearance (data not shown),

expression of the carotenoid staphyloxanthin was measured. For the assay of pigment production, each of the *S. aureus* strain backgrounds were cultured for 24 h to compare the wild-type and *pgd* mutant with their *pgd* complementation plasmid variants (section: 5.2.3). Methanol extraction was performed with suspended cell pellets to extract pigment.

Deletion of the *pgd* gene decreased staphyloxanthin pigment production in a *S. aureus* Newman *pgd* mutant, but did not with mutation of *pgd* in the SF8300, SH1000 or BH1CC strain backgrounds. This was clearly visualised from comparison of cell pellets with their respective parent strains (Fig 5.3.). The observed differences were confirmed by comparing the spectral profiles of extracted staphyloxanthin from both parent and *pgd* mutant, together with the pJAL-*pgd* (pSK5632 plus *pgd* gene) plasmid containing strains. The *S. aureus* Newman *pgd* mutant staphyloxanthin absorbance spectrum shows characteristic peaks at 430, 462 and 491 nm that were absent in the wild-type parent strain profile. Complementation of Newman *pgd* with pJAL-*pgd* did not fully restore pigmentation to wild-type levels (Fig. 5.3A1; B1). In two different strain backgrounds, mutant complementation decreased pigmentation (SF8300 *pgd* pJAL-*pgd* and SH1000 *pgd* pJAL-*pgd*) and the strains lacked the absorbance peaks (430, 462 and 491 nm) characteristic of staphyloxanthin (Katzif *et al.*, 2005) when compared with spectral profiles of their parent strains (Fig 5.3).

The incomplete complementation of staphyloxanthin expression could relate to the gene sequence cloned with respect to its regulatory sequences or due to gene dosage arising from the construction and copy number of the pJAL-*pgd* vector. The plasmid was assembled by cloning the full *pgd* transcriptional unit sequence, including a

candidate promoter located ~170 bp of DNA upstream of the start codon. In addition ~50 bp of sequence located 3' of the termination codon was cloned, which was predicted to include a terminator sequence. The plasmid used for complementation, pSK5632 (Grkovic *et al*., 2003) replicates and maintains a copy number of ~10 per cell, at least under conditions of testing in *S. aureus* RN4220. While at the lower end of copy numbers for complementation plasmids used in staphylococcal studies, the vector will still result in multiple copies of both the *pgd* gene and its regulatory sequences present in the cloned promoter region. While the mechanism of regulation of *pgd* expression in *S. aureus* is unknown, there is a likelihood of the MgrA transcriptional repressor being a contributory element from available transcriptional data and there could be an activator modulating transcription. The gene copy number could titrate two component system regulatory proteins e.g. WalKR, LytSR known to control autolysis and cell surface decoration producing consequential phenotypes (section 1.1.14.5. and 1.1.14.6.).

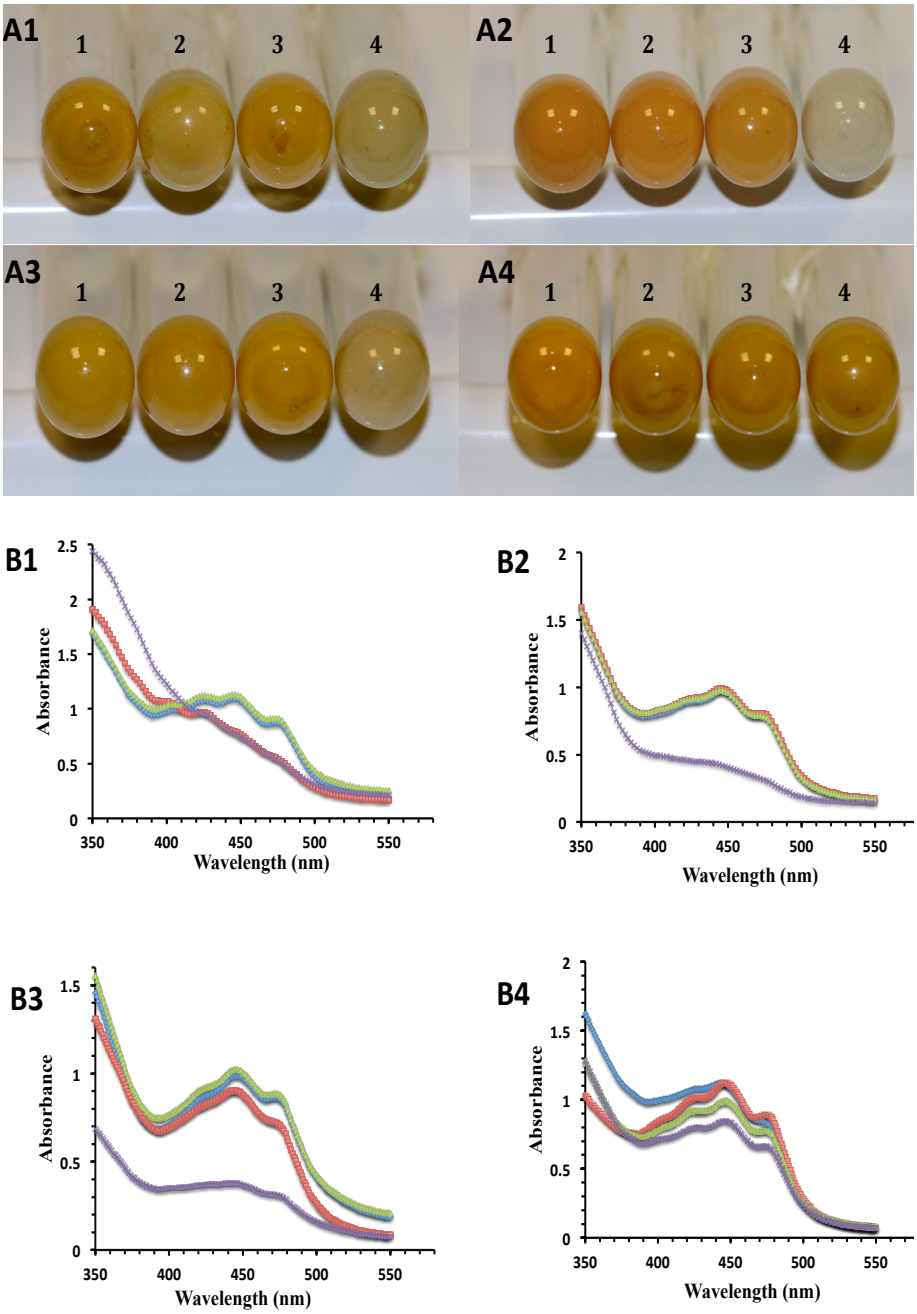

Fig 5.3. The effect of *pgd* on pigment production in *S. aureus* strains. Cell pellets after culture of (A1) Newman, (A2) SF8300, (A3) SH1000 and (A4) BHICC**.** Tubes numbered 1, 2, 3 and 4 represent wild type, *pgd*, and complementation strains wild-type plus pJAL-*pgd* and *pgd* plus pJAL-*pgd*, respectively. Strains were grown in 50 ml BHI (v/v) at 37^{O}C with shaking. After 24 h, cells were centrifuged and washed three times with PBS. Absorbance spectra ($A_{350-550}$) of strains: (B1) Newman, (B2) SF8300, (B3) SH1000 and (B4) BHICC. Lines coloured blue, red, green and purple correspond to wild type; *pgd*; wild-type plus pJAL-*pgd*; and *pgd* plus pJAL-*pgd*, respectively. The absorbance spectrum of each supernatant was measured. Experiments were repeated on three separate occasions and representative data of one experiment is shown.

Staphyloxanthin is a membrane-bound carotenoid of *S. aureus*. Most *S. aureus* clinical isolates produce the carotenoid pigment, though the expression levels vary widely, ranging from pale yellowish to bright orange after aerobic overnight culture on solid medium (Duthie and Lorenz, 1952). The levels of staphyloxanthin in the cell membrane are linked with increased bacterial survival from reactive oxygen species since the pigment has antioxidant properties (Chamberlain *et al.*, 1991; Dye and Kapral, 1980; Giachino *et al.*, 2001; Grinsted and Lacey, 1973; Lee and Bergdoll, 1985; Pelz *et al.*, 2005). The pigment contributes to *S. aureus* virulence and was demonstrated to increase the severity of skin abscess infections by comparison of wild-type and *crt* gene mutants (Liu *et al.*, 2005). Staphyloxanthin impairs the antimicrobial action of neutrophil ROS by virtue of its antioxidant roles (Clauditz *et al.*, 2006; Liu *et al.*, 2005; Olivier *et al.*, 2009). The carotenoid pigment also functions to modulate membrane fluidity to increase stiffness, which imparts resistance to cationic antimicrobial peptides. The proposed mechanism that directs this is unknown, though it was determined that neither phospholipid composition, surface charge, the complement of fatty acids or cell wall thickness wall appear to differ in a *S. aureus* mutant overexpressing crtMN of the *crtOPQMN* operon (Mishra *et al.*, 2011).

The yellow and orange carotenoid pigments of *S. aureus* are synthesised via a C_{30} triterpenoid biosynthetic pathway (Marshall and Wilmoth, 1981). The yellow pigment of carotenoid corresponds to 4,4'-diaponeurosporene which is converted to an orange pigment called staphyloxanthin as the pathway end product. The *crtOPQMN* operon encodes the biosynthetic enzymes for staphyloxanthin and *crtM* is responsible for the first step of carotenoid production, encoding dehydrosqualene

synthase. CrtM combines two farnesyl pyrophosphate molecules to create a 4,4'-diapophytoene. Subsequently, this molecule undergoes three cycles of dehydrogenation catalysed by CrtN, a 4,4'-diapophytoene desaturase, to produce the yellow pigment 4,4'-diaponeurosporene (Raisig and Sandmann, 1999). Following dehydrogenation the yellow pigment is converted to the orange pigment staphyloxanthin via the activities of CrtO, CrtP and CrtQ. Staphyloxanthin is regulated by the *rsbUVWsigB* operon (Giachino *et al.*, 2001; Horsburgh *et al.*, 2002b; Kullik *et al.*, 1998; Morikawa *et al.*, 2001; Palma and Cheung, 2001), with the alternative sigma factor SigB solely directing transcription of the *crtOPQMN* operon (Bischoff *et al.*, 2004). In addition, there are several reported genetic factors that modulate expression, including a cold shock gene, *cspA*, which was reported to modulate pigment production in *S. aureus* via a SigB-dependent pathway (Katzif *et al.*, 2005).

The data presented here indicates that deletion of *pgd* and changes to its expression can lead to altered pigment levels in certain strains, and needs more investigation but this must be influenced by other factors given the strain variation that is evident. Regardless of this, there would appear to be potentially undescribed pathways leading to altered pigment expression; this could be related to a potential cell wall activity.

5.3.3 Contribution of Pgd to cell surface properties

5.3.3.1. Cell surface hydrophobicity

To determine whether Pgd has a role in modifying properties of the *S. aureus* cell surface the hydrophobicity of cells was assayed. The previously described set of strains were cultured overnight, then washed and suspended in PBS buffer, pH 7.2. Each strain suspension was tested for microbial adhesion to hydrocarbon (MATH test) using hexadecane as the hydrophobic organic solvent (Section 5.2.4). The difference between the turbidity prior to and subsequent to mixing with hexadecane was used to determine adhesion (cell hydrophobicity). The experiment was performed with triplicate biological samples and the results expressed as percentage hydrophobicity for each individual strain (Fig. 5.4.).

The results clearly identified that in three strain backgrounds: Newman; SF8300*;* and BH1CC*,* mutation of *pgd* significantly lowers adhesion to hexadecane ($P < 0.01$). This phenotype is shown by the increased absorbance of the buffer phase for each mutants compared with their respective parent strains. These data indicate decreased hydrophobicity of the *pgd* mutant cell surface. In contrast, the SH1000 *pgd* mutant revealed the opposite phenotype with an increased hydrophobicity of its cell surface. In each case, the *pgd* mutant phenotypes were restored to similar hydrophobicity levels as their parent strains.

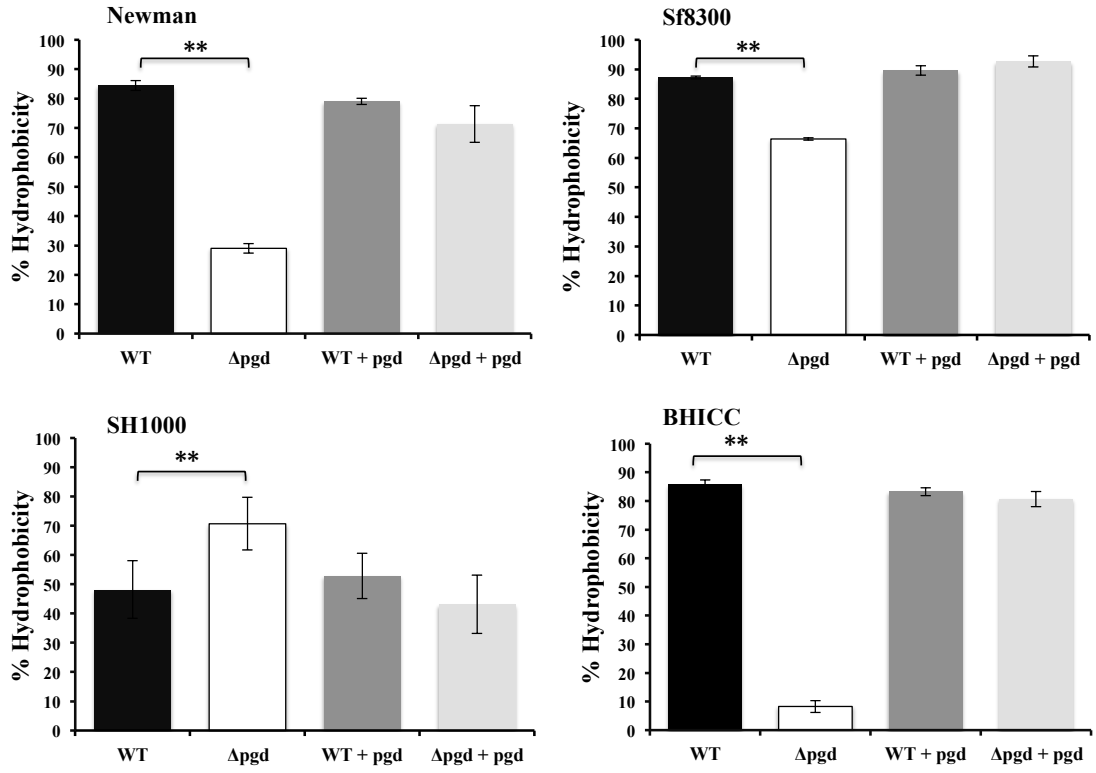

Fig. 5.4. Hydrophobicity of *S. aureus* cell surface based on adhesion to hexadecane. Cell surface hydrophobicity was evaluated by reduction in absorbance (OD_{450} nm) of the aqueous phase once separated from hydrocarbon. Strains: wild-type (black), Δ*pgd* (white), wild-type plus pJAL-*pgd* [WT + *pgd*] (dark grey) and complementation strain *pgd* plus pJAL-*pgd* (Δ*pgd* + *pgd*) (light grey). A minimum of triplicate experiments were performed and error bars represent standard deviation, using 2-tailed Student t-test, ** indicates $P<0.005$ value.

These data obtained from the MATH test clearly indicate that *pgd* contributes to hydrophobicity of the *S. aureus* cell surface. The phenotype is similar to that of a *S. mutans pgd* strain, where reduced hydrophobicity was observed (Deng *et al.*, 2009). *S. aureus* cells are typically hydrophobic and when examined in other studies for the contributing factors by gene deletion, it was identified that mutants that lacked protein A, teichoic acid or coagulase remained hydrophobic. However,

peptidoglycan extracted from different *S. aureus* strains is hydrophilic, indicating that there is likely to be one or more protein-associated molecule, presumably localised at the cell membrane or cell wall, capable of changing hydrophobicity of the cell surface (Reifsteck *et al.*, 1987). Hydrophobicity and charge of the *S. aureus* cell surface have been investigated across growth phases. Hydrophobicity was significantly increased during exponential phase and greatest in stationary phase, however, surface charge decreased during exponential phase yet significantly increased in stationary phase. These changes support different structures in *S. aureus* contributing to changing both charge and hydrophobicity of the cell surface during growth (Beck *et al.*, 1988).

The PgdA protein of *S. mutans* strain shares homology with Pgd proteins from *L. monocytogenes* and *S. pneumoniae* with each possessing catalytic domains corresponding to peptidoglycan N-acetylglucosamine deacetylase. Deletion of *pgdA* in *S. mutans* was reported to only slightly affect hydrophobicity and the mutant exhibited a dissimilar colony texture to the wild-type. These features were not reported for the *pgd* mutants of either *L. monocytogenes* or *S. pneumoniae*, and furthermore *S. mutans pgd* was not hypersensitive to lysozyme which was reported as a key phenotype of both *S. pneumoniae* and *L. monocytogenes* mutants (Deng *et al.*, 2009).

Based on the protein homology between the *S. aureus* candidate Pgd and the other species' Pgd proteins, plus the findings of altered hydrophobicity and pigmentation there is supporting evidence that the *pgd* gene contributes to cell surface properties. The protein is proposed from the structural work in chapter 3 to be a peptidoglycan

N-acetylglucosamine deacetylase. This enzyme activity can lead to a change of nett positive charge on the cell surface due to increased acetyl groups and this might be an explanation for the observations described above. A reduced level of positively charged peptidoglycan associated with the *S. aureus pgd* mutant surface, if verified, might lead to altered properties essential for normal cell growth. Decreasing the cell wall surface positive charge might be expected to alter resistance to cationic antimicrobial peptides, which are essential elements produced during innate immune system (Peschel, 2002). Modification of cell surface charge to change peptidoglycan properties might also be expected to alter the activity of peptidoglycan synthesis enzymes, particularly the activity of hydrolases, and in this respect altered lysozyme resistance is reported as a phenotype of *pgd* mutants of several species.

5.3.4. Autolysis.

Experiments were designed to examine the relative level of autolysis for the *S. aureus pgd* mutant compared with isogenic wild type and complementation control strains described above, but without study of BH1CC strains because this strain was incorporated into the study after these experiments were performed. Within these assays an *atl* mutant was included as an autolysis reference strain to provide a control for challenged cells. Briefly, harvested cells were washed and suspended in 50 mL sterile PBS containing either 0.1 mg ml^{-1} Penicillin-G or 0.1 % (v/v) Triton X-100. After addition of these autolysis trigger molecules, the mixture was incubated at $37^{O}C$ with shaking and lysis of cells was monitored by spectrophotometry (Fig. 5.5.) The extent of autolysis due to *pgd* mutation of both Newman and SF8300 strain backgrounds was clearly increased compared with wild-type, following challenge with Triton X-100 and Penicillin-G. Similar rates of autolysis were observed with

both strain Newman *pgd* and SF8300 *pgd*. In contrast, SH1000 *pgd* did not exhibit altered autolysis in either condition compared with its parental strain. Notably there was no complementation of the *pgd* mutation in this experiment with no explanation yet and the *pgd* complementation strains of Newman and SF8300 had higher autolysis rates than their isogenic parents and rates similar to Newman *pgd* and SF8300 *pgd*. These data do identify that the *pgd* mutation can be assigned with multiple phenotypes relating to the cell surface and autolysis, similar to *pgd*A inactivation of *L. monocytogenes* (Popowska *et al.*, 2009).

In bacteria, autolysins are peptidoglycan (murein) hydrolases that have specific hydrolytic activities for different components of peptidoglycan structure (Ingavale *et al.*, 2003). Autolysins control turnover, maturation and degradation of peptidoglycan (Bose *et al.*, 2012) meaning they play important roles in critical biological processes such as growth, cell wall synthesis, cell division, and peptidoglycan recycling (Fujimoto and Bayles, 1998). Biosynthesis of peptidoglycan in staphylococci, as in other bacteria, is a multistep process occurring across three different subcellular compartments; the cytoplasm, cell membrane and cell wall. UDP-MurNAc-pentapeptide is a final product of the cell wall biosynthetic pathway, which is transferred to the lipid membrane and modified by addition of GlcNAc residues and a peptidoglycan-bridge; this structure is translocated to the outer surface of the membrane (Ingavale *et al.*, 2003). Peptidoglycan assembly is catalysed by transpeptidases and carboxypeptidases, such as penicillin-binding proteins (Navarre and Schneewind, 1999). The staphylococcal peptidoglycan hydrolases include N-acetyl glucosaminidase, N-acetyl muramidase, endopeptidase, and N-acetylmuramyl-L-alanine amidase activities (Ramadurai *et al.*, 1999; Sugai *et al.*, 1995). Due to their

cell wall enzymatic activity, they are tightly regulated to prevent autolysin-mediated lysis. Previous studies demonstrated that autolysis enzymes are controlled transcriptionally (Fujimoto and Bayles, 1998) and indicated that multiple regulators including, SarA, LytSR, AgrCA, ArlRS and MgrA (Rot) affect autolysin expression in *S. aureus* (Ingavale *et al.*, 2003). Mutation of *S. aureus agr* leads to a decreased autolysis rate, while inactivation of several Sar-family genes results in an increased autolysis rate (Fujimoto and Bayles, 1998). Atl is the major autolysin activity of *S. aureus* and this enzyme contains two domains; amidase (AM) and glucosaminidase (GL), which must both be catalytically active for a bacterium to form a biofilm. Atl is the key enzyme activity associated with autolysis and a gene mutant has majorly reduced autolysis (see Fig 5.6) (Bose *et al.*, 2012).

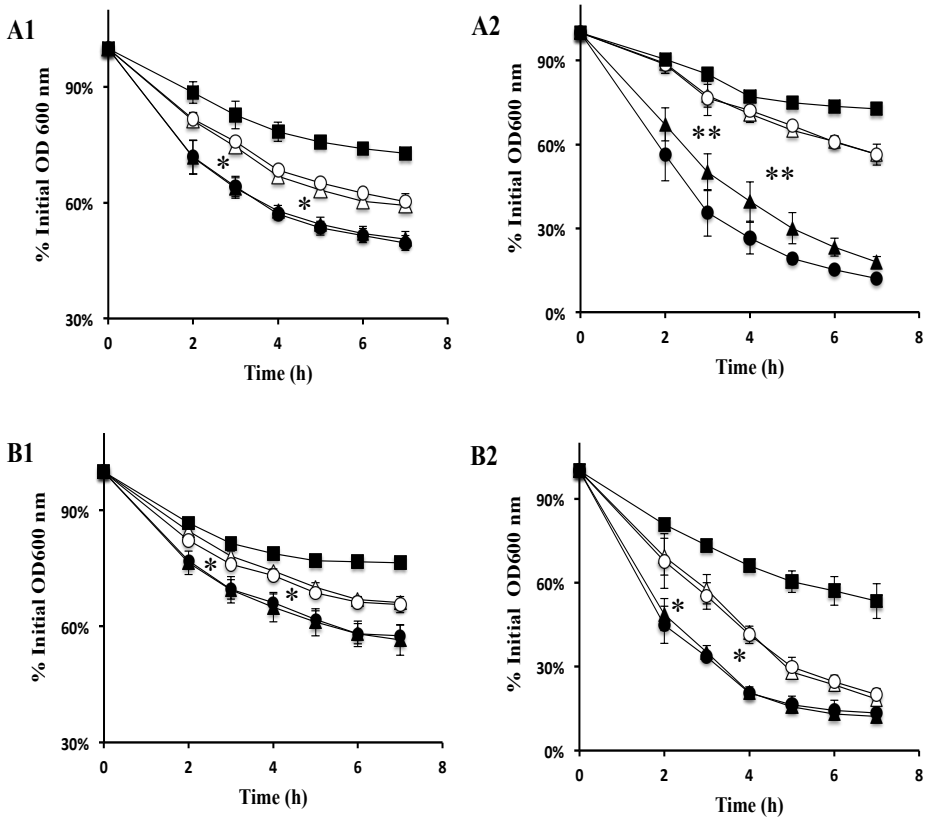

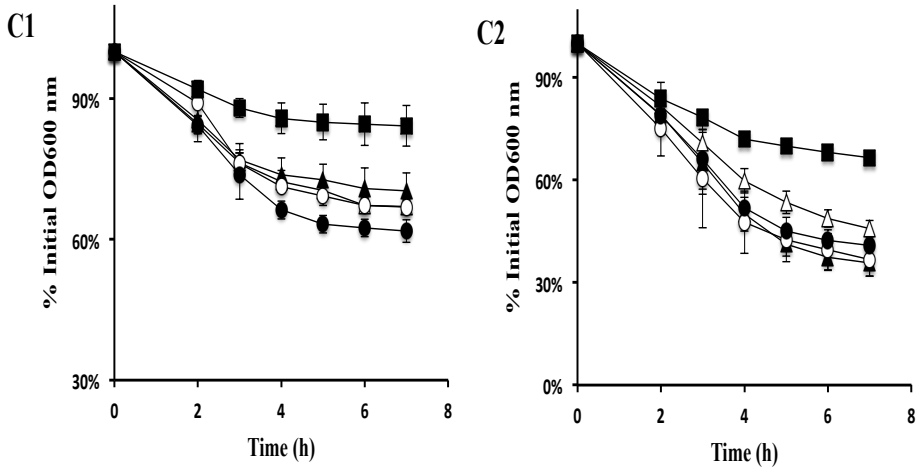

Fig. 5.5. Autolysis of *S. aureus pgd* mutants compared with isogenic strains.
Autolysis was induced in mid-exponential growth phase cells after adding Triton-X-100 [0.1% (v/v)] or Penicillin-G [0.1 mg ml^{-1}] in 50 mL PBS. Comparison are made with *S. aureus* wild-type strains (empty triangle), *atl* (solid square), Δ*pgd* (solid triangle), wild-type with pJAL-*pgd* plasmid (empty circle) and Δ*pgd* complemented with pJAL-*pgd* (solid circle). Strains Newman, SF8300 and SH1000 were challenged with (A1, B1, C1) Penicillin G or (A2, B2, C2) Triton-X-100, respectively. Data represents the mean of triplicate biological samples with standard deviation shown. In both experiments, statistically significant differences (*) between WT and Δ*pgd* are indicated ($p<0.05$) and determined using student's *t*-test

5.3.5. The role of Pgd in lysozyme resistance

Two separate experiments were performed to test the contribution of Pgd to lysozyme resistance of *S. aureus*. The assay approaches included: disc-diffusion of lysozyme (20 mg mL^{-1}) on agar; or challenge of planktonic post-exponential growth phase cells with lysozyme (30 mg mL^{-1}). Isogenic strain sets were assayed: Newman; SF8300; and SA113, with each set containing WT, *pgd, oatA* and double mutant *pgd oatA* (Table 3.2). In both lysozyme resistance experiments the *S. aureus* strains were grown in TSB medium. Optimisation of the lysozyme disc-diffusion agar assay was performed to determine conditions to compare resistance levels. This optimisation was required because the published assay of Bera *et al*. (2005) was established with

S. aureus SA113, which was identified here to be markedly less resistant to lysozyme than either Newman or SF8300 strains upon inactivation of resistance genes. The optimal test conditions were determined to be a lysozyme disc-diffusion agar plate overlaid with 6 mm paper discs prepared with 20 mg mL^{-1} lysozyme, or broth grown post-exponential phase cells challenged with lysozyme added to 30 mg mL^{-1} final concentration. The data from both optimised experiments is presented in Fig. 5.6.

As expected, each wild-type strain (Newman, SF8300 and SA113) was completely resistant to lysozyme (Fig.5.6 A3, B3, C3). Further, it was determined that all *pgd* mutants remained resistant and their growth was unaffected on lysozyme disc-diffusion agar plates and by lysozyme challenge in broth, even at the highest concentrations tested >30 mg mL^{-1} in the assays (Fig 5.7). The mutant Newman *oatA* was lysozyme sensitive at a level similar to that of SA113 *oatA* described by Bera *et al*., (2005). In sharp contrast and without explanation, SF8300 *oat*A was not lysozyme sensitive in either assay.

Newman *pgd oatA* and SA113 *pgd oatA* double mutant strains exhibited a reduced zone (~50%) of clearing on lysozyme diffusion agar plates. This is reduction in resistance was demonstrated more clearly in the broth lysozyme challenge assays with an increased lysozyme resistance of a *pgd oatA* double mutant compared with *oatA* mutation alone in the same strain backgrounds (Fig.5.6). From these data it is evident that Pgd contributes to lysozyme resistance and raises questions about whether there is coordinated OatA expression given potential compensatory roles.

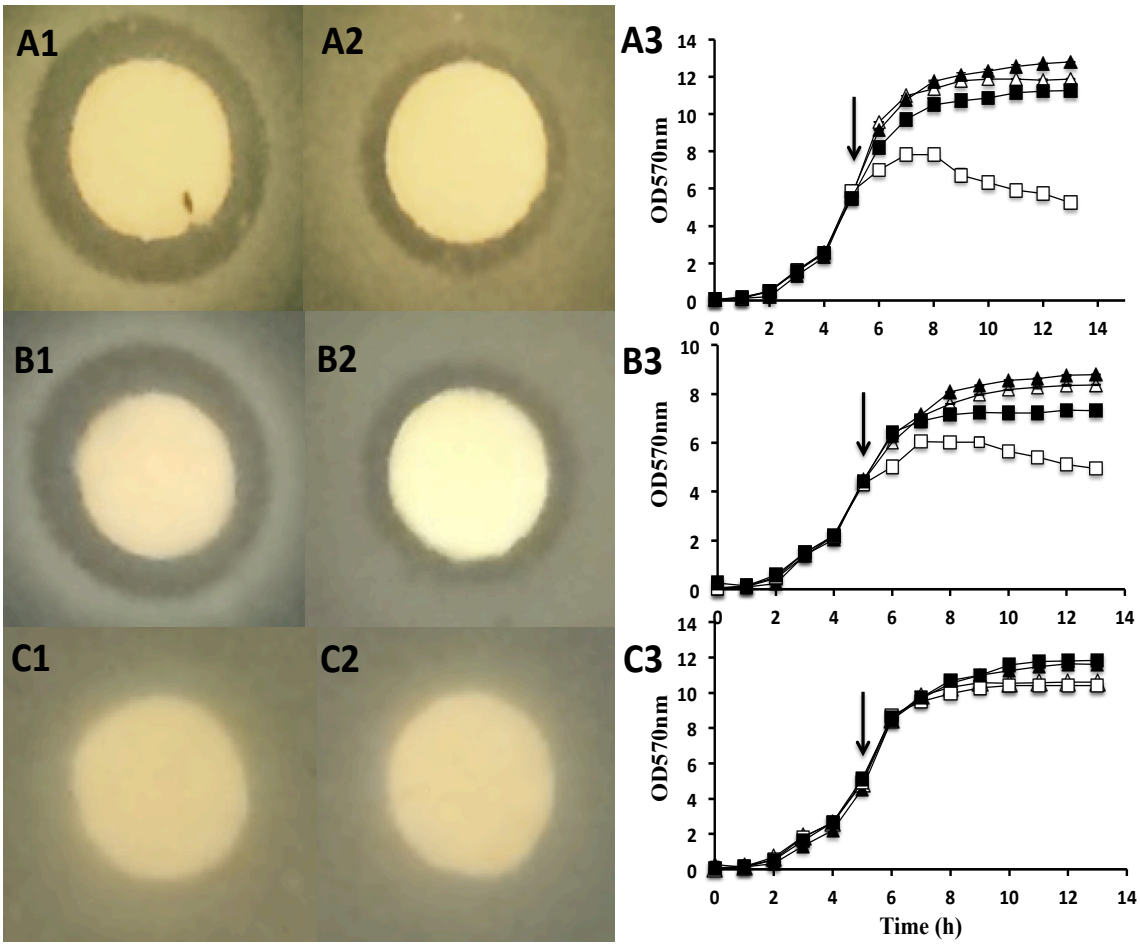

Fig. 5.6. The role of *pgd* in *S. aureus* resistance to lysozyme. Growth inhibition from lysozyme was assessed on TSA plates. Overnight cultures were diluted 10-fold in soft agar and poured onto plates. A paper disc (6 mm) containing lysozyme (20 mg) was placed on the plates and incubated at 37^{O}C overnight. Growth of *S. aureus* strains; SA113 *oatA* (A1), SA113 *oatA pgd* (A2), Newman *oatA* (B1), Newman *oatA pgd* (B2) and SF8300 *oatA* (C1) and SF8300 *oatA pgd* (C2). Cultures of SA113, Newman and SF8300 strains (A3, B3, C3) were challenged with lysozyme during late exponential growth phase in TSB after addition of 30mg ml^{-1} lysozyme (arrow). Wild-type (empty triangle), *pgd* (solid triangle), *oatA* (empty squares) and *oatApgd* (solid squares).

Many bacterial pathogens display resistance activity for bactericidal components produced by host tissues, including antimicrobial peptides and enzymes. This resistance frequently results from structural properties of the cell surface and the modification of these. For example, in *S. aureus* D-alanine is incorporated into teichoic acids by the DltA enzyme (Peschel *et al.*, 1999), O-acetylation of peptidoglycan is catalysed by OatA (Bera *et al.*, 2005) and MprF adds lysine to phosphatidylglycerol (Staubitz *et al.*, 2004); each modification contributes to surface defences to a range of molecules, including antimicrobial peptides. Thus, mutation in one of these genes was shown to decrease virulence. In addition to these activities, *S. aureus* similar to some other pathogens, has additional regulation of biochemical and structural features that increase resistance to host defence from bactericides. Lysozyme resistance is part of this defence system, to protect from the enzyme activity that cleaves peptidoglycan between the glycosidic beta-1,4-linked of *N*-acetylglucosamine (NAG) and *N*-acetylmuramic acid (NAM) (Bera *et al.*, 2005).

In this study (Chapter 3), *S. aureus* Pgd was revealed to show homology with the peptidoglycan deacetylation catalytic domains from *L. monocytogenes, S. pneumoniae* and *S. mutans*, which are members of the carbohydrate esterase family 4 enzymes (CE4) contributing to defence from human and animal mucosal lysozyme. It was reported that *pgd* mutants in several species lack peptidoglycan (GlcNac) deacetylase activity resulting in sensitivity to lysozyme digestion; for example mutants of *L. monocytogenes* (Popowska *et al.*, 2009), *S. pneumoniae* (Blair *et al.*, 2005a) and *Bacillus cereus* (Psylinakis *et al.*, 2005). In contrast, the *pgd* mutant of *S. mutans* was not sensitive to lysozyme (Deng *et al.*, 2009). Counter to these studies, the *S. aureus pgd* mutation apparently contributes to lysozyme resistance, which is

clearly demonstrated when the mutation is combined with *oatA* mutation revealing the double mutant has increased resistance. This warrants further investigation to identify the interrelationship between the two activities. Also prime for further investigation is the complete lysozyme resistance of the CA-MRSA strain SF8300 *oatA*. The underlying mechanism for this resistance could be a novel aspect or could be due to major compensation of absent O-linked acetylation of MurNAc with O-linked teichoic acid, catalysed by TagO (Bera *et al*., 2005). This would represent a marked difference in the described extent of the activity of TagO. Unfortunately, the lysozyme resistance in respect of *tagO* could not be investigated further at this stage due to the presence of *erm* resistance in strain SF8300.

5.3.6. The role of Pgd in biofilm formation

S. aureus causes a broad spectrum of infections in humans such as, soft tissue diseases and abscesses, endocarditis, and osteomyelitis. These diseases are largely due to *S. aureus* encoding a large set of virulence factors that allow the bacteria to infect various tissues within hosts. In addition to these secreted factors, *S. aureus* has the ability to form multicellular structures called biofilm. This biofilm structure is a functional multi-layered community with the bacteria attached to a surface and to each other while embedded in their synthesised extracellular matrix (O'Toole *et al.*, 2000). Biofilm formation is known as a form of bacterial protection from influences of hostile environments and is observed in many bacteria that infect animal and human tissues (O'Toole *et al.*, 2000).

Clinically, biofilm infections are important since bacterial biofilms display recalcitrance to antimicrobial peptides and host defence enzymes and immune

components and phagocytes. Biofilm development is a complex process and is structured, being commonly divided into three phases: initial attachment, maturation/accumulation and dispersal/detachment (O'Toole *et al.*, 2000; Otto, 2013).

The primary attachment phase can occur on biotic or inert surfaces and in staphylococcal infections the initial attachment can frequently be to an inert surface such as an indwelling medical implant, with colonisation of either a metal surface e.g. devices (prosthetic joints) or plastic surfaces e.g. central venous catheters, lines. Adherence is reliant on both the chemical characteristics of the material surface and bacterial surface components. The latter components include autolysin, Atl (Houston *et al.*, 2011), wall teichoic acid (WTA) and lipoteichoic acid (Gross *et al.*, 2001). For example, *atl* inactivation in several clinical *S. aureus* strains led to decreases in the initial attachment rate and reduced FnBP (fibronectin-binding protein)-dependent biofilm formation on hydrophilic polystyrene plates. In contrast, biofilm formation developed by FnBP or PIA proteins required *atl* gene expression on hydrophobic polystyrene plates (Houston *et al.*, 2011). The accessory sigma factor B (σ^B) is required for FnBP-mediated biofilm formation, and functions to repress expression of RNAIII and protease production. Mutation of *sigB* reduced initial attachment of MRSA strain BHICC during biofilm development due to reduced *atl* expression (Houston *et al.*, 2011). Extracellular DNA (eDNA) has an important contribution to early development steps of FnBP-dependent and Atl-dependent biofilm formation (Houston *et al.*, 2011). In *S. epidermidis*, autolysin AtlE promoted lysis of cells to release eDNA as a component of the biofilm matrix (Qin *et al.*, 2007), whereas

an Atl-enhanced lysis in *S. aureus,* leads to release of eDNA during the early steps of *ica*-independent biofilm (Houston *et al.*, 2011).

Primary attachment to a biotic surface, e.g. tissue cells or a synthetic surface coated with fibrinogen, fibronectin or vitronectin, is controlled largely by multiple cell wall-anchored (CWA) proteins including fibrinogen-binding protein (FnbpA), fibronectin-binding protein (FnbpB) and clumping factors A/B (Vaudaux *et al.*, 1995). After attachment, in both cases, staphylococcal biofilms develop through proliferation and production of an extracellular matrix as a scaffold (O'Toole *et al.*, 2000; Otto, 2013).

The extracellular matrix of biofilm is complex. However, until recently, few components of this structure were fully described: poly-N-acetyl-glucosamine (PNAG) also termed polysaccharide intercellular adhesin (PIA) (Mack *et al.*, 1996), and extracellular DNA (eDNA) (Montanaro *et al.*, 2011) are both recognised as key components. Both constituents direct development of the biofilm structure with the presence of eDNA being critical for stability. The polysaccharide intercellular adhesin (PIA) of *S. aureus* and *S. epidermidis* biofilm is encoded by the *icaADBC* locus and, in PIA-dependent biofilms, considered to be the major substance connecting cells in the matrix (Montanaro *et al.*, 2011). Aside from the primary attachment phase, an additional contribution of CWA proteins is promoting the accumulation phase within *ica*-dependent biofilm (Foster *et al.*, 2014). Thus, these proteins mediate all biofilm phases including intercellular adhesion. Varying numbers of different CWA proteins that contribute are present on the cell surface of *S. aureus*, based on growth conditions, but the bacteria can express up to 24 proteins, whereas *S. epidermidis* express a lower number (Foster *et al.*, 2014).

The *pgd* mutant is hypothesised to be incapable of N-acetylglucosamine deacetylation, which would lead to a change in the net charge and/or hydrophobicity of the surface. This functional prediction is consistent with the data presented so far including protein sequence homology. Hydrophobicity assay indicated that the *pgd* mutant of the three strains tested was significantly less hydrophobic compared with their parent strains (Section 5.3.3.1). If the *pgd* mutant is locked into increased acetylation of peptidoglycan producing altered surface properties, what is the role of Pgd in the biofilm formation where surface interactions are influenced by cell surface charge?

5.6.7. Biofilm formation

Various assays and experimental conditions were used in this study to evaluate biofilm formation. The development of biofilm was monitored after growth in BHI broth, either alone or supplemented with 1% (w/v) glucose or 4% (w/v) NaCl. To determine the effect of the abiotic surface upon which the biofilm was developing, various microtitre plates were used in the experiments: polystyrene plates which have a hydrophobic surface; or Nunclon plates that were oxygen plasma-treated, so called 'tc-treated', which introduces polar groups (e.g. carbonyl and carboxylic acid) rendering a hydrophilic surface.

5.6.7.1. Microtitre plate assay for biofilm formation

5.6.7.1.1. Biofilm formation on untreated polystyrene

Given the extent of strain variation observed in previous assays, biofilm formation was investigated with all four strains: Newman, SF8300, SH1000 and BHICC; testing wild type, *pgd*, wild type plus pJAL-*pgd* and the complemented *pgd* mutant with pJAL-*pgd* (section: 5.2.1.). Biofilm development was examined after culture with BHI broth or BHI supplemented with 1% (w/v) glucose. Experiments were performed with 96-well microtitre plates composed of polystyrene, an untreated surface described by the manufacturer as relatively hydrophobic.

After 24 h of incubation at 37°C, plates were washed and stained with crystal violet dye. From these assays, both wild-type strains and their *pgd* isogenic mutants did not form biofilm when cultured in unsupplemented BHI. However, both the SF8300 and Newman wild type strains displayed biofilm formation with 1% (w/v) glucose-supplemented BHI broth, while their respective *pgd* mutants did not (Fig.5.7.).

5.6.7.1.2. Biofilm formation on treated polystyrene

Biofilm growth followed by staining with crystal violet dye was performed as described in the previous section, except the microtitre plates were exchanged for Nunclon plates plasma-treated during production. These plates have a surface that is considered to be hydrophilic as indicated by the manufacturer.

The *S. aureus* strains were tested for their biofilm development in Nunclon plates after culture in BHI broth or BHI supplemented with 1% (w/v) glucose. The observed biofilms revealed that there were, again, no difference between wild type strains and their isogenic *pgd* mutants in BHI broth alone (data not shown).

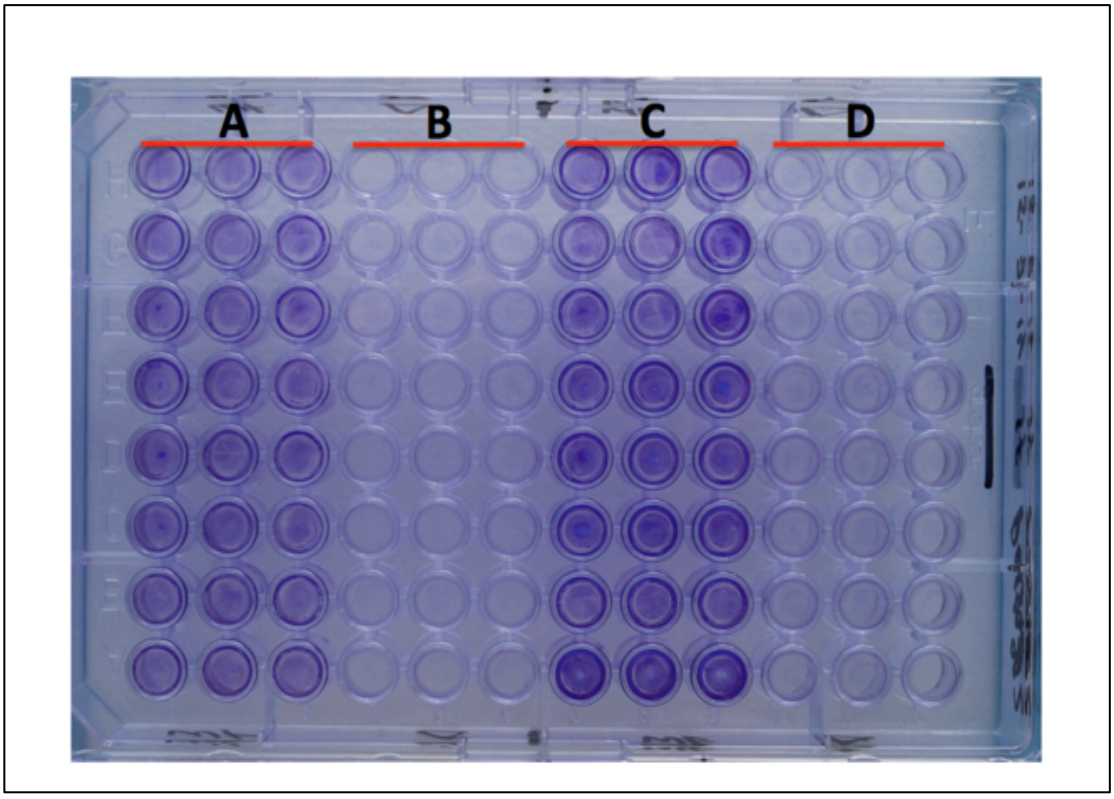

Fig. 5.7. The role of *pgd* in biofilm formation on a hydrophobic polystyrene surface. *S. aureus* strains: (A) Newman, (B) Newman *pgd* (C) SF8300 and (D) SF8300 *pgd* were cultured at 37°C for 24 h in BHI supplemented with 1% (w/v) glucose. Plates were washed with dH_2O before staining with crystal violet dye. The experiment displayed is representative of a minimum of triplicate experiments and each strain was assayed as three columns of technical replicates as indicated (red line).

In contrast, when the suite of *S. aureus* strains were cultured in BHI supplemented with 1% glucose, both of the Newman *pgd* and SF8300 *pgd* mutants developed greater levels of biofilm in comparison with their respective isogenic parents, Newman and SF8300 (Fig. 5.8 & 5.9). These results indicate there is an opposite effect of the nature of the polystyrene surface upon biofilm formation depending on it being either hydrophobic or hydrophilic in nature.

In comparison, both SH1000 and BHICC strains were examined for biofilm formation as described above but both displayed different outcomes for the *pgd* mutation when comparing the wild type and mutant strains (Fig. 5.8). Thus in these two strains inactivation of *pgd* produced no effect upon biofilm formation. Additionally, for confirmation, the biofilm was measured for all strains (A_{490}) with crystal violet dye-extraction using a FLUOstar Omega plate reader. From these assays it was observed that while biofilm formation of both Newman *pgd* and SF8300 *pgd* is significantly reduced ($p<0.05$), the SH1000 *pgd* and BH1CC *pgd* mutants are not significantly different ($p>0.05$), when each are compared with their respective isogenic parent strains (Fig. 5.10).

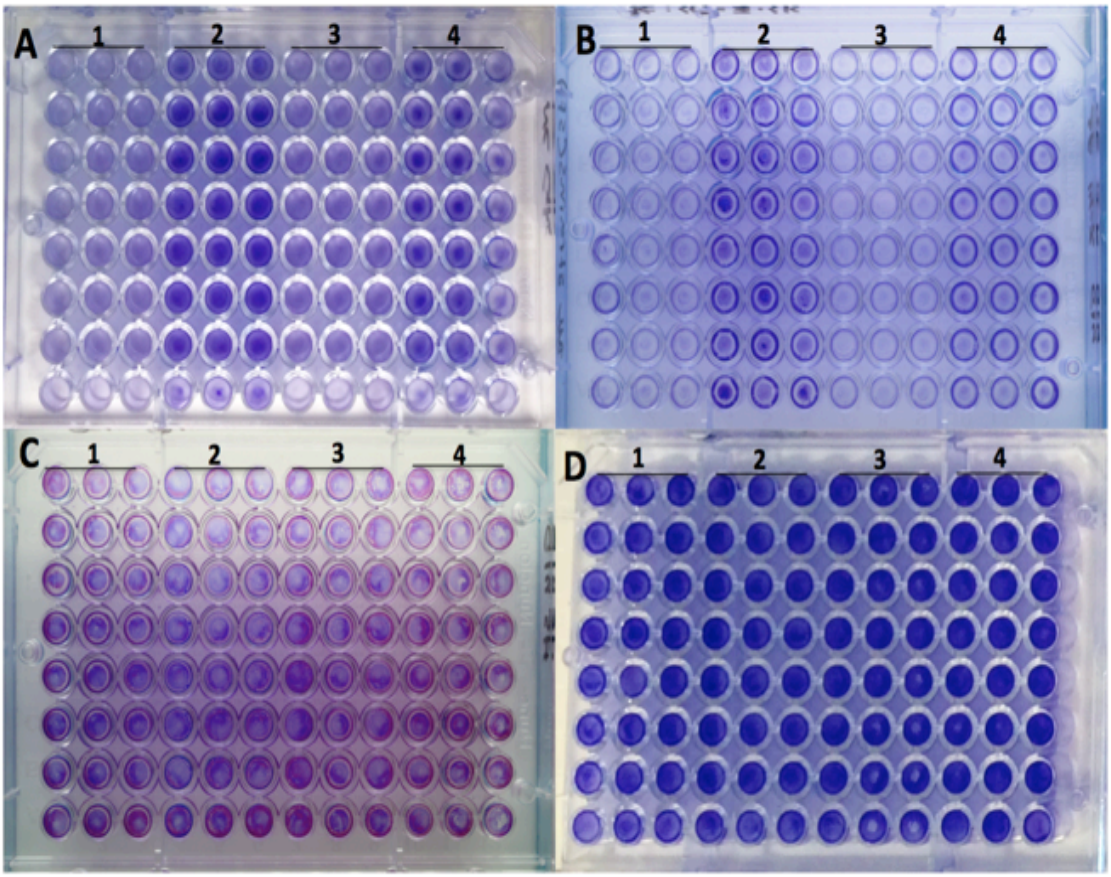

Fig. 5.8. The role of *pgd* in biofilm formation on a hydrophophilic (tc-treated) polystyrene surface. *S. aureus* strains: (A) Newman, (B) Newman *pgd* (C) SF8300 and (D) SF8300 *pgd* were cultured at 37°C for 24 h in BHI supplemented with 1% (w/v) glucose. Plates were washed with dH_2O before staining with crystal violet dye. The experiment displayed is representative of a minimum of triplicate experiments and each strain was assayed as three columns of technical replicates as indicated (red line).

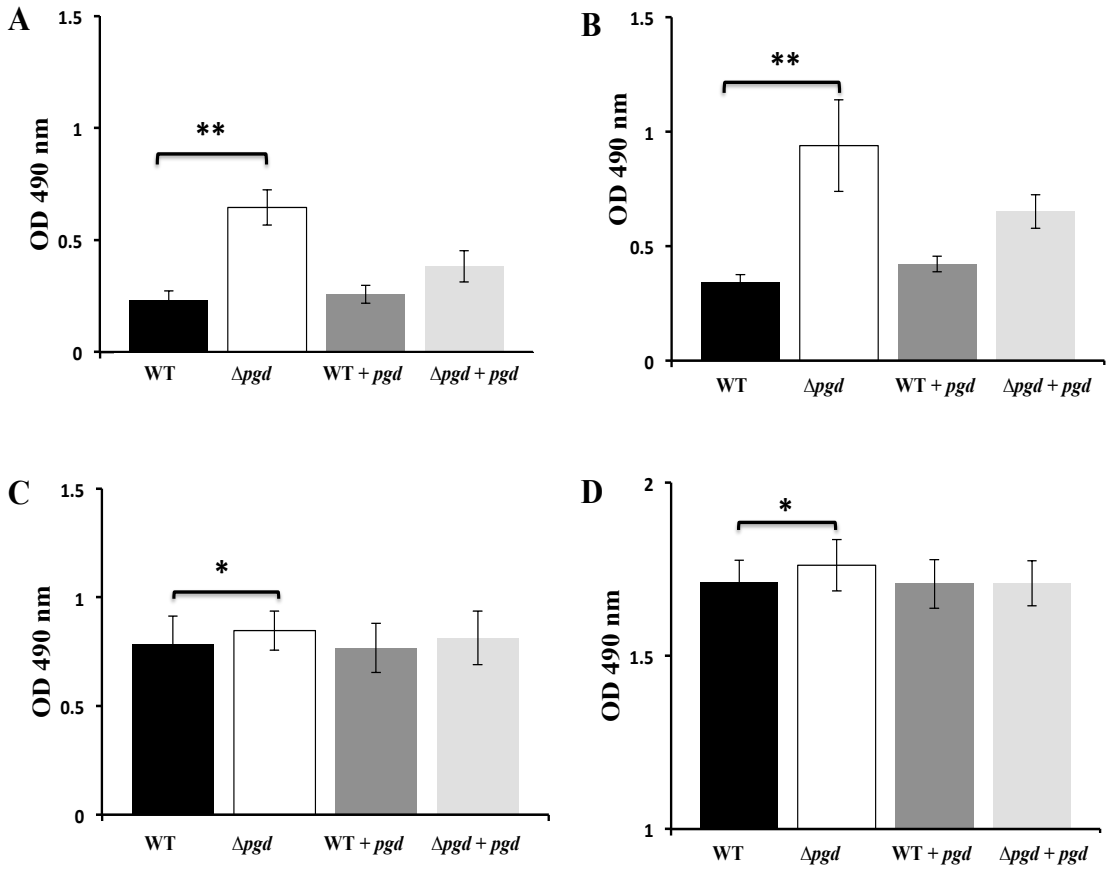

Fig. 5.9. *S. aureus* biofilm formation on a hydrophilic (tc-treated) polystyrene surface. *S. aureus* strains: (A) Newman, (B) SF8300 (C) SH1000 and (D) BH1CC were cultured at 37°C for 24 h in BHI supplemented with 1% (w/v) glucose. Plates were washed with dH_2O before staining with crystal violet dye. Next, 33% (v/v) acetic acid was added to extract the dye and OD_{490} was measured. Extracted dye values are presented for four strains in each graph: wild-type in (black), Δ*pgd* (white), wild-type plus pJAL-*pgd* [WT + *pgd*] (dark grey) and complementation strain *pgd* plus pJAL-*pgd* [Δ*pgd* + *pgd*] (light grey). A minimum of triplicate experiments were performed and error bars represent standard deviation. ** indicates $P<0.005$ value. Error bars are standard deviation with student's t-test used for statistical analysis.

5.6.7.1.3. Biofilm formation images by confocal laser microscopy (CLSM)

Since there was good evidence for increased biofilm production with Newman and SF8300 *pgd* mutant strains on a hydrophilic polystyrene surface, this was investigated further using poly-lysine-coated glass. The aim was to confirm the biofilm phenotype to enable further study using microscopy to examine the nature of the biofilm produced. Confocal laser scanning microscopy (CLSM) was combined with cell staining to visualise the biofilm, measure its thickness and examine cell viability. Paired strains were used in this experiment, Newman and SF8300 plus their *pgd* mutants. After culture of cells, as described above, the slides were washed and stained with the Live/Dead viability staining dye mixture (SYTO-9 and propidium iodide) and then immediately imaged using CLSM (Fig. 5.10). A greater depth of biofilm was produced by both *pgd* mutants, with a thickness of ~17-20 μm in comparison with their parental strains, which exhibited a thickness ~2-4 μm. Similar to several previous assays the complemented strains did not fully restore biofilm formation to the level of the parental strains but showed an intermediate phenotype.

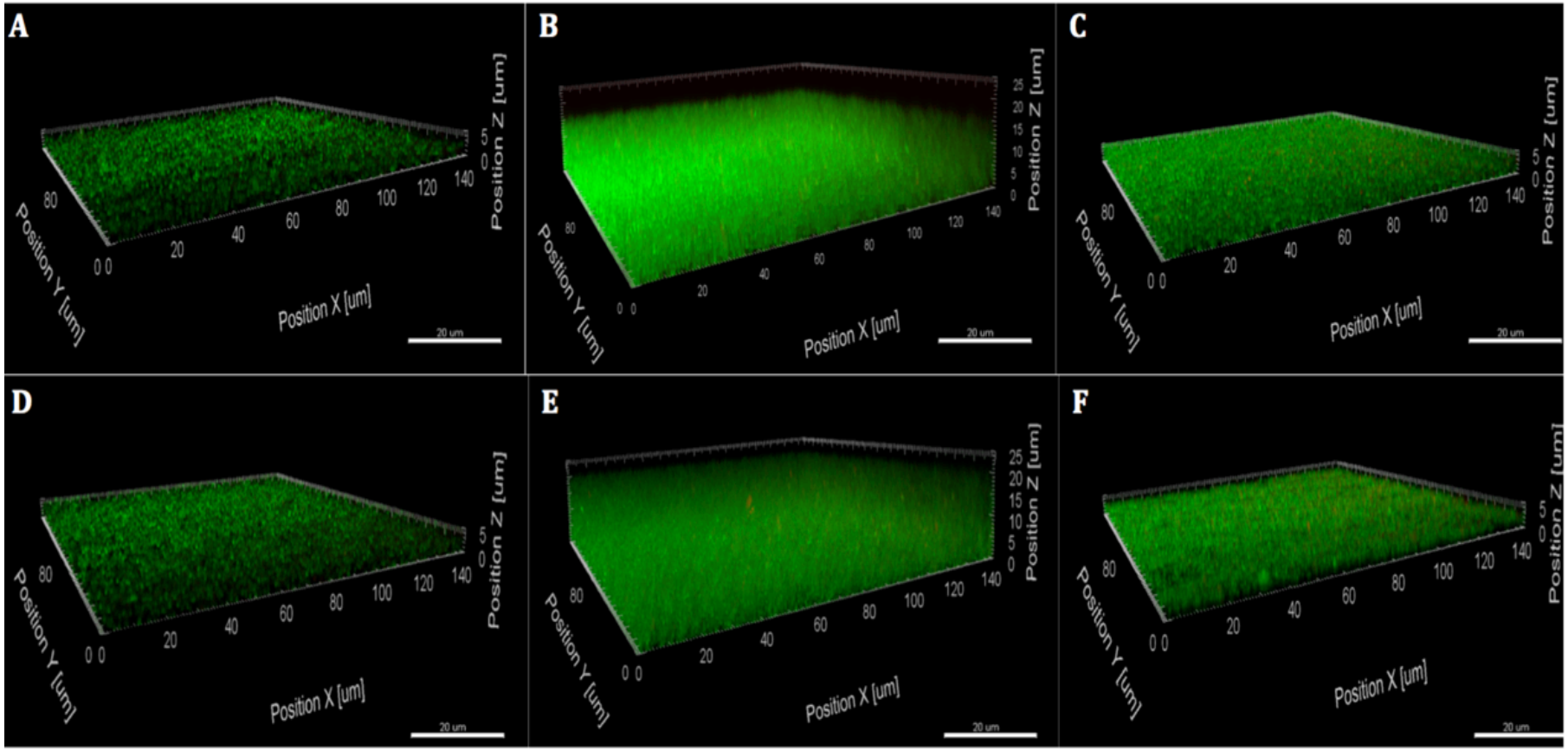

Fig 5.10. Confocal laser scanning microscopy (CLSM) imaging of *S. aureus* biofilm formation. Strain Newman (A-C) and strain SF8300 (D-F) were cultured on BHI supplemented with 1% (v/v) glucose at 37^{O}C for 24 h. Formed biofilms were stained with Syto9 and propidium iodide. 3D images were reconstructed from CLSM optical sections with Imaris software and thickness was measured using imageJ software**.** (A,D) wild-type; (B,E) Δ*pgd;* (C,F) Δ*pgd* with pJAL-*pgd.*

5.6.7.2. Hydrodynamic flow biofilm formation

While this study identified a biofilm phenotype for *pgd* mutation using standard methods of static biofilm formation, there has been a recent trend to investigate the formation of biofilm on a surface exposed to hydrodynamic flow using microfluidics. These conditions subject the forming biofilm to hydrodynamic shear within the continuous flow cell where biofilm forms and this can be visualised using light and fluorescence microscopy. Since this setup is considered to more closely resemble natural conditions under which biofilm assembly occurs it provided an important comparator for the previous assays that were performed in the study of Pgd. The BioFlux method was developed to be used also as a high-throughput (HTP) method for the screening of biofilm formation and viability (Benoit *et al.*, 2010). The surface within a bioFlux flow cell is a plate of glass that is plasma-treated to remove organic material, causing exposure of carbonyl and acetyl groups that generate a hydrophilic surface, but its properties alter to hydrophobic over time, as described by the manufacturer http://fluxionbio.com/bioflux/. For the study here, bioFlux flow cell biofilms were set up in collaboration with Nikki Black in the laboratory of Infectious Disease Microbiology at University of Ireland, Galway. Given the need to focus on one host strain for this part of the study, SF8300 was chosen to compare with its isogenic *pgd* mutant, complemented mutant and SF8300 with the *pgd* plasmid. In addition the role of *oatA* deletion in biofilm formation was assessed alone and in combination with *pgd* inactivation (SF8300 *oat*A; SF8300 *pgd oat*A).

The bioFlux system records biofilm development with video and from this recording still images were taken for each sample at time intervals. Three different cultural conditions were tested to examine biofilm development using the bioFlux system:

growth in BHI broth alone; growth in BHI broth supplemented with 1% (w/v) glucose; and growth in BHI supplemented with 4% (w/v) NaCl. Images were captured over the time-course once flow had begun.

None of the *S. aureus* SF8300 strains tested were able to form biofilm, neither in BHI alone nor supplemented with NaCl (data not shown) Both strains SF8300 (wild type) and SF8300 pJAL-*pgd* strains formed biofilm BHI medium supplemented with 1% glucose but, the latter strain forms greater amounts of biofilm formation at 18 h in comparison with former strain (Fig. 5.11). The wild-type strain, *S. aureus* SF8300 exhibits four steps to form biofilm, initial attachment between 0.5-1 h, microcolony formation evident at ~3 h, followed by development at (6 h) to fully formed biofilm at (12-18 h). Contrastingly, SF8300 *pgd* and the plasmid complementation strain SF8300 *pgd* pJAL-*pgd* were unable to form biofilm by 18 h, and visually appeared unable to remain attached to the glass in the bioFlux microfluidics channel. Complementation of *pgd* did not restore fully the capability to develop biofilm but there was clearly increased adherence to the channel surface after 6 h, indicating partially restored function (Fig. 5.11).

An unexpected finding was that both SF8300 *oat*A and SF8300 *oat*A *pgd* mutants were unable to form biofilm although their initial adherences appeared similar to wild-type. Both strains displayed adherence at 18 h (Fig. 5.11).

Discussion

Data obtained from the flow biofilm experiments were compared with that from the static biofilms and provided some clear contrasts between the same strains that need

explained from further study. For example, the SF8300 *pgd* mutant was able to form a biofilm in a tc-treated 96-well microtitre plate (static biofilm), however this mutant was not able to form biofilm under flow conditions although the media, BHI supplemented with 1% glucose, was the same in both experiments. The question raised is whether this discrepancy is simply due to material surface properties, such as hydrophobicity or charge, or just due to the hydrodynamic shear influencing the cells at the surface?

There is a precedent for the difference between the biofilm assay outcomes, where a similar situation was reported by Benoit *et al.*, (2010). Their study indicated a similar situation where a flow biofilm differed from a static biofilm in the study of *rpoS*-deficient *E. coli* that had impaired biofilm development under flow condition but biofilm developed in static conditions to an enhanced extent enhanced compared with its isogenic parent (Benoit *et al.*, 2010; Lee *et al.*, 2008). The reasoning proposed was that cell signalling is affected by hydrodynamic flow, particularly velocity and turbulence of the medium. A further possibility that might explain the difference comes from a study by Pozzi *et al* 2012, which indicated that in relative terms the surface of the glass bioFlux channel is more hydrophobic than the highly hydrophilic surface of a tc-treated polystyrene plate. In their study, they reported that MSSA clinical isolates cultured in BHI supplemented with glucose expressed a PNAG-dependent biofilm formation on a hydrophilic surface. In contrast, on a hydrophobic surface there formed a PNAG/Atl-dependent or complex biofilm that was also dependent on protein adhesins and eDNA (not solely dependent on PNAG). Other *S. aureus* surface proteins are reported to be associated with biofilm formation, including protein A, SasC, SasG, and biofilm-associated protein (Bap) in bovine

isolates, suggesting functional redundancy within the assortment of cell surface proteins contributing to biofilm and surface attachment (Pozzi *et al.*, 2012).

This study confirmed that the activity of *S. aureus* Pgd contributes to biofilm formation and this seems to be an indirect action by altering bacterial surface properties. While the consequential effect is unclear it may be due one or more factors, including release of eDNA from dead cells, alterations in expression or secretion of proteins concerned with biofilm formation and properties of peptidoglycan. The CFU of the *pgd* mutant, determined when the culture OD_{600} was 0.5, indicated that fewer mutant bacteria cultured on agar. The presence of fewer viable cells than the parent strain (data not shown), indicated either a plating defect or a greater number of dead cells. The latter explanation could implicate that eDNA involvement in the complex of biofilm formed by the *pgd* mutant on a treated plated. This could be confirmed by further investigation using DNase and protease to examine the biofilm that is formed.

The *oat*A mutant was shown to be less sensitive to lysozyme when combined with a *pgd* mutation (section 5.3.5). This study identified that *oat*A and *oat*A *pgd* mutants were unable to form biofilm on tc-treated plates but showed pronounced adherence on the glass of biofilux channel, indicating an important role of these genes in surface interaction, presumably arising from their roles in the modification of the peptidoglycan surface. Both *pgd* and *oatA* mutants need to be investigated further in new studies for their clear involvement in surface interactions and biofilm development.

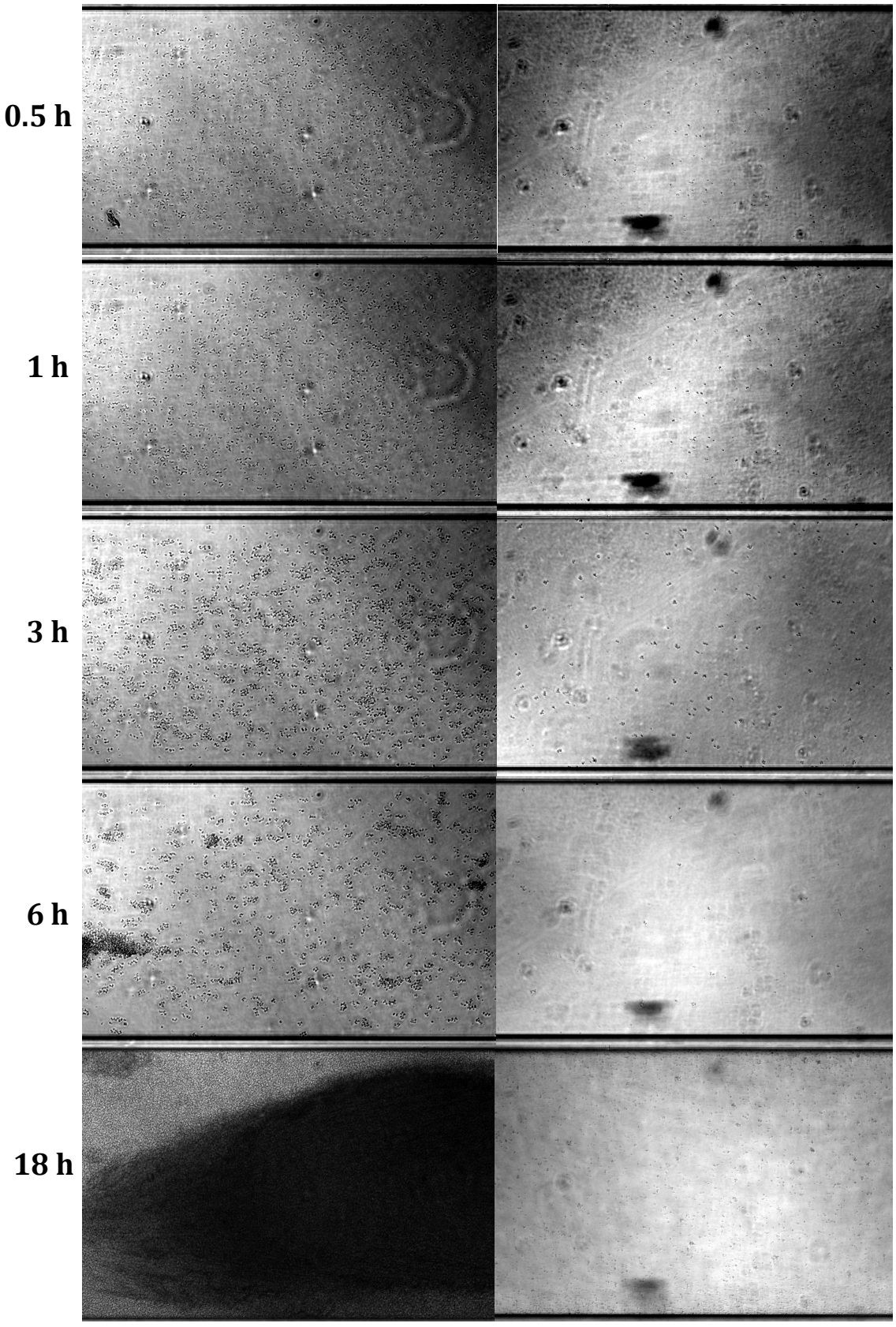
Sf8300 (WT) in Glucose
Mutant (Δpgd) in Glucose
0.5 h
1 h
3 h
6 h
18 h

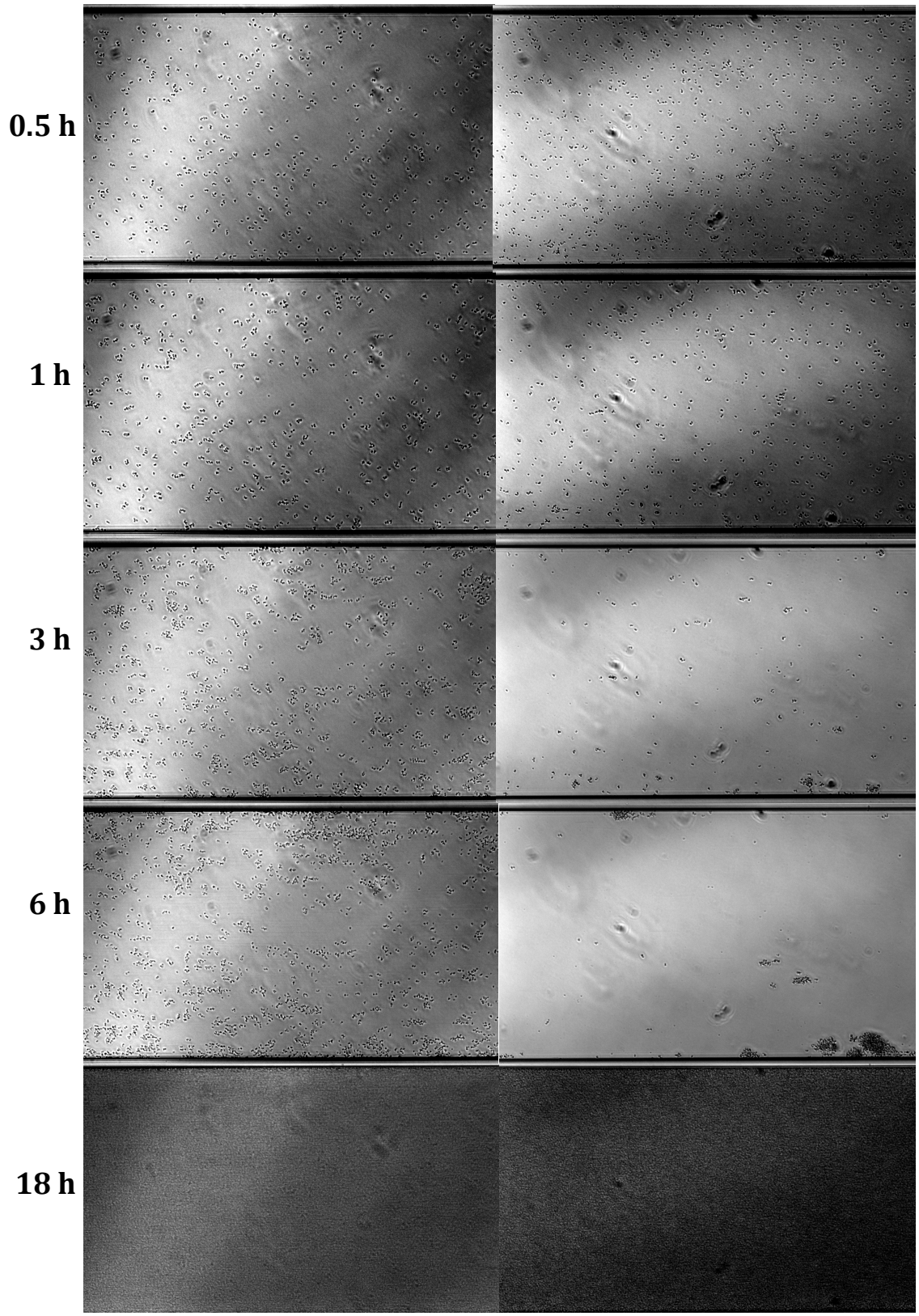
Mutant (*oat*A) in Glucose
Mutant (*oat*A *pgd*) in Glucose
0.5 h
1 h
3 h
6 h
18 h

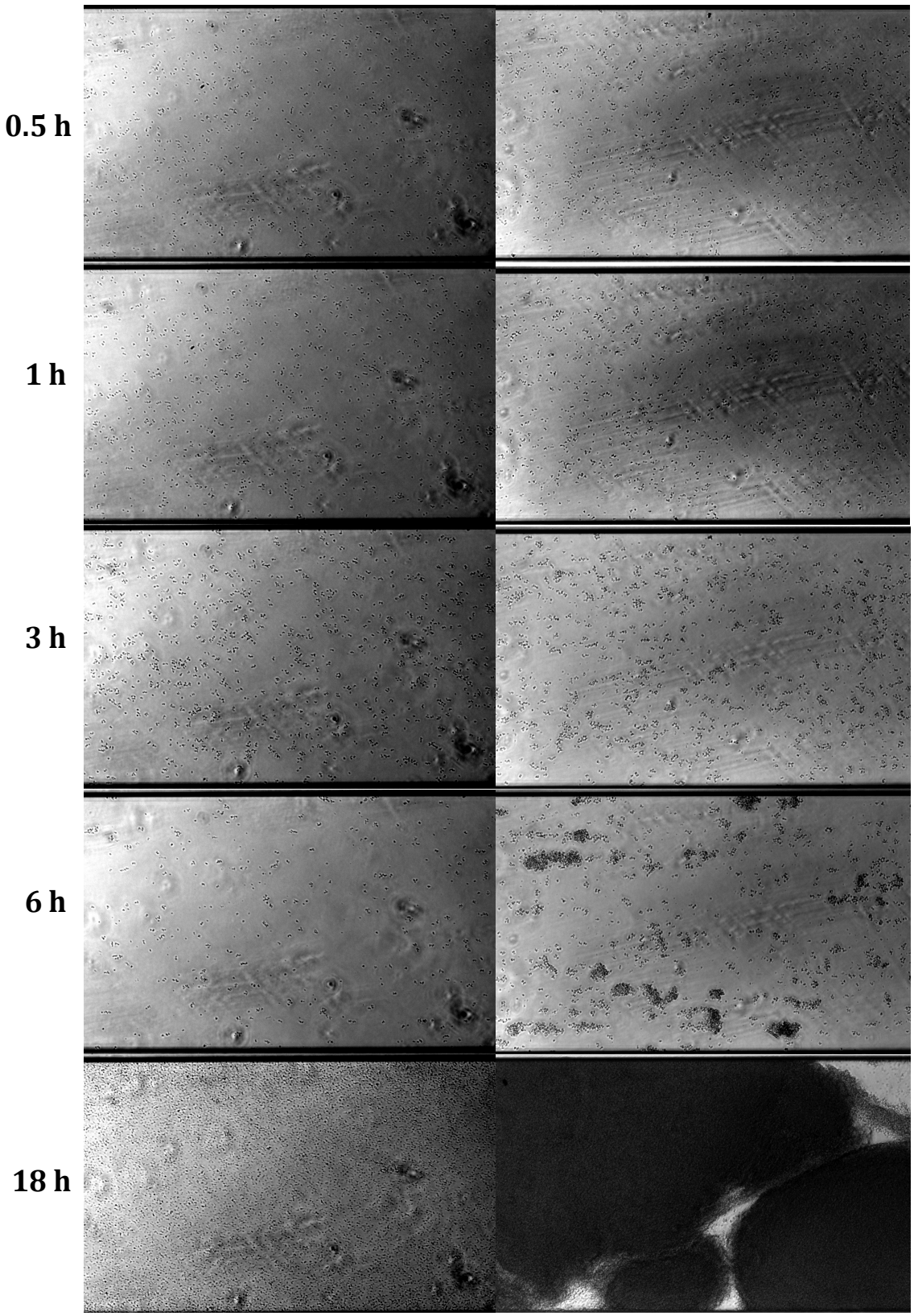
(Sf8300 pJAL-*pgd*) in Glucose
(Δ*pgd* pJAL-*pgd*) in Glucose
0.5 h
1 h
3 h
6 h
18 h

Fig. 5.11. Biofilm formation and development of *S. aureus* in bioFlux microfluid channel. Strains: SF8300 (WT) and isogenic mutants *pgd*, *oat*A and *pgd oat*A, SF8300+pJAL-*pgd* and *pgd*+pJAL-*pgd.* Cells were grown in BHI supplemented with 1% glucose. Images were captured over the time course once flow had begun. In comparison with the WT strain, initial attachment between 0.5-1 h, microcolony formation evident at 3 h, development at 6 h with maximally formed biofilm at (18 h). Each experiment was repeated with three biological replicates.

5. 6. 8. Alamar Blue assay

Alamar blue dye is a proprietary reagent consisting of resazurin, a non-toxic cell permeable compound, that is used extensively for assaying cytotoxicity and viability of cells, including yeast, fungi, bacteria and mammalian cells. Resazurin is a useful indicator to assess both cellular health and metabolic activity of cells, by indicating the energy capacity (ATP status) of cells (Rampersad, 2012). Since cell metabolic activity can be monitored by Alamar blue, it was used in this study to assess relative differences in the viability, cellular health and metabolic status of *pgd* mutants of strains Newman and SF8300 grown in broth media and compared with their parent strain. Overnight-cultured cells were harvested and suspended in 10 mL BHI (pH 7.2) broth until the OD_{600} reached 0.5. Next, 200 µL of cell suspension was mixed with 20 µL Alamar blue and incubated at 37 ^{O}C in the dark. A negative control (BHI plus Alamar blue) was included and for each sample the absorbance was monitored by measuring wavelengths at 570 nm and 600 nm, which represents the absorbance maxima of resorufin/resazurin (Fig. 5.12). The experiment was repeated at least 3 times.

The experiment indicated that Alamar blue was rapidly reduced by both wild type strains as evidenced by the medium turning pink in colour due to reduction of Alamar blue. In contrast, both *pgd* mutants were unable to reduce Alamar blue within 30 min. In addition, complementation of both the Newman *pgd* pJAL-*pgd* and SF8300 *pgd* pJAL-*pgd* strains fully restored metabolic activity, such that Alamar blue was again reduced to pink.

The Alamar blue assays revealed an unexpected alteration in the metabolism of the *pgd* mutants of both strains, Newman and SF8300 during exponential phase. This difference in the capacity for reduction of resazurin in the *pgd* mutants might explain the observed growth lag when the *pgd* mutants are cultured (section 5.3.1). The metabolism defect was fully complemented indicating the defect might be directly linked with Pgd activity. Although, the Alamar blue bioassay measured metabolism via the reduction/oxidation (redox) indicator and is used for assessing cellular health and metabolic function (Rampersad, 2012), it requires further investigation, including cfu quantification, to explain the link between the proposed cell wall function of Pgd and the apparent intracellular metabolism differences recorded here. A combination of proteomics and metabolomics approaches would be appropriate to gain insight.

A

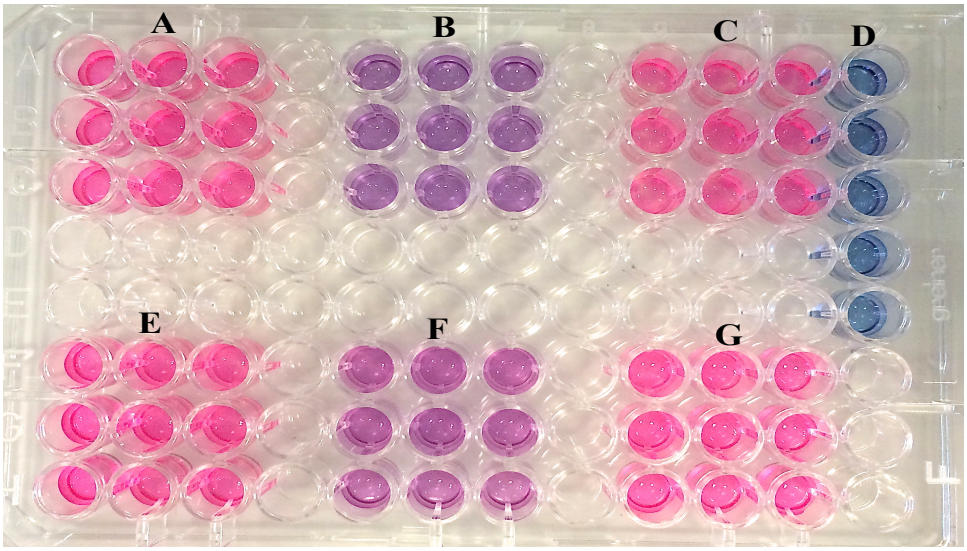

B

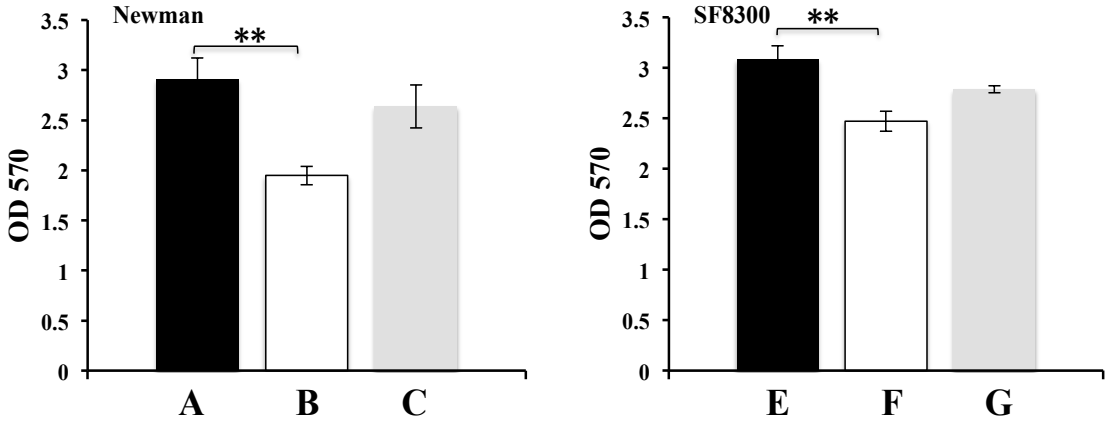

Fig. 5.12. Measurement of cell viability using Alamar blue assay. Overnight strains Newman (A-C) and SF8300 (E-G) were cultured to OD_{600}=0.05 in BHI and allowed cells to grow until around OD_{600}=0.5 nm. Next, the OD of culture was adjusted to OD_{600}=0.05 in BHI and then 10% Alamar blue was added to the culture and incubated at 37^{O}C for 30 min. Fig 5.14A- Colour change in response to chemical reduction was recorded at A_{570}**.** Fig 5.14B, Strains (A,E) wild-type; (B,F) *pgd;* (C,G) *pgd* with pJAL-*pgd* and (D) Control - BHI broth with 10 % Alamar blue. (D) The experiment displayed is representative of a minimum of triplicate experiments as indicated.

CHAPTER 6

6. Biochemical and biophysical analysis of *S. aureus pgd*

6. 1. Introduction

A putative *S. aureus* peptidoglycan deacetylase (Pgd) enzyme sequence belonging to the CE-4 esterase family was identified using bioinformatics methods, as described in chapter 2. Experiments presented in chapters 4 and 5 reveal that *pgd* deletion produces multiple phenotypes, such as a delay in growth, altered pigmentation, cell surface hydrophobicity, increased autolysis and increased resistance to lysozyme. Taken together these phenotypes indicate a cell wall modification that affects many properties and cell metabolism.

From the bioinformatic data it was predicted that Pgd protein is located at the cell surface via a lipobox sequence and may act in concert with other proteins. Pgd joins a set of surface-located protein activities, including TagO and OatA, that are responsible for peptidoglycan modification, and whose interaction and activity in relation to environmental conditions are incompletely understood. The research in this chapter was focused on attempts to investigate both biochemical and biophysical effects of *pgd* mutation to better understand the contribution made by the encoded activity in cellular processes and virulence.

6. 2. Materials and methods

6. 2. 1. Strains and growth condition

The *pgd* mutants and parent strains used in this chapter were descried previously (section 5.2.1).

6. 2. 2. Transmission electron microscopy (TEM)

Samples were prepared for TEM by using a modification of methods described for *S. aureus* (Fischer *et al.*, 2013). Strains were cultured overnight as described (section 5.2.2.); BHI broth was inoculated from overnight cultures to OD_{600}=0.05. Cultures were incubated at $37^{O}C$ with shaking until OD_{600} reached 0.2 then cells were harvested by centrifugation at 1500 rcf for 10 min. Next, cells were washed with PBS (pH 7.2) and then fixed in 2.5% (w/v) glutaraldehyde in 0.1 M cacodylate buffer, pH 7.2 for 3 h at RT. Next, cells were washed twice in 0.1 M cacodylate buffer, pH 7.2. Subsequently, cells were resuspended in molten 1% agarose (Sigma) at $37^{O}C$ and then agarose was solidified on wet ice for 15 min, followed by cutting the agarose contained sample into small pieces 1 mm cube. Next, cubes of agarose were treated with 1% (w/v) osmium tetroxide (Agar scientific, Essex) for one hour, and washed five times with dH_2O, and then treated with 1% (w/v) TAAB EM stain (uranyl acetate alternative) for 12 h at $4^{O}C$, followed by same washes with dH_2O. Next, samples were dehydrated in a series of 30%, 60%, 90%, 100% ethanol followed by two times cleared in 99.5 % propylene oxide (Aldrich). Cubes of agarose containing bacteria were washed again with a resin series dilution of 50%, 75% and then embedded into 100% resin (TAAB 812 Resin Embedding Kit, TAAB) followed by the incubation at RT overnight. Next, resin containing the sample was

cut into sections of 75 nm using an ultramicrotome (LEICA EM UC6, Leica). These sections were mounted on formvar 200 mesh copper grids (TAAB) coated with pioloform (SPI-CHEM, West Chester) and stained again with 4% (w/v) uranyl and Reynolds Lead citrate (sodium citrate and lead nitrate) before examining using a transmission electron microscope (FEI Tecnai T12 Biotwin -120 kv).

6.2.2.1. Dimensions and analysis of cells

Cells were randomly chosen and photographed. To determine the observed effects of *pgd* mutation on the cell wall (peptidoglycan) thickness, each cell was measured for its dimensions using TEM software (MegaView 3 analySIS). The measurements of a single bacterium were taken from the approximated middle of the vertical diameter and also for the cell wall thickness. These measurements were performed for n= 25 cells per strain and analyses were based on a minimum of 6 measurements for each cell.

6.2.3. Nuclear Magnetic Resonance spectroscopy (NMR)

Nuclear Magnetic Resonance spectroscopy (NMR) is a powerful device used for obtaining a wide range of information on the conformation, solvation and electronic structure of molecules, including the structure of cell wall peptidoglycan (Lapidot and Irving, 1977). In addition, NMR has been used to analysis lipoteichoic acids (LTAs), which is able to identify the methine group of the *sn*-glycerol repeating unit, d-alanine (d-Ala), *N*-acetylglucosamine (NGA), and fatty acids (e.g. CH_2 and CH_3). The average chain length of backbone and the degree of substitution are quantified directely by ^{1}H NMR spectrum (Morath *et al.*, 2001). Thus, this study, samples were

prepared and purified peptidoglycan from ruptured cells was analysed using NMR by Dr. Edwin Yates, Department of Biochemistry, University of Liverpool

6.2.3.1. Peptidoglycan isolation

The method used for the purification of PG was described by (Rosenthal and Dziarski, 1994). Two litre volumes of BHI broth were inoculated from overnight cultures of wild type *S. aureus* SF8300 or *pgd* strains and were grown until OD_{600} of ~ 0.8 nm (mid-exponential phase). Cells were then harvested at 1500 rcf for 10 min and washed with sterile PBS, followed by autoclaving for 15 min. The cells were then ruptured, using a French pressure cell at 15,000 psi six-times to obtain maximum breakage. Broken cells were harvested at 15900 rcf for 10 min and treated in SDS buffer, then boiled five times in SDTE buffer for 10 min (each time the pellet was collected at 21200 rcf for 10 min). The final collected pellet was boiled again and washed five-times in dH_2O. The peptidoglycan layer (PG) appeared as a white layer above the yellow cell debris. Peptidoglycan was then collected by gently shaking with sterile dH_2O followed by harvesting PG by centrifugation at 21200 rcf for 10 min and then resuspension in 2 ml sterile dH_2O. The turbidity was measured at OD_{660} and PG was stored at - 20 ^{O}C until use.

6.2.3.2. Peptidoglycan structural analysis by NMR spectra

The method used to digest PG was based on that reported by Eckert (Eckert *et al.*, 2006). An aliquot of 10 OD_{600} units of PG was incubated at 37 ^{O}C overnight with 45 µg mutanolysin (Sigma) with 0.1 mM $MgCl_2$ in 1 ml of phosphate buffer (pH 6). The

supernatant containing soluble muropeptides was collected after centrifugation at 21200 rcf for 30 min.

Soluble muropeptides were then freeze dried (LABCONCO) to remove excess water and replaced with deuterium oxide (HDO) (Sigma-Aldrich). Next, samples were loaded into a NMR tube (Wilmad, LabGlass) and examined by NMR spectroscopy. The ^{1}H NMR spectra were recorded on a Bruker Avance DPX300 NMR instrument at 300 MHz (300k) referenced to an external standard (TSP).

6.2.4. Pneumonia and bacteraemia infection models

6.2.4. 1. Ethics statement

This study was performed with the approval of and in strict accordance with the UK Home Office and the University of Liverpool ethics committee (Home Office Project License Number 40/3602 to Prof. Aras Kadioglu, University of Liverpool). Every effort was made to minimize suffering. All animal experiments were carried out at the Universities of Liverpool and handling/procedures were performed by Dr Elaine Waters, University of Liverpool.

6.2.4. 2. Infection experiments

Female CD1 mice aged 6-8 weeks and age matched (Charles River, UK) were used for both pneumonia and bacteraemia models. Bacterial inocula for infections were prepared by growing the bacteria in BHI (Oxoid) with shaking until the OD_{600} reached 3.0. Cells were harvested, washed in PBS and then adjusted to the

appropriate cell numbers for each procedure. Each experiment was repeated twice with 5 mice per group to give a total of 10 per group per time point. Statistical analysis was done using 2-tailed Student t-test.

6.2.4. 2. 1. Pneumonia model

For induction of non-lethal pneumonia, mice were anesthetised with a mixture of O_2 and isofluorane, and then inoculated intranasally (IN) with 2×10^7 CFU *S. aureus* SF8300 or isogenic SF8300 *pgd* in PBS.

6.2.4. 2. 2. Bacteraemia model

For induction of bactereamia, 5×10^6 CFU were injected into the tail vein (IV). Mice did not develop visible signs of disease and were culled at predetermined times post-infection by cervical dislocation.

Lungs and nasopharnx were collected for the pneumonia model while kidney, spleen, heart and blood were collected for the bacteraemia model. All organs and nasopharnx were homogenised, serially diluted and plated on either mannitol salt agar (lungs and nasopharnx) or blood plates.

6. 2. 5. Label free quantitative proteomics analysis

Proteomics of *S. aureus* cells was performed by the Centre for Protein Research at the Institute of Integrative Biology, University of Liverpool. *S. aureus* strains SF8300 (wild-type) and SF8300 *pgd* were cultured overnight as described (section 5.2.2). BHI broth was inoculated from overnight culture to OD around 0.05 and cells

grown until OD_{600} ~0.5. After, The culture was centrifuged at 1500 rcf for 10 min and the pellet washed with sterile PBS. Next, the pellet was resuspended in 100 µl of 25 mM ammonium bicarbonate (AMBIC).

To analyse for protein content, 0.05% RapiGest™ (Waters, Manchester) in 25 mM AMBIC was added and the samples were shaken at 1600 rcf for 10 min at 80°C. The samples were then reduced (addition of 10 µl of 60 mM DTT with incubation at 60 °C for 10 min) and alkylated (addition of 10 µl of 180 mM iodoacetamide with incubation at RT for 30 min in the dark).

6. 2. 5. 1. Protein digestion

Trypsin (Promega U.K. Ltd., Southampton, proteomics grade) was reconstituted in 50 mM acetic acid to a concentration of 0.2 µg $µl^{-1}$ and 10 µL was added to the samples prior to overnight incubation at 37 °C. The digestion was terminated and RapiGest™ removed by acidification (1 µl of TFA and incubation at 37°C for 45 min) and centrifugation (15,000 x g for 15 min). To check for complete digestion, each sample was analysed pre- and post-acidification by SDS-PAGE.

6. 2. 5. 2. LC-MS/MS analysis

For LC-MS/MS analysis, a 2µl (1 µg) injection was analysed using an Ultimate 3000 RSLC™ nano system (Thermo Scientific, Hemel Hempstead) coupled to a QExactiveHF™ mass spectrometer (Thermo Scientific). The samples were loaded onto the trapping column (Thermo Scientific, PepMap100, C18, 300µm X 5 mm), using partial loop injection, for seven min at a flow rate of 4 µl min^{-1} with 0.1% (v/v)

FA. The samples were resolved on the analytical column (Easy-Spray C18 75 µm x 500 mm 2 µm column) using a gradient of 97% A (0.1% v/v formic acid) 3% B (99.9% v/v ACN 0.1% v/v formic acid) to 70% A: 30% B over 120 min at a flow rate of 300 nl min^{-1}. The data-dependent program used for data acquisition consisted of a 60,000 resolution full-scan MS scan (AGC set to 3e6 ions with a maximum fill time of 100 ms) and the 18 most abundant peaks were selected for MS/MS using a 30,000 resolution scan (AGC set to 1e5 ions with a maximum fill time of 45 ms) with an ion selection window of 1.2 *m/z* and a normalised collision energy of 28. To avoid repeated selection of peptides for MSMS the program used a 30 s dynamic exclusion window.

6. 2. 6. Bradford Assay

The pellet was suspended in 200 µl of 25 mM AMBIC as described before, and then sonicated using a Sonics, Vibra Cell (Sonics & Materials, Newtown, USA) with a 250 µl to 10 ml probe. This was carried out in cycles of 10 s of 30% amplitude in each 60 s, to a maximum of 120 joules then stored at -80°C. Further the pellets from the wild type and mutant were suspended in 200 µl of 25 mM AMBIC and 10 µl of Rapigest detergent and heated to 80°C for 10 min. The protein content of wild type and *pgd* mutant were measured using a Bradford assay and ran 10 µl on PAGE.

The data was searched against *S. aureus* USA300 database using Mascot (Matrix Science, London, UK). A fixed carbamidomethyl modification for cysteine and variable oxidation modification for methionine were specified. A precursor mass tolerance of 10 ppm and a fragment ion mass tolerance of 0.01 Da were applied. The results were then filtered to obtain a peptide false discovery rate of 1%.

6. 2. 7. Complement deposition on *S. aureus*

Immunological assays were performed by Märtje Rujken in the laboratory of Dr Suzan Rooijakkers at Utrecht University, The Netherlands. To analyse C3b deposition on the surface of bacteria, *S. aureus* Newman (WT), Newman *pgd* and Newman *pgd* pJAL-*pgd*) were grown overnight in BHI with appropriate antibiotic as (section 5.2.2). Next, BHI broth was inoculated from overnight to OD_{600}=0.05, followed by allowing cells to grow until OD_{600}=0.5. Subsequently, the cells were harvested, washed and adjusted OD_{600}=1.0 in veronal buffer (2.5 mM $MgCl_2$, 0.5 mM $CaCl_2$) containing 1% (w/v) bovine serum albumin (BSA) to block nonspecific hydrophobic binding. Dilute 10x culture in veronal-buffered saline buffer (VBS++ 1% BSA, and then 50 µL from this dilution bacteria mixed, in 96-well round bottom plate, with series dilution of 0.0, 0.03, 0.1, 1, 3, 10 and 30 % serum followed by incubating at 37^{O}C for 30 min with shaking to allow complement deposition on the surface of the bacteria. Subsequently, the plates were centrifuged at 1320 rcf for 7 min and the supernatant removed. Next, 200 µL of 0.1% BSA in PBS was added to the cells and mixed followed by removing the supernatant. Afterward, 50 µL PBS+0.1% BSA with specific antibody (anti-human-C3 FITC-conjugated goat $F(ab')_2$ 1/50, Protos Immunoresearch, Burlingame, CA) added to cells and incubated for 30 min with shaking at 4 ^{O}C. Next, cells were washed with 0.1% BSA in PBS as before and finally 150 µL of this buffer was added to cells. A flow cytometer (FACS Verse, BD) was used to measure C3b deposition level on the surface of bacteria.

6. 2. 8. Bacterial killing in serum

Strains were grown from overnight cultures in BHI until $OD_{600=}0.5$ as outlined in (section 5.2.2.). Cells (1 ml) were harvested, washed and resuspended in 1ml sterile RPMI buffer plus human serum albumin (HSA), followed by diluting cells 10^4 ml^{-1}. Next, 50 µl of bacteria were mixed in an Eppendorf tube with 50 µl RPMI buffer, plus either 50% (v/v) normal human serum (NHS), 50% (v/v) heat-inactivated serum (HI) that is complement inactived, or NHS plus compstatin (10 µM). The tubes were incubated 37 ^{O}C with shaking for 60 min. Subsequently, 20 µl of incubated cells were mixed with 180 µl PBS in an Eppendorf tube with 50 µl RPMI buffer and plated immediately. Viability of strains was assessed by colony enumeration after serial dilution.

6. 2. 9. Neutrophil (PMN) killing assay

Strains were cultures as per section 5.2.1.2. Next, a culture was grown in BHI to $OD_{600=}1.5$ and then diluted as a starter culture 1:100 in 3 ml BHI in a 10 ml tube. Cells were grown to $OD_{600=}0.5$ nm (~ $2x10^8$ cfu ml^{-1}) at 37^{O}C with shaking at 500 rpm for about 2 h, followed by the opsonisation of bacteria for 15 min in a FACS tube at RT as follows: 175 µl RPMI buffer/HSA, 20 µl pooled human serum and 5 µl bacteria of $OD_{600=}0.5$. Subsequently, PMNs were diluted in RPMI (100 µl of 1E+07 PMN per ml and 900 µl RPMI-HSA) and added to the FACS tube as follows: 90 µl diluted PMN/RPMI buffer (or only RPMI buffer as control) plus 10 µl opsonised bacteria. For the zero time-point (pre-incubation), the mixture of cells was plated without incubation immediately on THA plates, while other samples were incubated at 37 ^{O}C with shaking at 500 rpm and the killing/growth was determined at time

points including 0, 30, 60 and 90 min. To stop the reaction, 900 µl/ml ice-cold MQ (milliQ water) plus 0.1% (w/v) saponin (S02) was added and incubated for 15 min at 4 ^{O}C, followed by viable counting. Finally, cells were also counted after overnight incubation at 37^{O}C.

6.3. Results and discussions

6.3. 1. Transmission electron microscopy (TEM)

As described in the previous chapter, this study observed that deletion of the *S. aureus pgd* gene in strains Newman and SF8300 strains led to altered surface properties. Pigmentation, hydrophobicity and surface attachment of the *pgd* mutant were affected and the mutation increased autolysis.

To examine further these surface-associated phenotypes, the *pgd* mutants of strain Newman and SF8300 were visualised by transmission electron microscopy (TEM) and compared with their isogenic parent strains. Cells were prepared for TEM (Section 6.2.2) and measured with the TEM-software Megaview 3 analySIS from photographic images at magnification of x60,000 (Section 6.2.2.1). Three independent experiments (biological replicates) were performed, with twenty-five randomly selected cells from each strain used to measure the cell diameter and the thickness of the extracellular cell wall.

The results obtained from TEM indicate that inactivation of *pgd* in both *S. aureus* Newman and SF8300 led to a decrease peptidoglycan thickness of around 25%

compared with parent strains. (Fig.6.1.). Mean peptidoglycan thickness of Newman, and SF8300 and Newman *pgd*, SF8300 *pgd* were 23.37 nm, 22.49 nm, 34.08 nm and 33.03 nm, respectively (Table.6.1.). The differences between cell wall thickness of wild type and mutant was statically significant ($P< 0.001$), using students' two-tailed *t*-test.

Discussion

Given the previously described differences with cell autolysis, there is the possibility that *pgd* mutants of both Newman and SF8300 lysed more rapidly and to a greater extent compared with their parent strains due to the reduced peptidoglycan thickness. Various relationships between cell wall thickness and autolysis have been previously reported. For example, a correlation between susceptibility of strain SF8300 to vancomycin, its cell wall thickness and autolysis was previously reported. In one case the vancomycin-sensitive parent strain (MIC 1µg/ml; A1-VSSA) was compared with a clone with reduced susceptibility to vancomycin (MIC 8µg/ml; A2 – VSIA) strains. The A2 –VSIA clone presented a significantly thicker cell wall (~50 nm) and reduced autolysis following Triton X-100 challenge compared with its parent A1-VSSA (cell wall ~ 40 nm) (Passalacqua *et al.*, 2012). In addition, a further study compared the VISA strain Mu50 with the heteroresistant hVISA strain Mu3 indicated that multiple distinct SNPs in the two-component regulator system gene *graR* (up to 16 mutations) and especially that leading to the amino acid change (N197S) converted hVISA Mu3 into VISA strain Mu50, in turn producing enhanced cell wall thickness and decreased autolysis (Howden *et al.*, 2010).

Table. 6. 1. Cell wall dimensions measured using transmission electron microscopy (TEM).

Strain	Cell diameter (nm)*	Cell wall thickness (nm)*
Newman	1004.71 ± 56.95	34.08 ± 3.62
Newman *pgd*	963.87 ± 46.60	23.37 ± 2.63
SF8300	993.83 ± 51.85	33.03 ± 3.07
SF8300 *pgd*	910.61 ± 64.43	22.49 ± 2.44

*The measurements (nm) are mean ± standard deviations.

The value for strains Newman *pgd* and SF8300 *pgd* were significantly different (*P*< 001) from their isogenic parent strains using Students two-tailed t-test.

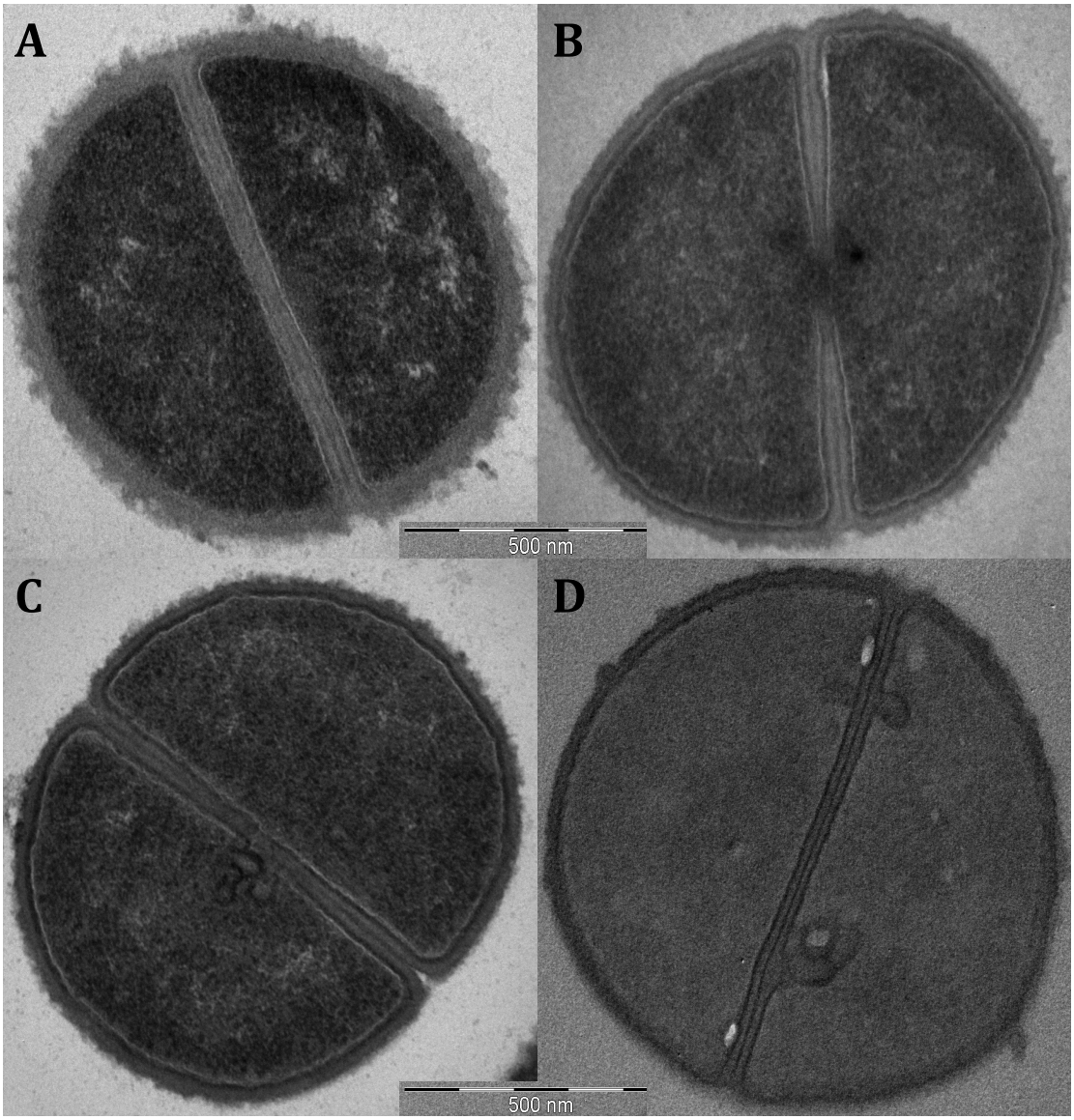

Fig. 6. 1. Cell dimensions measured by transmission electron microscopy. Representative TEM images at x60,000 of mid-exponential growth phase cells from strains Newman (A), Newman *pgd* (B), SF8300 (C) and SF8300 *pgd* (D). Measurements of cell wall thicknesses are given in Table 6.1**.**

6.3. 2. Nuclear magnetic resonance spectroscopy (NMR)

The molecular structure of peptidoglycan was studied by NMR spectroscopy to investigate the extent to which the *pgd* gene contributes to those features that can be distinguished using this technique. Samples were prepared and purified

peptidoglycan from ruptured cells was analysed using NMR by Dr. Edwin Yates, Department of Biochemistry, University of Liverpool. The ^{1}H NMR signals arising from 5mg of mutanolysin-digested peptidoglycan were consistent with assignments reported in the literature for specific structural component moieties (Morath *et al.*, 2001). The ^{1}H NMR signals arising from N-acetyl glucosamine (NAG) between 2.0 and 2.15 ppm were integrated and measured employing iNMR software. The NAG signal was twofold increased in the strain SF8300 *pgd* mutant compared with the wild-type SF8300 strain. It was noticeable that other signals were also increased, including those corresponding to CH_2 at 1.7 ppm and d-Ala at 4.3 ppm, which were increased ~1.5 and ~1.75-fold, respectively. Experiments were repeated at least three times and the error bars are indicated.

Discussion

The data obtained from the NMR analysis indicated that *pgd* deletion led to increased acetyl groups on the peptidoglycan and this would be predicted given the bioinformatics analysis of the *S. aureus* Pgd protein sequence (Chapter 2.). Thus, the increasing signal of NAG, is a result of overproduction of $COCH_3$ (CH_3) in the peptidoglycan sample. However, the peptidoglycan structure is composed of two sugars; N-acetyl glucosamine (NAG) and N-acetyl muramic acid (NAM), and both possess N-acetyl (and hence, CH_3) groups. This study suggests that the peptidoglycan has been affected through reduction of Pgd-dependent deacetylation, but needs further investigation to determine the extent to which the N-acetyl CH_3 group was increased in the peptidoglycan structure. Particularly noticeable is the O-acetyl group (1.9 ppm), which was shown to be increased twofold and also relevant to this analysis is the increased ratio of CH_2:CH_3 in the *pgd* mutant.

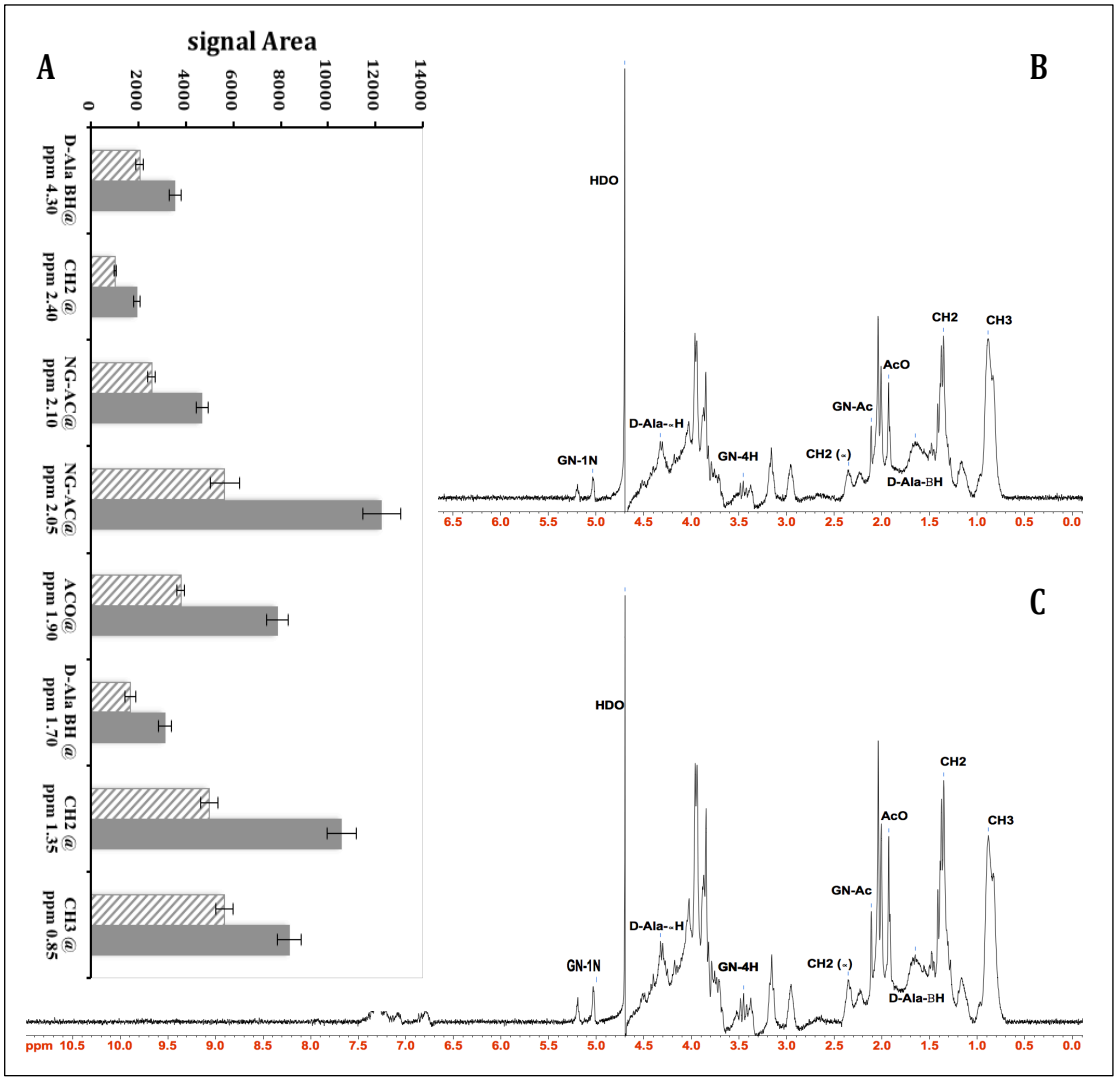

Fig. 6.2. Peptidoglycan structure of *S. aureus* SF8300 and an isogenic *pgd* mutant using NMR spectroscopic analysis. Experiments were repeated in triplicate from individual biological replicates and the mean values (**A**) were determined, SF8300 (stippled grey) and SF8300 *pgd* (grey). The signals 2.0-2.15 ppm are assigned to the acetyl group ($COCH_3$) of N-acetyl glucosamine. NMR spectra of SF8300 (**B**) and *pgd* mutant (**C**). Error bars are standard deviation.

6.3. 3. Investigating the role of Pgd in virulence using infection models

S. aureus is a pathogen that can cause a wide variety of infections, such as pneumonia, sepsis and skin infection. The pathogenicity of this bacterium is dependent on multiple virulence factors including cell wall-anchored (CWA) proteins, polysaccharide and toxins as discussed in the thesis introduction.

The peptidoglycan analysis of the *pgd* mutant described in the previous section, together with the altered extent of TEM-visible cell wall might indicate that the surface protein presentation and thus virulence factor of the strain might be altered, To investigate this possibility, the *pgd* mutant was compared with its isogenic parent using pneumonia and bacteraemia infection models, Samples of SF8300 and SF8300 *pgd* were prepared and used to inoculate CD1 mice (Table. 6. 1.), by Dr. Elaine Waters, Institute of Infection and Global Health, University of Liverpool.

6.3. 3. 1. Pneumonia model of infection

CD1 mice were challenged by intranasal (IN) administration with $2x10^7$ CFU *S. aureus* SF8300 or SF8300 *pgd.* The lungs and nasopharynx were collected after 12 and 48 h and the viable bacteria counted. A marginal decrease was determined in the CFU of *pgd* mutant cells in both nasopharynx and lung at 12 h, but this was not significant in comparison with parent strain, SF8300 (Fig. 6. 3. 1.). After 48 h, the CFU of the *pgd* mutant was again marginally and non-significantly decreased in the nasopharynx. In contrast, the pgd mutant was significantly decreased in number in the lungs after 48 h. The reason for this is unclear but could relate to differences in

cell persistence due to changes in the cell surface and interactions with the host. These changes could also impact on survival from the immune system of mouse.

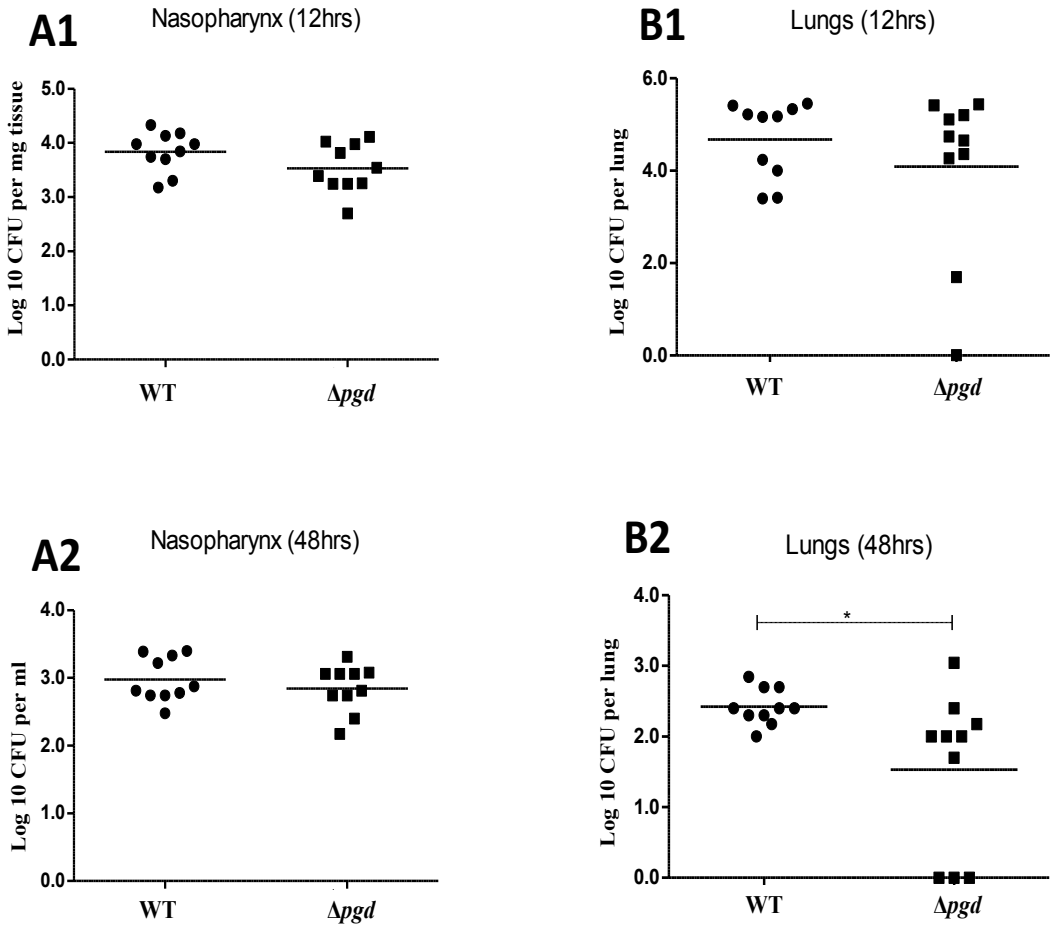

Fig 6.3.1. Bacterial burden after intranasal inoculation with *S. aureus* SF8300. CD1 mice were intranasally inoculated with 2×10^7 CFU of SF8300 (circle) or SF8300 *pgd* (square). Bacterial numbers in the nasopharynx were determined after 12 h (**A1**) and 48 h (**A2**), and in the lungs after 12 h (**B1**) and 48 h (**B2**). Each experiment was repeated twice with 5 mice per group to give a total of 10 per group per time point. Horizontal lines refer to the mean value for each group and each symbol indicates an individual animal. * indicates $P< 0.05$.

6. 3. 3. 2. Bacteraemia (sepsis) model of infection

CD1 mice were challenged by intravenous administration with $5x10^6$ CFU of *S. aureus* SF8300 or SF8300 *pgd*. Bacteria were recovered from kidney, spleen, heart and blood at two time points post-inoculation: 18 h and 7 d, by organ disruption followed by enumeration on agar (Fig 6. 3. 2). Across the various organs that were harvested it was determined that there was no significant difference in bacterial numbers after 18 h with the CFU of the *pgd* mutant similar to that of the parent. After 7 d, however, there were significantly ($P<0.05$) fewer CFU of the *pgd* mutant recovered from the spleen, but no significant differences in the numbers between the *pgd* mutant and parent for the other organs.

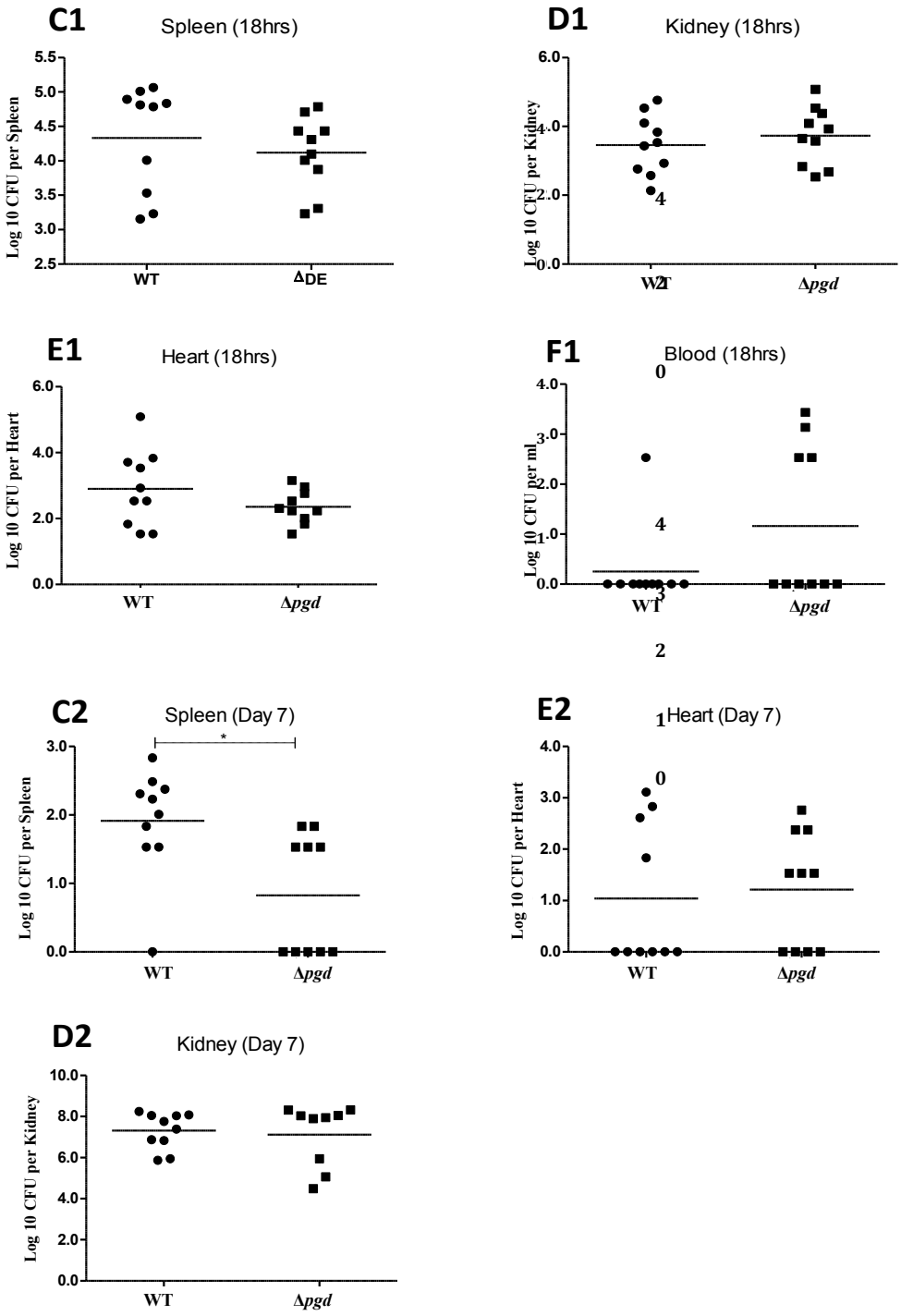

Fig. 6.3.2. Bacterial burden after intravenous inoculation with *S. aureus* SF8300. CD1 mice were injected into the tail vein with 5×10^6 CFU of SF8300 (circle) or SF8300 *pgd* (square). Bacteria were enumerated from recovered organs after 18 h (C1-F1) or 7 d (C2-E2): spleen at 18 h, 7 d (C), kidney 18 h, 7 d (D), heart 18 h, 7 d (E), and blood at 18 h (F1). Horizontal lines refer to the mean value for each group and each symbol represents an individual mouse. **P*<0.05 indicated.

Discussion

There were clear reductions in the survival of the *pgd* mutant in two of the models of infection studied. The reason for the reduced bacterial numbers recovered with the mutant is not clear given the finding of differential survival in the lungs and the spleen. The observed differences in the cell surface that were described above might account for the phenotype, but further experiments are necessary to reveal the defects encountered with the mutant as they actually relate to these niches. The necessary virulence factors for extended survival at these sites might be reduced on the mutant cell surface altering colonisation, immune evasion or replication.

6. 3. 4. The contribution of Pgd to host immune survival.

The complement system signals to the innate defence mechanisms that there are invading microorganisms like *S. aureus* present. The activation of complement leads to a labelling of the bacterial cell surface with the opsonins C3b and iC3b, which promotes neutrophil phagocytosis. To investigate whether Pgd has a role in defence of *S. aureus* from opsonophagocytosis, the strains Newman, Newman *pgd* and Newman *pgd* pJAL-*pgd*) tested. Three separate experiments were performed in collaboration with Dr Suzan H. M. Rooijakkers (Medical Microbiology, University Medical Center, Utrecht, the Netherlands: C3b deposition level, *S. aureus* killing in serum and neutrophil (PMN) killing assays.

6. 3. 4. 1. Complement deposition on *S. aureus*

The immunological study first analysed deposited C3b on the bacterial surface, using a specific antibody specific for human C3. Samples were prepared as described (section 6.2.7) and the amount of C3b was measured using flow cytometry. The

assay revealed a dose-dependent relationship between the amount of serum and the extent of C3b deposition on the cell surface of *S. aureus* Newman, in which, the level of C3b molecules gradually increased with increasing serum levels from 0.03 - 30 % (Fig. 6. 4.). It was also determined that the level of C3b on the surface of *pgd* mutant was not statistically significantly different at any serum concentration.

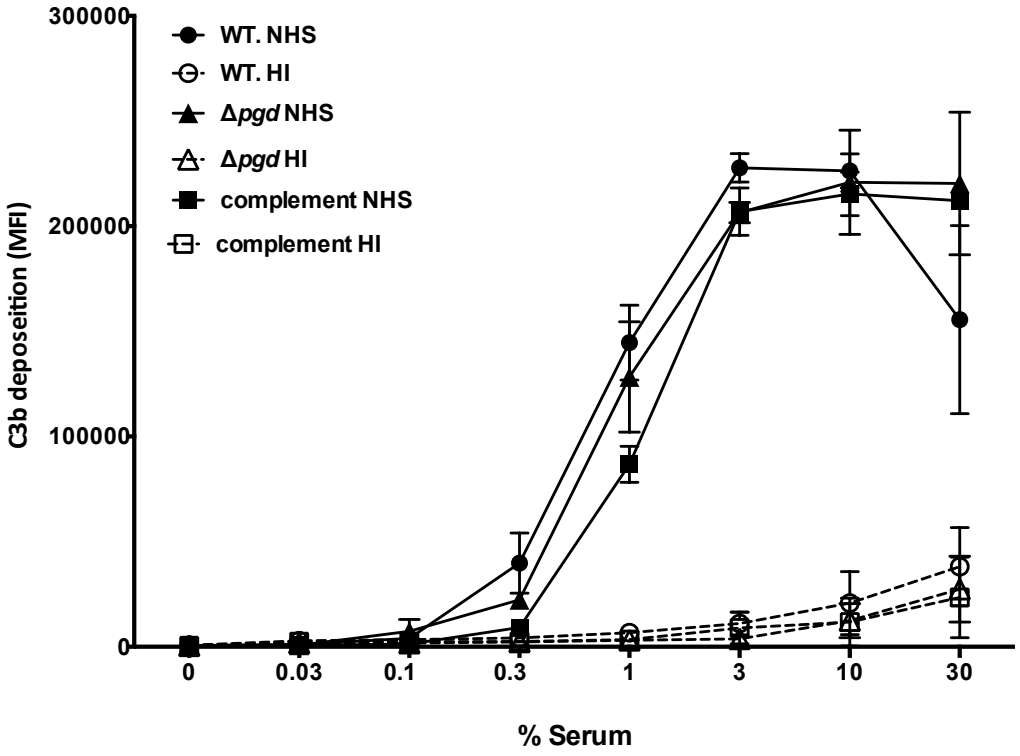

Fig. 6.4. Complement deposition on *S. aureus*. The levels of C3b deposition on strains Newman (circles), Newman *pgd* (triangles) and Newman *pgd* pJAL-*pgd* (squares) was measured by flow cytometry after incubation in the absence or presence of normal human serum or heat-inactivated (HI) serum. Data represents the mean and standard error of three individual experiments.

6. 3. 4. 2. *S. aureus* survival in human serum

To evaluate the contribution of Pgd to survival of *S. aureus* Newman in human serum the *pgd* mutant and complementation strains were compared with their isogenic parent. The relative survival of these strains was determined after incubating these strains for 1 h at 37^{O}C with either normal human serum (NHS), heat-inactivated (HI) serum or NHS plus compstatin (Fig. 6. 5.). Viability was assessed by the Miles and Misra method, to determine colony forming unit (CFU) after overnight incubation at 37^{O}C (section 6.2.8).

Comparable levels survival were observed across all of the strains examined revealing that the *pgd* mutant is not affected by the activity of complement in serum, at least under the conditions studied in the described assay. The presence of the C3 inhibitor compstatin did not affect relative survival, where this compound was included to evaluate if there were complement-independent affects on serum survival.

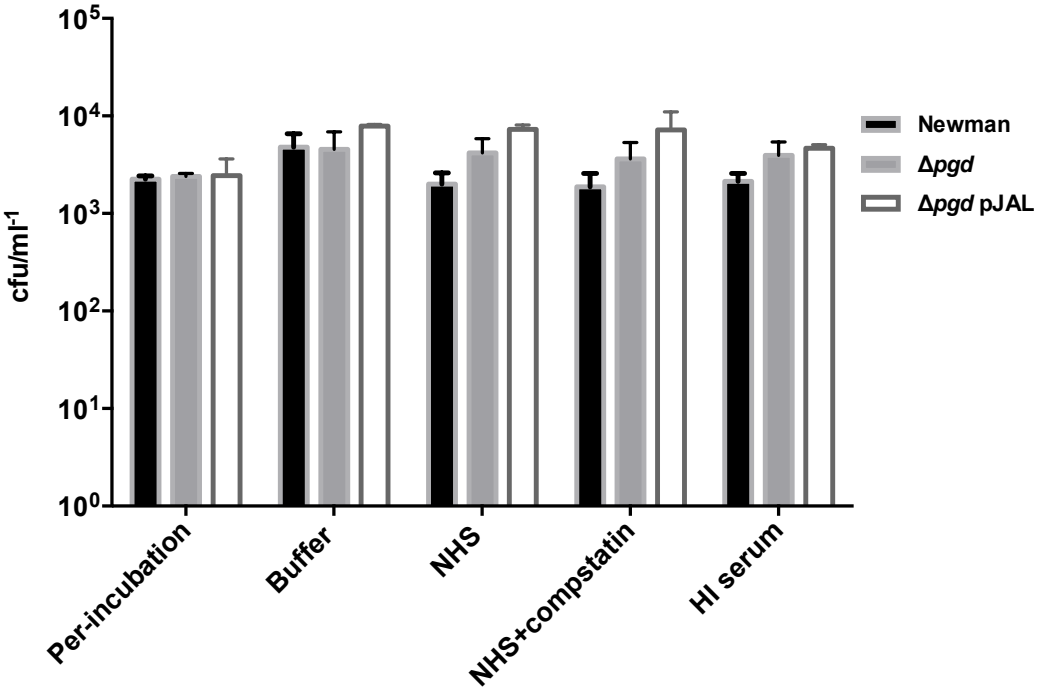

Fig. 6.5. *S. aureus* survival in the presence of human serum. The viability of *S. aureus* strains was assessed after incubation for 1 h with 50% (v/v) NHS, HI serum or NHS + compstatin (10 mM), with serum and incubation controls. Data represents the mean CFU ± standard error of the average of three experiments.

6. 3. 4. 3 Neutrophil (PMN) killing assay

A further experiment was performed to investigate the effect of Pgd in immune survival by testing neutrophil killing in an opsonophagocytosis assay. Freshly isolated neutrophils (PMN) from human volunteers were added to NHS-opsonised *S. aureus* strains and the viability of each strain were determined by lysing the neutrophils and enumeration using the Miles and Misra method (section 6.2.9). It was determined from this assay that *S. aureus pgd* was killed faster than its isogenic Newman parent strain by neutrophils at 60 min and 90 min of incubation (Fig. 6. 6.). This reduced survival was statistically significant at these time points using the

students *t*-test $P<0.05$. In this assay, as with several other assays, the *pgd* complementation strain did not show restored viability (*S. aureus pgd* pJAL-*pgd*).

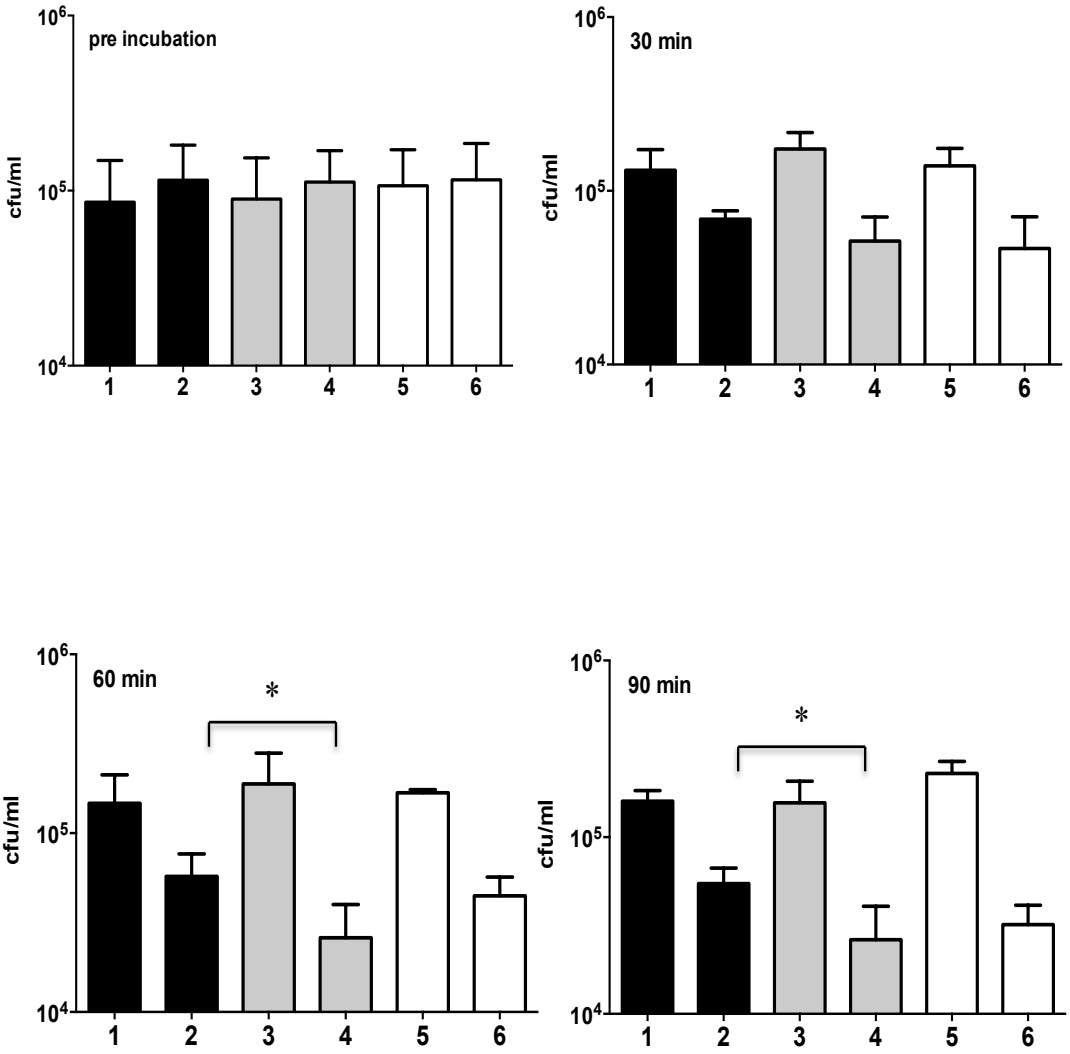

Fig. 6. 6. Neutrophil killing of *S. aureus*. Bacterial viability (CFU ml^{-1}) was assessed for PMN survival at the indicated times with NHS-opsonised *S. aureus* Newman (black), Newman *pgd* (grey) and Newman *pgd* pJAL-*pgd* (white). Assay controls, strains incubated with only RPMI buffer are labelled 1, 3 and 5, and those incubated with PMN are labelled 2, 4 and 6). Data represents the mean number of recovered colonies ± standard error of three separate experiments, using student's *t*-test.

Discussion

C3b molecules can randomly attach via amine group or hydroxyl groups on the cell surface, and deposition of C3b is an important part of innate immune defence leading to opsonophagocytosis (Berends *et al.*, 2013). In addition to opsonisation from activated serum proteins of the complement cascade, neutrophils can recognise peptidoglycan (PG) structure by binding via the PGRPb receptor (An *et al.*, 2013; Kobayashi *et al.*, 2005; Liu *et al.*, 2000). This study assessed the level of deposition of C3b and observed no significant difference between the *pgd* mutant and parent strain, suggesting C3b binding despite the observed differences in structural composition by NMR and the reduced cell wall thickness.

The neutrophil killing assay in contrast indicated that *pgd* mutant was killed more rapidy than the wild-type strain which might indicate that either phagocytosis was greater with the *pgd* mutant or that once phagocytosed the bacteria were more rapidly killed. Thus, so far, this study suggests that the *pgd* mutant killing is not directly related to opsonisation or serum killing, but could result from increased ability of the neutrophils to recognise PG directly e.g. via its PGRPb receptor, another serum factor(s) or an increased killing rate after phagocytosis. Since the *pgd* mutant exhibits less thick PG and lyses faster under stress of Penicillin G and Triton, it could be most likely that the mutant is digested by PMN faster than the parent strain or killing by antimicrobial molecules that are release from neutrophils (granular and/or via NETs) during interactions with bacterium (see section 1.1.2.6.).

6. 3. 5. Proteome analysis of *S. aureus pgd* using label-free quantitative analysis

The proteome includes all translated proteins and this term was used first by Marc Wilkins in 1994 meaning "the protein complement of the genome" (Wasinger *et al.*, 1995). The term proteomics describes the analysis of proteins on a large scale, being a complement derived from a cell fraction, organelle, whole cell or community. Global methods for proteomic analysis include gel-free and gel-based techniques. The latter method can be used to pre-fractionate, a complex protein mixture by using gel electrophoresis. More recent advances use gel-free techniques and these methods now typically employ chromatographic separation after digestion of proteins using the protease trypsin. Peptide analysis is achieved by liquid chromatography mass spectrometry (LC-MS) that utilises nano-flow liquid chromatography based on affinity separation coupled to tandem mass spectrometers (LC-MS/MS). Trypsin is used in most mass-spectrometry based proteomics, because of the ease and reliability of converting a protein mixture into peptide fragments by C-terminal cleavage of peptide bonds between K and R residues (Eng *et al.*, 1994; Olsen *et al.*, 2004).

On the basis that the described results revealed altered peptidoglycan and cell metabolism of the *pgd* mutant, the study aimed to quantify any differences in the protein complement of the *pgd* mutant compared with its parent. It was hypothesised that this approach might answer the questions as to what were the underlying bases for the metabolic and cell surface changes of the *pgd* mutant.

The strains SF8300 and SF8300 *pgd* were cultured and washed and the whole cells were trypsin digested and separated using an Ultimate 3000 RSLC system coupled to

a QExactiveHF mass spectrometer (section: 6. 2. 5.). This work was performed at University of Liverpool in collaboration with Dr. Josephine Moran (Microbiology) and Dr. Lynn McLean (Biochemistry) from The Institute of Integrative Biology. Five biological samples for each strain were analysed and the differential protein abundance was determined.

Bradford assay indicated that the total of protein content of the digest for SF8300 *pgd* was 0.126 μg μl^{-1} and the wild type strain, SF8300 was 0.181 μg μl^{-1}. The protein identification based on the peptide analyses using LC-MS/MS methods enabled differential protein quantitation between both strains (Table 6. 2.a-b). Comparison of the peptide datasets revealed a total of 33 proteins that were identified as being differentially expressed; significance was based upon Anova with $P<0.05$ and with a 1.5-fold increase or decrease in expression.

The SF8300 *pgd* strain dataset revealed that out of the 33 differentially expressed proteins 11 were present at increased levels including the cell surface proteins IsaA, FnbA and SdrE (Table 6. 2.a.), while 22 proteins were present at decreased number including Spa, PBP2a, SarS and Sbi (Table 6. 2.b.).

Table 6.2.a. Proteins with increased expression in SF8300 *pgd* using quantitative proteomics. Eleven proteins in the proteome of SF8300 *pgd* were increased in comparison with its isogenic parent, SF8300. Five separate culture samples were assayed for each strain with two peptides being the minimum for searching. Values are the average between samples and *p*-value determined using Anova.

ID	**Peptides**	**Score**	***P* value**	**Fold**	**Protein name**
Q2FDZ7	6	263.19	0.000044	3.19	FeoB
Q2FHR7	6	356.83	0.00118	2.42	ArcC1 Carbamate kinase
Q2FDL8	2	61.5	0.00417	2.22	PTS IIABC mannose
Q2FDT8	5	409.01	0.0000453	2.2	IsaA
Q2FES7	2	56.22	0.00931	2.18	BudA (AlsD)
Q2FE03	17	1397.52	0.00236	1.96	FnbA
Q2FHN1	2	48.35	0.03	1.77	Unknown
Q2FJ77	22	1406.1	0.000205	1.74	SdrE
Q2FKI1	4	219.36	0.04	1.64	Lipoprotein
Q2FFB7	2	120.25	0.00609	1.56	RecT recombinase
Q2FJI3	2	53.61	0.04	1.53	Sodium-dependent transporter

Table 6. 2.b. Proteins with decreased expression in SF8300 *pgd* using quantitative proteomics. Twenty-two proteins in the proteome of SF8300 *pgd* were decreased in comparison with its isogenic parent, SF8300.

ID	Peptides	Score	*P* value	Fold	Protein name
Q2FJH8	3	162.56	0.0000498	3.65	Methionine ABC transport protein
Q2FKD2	6	547.52	0.0000016	3.63	Diacetyl reductase (ButA)
Q2FKE8	28	3103.13	0.000105	3.16	Protein A (Spa)
Q2FG28	7	687.07	0.000155	2.47	Universal stress protein (UspA)
Q2FK44	33	2787.51	0.0000261	2.41	Acetyltransferase (PflB)
Q2FDV8	20	1247.24	0.02	2.27	Clp protease ATP-binding subunit ClpL
Q2FDZ1	11	654.93	0.00157	2.16	Lantibiotic ABC transporter
Q2FK74	6	317.87	0.000333	2.02	Pyruvate decarboxylase (IpdC)
Q2FJ31	14	1234.37	0.00849	1.92	Alcohol dehydrogenase (Adh1)
Q2FJZ0	21	1441.99	0.000166	1.83	Unknown
Q2FIN9	5	271.49	0.00223	1.77	Ribosome-associated factor Y
Q2FDR6	2	77.19	0.00396	1.73	AAA ATPase
Q2FDG7	2	55.64	0.00151	1.71	2-oxoglutarate translocator
Q2FHW6	32	1764.34	0.02	1.65	Pyruvate carboxylase (Pyc)
Q2FKN3	2	111.77	0.00379	1.64	Adenosine synthase (AdsA)
Q2FK34	3	194.9	0.03	1.61	PrsS protease (PrsW-like)
Q2FKM6	13	682.51	0.00815	1.6	Penicillin-binding protein (Pbp2a) transpeptidase
Q2FEH9	2	134.43	0.04	1.6	RpiR
Q2FDQ7	9	695.29	0.00345	1.53	L-lactate dehydrogenase (Ldh2)
Q2FHA5	3	232.33	0.04	1.53	Putative homoserine dehydrogenase (Hdh)
Q2FKE7	9	395.85	0.02	1.51	SarS
Q2FE79	6	357.79	0.00424	1.51	Immunoglobulin-binding protein (Sbi)

Discussion

The expression levels of the cell surface proteins, Protein A (Spa) and Immunoglobulin-binding protein (Sbi), were decreased in SF8300 *pgd* mutant compared with the parent strain (Table 6. 2.b). While these proteins are both ascribed roles in virulence and immune evasion, they might be implicated in other identified phenotypes of the *pgd* mutant and this is outlined below.

S. aureus binds to numerous serum proteins including, fibronectin, fibrinogen and immunoglobulin (IgG). This binding is widely recognised as contributing to protecting the bacterium from innate immune defences of the host (Zhang *et al.*, 1998) The Spa and Sbi proteins are both immunoglobulin G (IgG)-binding. These secreted surface-attached proteins enable *S. aureus* to bind the Fc region of IgG to prevent complement fixation and thus recognition by the neutrophil FcγR receptor to inhibit opsonophagocytosis (Smith *et al.*, 2011b). The N-terminus of Sbi protein contains two IgG-binding domains in comparison with five consecutive IgG-binding domains in the Spa protein sequence. In addition, the C-terminus of Spa comprises a proline-rich region followed by a cell wall-anchoring LPXTG motif, which is used to covalently link the protein to peptidoglycan. Sbi contains the proline-rich region but is not covalently-attached (Smith *et al.*, 2011b; Zhang *et al.*, 1998) meaning that Sbi protein is released into supernatant of *S. aureus* culture in addition to its association with the cell wall. Both Spa and Sbi contribute to innate immune defense and their expression was found to be affected by the levels of iron in culture medium (Smith *et al.*, 2011a). In a neutrophil killing assay, using whole human blood, the survival of *spa* and *sbi* mutants was reduced by half in comparison with the parent, in the Newman strain (Smith *et al.*, 2011a), implying that these proteins do limit

opsonophagocytosis by limiting both complement fixation and interaction with neutrophil Fc-binding receptors (Foster, 2005).

The reduced expression of both Spa and Sbi in the *pgd* mutant in the study described here might therefore partly explain the reductions in virulence with the spleen and lung organ numbers and reduced survival in lung and spleen assay. Moreover, it could also contribute to the increased rate of neutrophil killing observed with the *pgd* mutant in this study.

The SarS transcriptional repressor protein is a member of the SarA-like family and its expression is regulated negatively by both *agr* and *sarA* regulators. SarS is an activator for the transcription of *spa* by binding directly to the *spa* promoter region. SarS thus functions as an intermediary for the regulation of Spa expression controlled by both SarA and *agr* (Bronner *et al.*, 2004).

In this study, SarS protein levels were reduced ~1.5 fold in the *pgd* mutant compared with the parent strain, suggesting this decrease in the level of SarS is an effector for the reduced level of the Spa protein in the *pgd* mutant. However, in this study, the global regulators *agr* and SarA were not investigated and may also be responsible for the observed changes in Spa expression.

SdrE is one of *S. aureus'* family of MSCRAMMs (section; 1.1.3.1.), and this surface-associated protein contributes to immune defence. Specifically, SdrE was reported function similar to complement regulatory protein factor H and when expressed it disrupts the alternative pathway of complement fixation by cleaving C3b

to iC3b, thereby reducing C3-fragment deposition and in turn reducing C5a generation. Furthermore, expression of SdrE in serum was found to provide a survival advantage for the bacterium (Foster *et al.*, 2014; Sharp *et al.*, 2012), meaning that observed changes in SdrE expression in the *pgd* mutant might contribute to altered survival in the immune evasion and virulence assays .

A noted phenotype of the *pgd* mutant was the indication of a metabolism alteration when the strain was assayed using an Alamar blue viability assay. Considerable insight was provided by the proteomic investigation. In *S. aureus*, carbohydrates such as glucose are metabolised to pyruvate for subsequent supply to the tricarboxylic acid (TCA) or fermentive metabolism pathways (Friedman *et al.*, 2006), which provides biosynthetic intermediates, ATP, NADH and FADH to drive cellular processes (Chaffin *et al.*, 2012). Within the differential protein expression data obtained for the *pgd* mutant there were clearly altered levels of proteins in pyruvate and acetoin metabolism plus lower expression of multiple fermentative metabolism proteins were reduced. Under excess glucose, the products of the *alsSD* operon converts acetolactate derived from pyruvate metabolism to acetoin. Acetoin produced can also be converted to 2,3-butanediol by acetoin reductase (ButA), which could be readily utilised at a later time (Rice and Bayles, 2008). Within the differentially expressed proteins of the *pgd* mutant there was an increased level of AlsD (BudA1) and reduced levels of ButA, producing (*S*)-2-acetoin and (*R*)-2-acetoin, respectively, indicating an altered balance of steeorisomers of acetoin, although the significance of this is not clear. The increased expression of AlsD may also integrate the observed effects of increased autolysis in this study and suggests

that cell viability in post-stationary phase should be examined on the basis of the work described by (Yang *et al.*, 2006).

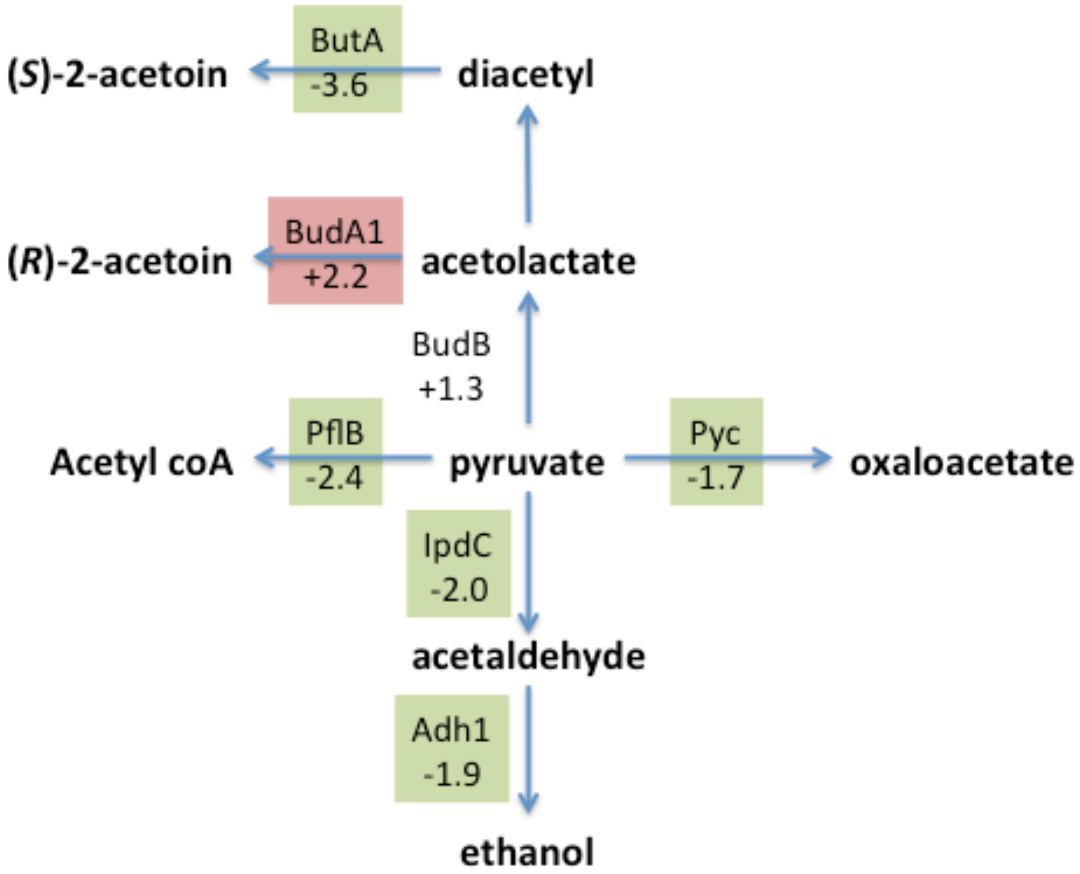

Fig. 6. 7. Pyruvate and acetoin metabolism enzymes with altered expression in *S. aureus pgd*. Red = increased expression, greeen = decreased expression and no shading = change in expression <1.5-fold.

This results and alamar Blue observation (section 5.6.8.), together indicating that *pgd* mutant is indeed affected its metabolic activity and maybe not able to adapt itself with environment.

However, in this proteomics study, there are some proteins of known function were increased such as, immunodominant staphylococcal antigen A (IsaA), fibronectin-

binding protein (FnbA) and surface-associated protein (SdrE) with 2.2, 1.96 and 1.74 fold increased compared to wild type strain (Table 6.3.a), and as described before.

IsaA is an enzyme involved with the metabolism of cell wall. As peptidoglycan of bacteria is a dynamic structure, IsaA enzyme has autolytic activity (lytic transglycosylase) and able to act on peptidoglycan structure, allowing cell wall of bacterium to grow and divide. Moreover, IsaA is located in the cell wall-attached with ionically bound. IsaA production can be upregulated by several genes such as, *sarA*, *sigB*, *agrB* or *saeR* but, also was found to be downregulated at anaerobic condition, implying the control of IsaA expression is complex (Lorenz *et al.*, 2011; Stapleton *et al.*, 2007).

FnbA and FnbB are surface-anchored protein that involved for promoting biofilm formation in *S. aureus*. *finbA* mutant was less biofilm formation but not substantially affected as double mutants *finbA finbB* (O'Neill *et al.*, 2008). However, deletion of *finbA* in *rsp* mutant was restored biofilm formation to parent strain level (Lei *et al.*, 2011).

Thus, deletion *pgd* gene led to increase the level of these proteins in the surface of *pgd* mutant. Increasing the level of IsaA protein could be affected the cell wall peptidoglycan and therefore can lead to increase the autolysis activity, which was observed under stresses of penicillin-G and triton X-100 assays (section: 5.3.4). Moreover, increasing FnbA maybe related to *pgd* mutant, while SdrE related to improve *pgd* mutant in serum assay.

CHAPTER 7

7.1. General Discussion

At the outset of this study the aim was to identify novel activities of *S. aureus* secreted proteins. Based upon database and literature searches, modification of peptidoglycan by deacetylation in *S. aureus* has not been reported previously. In this regard, the study was successful at identifying a novel function for the species, albeit one characterised for a handful of other bacteria. With the identification of a putative deacetylase enzyme, gene mutants were generated to determine the role of *pgd* encoding this activity. Constructed *pgd* mutants of *S. aureus* were studied to examine the effect of gene inactivation upon peptidoglycan acetylation as well as growth, virulence and survival.

Throughout the study it was clear that there was pronounced strain variation in several of the phenotypes. Particularly, the use of four strain backgrounds (SH1000, Newman, BH1CC, SF8300) to study the *pgd* mutation produced data where one or more strain background had a phenotype matching the wild-type or had an opposite phenotype as the other *pgd* mutant strain backgrounds. This latter effect was prominent with the hydrophobicity of SH1000 *pgd* compared with the other *pgd* mutants of Newman, BH1CC and SF8300. To assess hydrolytic activity of the *pgd* mutant in each strain background the mutants and parent strains were challenged with Triton X-100 and penicillin-G in autolysis assays. The *pgd* mutants of both Newman and SF8300 strains exhibited higher autolysis rates compared with the parent strains, indicating peptidoglycan or autolysisn levels were altered. Strain,

SH1000 *pgd* exhibited no alteration to autolysis upon challenge with either Triton X-100 or penicillin, revealing differences between the strains being studied.

Within the research field there is much discussion over the use of more than one strain of *S. aureus* to investigate the effects of gene function to rule out strain-specific effects. The use of the four strain backgrounds identified variation in cell wall properties. Some of the data presented here certainly suggests differences between strains in terms of cell wall charge, hydrophobicity and decoration with teichoic acids and acetyl groups (N- and O-linked). This would be a promising area of future study to identify the correlations between gene expression and surface properties.

Deletion of *pgd* in two *S. aureus* strains, SF8300 and Newman, reduced peptidoglycan thickness by 18-25 %, indicating that cell surface PG was affected at a gross level. This phenotype has not been reported in other studies of Pgd homologs. Increased acetylation was identified by NMR assay for the PG of the mutant strain compared with parent strain relates, however it is not clear how this relates to the cell wall thickness phenotype. Perhaps the change in acetylation causes a degree of disorder in PG synthesis by altering the localisation of PBPs and/or autolysins during biosynthesis, for example.

What could cause reduced peptidoglycan thickness? From the proteomic analysis of the *pgd* mutant the consequence of increased peptidoglycan *N*-acetylation was altered levels of multiple secreted proteins, including IsaA that has cell wall autolytic activity. This *S. aureus* protein is one of only nine with peptidoglycan hydrolytic

activity (Dubrac and Msadek, 2004) and IsaA functions as a lytic transglycosylase to modify peptidoglycan structure (Lorenz *et al.*, 2011; Stapleton *et al.*, 2007). From the proteomic data of SF8300 *pgd* (Table 6.2a), the IsaA protein was increased 2.2-fold, compared with its parent strain. This increased level of IsaA has the potential to modulate cell wall turnover and cause disorder in PG synthesis. Tannic acid was reported to interfere with biofilm activity and the limiting factor was determined to be an elevation of IsaA activity (Payne *et al.*, 2013). Of particular interest is the link between IsaA levels and biofilm formation, since the *pgd* mutant also exhibited altered biofilm phenotypes in this study. This link needs to be investigated further through the use of multiple mutants and to assess the specific consequences of IsaA levels upon peptidoglycan structure, which requires closer scrutiny beyond the functional determination previously reported (Stapleton *et al.*, 2007).

Lysozyme is an important component of the animal host defense system, and it is presumed that many Gram-positive bacteria, including *S. aureus* are completely resistant. Several reports describe that *O*-acetylation, *N*-acetylation and *N*-deacetylation of peptidoglycan are important processes, conferring intrinsic resistance to hydrolysis or autolysis (Dupont and Clarke, 1991; Rae *et al.*, 2011; Raymond *et al.*, 2005; Vollmer and Tomasz, 2000). In Gram-positive bacteria, the enzymes responsible for these activities encode peptidoglycan N-acetylglucosamine deacetylase (Pgd) and O-acetyltransferase A (OatA).

Mutation of *pgd* in *S. aureus* Newman, SF8300 or SA113 did not affect lysozyme resistance when assaying cells cultured in broth or agar. Assay of *pgd oatA* double mutants in strains Newman and SA113 revealed that the double mutant was more

lysozyme resistant than Newman *oatA* and SA113 *oatA* strains. From these data it is evident that Pgd contributes to lysozyme resistance and raises questions about the potential for coordinated Pgd and OatA expression and compensatory roles in their activity. How this coordination would be regulated requires investigation. Firstly though, the genetic regulation of *pgd* transcription must be determined and efforts towards this aim are ongoing in the Horsburgh lab using promoter fusions combined with transposon mutagenesis. In addition genome resequencing of *pgd, oatA, oatAtagO* mutants selected for increased lysozyme resistance is being undertaken to identify SNPs contributing to improved growth in high concentrations of lysozyme. The *pgd* promoter contains an inverted repeat sequence that is unique in the genome and might indicate the binding site of a novel regulator. Alternatively, one or more of the cell wall regulators, such as *WalKR, GraRS, LytRS or MgrA* might regulate *pgd* transcription. Data from the transcriptomic database maintained by the Elasri lab (http://www.bioinformatics.org/sammd/) indicates that MgrA might act as either a direct or indirect regulator of *pgd*. Such regulation would coordinate autolysis activity with cell wall modifications; this regulation would fit within the described regulatory network encompassing the lytic transglycosylase activity of IsaA.

To further investigate the actions of Pgd and OatA in *S. aureus*, this study characterised the *pgd*, *oatA* and double mutants to identify their relative roles in resistance to the hydrolytic action of lysozyme. In agreement with previous studies, deletion of *oatA* caused high sensitivity to lysozyme in *S. aureus* SA113 (Bera *et al.*, 2005). This phenotype was extended in this study using *S. aureus* Newman. However, in contrast SF8300 *oatA* was not lysozyme sensitive in either assay. Since SF8300 is a representative of the USA300 strain lineage that has evolved increased

virulence as CA-MRSA, this lysozyme resistance phenotype independent of *oatA* warrants further investigation and further highlights the strain differences observed with respect cell wall properties. One explanation for this phenotype is that the absence of O-acetyl is fully compensated by the addition of teichoic acid, which is competitively added to the same position on MurNAc. This might indicate that the teichoic acid transferase activity (TagO) is higher in this strain or that peptidoglycan deacetylase (Pgd) activity is repressed; other possibilities are currently hard to envisage.

The proteomics data of the *pgd* mutant compared with the wild-type SF8300 strain indicated that SarS expression was decreased in the *pgd* mutant. This decrease is likely to be the basis for the decreased levels of protein A (Spa). Since this altered Spa expression could be important for immune evasion and biofilm formation, it will be important to understand the basis for the pgd mutation leading to the signal transduction via SarS. This SarA-like protein is a member of a suite of purported environmental signal-transducing transcriptional repressors, but the actual basis for the extracytoplasmic signal transduction leading to altered SarA-like family protein activity is mostly incompletely understood, despite many extensive analyses. The data presented here provides another environmental input via N-acetylation changes.

In contrast to *S. aureus*, mutation of *pgd* in *Streptococcus pneumoniae*, *Listeria monocytogenes* and *Lactococcus lactis* resulted in clear lysozyme sensitivity (Boneca *et al.*, 2007; Meyrand *et al.*, 2007; Vollmer and Tomasz, 2000). Other studies with *S. mutans* and *Enterococcus faecalis* revealed no difference when comparing parent strains with *pgd* mutants, while with *Bacillus anthracis* the results were equivocal

(Deng *et al.*, 2009; Fukushima *et al.*, 2005; Hebert *et al.*, 2007). Inactivation of *oatA*, *pgdA*, *dltA* or *sigV* encoding the extracytoplasmic sigma factor σ^V, in *E. faecalis* had no impact on lysozyme resistance levels compared with their parent strain (Benachour *et al.*, 2012). Deletion of *sigV* in *B. subtilis* increased lysozyme sensitivity, while overexpression of *oatA* in the *sigV* mutant restored lysozyme resistance revealing a contribution of σ^V to OatA expression (Ho *et al.*, 2011). Although *S. aureus* has no σ^V homolog, it has an equivalent mechanism of lysozyme resistance through increased expression of DltA, which is responsible for addition of positively-charged D-alanine to cell wall teichoic acid, plus OatA-mediated MurNAc O-acetylation. *S. aureus* mutated for both genes has a significant increase in lysozyme sensitivity.

Compared with their parent strains, *pgd* mutants of Newman and SF8300 exhibited biofilm formation when cultured with 1 % glucose on both plasma-treated plates (tissue culture plate) or poly-lysine-coated glass. These strains did not form biofilm on a polystyrene plate, an untreated surface. Additionally, the SF8300 *pgd* mutant was unable to attach and form biofilm within a glass microfluidics channel of bioFlux system. These data reveal a striking contrast between assays when using the same material with similar surface properties (treated glass), producing either a biofilm or no biofilm. These experiments raise a question as to whether this discrepancy is due to material surface properties (hydrophobicity or charge) combined with the increased PG acetylation of the *pgd* mutant, or simply due to the hydrodynamic shear influencing behaviour of cells differently at the surface. Nevertheless, it is clear that a *pgd* mutant has a biofilm phenotype in certain strains of *S. aureus*, and this could be examined further to determine the critical parameters

influencing the cell surface/ material surface interaction under hydrodynamic flow and static conditions. There is a precedent for the difference between the biofilm assay outcomes as reported by (Benoit *et al.*, 2010). Their study indicated a similar situation where a flow biofilm differed from a static biofilm in their study of *rpoS*-deficient *E. coli* that had impaired biofilm development under flow condition but developed biofilm under static conditions to an enhanced extent when compared with its isogenic parent (Benoit *et al.*, 2010; Lee *et al.*, 2008). The reasoning proposed was that cell signalling is affected by hydrodynamic flow, particularly due to velocity and turbulence of the medium and these conditions altered biofilm development. A further possibility that might explain the difference comes from a study by Pozzi *et al* 2012, which indicated that in relative terms the surface of the glass bioFlux channel is more hydrophobic than the highly hydrophilic surface of a tc-treated polystyrene plate.

In this study Pgd was determined to have roles in the virulence of *S. aureus.* Inactivation of *pgd* in *S. aureus* therefore has a similar infection outcome to that seen with the reduced *in vivo* survival of *S. pneumoniae pgd* and *E. faecalis pgd* in animal models (Blair *et al.*, 2005a; Hebert *et al.*, 2007; Vollmer and Tomasz, 2000). Reduced *in vitro* survival was previously reported for *Listeria monocytogenes pgd* and *Shigella flexneri pgd* mutants in survival assays with polymorphonuclear neutrophils (PMNs) (Rae *et al.*, 2011) which matches the decreased virulence *S. aureus* SF8300 *pgd* for PMN survival. These *in vivo* phenotypes of the *S. aureus* mutant may result from the reduced fitness observed in several assays, including increased hydrolytic activity that could lead to PG fragments being released to activate innate immune pathways. The decreased expression of the surface

immunoglobulin G (IgG)-binding proteins protein A (Spa) and Sbi shown in the proteomics data (Table 6.2b) may increase complement deposition and recognition by the neutrophil (FcyR) receptor to limit their inhibition of opsonophagocytosis (Smith *et al.*, 2011b). The decreased virulence of *S. aureus* SF8300 *pgd* in the infection models could be related to increased IsaA expression, which is highly immunogenic meaning it may increase host immune responses. A higher titre of antibody against IsaA was reported as being detected following *S. aureus* infections (Lorenz *et al.*, 2011; Payne *et al.*, 2013).

In summary, many *pgd* mutant phenotypes were identified in this study and further study of the mutant cell wall structure and function will advance our understanding of *S. aureus* as a biofilm-forming pathogen. This increased understanding from further such studies will contribute to the long-term objective of new and improved antimicrobial therapies. Pgd of *S. aureus* may also represent a promising target for vaccine design.

References

Akita, M., Sasaki, S., Matsuyama, S., and Mizushima, S. (1990). SecA interacts with secretory proteins by recognizing the positive charge at the amino terminus of the signal peptide in *Escherichia coli*. *The Journal of Biological Chemistry* ***265***, 8164-8169.

An, J.H., Kurokawa, K., Jung, D.J., Kim, M.J., Kim, C.H., Fujimoto, Y., Fukase, K., Coggeshall, K.M., and Lee, B.L. (2013). Human SAP is a novel peptidoglycan recognition protein that induces complement-independent phagocytosis of *Staphylococcus aureus*. *Journal of Immunology* ***191***, 3319-3327.

Antelmann, H., Tjalsma, H., Voigt, B., Ohlmeier, S., Bron, S., van Dijl, J.M., and Hecker, M. (2001). A proteomic view on genome-based signal peptide predictions. *Genome Research* ***11***, 1484-1502.

Archer, G.L. (1998). *Staphylococcus aureus*: A well-armed pathogen. *Clinical Infectious Diseases* ***26***, 1179-1181.

Arvidson, S., and Tegmark, K. (2001). Regulation of virulence determinants in *Staphylococcus aureus*. *International Journal of Medical Microbiology* ***291***, 159-170.

Asheshov, E.A., and Jevons, M.P. (1963). The effect of heat on the ability of a host strain to support the growth of a *Staphylococcus* phage. *Journal of General Microbiology* ***31,*** 97-107.

Baba, T., Bae, T., Schneewind, O., Takeuchi, F., and Hiramatsu, K. (2008). Genome sequence of *Staphylococcus aureus* strain Newman and comparative analysis of *staphylococcal* genomes: polymorphism and evolution of two major pathogenicity islands. *Journal of Bacteriology* ***190***, 300-310.

Baek, K.T., Grundling, A., Mogensen, R.G., Thogersen, L., Petersen, A., Paulander, W., and Frees, D. (2014). beta-Lactam resistance in methicillin-resistant *Staphylococcus aureus* USA300 is increased by inactivation of the ClpXP protease. *Antimicrob Agents Chemother* ***58***, 4593-4603.

Bagos, P.G., Tsirigos, K.D., Liakopoulos, T.D., and Hamodrakas, S.J. (2008). Prediction of lipoprotein signal peptides in Gram-positive bacteria with a Hidden Markov *Model. J Proteome Res 7*, 5082-5093.

Bauer, J., Siala, W., Tulkens, P.M., and Van Bambeke, F. (2013). A combined pharmacodynamic quantitative and qualitative model reveals the potent activity of daptomycin and delafloxacin against *Staphylococcus aureus* biofilms. *Antimicrob Agents Chemother* ***57***, 2726-2737.

Bayer, M.G., Heinrichs, J.H., and Cheung, A.L. (1996). The molecular architecture of the sar locus in *Staphylococcus aureus. Journal of Bacteriology* ***178***, 4563-4570.
Beck, G., Puchelle, E., Plotkowski, C., and Peslin, R. (1988). Effect of growth on surface charge and hydrophobicity of *Staphylococcus aureus*. *Ann Inst Pasteur Microbiol* ***139***, 655-664.

Belcheva, A., and Golemi-Kotra, D. (2008). A close-up view of the VraSR two-component system. A mediator of *Staphylococcus aureus* response to cell wall damage. *The Journal of Biological Chemistry* ***283***, 12354-12364.

Benachour, A., Ladjouzi, R., Le Jeune, A., Hebert, L., Thorpe, S., Courtin, P., Chapot-Chartier, M.P., Prajsnar, T.K., Foster, S.J., and Mesnage, S. (2012). The lysozyme-induced peptidoglycan N-acetylglucosamine deacetylase PgdA (EF1843) is required for *Enterococcus faecalis* virulence. *Journal of Bacteriology* ***194***, 6066-6073.

Benoit, M.R., Conant, C.G., Ionescu-Zanetti, C., Schwartz, M., and Matin, A. (2010). New device for high-throughput viability screening of flow biofilms. *Applied and Environmental Microbiology* ***76***, 4136-4142.

Bera, A., Biswas, R., Herbert, S., Kulauzovic, E., Weidenmaier, C., Peschel, A., and Gotz, F. (2007). Influence of wall teichoic acid on lysozyme resistance in *Staphylococcus aureus*. *Journal of Bacteriology* ***189***, 280-283.

Bera, A., Herbert, S., Jakob, A., Vollmer, W., and Gotz, F. (2005). Why are pathogenic *staphylococci* so lysozyme resistant? The peptidoglycan O-acetyltransferase OatA is the major determinant for lysozyme resistance of *Staphylococcus aureus*. *Molecular Microbiology* ***55***, 778-787.

Berends, E.T., Dekkers, J.F., Nijland, R., Kuipers, A., Soppe, J.A., van Strijp, J.A., and Rooijakkers, S.H. (2013). Distinct localization of the complement C5b-9 complex on Gram-positive bacteria. *Cell Microbiol* ***15***, 1955-1968.

Berman, H.M., Westbrook, J., Feng, Z., Gilliland, G., Bhat, T.N., Weissig, H., Shindyalov, I.N., and Bourne, P.E. (2000). The Protein Data Bank. *Nucleic Acids Research* ***28***, 235-242.

Bischoff, M., Dunman, P., Kormanec, J., Macapagal, D., Murphy, E., Mounts, W., Berger-Bachi, B., and Projan, S. (2004). Microarray-based analysis of the *Staphylococcus aureus* sigmaB regulon. *Journal of Bacteriology* ***186***, 4085-4099.

Blair, D.E., Hekmat, O., Schuttelkopf, A.W., Shrestha, B., Tokuyasu, K., Withers, S.G., and van Aalten, D.M. (2006). Structure and mechanism of chitin deacetylase from the fungal pathogen *Colletotrichum lindemuthianum*. *Biochemistry* ***45***, 9416-9426.

Blair, D.E., Schuttelkopf, A.W., MacRae, J.I., and van Aalten, D.M. (2005a). Structure and metal-dependent mechanism of peptidoglycan deacetylase, a *streptococcal* virulence factor. *Proceedings of The National Academy of Sciences of The United States of America* ***102***, 15429-15434.

Blair, D.E., Schuttelkopf, A.W., MacRae, J.I., and van Aalten, D.M.F. (2005b). Structure and metal-dependent mechanism of peptidoglycan deacetylase, a *Streptococcal* virulence factor. *Proceedings of the National Academy of Sciences of The United States of America* ***102***, 15429-15434.

Blake, K.L., O'Neill, A.J., Mengin-Lecreulx, D., Henderson, P.J., Bostock, J.M., Dunsmore, C.J., Simmons, K.J., Fishwick, C.W., Leeds, J.A., and Chopra, I. (2009). The nature of *Staphylococcus aureus* MurA and MurZ and approaches for detection of peptidoglycan biosynthesis inhibitors. *Molecular Microbiology* ***72***, 335-343.

Boneca, I.G., Dussurget, O., Cabanes, D., Nahori, M.A., Sousa, S., Lecuit, M., Psylinakis, E., Bouriotis, V., Hugot, J.P., Giovannini, M.*, et al.* (2007). A critical role for peptidoglycan N-deacetylation in *Listeria* evasion from the host innate immune system. *Proceedings of The National Academy of Sciences of The United States of America* ***104***, 997-1002.

Bose, J.L., Lehman, M.K., Fey, P.D., and Bayles, K.W. (2012). Contribution of the *Staphylococcus aureus* Atl AM and GL murein hydrolase activities in cell division, autolysis, and biofilm formation. *PloS one 7*, e42244.

Bronner, S., Monteil, H., and Prevost, G. (2004). Regulation of virulence determinants in *Staphylococcus aureus*: complexity and applications. *FEMS Microbiol Rev* ***28***, 183-200.

Brunskill, E.W., and Bayles, K.W. (1996). Identification of LytSR-regulated genes from *Staphylococcus aureus*. *Journal of Bacteriology* ***178***, 5810-5812.

Burns, D.M., and Beacham, I.R. (1986). Nucleotide sequence and transcriptional analysis of the *E. coli ushA* gene, encoding periplasmic UDP-sugar hydrolase (5'-nucleotidase): regulation of the *ushA* gene, and the signal sequence of its encoded protein product. *Nucleic Acids Research* ***14***, 4325-4342.

Byth, H.A., McHunu, B.I., Dubery, I.A., and Bornman, L. (2001). Assessment of a simple, non-toxic Alamar blue cell survival assay to monitor tomato cell viability. *Phytochemical Analysis* ***12***, 340-346.

Cantarel, B.L., Coutinho, P.M., Rancurel, C., Bernard, T., Lombard, V., and Henrissat, B. (2009). The Carbohydrate-Active EnZymes database (CAZy): an expert resource for Glycogenomics. *Nucleic Acids Research* ***37***, D233-238.

Chaffin, D.O., Taylor, D., Skerrett, S.J., and Rubens, C.E. (2012). Changes in the *Staphylococcus aureus* transcriptome during early adaptation to the lung. *PloS one 7,* e41329.

Chamberlain, N.R., Mehrtens, B.G., Xiong, Z., Kapral, F.A., Boardman, J.L., and Rearick, J.I. (1991). Correlation of carotenoid production, decreased membrane fluidity, and resistance to oleic acid killing in *Staphylococcus aureus* 18Z. *Infection and Immunity* ***59***, 4332-4337.

Chambers, H.F., and Deleo, F.R. (2009). Waves of resistance: *Staphylococcus aureus* in the antibiotic era. *Nature Reviews Microbiology 7*, 629-641.

Chambers, H.F., and Miick, C. (1992). Characterization of penicillin-binding protein 2 of *Staphylococcus aureus*: deacylation reaction and identification of two penicillin-binding peptides. *Antimicrob Agents Chemother* ***36***, 656-661.

Cheung, A.L., Bayer, A.S., Zhang, G., Gresham, H., and Xiong, Y.Q. (2004). Regulation of virulence determinants in vitro and in vivo in *Staphylococcus aureus. FEMS Immunol Medical Microbiology* ***40*****,** 1-9.

Cheung, A.L., Nishina, K.A., Trotonda, M.P., and Tamber, S. (2008). The SarA protein family of *Staphylococcus aureus*. *Int J Biochemical Cell Biology* ***40***, 355-361.

Christensen, G.D., Simpson, W.A., Younger, J.J., Baddour, L.M., Barrett, F.F., Melton, D.M., and Beachey, E.H. (1985). Adherence of coagulase-negative *Staphylococci* to plastic tissue culture plates: a quantitative model for the adherence of *Staphylococci* to medical devices. *Journal of Clinical Microbiology* ***22***, 996-1006.

Clauditz, A., Resch, A., Wieland, K.P., Peschel, A., and Gotz, F. (2006). Staphyloxanthin plays a role in the fitness of *Staphylococcus aureus* and its ability to cope with oxidative stress. *Infection and Immunity* ***74***, 4950-4953.

Corvaglia, A.R., Francois, P., Hernandez, D., Perron, K., Linder, P., and Schrenzel, J. (2010). A type III-like restriction endonuclease functions as a major barrier to horizontal gene transfer in clinical *Staphylococcus aureus* strains. *Proceedings of The National Academy of Sciences of The United States of America* ***107*****,** 11954-11958.

Cramton, S.E., Gerke, C., Schnell, N.F., Nichols, W.W., and Gotz, F. (1999). The intercellular adhesion (ica) locus is present in *Staphylococcus aureus* and is required for biofilm formation. *Infection and Immunity* ***67***, 5427-5433.

David, M.Z., and Daum, R.S. (2010). Community-associated methicillin-resistant *Staphylococcus aureus*: epidemiology and clinical consequences of an emerging epidemic. *Clinical Microbiology Reviews* ***23*****,** 616-687.

Delaune, A., Dubrac, S., Blanchet, C., Poupel, O., Mader, U., Hiron, A., Leduc, A., Fitting, C., Nicolas, P., Cavaillon, J.M*., et al.* (2012). The WalKR system controls major *Staphylococcal* virulence genes and is involved in triggering the host inflammatory response. *Infection and Immunity* ***80***, 3438-3453.

DeLeo, F.R., Otto, M., Kreiswirth, B.N., and Chambers, H.F. (2010). Community-associated meticillin-resistant *Staphylococcus aureus*. *Lancet* ***375***, 1557-1568.

Deng, D.M., Urch, J.E., ten Cate, J.M., Rao, V.A., van Aalten, D.M., and Crielaard, W. (2009). *Streptococcus mutans* SMU.623c codes for a functional, metal-dependent polysaccharide deacetylase that modulates interactions with salivary agglutinin. *Journal of Bacteriology* ***191***, 394-402.

Depardieu, F., Podglajen, I., Leclercq, R., Collatz, E., and Courvalin, P. (2007). Modes and modulations of antibiotic resistance gene expression. *Clinical Microbiology Reviews 20*, **79**-114.

Didier, J.P., Cozzone, A.J., and Duclos, B. (2010). Phosphorylation of the virulence regulator SarA modulates its ability to bind DNA in *Staphylococcus aureus*. *FEMS Microbiology letters* ***306***, 30-36.

Dinges, M.M., Orwin, P.M., and Schlievert, P.M. (2000). Exotoxins of *Staphylococcus aureus*. *Clinical Microbiology Reviews* ***13***, 16-34, table of contents.

Dreisbach, A., van der Kooi-Pol, M.M., Otto, A., Gronau, K., Bonarius, H.P., Westra, H., Groen, H., Becher, D., Hecker, M., and van Dijl, J.M. (2011). Surface shaving as a versatile tool to profile global interactions between human serum proteins and the *Staphylococcus aureus* cell surface. *Proteomics* ***11***, 2921-2930.

Dubrac, S., Boneca, I.G., Poupel, O., and Msadek, T. (2007). New insights into the WalK/WalR (YycG/YycF) essential signal transduction pathway reveal a major role in controlling cell wall metabolism and biofilm formation in *Staphylococcus aureus. Journal of Bacteriology* ***189***, 8257-8269.

Dubrac, S., and Msadek, T. (2004). Identification of genes controlled by the essential YycG/YycF two-component system of *Staphylococcus aureus. Journal of Bacteriology* ***186***, 1175-1181.

Dunman, P.M., Murphy, E., Haney, S., Palacios, D., Tucker-Kellogg, G., Wu, S., Brown, E.L., Zagursky, R.J., Shlaes, D., and Projan, S.J. (2001). Transcription profiling-based identification of *Staphylococcus aureus* genes regulated by the *agr* and/or *sarA* loci. *Journal of Bacteriology* ***183*****,** 7341-7353.

Dupont, C., and Clarke, A.J. (1991). Evidence for N----O acetyl migration as the mechanism for O acetylation of peptidoglycan in Proteus mirabilis. *Journal of Bacteriology* ***173***, 4318-4324.

Duthie, E.S., and Lorenz, L.L. (1952). Staphylococcal coagulase; mode of action and antigenicity. *Journal of General microbiology* ***6*****,** 95-107.

Dye, E.S., and Kapral, F.A. (1980). Partial characterization of a bactericidal system in *Staphylococcal* abscesses. *Infection and immunity* ***30***, 198-203.

Eckert, C., Lecerf, M., Dubost, L., Arthur, M., and Mesnage, S. (2006). Functional analysis of AtlA, the major N-acetylglucosaminidase of *Enterococcus faecalis. Journal of Bacteriology* ***188***, 8513-8519.

Eng, J.K., McCormack, A.L., and Yates, J.R. (1994). An approach to correlate tandem mass spectral data of peptides with amino acid sequences in a protein database. *Journal of the American Society for Mass Spectrometry* ***5***, 976-989.

Falkow, S. (1988). Molecular Koch's postulates applied to microbial pathogenicity. *Reviews of Infectious Diseases 10 Suppl* ***2***, S274-276.

Firon, A., Dinis, M., Raynal, B., Poyart, C., Trieu-Cuot, P., and Kaminski, P.A. (2014). Extracellular nucleotide catabolism by the Group B *Streptococcus* ectonucleotidase NudP increases bacterial survival in blood. *The Journal of Biological Chemistry* ***289***, 5479-5489.

Fischer, C.L., Walters, K.S., Drake, D.R., Blanchette, D.R., Dawson, D.V., Brogden, K.A., and Wertz, P.W. (2013). Sphingoid bases are taken up by *Escherichia coli* and *Staphylococcus aureus* and induce ultrastructural damage. *Skin Pharmacology Physiology* ***26***, 36-44.

Foster, S.J. (1995). Molecular characterization and functional analysis of the major autolysin of *Staphylococcus aureus* 8325/4. *Journal of Bacteriology* ***177***, 5723-5725.

Foster, T.J. (2005). Immune evasion by *Staphylococci. Nat Rev Microbiol* ***3***, 948-958.

Foster, T.J. (2009). Colonization and infection of the human host by *Staphylococci*: adhesion, survival and immune evasion. *Veterinary Dermatology* ***20***, 456-470.

Foster, T.J., Geoghegan, J.A., Ganesh, V.K., and Hook, M. (2014). Adhesion, invasion and evasion: the many functions of the surface proteins of *Staphylococcus aureus. Nature Reviews Microbiology* ***12***, 49-62.

Foster, T.J., and Hook, M. (1998). Surface protein adhesins of *Staphylococcus aureus. Trends Microbiology* ***6***, 484-488.

Fournier, B. (2008). Global Regulators of *Staphylococcus aureus* virulence genes. *Staphylococcus*: molecular genetics. *Molecular Microbiology* ***9***, 222-211.

Fournier, B., Klier, A., and Rapoport, G. (2001). The two-component system ArlS-ArlR is a regulator of virulence gene expression in *Staphylococcus aureus*. *Molecular Microbiology* ***41***, 247-261.

Fournier, B., and Philpott, D.J. (2005). Recognition of *Staphylococcus aureus* by the innate immune system. *Clinical Microbiology Reviews* ***18***, 521-540.

Francois, P., Scherl, A., Hochstrasser, D., and Schrenzel, J. (2010). Proteomic approaches to study *Staphylococcus aureus* pathogenesis. *Journal of Proteomics* ***73***, 701-708.

Frankel, M.B., and Schneewind, O. (2012). Determinants of murein hydrolase targeting to cross-wall of *Staphylococcus aureus* peptidoglycan. *The Journal of Biological Chemistry* ***287***, 10460-10471.

Friedman, D.B., Stauff, D.L., Pishchany, G., Whitwell, C.W., Torres, V.J., and Skaar, E.P. (2006). *Staphylococcus aureus* redirects central metabolism to increase iron availability. *PLoS Pathog* ***2***, e87.

Fujimoto, D.F., and Bayles, K.W. (1998). Opposing roles of the *Staphylococcus aureus* virulence regulators, *Agr* and *Sar*, in Triton X-100- and penicillin-induced autolysis. *Journal of Bacteriology* ***180***, 3724-3726.

Fukushima, T., Kitajima, T., and Sekiguchi, J. (2005). A polysaccharide deacetylase homologue, PdaA, in *Bacillus subtilis* acts as an N-acetylmuramic acid deacetylase in vitro. *Journal of Bacteriology* ***187***, 1287-1292.

Gao, R., and Stock, A.M. (2009). Biological insights from structures of two-component proteins. *Annual Reviews Microbiology* ***63***, 133-154.

Gardete, S., Wu, S.W., Gill, S., and Tomasz, A. (2006). Role of VraSR in antibiotic resistance and antibiotic-induced stress response in *Staphylococcus aureus*. *Antimicrobial Agents Chemotherapy* ***50***, 3424-3434.

Giachino, P., Engelmann, S., and Bischoff, M. (2001). Sigma(B) activity depends on RsbU in *Staphylococcus aureus. Journal of Bacteriology* ***183***, 1843-1852.

Giraudo, A.T., Calzolari, A., Cataldi, A.A., Bogni, C., and Nagel, R. (1999). The sae locus of *Staphylococcus aureus* encodes a two-component regulatory system. *FEMS Microbiology Letters* ***177***, 15-22.

Giraudo, A.T., Cheung, A.L., and Nagel, R. (1997). The sae locus of *Staphylococcus aureus* controls exoprotein synthesis at the transcriptional level. *Arch Microbiol* ***168*****,** 53-58.

Gittelman, P.D., Jacobs, J.B., Lebowitz, A.S., and Tierno, P.M. (1991). *Staphylococcus aureus* Nasal Carriage in Patients with Rhinosinusitis. *Laryngoscope* ***101***, 733-737.

Glaser, F., Pupko, T., Paz, I., Bell, R.E., Bechor-Shental, D., Martz, E., and Ben-Tal, N. (2003). ConSurf: identification of functional regions in proteins by surface-mapping of phylogenetic information. *Bioinformatics* ***19***, 163-164.

Glaser, L., Melo, A., and Paul, R. (1967). Uridine diphosphate sugar hydrolase. Purification of enzyme and protein inhibitor. *The Journal of Biological Chemistry* ***242***, 1944-1954.

Grinsted, J., and Lacey, R.W. (1973). Ecological and genetic implications of pigmentation in *Staphylococcus aureus*. *Journal of General Microbiology* ***75***, 259-267.

Grkovic, S., Brown, M.H., Hardie, K.M., Firth, N., and Skurray, R.A. (2003). Stable low-copy-number *Staphylococcus aureus* shuttle vectors. *Microbiology* ***149***, 785-794.

Groicher, K.H., Firek, B.A., Fujimoto, D.F., and Bayles, K.W. (2000). The *Staphylococcus aureus lrgAB* operon modulates murein hydrolase activity and penicillin tolerance. *Journal of Bacteriology* ***182***, 1794-1801.

Gross, M., Cramton, S.E., Gotz, F., and Peschel, A. (2001). Key role of teichoic acid net charge in *Staphylococcus aureus* colonization of artificial surfaces. *Infection and Immunity* ***69***, 3423-3426.

Guerout-Fleury, A.M., Shazand, K., Frandsen, N., and Stragier, P. (1995). Antibiotic-resistance cassettes for *Bacillus subtilis. Gene* ***167***, 335-336.

Gustafsson, E., and Oscarsson, J. (2008). Maximal transcription of aur (aureolysin) and sspA (serine protease) in *Staphylococcus aureus* requires *staphylococcal* accessory regulator R (sarR) activity. *FEMS Microbiology Letters* ***284***, 158-164.

Hanahan, D., Jessee, J., and Bloom, F.R. (1991). Plasmid transformation of *Escherichia coli* and other bacteria. *Methods in Enzymology* ***204***, 63-113.

Harris, L.G., Foster, S.J., and Richards, R.G. (2002). An introduction to *Staphylococcus aureus*, and techniques for identifying and quantifying *S. aureus* adhesins in relation to adhesion to biomaterials: review. *Journal of European Cells and Materials* ***4***, 39-60.

Hebert, L., Courtin, P., Torelli, R., Sanguinetti, M., Chapot-Chartier, M.P., Auffray, Y., and Benachour, A. (2007). *Enterococcus faecalis* constitutes an unusual bacterial model in lysozyme resistance. *Infection and Immunity* ***75***, 5390-5398.

Hecker, M., Becher, D., Fuchs, S., and Engelmann, S. (2010). A proteomic view of cell physiology and virulence of *Staphylococcus aureus*. *International Journal of Medical Microbiology* ***300***, 76-87.

Ho, T.D., Hastie, J.L., Intile, P.J., and Ellermeier, C.D. (2011). The *Bacillus subtilis* extracytoplasmic function sigma factor sigma(V) is induced by lysozyme and provides resistance to lysozyme. *Journal of Bacteriology* ***193***, 6215-6222.

Holbrook, K.A., and Lowy, F.D. (1998). beta-lactam antibiotics. *Cancer Investigation* ***16***, 405-412.

Horsburgh, M.J., Aish, J.L., White, I.J., Shaw, L., Lithgow, J.K., and Foster, S.J. (2002a). sigma(B) modulates virulence determinant expression and stress resistance: Characterization of a functional rsbU strain derived from *Staphylococcus aureus* 8325-4. *Journal of Bacteriology* ***184***, 5457-5467.

Horsburgh, M.J., Aish, J.L., White, I.J., Shaw, L., Lithgow, J.K., and Foster, S.J. (2002b). sigmaB modulates virulence determinant expression and stress resistance: characterization of a functional rsbU strain derived from *Staphylococcus aureus* 8325-4. *Journal of Bacteriology* ***184***, 5457-5467.

Houston, P., Rowe, S.E., Pozzi, C., Waters, E.M., and O'Gara, J.P. (2011). Essential role for the major autolysin in the fibronectin-binding protein-mediated *Staphylococcus aureus* biofilm phenotype. *Infection and Immunity* ***79***, 1153-1165.

Howden, B.P., Davies, J.K., Johnson, P.D., Stinear, T.P., and Grayson, M.L. (2010). Reduced vancomycin susceptibility in *Staphylococcus aureus*, including vancomycin-intermediate and heterogeneous vancomycin-intermediate strains: resistance mechanisms, laboratory detection, and clinical implications. *Clin Microbiology Reviews* ***23***, 99-139.

Hutchings, M.I., Palmer, T., Harrington, D.J., and Sutcliffe, I.C. (2009). Lipoprotein biogenesis in Gram-positive bacteria: knowing when to hold 'em, knowing when to fold 'em. *Trends Microbiology **17***, 13-21.

Ingavale, S., van Wamel, W., Luong, T.T., Lee, C.Y., and Cheung, A.L. (2005). Rat/MgrA, a regulator of autolysis, is a regulator of virulence genes in *Staphylococcus aureus*. *Infection and Immunity **73***, 1423-1431.

Ingavale, S.S., Van Wamel, W., and Cheung, A.L. (2003). Characterization of RAT, an autolysis regulator in *Staphylococcus aureus*. *Molecular Microbiology **48***, 1451-1466.

Juncker, A.S., Willenbrock, H., Von Heijne, G., Brunak, S., Nielsen, H., and Krogh, A. (2003). Prediction of lipoprotein signal peptides in Gram-negative bacteria. *Protein science : A Publication of The Protein Society **12***, 1652-1662.

Katzif, S., Lee, E.H., Law, A.B., Tzeng, Y.L., and Shafer, W.M. (2005). CspA regulates pigment production in *Staphylococcus aureus* through a SigB-dependent mechanism. *Journal of Bacteriology **187***, 8181-8184.

Kelleher, J.E., and Raleigh, E.A. (1991). A novel activity in *Escherichia coli* K-12 that directs restriction of DNA modified at CG dinucleotides. *Journal of Bacteriology **173***, 5220-5223.

Knofel, T., and Strater, N. (1999). X-ray structure of the Escherichia coli periplasmic 5'-nucleotidase containing a dimetal catalytic site. *Nature Structural & Molecular Biology **6***, 448-453.

Knofel, T., and Strater, N. (2001). Mechanism of hydrolysis of phosphate esters by the dimetal center of 5'-nucleotidase based on crystal structures. *Journal of Molecular Biology **309***, 239-254.

Kobayashi, S.D., Voyich, J.M., Burlak, C., and DeLeo, F.R. (2005). Neutrophils in the innate immune response. *Archivum Immunologiae Therapia Experimentalis* ***53***, 505-517.

Korkmaz, B., Horwitz, M.S., Jenne, D.E., and Gauthier, F. (2010). Neutrophil elastase, proteinase 3, and cathepsin G as therapeutic targets in human diseases. *Pharmacology Reviews* ***62***, 726-759.

Kovacs-Simon, A., Titball, R.W., and Michell, S.L. (2011). Lipoproteins of bacterial pathogens. *Infection and Immunity* ***79***, 548-561.

Kullik, I., Giachino, P., and Fuchs, T. (1998). Deletion of the alternative sigma factor sigmaB in *Staphylococcus aureus* reveals its function as a global regulator of virulence genes. *Journal of Bacteriology* ***180***, 4814-4820.

Kuroda, M., Kuroda, H., Oshima, T., Takeuchi, F., Mori, H., and Hiramatsu, K. (2003). Two-component system VraSR positively modulates the regulation of cell-wall biosynthesis pathway in *Staphylococcus aureus*. *Molecular Microbiology* ***49***, 807-821.

Kuroda, M., Ohta, T., Uchiyama, I., Baba, T., Yuzawa, H., Kobayashi, I., Cui, L.Z., Oguchi, A., Aoki, K., Nagai, Y.*, et al.* (2001). Whole genome sequencing of meticillin-resistant *Staphylococcus aureus*. *Lancet* ***357***, 1225-1240.

Lan, L., Cheng, A., Dunman, P.M., Missiakas, D., and He, C. (2010). Golden pigment production and virulence gene expression are affected by metabolisms in *Staphylococcus aureus*. *Journal of Bacteriology* ***192***, 3068-3077.

Lapidot, A., and Irving, C.S. (1977). Dynamic structure of whole cells probed by nuclear Overhauser enhanced nitrogen-15 nuclear magnetic resonance spectroscopy. *Proceedings of the National Academy of Sciences of the United States of America* ***74***, 1988-1992.

Lazarevic, V., Beaume, M., Corvaglia, A., Hernandez, D., Schrenzel, J., and Francois, P. (2011a). Epidemiology and virulence insights from MRSA and MSSA genome analysis. *Future Microbiology* ***6***, 513-532.

Lazarevic, V., Beaume, M., Corvaglia, A., Hernandez, D., Schrenzel, J., and Francois, P. (2011b). Epidemiology and virulence insights from MRSA and MSSA genome analysis. *Future Microbiology* ***6***, 513-532.

Lee, A.C., and Bergdoll, M.S. (1985). Spontaneous occurrence of *Staphylococcus aureus* mutants with different pigmentation and ability to produce toxic shock syndrome toxin 1. *Journal of Clinical Microbiology* ***22***, 308-309.

Lee, J.H., Kaplan, J.B., and Lee, W.Y. (2008). Microfluidic devices for studying growth and detachment of *Staphylococcus epidermidis* biofilms. *Biomed Microdevices* ***10***, 489-498.

Lehman, M.K., Bose, J.L., Sharma-Kuinkel, B.K., Moormeier, D.E., Endres, J.L., Sadykov, M.R., Biswas, I., and Bayles, K.W. (2015). Identification of the amino acids essential for LytSR-mediated signal transduction in *Staphylococcus aureus* and their roles in biofilm-specific gene expression. *Molecular Microbiology* ***95***, 723-737.

Lei, M.G., Cue, D., Roux, C.M., Dunman, P.M., and Lee, C.Y. (2011). Rsp inhibits attachment and biofilm formation by repressing fnbA in *Staphylococcus aureus* MW2. *Journal of Bacteriology* ***193***, 5231-5241.

Lew, D.P., and Waldvogel, F.A. (2004). Osteomyelitis. *Lancet* ***364***, 369-379.

Lindsay, J.A. (2008). Staphylococcus: Molecular Genetics (*Norfolk, UK: Caister Academic Press*).

Little, D.J., Poloczek, J., Whitney, J.C., Robinson, H., Nitz, M., and Howell, P.L. (2012). The structure- and metal-dependent activity of *Escherichia coli PgaB* provides insight into the partial de-N-acetylation of poly-beta-1,6-N-acetyl-D-glucosamine. *The Journal of Biological Chemistry* ***287***, 31126-31137.

Liu, C., Gelius, E., Liu, G., Steiner, H., and Dziarski, R. (2000). Mammalian peptidoglycan recognition protein binds peptidoglycan with high affinity, is expressed in neutrophils, and inhibits bacterial growth. *The Journal of Biological Chemistry* ***275***, 24490-24499.

Liu, G.Y., Essex, A., Buchanan, J.T., Datta, V., Hoffman, H.M., Bastian, J.F., Fierer, J., and Nizet, V. (2005). *Staphylococcus aureus* golden pigment impairs neutrophil killing and promotes virulence through its antioxidant activity. *The Journal of Experimental Medicine* ***202***, 209-215.

Liu, Y., Manna, A.C., Pan, C.H., Kriksunov, I.A., Thiel, D.J., Cheung, A.L., and Zhang, G. (2006). Structural and function analyses of the global regulatory protein SarA from *Staphylococcus aureus*. *Proceedings of The National Academy of Sciences of The United States of America* ***103***, 2392-2397.

Lorenz, U., Lorenz, B., Schmitter, T., Streker, K., Erck, C., Wehland, J., Nickel, J., Zimmermann, B., and Ohlsen, K. (2011). Functional antibodies targeting IsaA of *Staphylococcus aureus* augment host immune response and open new perspectives for antibacterial therapy. *Antimicrob Agents Chemother* ***55***, 165-173.

Lowy, F.D. (1998). *Staphylococcus aureus* infections. *The New England Journal of Medicine* ***339*****,** 520-532.

Lyon, G.J., and Novick, R.P. (2004). Peptide signaling in *Staphylococcus aureus* and other Gram-positive bacteria. *Peptides* ***25***, 1389-1403.

Mack, D., Fischer, W., Krokotsch, A., Leopold, K., Hartmann, R., Egge, H., and Laufs, R. (1996). The intercellular adhesin involved in biofilm accumulation of *Staphylococcus epidermidis* is a linear beta-1,6-linked glucosaminoglycan: purification and structural analysis. *Journal of Bacteriology* ***178***, 175-183.

Madigan, M.T., Martinko, J.M., Parker, J., and Brock, T.D. (2003). Brock biology of microorganisms, *Vol Prentice Hall international editions* (*Upper Saddle River, N.J.London: Prentice Hall, Pearson Education*).

Magrane, M., and Consortium, U. (2011). UniProt Knowledgebase: a hub of integrated protein data. Database (*Oxford*) *2011*, bar009.

Mainiero, M., Goerke, C., Geiger, T., Gonser, C., Herbert, S., and Wolz, C. (2010). Differential target gene activation by the *Staphylococcus aureus* two-component system saeRS. *Journal of Bacteriology* ***192***, 613-623.

Manna, A., and Cheung, A.L. (2001). Characterization of sarR, a modulator of sar expression in *Staphylococcus aureus*. *Infection and Immunity* ***69***, 885-896.

Manna, A.C., Bayer, M.G., and Cheung, A.L. (1998). Transcriptional analysis of different promoters in the sar locus in *Staphylococcus aureus*. *Journal of Bacteriology* ***180***, 3828-3836.

Manna, A.C., and Cheung, A.L. (2006). Transcriptional regulation of the agr locus and the identification of DNA binding residues of the global regulatory protein SarR in *Staphylococcus aureus*. *Molecular Microbiology* ***60***, 1289-1301.

Manna, A.C., Ingavale, S.S., Maloney, M., van Wamel, W., and Cheung, A.L. (2004). Identification of sarV (SA2062), a new transcriptional regulator, is repressed by SarA and MgrA (SA0641) and involved in the regulation of autolysis in *Staphylococcus aureus*. *Journal of Bacteriology* ***186***, 5267-5280.

Marchler-Bauer, A., Derbyshire, M.K., Gonzales, N.R., Lu, S., Chitsaz, F., Geer, L.Y., Geer, R.C., He, J., Gwadz, M., Hurwitz, D.I.*, et al.* (2015). CDD: NCBI's conserved domain database. *Nucleic Acids Research* ***43***, D222-226.

Marshall, J.H., and Wilmoth, G.J. (1981). Proposed pathway of triterpenoid carotenoid biosynthesis in *Staphylococcus aureus*: evidence from a study of mutants. *Journal of Bacteriology* ***147***, 914-919.

Martin, P.K., Li, T., Sun, D., Biek, D.P., and Schmid, M.B. (1999). Role in cell permeability of an essential two-component system in *Staphylococcus aureus*. *Journal of Bacteriology* ***181***, 3666-3673.

Maruyama, Y., Ochiai, A., Mikami, B., Hashimoto, W., and Murata, K. (2011). Crystal structure of bacterial cell-surface alginate-binding protein with an M75 peptidase motif. *Biochemical Biophysical Research Communication* ***405*****,** 411-416.

Massey, R.C., Kantzanou, M.N., Fowler, T., Day, N.P., Schofield, K., Wann, E.R., Berendt, A.R., Hook, M., and Peacock, S.J. (2001). Fibronectin-binding protein A of *Staphylococcus aureus* has multiple, substituting, binding regions that mediate adherence to fibronectin and invasion of endothelial cells. *Cell Microbiology* ***3***, 839-851.

Meyrand, M., Boughammoura, A., Courtin, P., Mezange, C., Guillot, A., and Chapot-Chartier, M.P. (2007). Peptidoglycan N-acetylglucosamine deacetylation decreases autolysis in *Lactococcus lactis*. *Microbiology* ***153***, 3275-3285.

Mishra, N.N., Liu, G.Y., Yeaman, M.R., Nast, C.C., Proctor, R.A., McKinnell, J., and Bayer, A.S. (2011). Carotenoid-related alteration of cell membrane fluidity impacts *Staphylococcus aureus* susceptibility to host defense peptides. *Antimicrob Agents Chemother* ***55***, 526-531.

Moffatt, B.A., and Studier, F.W. (1988). Entry of bacteriophage T7 DNA into the cell and escape from host restriction. *Journal of Bacteriology* ***170***, 2095-2105.

Monk, I.R., and Foster, T.J. (2012). Genetic manipulation of *Staphylococci*-breaking through the barrier. *Frontiers in Cellular and Infection Microbiology* ***2***, 49.

Monk, I.R., Shah, I.M., Xu, M., Tan, M.W., and Foster, T.J. (2012). Transforming the untransformable: application of direct transformation to manipulate genetically *Staphylococcus aureus* and *Staphylococcus epidermidis*. *American Society for Microbiology* (*mBio*) ***3***,266-280

Montanaro, L., Poggi, A., Visai, L., Ravaioli, S., Campoccia, D., Speziale, P., and Arciola, C.R. (2011). Extracellular DNA in biofilms. *The International journal of Artificial Organs* ***34***, 824-831.

Montgomery, C.P., Boyle-Vavra, S., and Daum, R.S. (2009). The arginine catabolic mobile element is not associated with enhanced virulence in experimental invasive disease caused by the community-associated methicillin-resistant *Staphylococcus aureus* USA300 genetic background. *Infection and Immunity* ***77***, 2650-2656.

Morath, S., Geyer, A., and Hartung, T. (2001). Structure-function relationship of cytokine induction by lipoteichoic acid from *Staphylococcus aureus*. *The Journal of Experimental Medicine* ***193***, 393-397.

Morfeldt, E., Taylor, D., von Gabain, A., and Arvidson, S. (1995). Activation of alpha-toxin translation in *Staphylococcus aureus* by the trans-encoded antisense RNA, RNAIII. *EMBO J* ***14***, 4569-4577.

Morikawa, K., Maruyama, A., Inose, Y., Higashide, M., Hayashi, H., and Ohta, T. (2001). Overexpression of sigma factor, sigma(B), urges *Staphylococcus aureus* to thicken the cell wall and to resist beta-lactams. *Biochemical Biophysical Research Communication* ***288***, 385-389.

Morrison, J.M., Anderson, K.L., Beenken, K.E., Smeltzer, M.S., and Dunman, P.M. (2012). The *staphylococcal* accessory regulator, SarA, is an RNA-binding protein that modulates the mRNA turnover properties of late-exponential and stationary phase *Staphylococcus aureus* cells. *Frontiers in Cellular and Infection Microbiology* ***2***, 26.

Nair, D., Memmi, G., Hernandez, D., Bard, J., Beaume, M., Gill, S., Francois, P., and Cheung, A.L. (2011). Whole-genome sequencing of *Staphylococcus aureus* strain RN4220, a key laboratory strain used in virulence research, identifies mutations that affect not only virulence factors but also the fitness of the strain. *Journal of Bacteriology* ***193***, 2332-2335.

Nakayama, H., Kurokawa, K., and Lee, B.L. (2012). Lipoproteins in bacteria: structures and biosynthetic pathways. *FEBS Journal* ***279***, 4247-4268.

Navarre, W.W., and Schneewind, O. (1999). Surface proteins of gram-positive bacteria and mechanisms of their targeting to the cell wall envelope. *Microbiology and Molecular Biology* reviews : *MMBR* ***63***, 174-229.

Neuhaus, F.C., and Baddiley, J. (2003). A continuum of anionic charge: structures and functions of D-alanyl-teichoic acids in gram-positive bacteria. *Microbiology and Molecular Biology* reviews : *Microbiology and Molecular Biology Reviews* ***67***, 686-723.

Notredame, C., Higgins, D.G., and Heringa, J. (2000). T-Coffee: A novel method for fast and accurate multiple sequence alignment. *Journal of molecular Biology* ***302***, 205-217.

Novick, R.P. (1991). Genetic systems in *Staphylococci*. *Methods In Enzymology* ***204*****,** 587-636.

Novick, R.P. (2003). Autoinduction and signal transduction in the regulation of *Staphylococcal* virulence. *Molecular Microbiology* ***48***, 1429-1449.

Novick, R.P., and Geisinger, E. (2008). Quorum sensing in *Staphylococci. Annual Review Of Genetics* ***42***, 541-564.

O'Neill, A.J. (2010). *Staphylococcus aureus* SH1000 and 8325-4: comparative genome sequences of key laboratory strains in *Staphylococcal* research. *Letters In Applied Microbiology* ***51***, 358-361.

O'Neill, E., Pozzi, C., Houston, P., Humphreys, H., Robinson, D.A., Loughman, A., Foster, T.J., and O'Gara, J.P. (2008). A novel *Staphylococcus aureus* biofilm phenotype mediated by the fibronectin-binding proteins, FnBPA and FnBPB. *Journal of Bacteriology* ***190***, 3835-3850.

O'Neill, E., Pozzi, C., Houston, P., Smyth, D., Humphreys, H., Robinson, D.A., and O'Gara, J.P. (2007). Association between methicillin susceptibility and biofilm regulation in *Staphylococcus aureus* isolates from device-related infections. *Journal of Clinical Microbiology* ***45***, 1379-1388.

O'Toole, G., Kaplan, H.B., and Kolter, R. (2000). Biofilm formation as microbial development. *Annual Review of Microbiology* ***54***, 49-79.

Oberbarnscheidt, L., Taylor, E.J., Davies, G.J., and Gloster, T.M. (2007). Structure of a carbohydrate esterase from *Bacillus anthracis*. *Proteins* ***66***, 250-252.

Olivier, A.C., Lemaire, S., Van Bambeke, F., Tulkens, P.M., and Oldfield, E. (2009). Role of rsbU and staphyloxanthin in phagocytosis and intracellular growth of *Staphylococcus aureus* in human macrophages and endothelial cells. *The Journal of Infectious Diseases* ***200***, 1367-1370.

Olsen, J.V., Ong, S.E., and Mann, M. (2004). Trypsin cleaves exclusively C-terminal to arginine and lysine residues. *Molecular and Cellular Proteomics* ***3***, 608-614.

Otto, M. (2013). *Staphylococcal* infections: mechanisms of biofilm maturation and detachment as critical determinants of pathogenicity. *Annual Review of Medicine* ***64***, 175-188.

Oudega, B. (2003). Protein secretion pathways in bacteria (The Netherlands).
Paetzel, M., Karla, A., Strynadka, N.C.J., and Dalbey, R.E. (2002). Signal peptidases. *Chemical Reviews* ***102***, 4549-4579.

Palma, M., and Cheung, A.L. (2001). sigma(B) activity in *Staphylococcus aureus* is controlled by RsbU and an additional factor(s) during bacterial growth. *Infection and Immunity* ***69***, 7858-7865.

Palmqvist, N., Patti, J.M., Tarkowski, A., and Josefsson, E. (2004). Expression of *staphylococcal* clumping factor A impedes macrophage phagocytosis. *Microbes Infect* ***6***, 188-195.

Park, J.H., and Batt, C.A. (2004). Restoration of a defective *Lactococcus lactis* xylose isomerase. *Applied and Environmental Microbiology* ***70***, 4318-4325.

Passalacqua, K.D., Satola, S.W., Crispell, E.K., and Read, T.D. (2012). A mutation in the PP2C phosphatase gene in a *Staphylococcus aureus* USA300 clinical isolate with reduced susceptibility to vancomycin and daptomycin. *Antimicrobial Agents and Chemotherapy* ***56***, 5212-5223.

Payne, D.E., Martin, N.R., Parzych, K.R., Rickard, A.H., Underwood, A., and Boles, B.R. (2013). Tannic acid inhibits *Staphylococcus aureus* surface colonization in an IsaA-dependent manner. *Infection and Immunity* ***81***, 496-504.

Peacock, S.J., Moore, C.E., Justice, A., Kantzanou, M., Story, L., Mackie, K., O'Neil, G., and Day, N.P.J. (2002). Virulent combinations of adhesin and toxin genes in natural populations of *Staphylococcus aureus*. *Infection and Immunity* ***70***, 4987-4996.

Pelz, A., Wieland, K.P., Putzbach, K., Hentschel, P., Albert, K., and Gotz, F. (2005). Structure and biosynthesis of staphyloxanthin from *Staphylococcus aureus*. The *Journal of Biological Chemistry* ***280***, 32493-32498.

Peschel, A. (2002). How do bacteria resist human antimicrobial peptides? *Trends In Microbiology* ***10***, 179-186.

Peschel, A., Otto, M., Jack, R.W., Kalbacher, H., Jung, G., and Gotz, F. (1999). Inactivation of the dlt operon in *Staphylococcus aureus* confers sensitivity to defensins, protegrins, and other antimicrobial peptides. *The Journal of Biological Chemistry* ***274***, 8405-8410.

Petersen, T.N., Brunak, S., von Heijne, G., and Nielsen, H. (2011). SignalP 4.0: discriminating signal peptides from transmembrane regions. *Nature Methods* ***8***, 785-786.

Phillipson, M., and Kubes, P. (2011). The neutrophil in vascular inflammation. *Nature Medicine* ***17***, 1381-1390.

Poirot, O., O'Toole, E., and Notredame, C. (2003). Tcoffee@igs: a web server for computing, evaluating and combining multiple sequence alignments. *Nucleic Acids Research* ***31***, 3503-3506.

Popowska, M., Kusio, M., Szymanska, P., and Markiewicz, Z. (2009). Inactivation of the wall-associated de-N-acetylase (PgdA) of Listeria monocytogenes results in greater susceptibility of the cells to induced autolysis. *Journal of Microbiology and Biotechnology* ***19***, 932-945.

Powers, K.A., Terpenning, M.S., Voice, R.A., and Kauffman, C.A. (1990). Prosthetic Joint Infections in the Elderly. *The American Journal of Medicine* ***88***, N9-N13.

Pozzi, C., Waters, E.M., Rudkin, J.K., Schaeffer, C.R., Lohan, A.J., Tong, P., Loftus, B.J., Pier, G.B., Fey, P.D., Massey, R.C.*, et al.* (2012). Methicillin resistance alters the biofilm phenotype and attenuates virulence in *Staphylococcus aureus* device-associated infections. *PLoS Pathogens* ***8*****,** e1002626.

Pragman, A.A., Ji, Y., and Schlievert, P.M. (2007). Repression of *Staphylococcus* aureus SrrAB using inducible antisense srrA alters growth and virulence factor transcript levels. *Biochemistry* ***46***, 314-321.

Pragman, A.A., Yarwood, J.M., Tripp, T.J., and Schlievert, P.M. (2004). Characterization of virulence factor regulation by SrrAB, a two-component system in *Staphylococcus aureus*. *Journal of Bacteriology* ***186***, 2430-2438.

Psylinakis, E., Boneca, I.G., Mavromatis, K., Deli, A., Hayhurst, E., Foster, S.J., Varum, K.M., and Bouriotis, V. (2005). Peptidoglycan N-acetylglucosamine deacetylases from *Bacillus cereus*, highly conserved proteins in *Bacillus anthracis*. *The Journal of Biological Chemistry* ***280***, 30856-30863.

Punta, M., Coggill, P.C., Eberhardt, R.Y., Mistry, J., Tate, J., Boursnell, C., Pang, N., Forslund, K., Ceric, G., Clements, J.*, et al.* (2012). The Pfam protein families database. *Nucleic Acids Research* ***40***, D290-301.

Qin, S., and Zhou, H.X. (2007). meta-PPISP: a meta web server for protein-protein interaction site prediction. *Bioinformatics* ***23***, 3386-3387.

Qin, Z., Ou, Y., Yang, L., Zhu, Y., Tolker-Nielsen, T., Molin, S., and Qu, D. (2007). Role of autolysin-mediated DNA release in biofilm formation of *Staphylococcus epidermidis*. *Microbiology* ***153***, 2083-2092.

Rae, C.S., Geissler, A., Adamson, P.C., and Portnoy, D.A. (2011). Mutations of the Listeria monocytogenes peptidoglycan N-deacetylase and O-acetylase result in enhanced lysozyme sensitivity, bacteriolysis, and hyperinduction of innate immune pathways. *Infection and Immunity* ***79***, 3596-3606.

Raisig, A., and Sandmann, G. (1999). 4,4'-diapophytoene desaturase: catalytic properties of an enzyme from the C(30) carotenoid pathway of *Staphylococcus aureus*. *Journal of Bacteriology* ***181***, 6184-6187.

Rajasekaran, M.B., Nilapwar, S., Andrews, S.C., and Watson, K.A. (2010). EfeO-cupredoxins: major new members of the cupredoxin superfamily with roles in bacterial iron transport. *Biometals* ***23***, 1-17.

Ramadurai, L., Lockwood, K.J., Nadakavukaren, M.J., and Jayaswal, R.K. (1999). Characterization of a chromosomally encoded glycylglycine endopeptidase of *Staphylococcus aureus*. *Microbiology* ***145*** *(Pt 4)*, 801-808.

Rampersad, S.N. (2012). Multiple applications of Alamar Blue as an indicator of metabolic function and cellular health in cell viability bioassays. *Sensors* (*Basel*) ***12***, 12347-12360.

Rasmussen, R.V., Fowler, V.G., Jr., Skov, R., and Bruun, N.E. (2011). Future challenges and treatment of *Staphylococcus aureus* bacteremia with emphasis on MRSA. *Future Microbiology* ***6***, 43-56.

Raymond, J.B., Mahapatra, S., Crick, D.C., and Pavelka, M.S., Jr. (2005). Identification of the namH gene, encoding the hydroxylase responsible for the N-glycolylation of the mycobacterial peptidoglycan. *The Journal of Biological Chemistry* ***280***, 326-333.

Recsei, P., Kreiswirth, B., O'Reilly, M., Schlievert, P., Gruss, A., and Novick, R.P. (1986). Regulation of exoprotein gene expression in *Staphylococcus aureus* by agar. *Molecular Genetics and Genomics* ***202***, 58-61.

Reed, P., Veiga, H., Jorge, A.M., Terrak, M., and Pinho, M.G. (2011). Monofunctional transglycosylases are not essential for *Staphylococcus aureus* cell wall synthesis. *Journal of Bacteriology* ***193***, 2549-2556.

Reifsteck, F., Wee, S., and Wilkinson, B.J. (1987). Hydrophobicity-hydrophilicity of *staphylococci*. *Journal of Medical Microbiology* ***24***, 65-73.

Remijsen, Q., Kuijpers, T.W., Wirawan, E., Lippens, S., Vandenabeele, P., and Vanden Berghe, T. (2011). Dying for a cause: NETosis, mechanisms behind an antimicrobial cell death modality. *Cell Death & Differentiation* ***18***, 581-588.

Remmert, M., Biegert, A., Hauser, A., and Soding, J. (2012). HHblits: lightning-fast iterative protein sequence searching by HMM-HMM alignment. *Nature Methods* ***9***, 173-175.

Rice, K.C., and Bayles, K.W. (2008). Molecular control of bacterial death and lysis. *Microbiology and Molecular Biology* reviews : *MMBR* ***72***, 85-109.

Rigden, D.J. (2009). From protein structure to function with bioinformatics (School of biological sciences, University of Liverpool, UK: Springer).

Rivas, J.M., Speziale, P., Patti, J.M., and Hook, M. (2004). MSCRAMM--targeted vaccines and immunotherapy for *Staphylococcal* infection. *Current Opinion in Drug Discovery and Development* ***7***, 223-227.

Rooijakkers, S.H., Ruyken, M., van Roon, J., van Kessel, K.P., van Strijp, J.A., and van Wamel, W.J. (2006). Early expression of SCIN and CHIPS drives instant immune evasion by *Staphylococcus aureus*. *Cellular Microbiology* ***8***, 1282-1293.

Rooijakkers, S.H., van Kessel, K.P., and van Strijp, J.A. (2005). *Staphylococcal* innate immune evasion. *Trends In Microbiology* ***13***, 596-601.

Rosano, G.L., and Ceccarelli, E.A. (2014). Recombinant protein expression in *Escherichia coli*: advances and challenges. *Frontiers In Microbiology* ***5***, 172.

Rosenthal, R.S., and Dziarski, R. (1994). Isolation of peptidoglycan and soluble peptidoglycan fragments. *Methods In Enzymology* ***235*****,** 253-285.

Rountree, P.M. (1956). Variations in a related series of *staphylococcal* bacteriophages. *Journal of General Microbiology* ***15***, 266-279.

Ruch, D.S., Vallee, J., Li, Z., Smith, B.P., Holden, M., and Koman, L.A. (2003). The acute effect of peripheral nerve transection on digital thermoregulatory function. *The Journal of Hand Surgery* ***28***, 481-488.

Schenk, S., and Laddaga, R.A. (1992). Improved method for electroporation of *Staphylococcus aureus*. *FEMS Microbiology Letters* ***73***, 133-138.

Schlievert, P.M. (1993). Role of superantigens in human disease. *The Journal of Infectious Diseases* ***167*****,** 997-1002.

Schmidt, K.A., Manna, A.C., Gill, S., and Cheung, A.L. (2001). SarT, a repressor of alpha-hemolysin in *Staphylococcus aureus*. *Infection and Immunity* ***69***, 4749-4758.

Sharif, S., Singh, M., Kim, S.J., and Schaefer, J. (2009). *Staphylococcus aureus* peptidoglycan tertiary structure from carbon-13 spin diffusion. *Journal of the American Chemical Society* ***131***, 7023-7030.

Sharp, J.A., Echague, C.G., Hair, P.S., Ward, M.D., Nyalwidhe, J.O., Geoghegan, J.A., Foster, T.J., and Cunnion, K.M. (2012). *Staphylococcus aureus* surface protein SdrE binds complement regulator factor H as an immune evasion tactic. *PloS one* ***7***, e38407.

Sibbald, M.J., Ziebandt, A.K., Engelmann, S., Hecker, M., de Jong, A., Harmsen, H.J., Raangs, G.C., Stokroos, I., Arends, J.P., Dubois, J.Y*., et al.* (2006). Mapping the pathways to *Staphylococcal* pathogenesis by comparative secretomics. *Microbiology and molecular biology* reviews : *MMBR* ***70***, 755-788.

Smith, E.J., Visai, L., Kerrigan, S.W., Speziale, P., and Foster, T.J. (2011a). The Sbi protein is a multifunctional immune evasion factor of *Staphylococcus aureus*. *Infection and Immunity* ***79*****,** 3801-3809.

Smith, E.J., Visai, L., Kerrigan, S.W., Speziale, P., and Foster, T.J. (2011b). The Sbi protein is a multifunctional immune evasion factor of *Staphylococcus aureus. Infection and Immunity* ***79***, 3801-3809.

Soding, J. (2005). Protein homology detection by HMM-HMM comparison. *Bioinformatics* ***21***, 951-960.

Soding, J., Biegert, A., and Lupas, A.N. (2005). The HHpred interactive server for protein homology detection and structure prediction. *Nucleic Acids Research* ***33***, W244-248.

Speziale, P., Pietrocola, G., Foster, T.J., and Geoghegan, J.A. (2014). Protein-based biofilm matrices in *Staphylococci*. *Frontiers In Cellular and Infection Microbiology* ***4***, 171.

Stapleton, M.R., Horsburgh, M.J., Hayhurst, E.J., Wright, L., Jonsson, I.M., Tarkowski, A., Kokai-Kun, J.F., Mond, J.J., and Foster, S.J. (2007). Characterization of IsaA and SceD, two putative lytic transglycosylases of *Staphylococcus aureus*. *Journal of Bacteriology* ***189***, 7316-7325.

Staubitz, P., Neumann, H., Schneider, T., Wiedemann, I., and Peschel, A. (2004). MprF-mediated biosynthesis of lysylphosphatidylglycerol, an important determinant in *Staphylococcal* defensin resistance. *FEMS Microbiology Letters* ***231***, 67-71.

Stobberingh, E.E., Schiphof, R., and Sussenbach, J.S. (1977). Occurrence of a class II restriction endonuclease in *Staphylococcus aureus*. *Journal of Bacteriology* ***131***, 645-649.

Studier, F.W., Rosenberg, A.H., Dunn, J.J., and Dubendorff, J.W. (1990). Use of T7 RNA polymerase to direct expression of cloned genes. *Methods In Enzymology* ***185***, 60-89.

Sugai, M., Komatsuzawa, H., Akiyama, T., Hong, Y.M., Oshida, T., Miyake, Y., Yamaguchi, T., and Suginaka, H. (1995). Identification of endo-beta-N-acetylglucosaminidase and N-acetylmuramyl-L-alanine amidase as cluster-dispersing enzymes in *Staphylococcus aureus*. *Journal of bacteriology 177*, 1491-1496.

Sutcliffe, I.C., and Russell, R.R. (1995). Lipoproteins of gram-positive bacteria. *Journal of Bacteriology* ***177***, 1123-1128.

Tamber, S., Reyes, D., Donegan, N.P., Schwartzman, J.D., Cheung, A.L., and Memmi, G. (2010). The *staphylococcus*-specific gene rsr represses agr and virulence in *Staphylococcus aureus*. *Infection and Immunity* ***78***, 4384-4391.

Thammavongsa, V., Kern, J.W., Missiakas, D.M., and Schneewind, O. (2009). *Staphylococcus aureus* synthesizes adenosine to escape host immune responses. *J Exp Med* ***206***, 2417-2427.

Throup, J.P., Zappacosta, F., Lunsford, R.D., Annan, R.S., Carr, S.A., Lonsdale, J.T., Bryant, A.P., McDevitt, D., Rosenberg, M., and Burnham, M.K. (2001). The srhSR gene pair from *Staphylococcus aureus*: genomic and proteomic approaches to the identification and characterization of gene function. *Biochemistry* ***40*****,** 10392-10401.

Tjalsma, H., Antelmann, H., Jongbloed, J.D., Braun, P.G., Darmon, E., Dorenbos, R., Dubois, J.Y., Westers, H., Zanen, G., Quax, W.J.*, et al.* (2004). Proteomics of protein secretion by *Bacillus subtilis*: separating the "secrets" of the secretome. *Microbiology and Molecular Biology Reviews* ***68*****,** 207-233.

Tjalsma, H., Bolhuis, A., Jongbloed, J.D., Bron, S., and van Dijl, J.M. (2000). Signal peptide-dependent protein transport in Bacillus subtilis: a genome-based survey of the secretome. *Microbiology and Molecular Biology Reviews* ***64***, 515-547.

Turlin, E., Debarbouille, M., Augustyniak, K., Gilles, A.M., and Wandersman, C. (2013). *Staphylococcus aureus* FepA and FepB proteins drive heme iron utilization in *Escherichia coli*. *PloS one* ***8***, e56529.

Typas, A., Banzhaf, M., Gross, C.A., and Vollmer, W. (2012). From the regulation of peptidoglycan synthesis to bacterial growth and morphology. *Nature Reviews of Microbiology* ***10***, 123-136.

Urch, J.E., Hurtado-Guerrero, R., Brosson, D., Liu, Z.L., Eijsink, V.G.H., Texier, C., and van Aalten, D.M.F. (2009). Structural and functional characterization of a putative polysaccharide deacetylase of the human parasite Encephalitozoon cuniculi. *Protein Science* ***18***, 1197-1209.

Vagner, V., Dervyn, E., and Ehrlich, S.D. (1998). A vector for systematic gene inactivation in *Bacillus subtilis*. *Microbiology* ***144*** *(Pt 11)*, 3097-3104.

van Kessel, K.P., Bestebroer, J., and van Strijp, J.A. (2014). Neutrophil-Mediated Phagocytosis of *Staphylococcus aureus*. *Frontiers Immunology* ***5***, 467.

Vandenesch, F., Naimi, T., Enright, M.C., Lina, G., Nimmo, G.R., Heffernan, H., Liassine, N., Bes, M., Greenland, T., Reverdy, M.E., *et al.* (2003). Community-acquired methicillin-resistant *Staphylococcus aureus* carrying Panton-Valentine leukocidin genes: worldwide emergence. *Emerging Infectious Diseases* ***9***, 978-984.

Vaudaux, P.E., Francois, P., Proctor, R.A., McDevitt, D., Foster, T.J., Albrecht, R.M., Lew, D.P., Wabers, H., and Cooper, S.L. (1995). Use of adhesion-defective mutants of *Staphylococcus aureus* to define the role of specific plasma proteins in promoting bacterial adhesion to canine arteriovenous shunts. *Infection and Immunity* ***63*****,** 585-590.

Verdon, J., Girardin, N., Lacombe, C., Berjeaud, J.M., and Hechard, Y. (2009). delta-hemolysin, an update on a membrane-interacting peptide. *Peptides* ***30***, 817-823.

Volkov, A., Liavonchanka, A., Kamneva, O., Fiedler, T., Goebel, C., Kreikemeyer, B., and Feussner, I. (2010). Myosin cross-reactive antigen of *Streptococcus pyogenes* M49 encodes a fatty acid double bond hydratase that plays a role in oleic acid detoxification and bacterial virulence. *The Journal of Biological Chemistry* ***285***, 10353-10361.

Vollmer, W., and Tomasz, A. (2000). The *pgdA* gene encodes for a peptidoglycan N-acetylglucosamine deacetylase in *Streptococcus pneumoniae*. *The Journal of Biological Chemistry* ***275***, 20496-20501.

Vonheijne, G. (1990). The Signal Peptide. J Membrane Biol *115*, 195-201.

Voyich, J.A., Braughton, K.R., Sturdevant, D.E., Whitney, A.R., Said-Salim, B., Porcella, S.F., Long, R.D., Dorward, D.W., Gardner, D.J., Kreiswirth, B.N., *et al.* (2005). Insights into mechanisms used by *Staphylococcus aureus* to avoid destruction by human neutrophils. *Journal of Immunology* ***175*****,** 3907-3919.

Waldron, D.E., and Lindsay, J.A. (2006). Sau1: a novel lineage-specific type I restriction-modification system that blocks horizontal gene transfer into *Staphylococcus aureus* and between *S. aureus* isolates of different lineages. *Journal of Bacteriology* ***188***, 5578-5585.

Wasinger, V.C., Cordwell, S.J., Cerpa-Poljak, A., Yan, J.X., Gooley, A.A., Wilkins, M.R., Duncan, M.W., Harris, R., Williams, K.L., and Humphery-Smith, I. (1995). Progress with gene-product mapping of the Mollicutes: *Mycoplasma genitalium. Electrophoresis* ***16*****,** 1090-1094.

Watson, J.D., and Thornton, J.M. (2009). Protein Function Prediction from Structure in Structural Genomics and Its Contribution to the Study of Health and Disease. *Nato Science For Peace Security* A **2,** 201-215.

Watts, A., Ke, D., Wang, Q., Pillay, A., Nicholson-Weller, A., and Lee, J.C. (2005). *Staphylococcus aureus* strains that express serotype 5 or serotype 8 capsular polysaccharides differ in virulence. *Infection and Immunity* ***73***, 3502-3511.

Waxman, D.J., and Strominger, J.L. (1983). Penicillin-binding proteins and the mechanism of action of beta-lactam antibiotics. *Annual Review of Biochemistry* ***52***, 825-869.

Whisstock, J.C., and Lesk, A.M. (2003). Prediction of protein function from protein sequence and structure. *Quarterly Reviews of Biophysics* ***36***, 307-340.

Wooldridge, K. (2009). Bacterial Secreted Proteins: Secretory Mechanisms and Role in Pathogenesis (*Norfolk, UK: Caister Academic Press*).

Xu, Q.P., Rawlings, N.D., Farr, C.L., Chiu, H.J., Grant, J.C., Jaroszewski, L., Klock, H.E., Knuth, M.W., Miller, M.D., Weekes, D., *et al.* (2011a). Structural and Sequence Analysis of Imelysin-Like Proteins Implicated in Bacterial Iron Uptake. *PloS one* ***6***.

Xu, S.Y., Corvaglia, A.R., Chan, S.H., Zheng, Y., and Linder, P. (2011b). A type IV modification-dependent restriction enzyme SauUSI from *Staphylococcus aureus* subsp. *aureus* USA300. *Nucleic Acids Research* ***39***, 5597-5610.

Yang, S.J., Dunman, P.M., Projan, S.J., and Bayles, K.W. (2006). Characterization of the *Staphylococcus aureus* CidR regulon: elucidation of a novel role for acetoin metabolism in cell death and lysis. *Molecular Microbiology* ***60***, 458-468.

Zhang, L., Jacobsson, K., Vasi, J., Lindberg, M., and Frykberg, L. (1998). A second IgG-binding protein in *Staphylococcus aureus. Microbiology* ***144*** *(Pt 4)*, 985-991.

Zhu, T., Lou, Q., Wu, Y., Hu, J., Yu, F., and Qu, D. (2010). Impact of the Staphylococcus epidermidis LytSR two-component regulatory system on murein hydrolase activity, pyruvate utilization and global transcriptional profile. *BMC Microbiology* ***10***, 287.

Zimmermann, H. (1996). Biochemistry, localization and functional roles of ecto-nucleotidases in the nervous system. *Progress in Neurobiology* ***49***, 589-618.

Appendix

Fig 4A. Analysis multi-sequence for their similarity, using Clustal Omega server. (In the top) Original *S. aureus* Newman *pgd* sequence, (second) cloned *pgd*PCR2 sequence (from pJAMAL2) and (third) cloned *pgd*PCR3 sequence (from pJAMAL2). Mutation in the sequence compared with original *pgd* sequence indicated by black triangle.

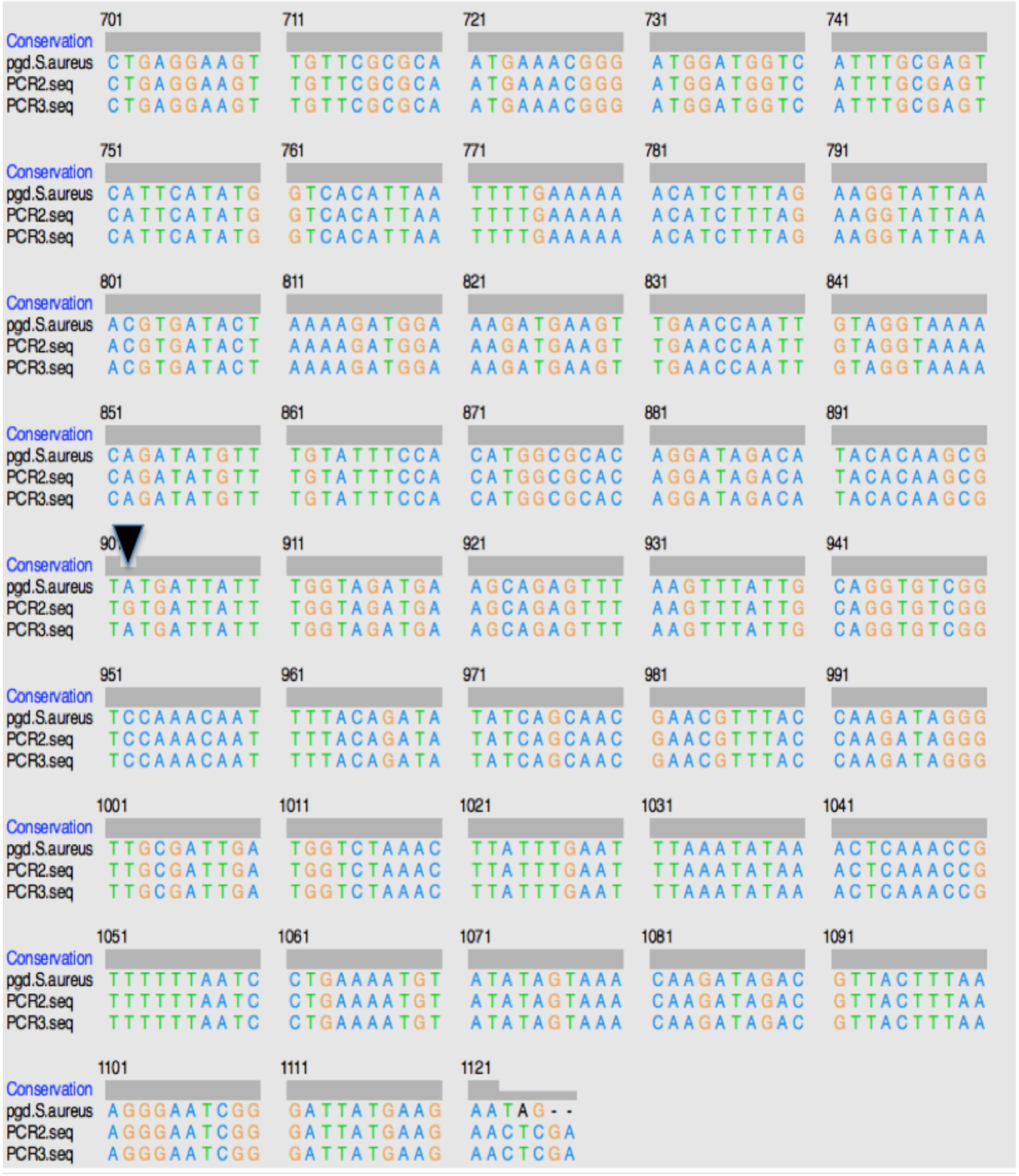
701 711 721 731 741
Conservation
pgd.S.aureus CTGAGGAAGT TGTTCGCGCA ATGAAACGGG ATGGATGGTC ATTTGCGAGT
PCR2.seq CTGAGGAAGT TGTTCGCGCA ATGAAACGGG ATGGATGGTC ATTTGCGAGT
PCR3.seq CTGAGGAAGT TGTTCGCGCA ATGAAACGGG ATGGATGGTC ATTTGCGAGT
751 761 771 781 791
Conservation
pgd.S.aureus CATTCATATG GTCACATTAA TTTTGAAAAA ACATCTTTAG AAGGTATTAA
PCR2.seq CATTCATATG GTCACATTAA TTTTGAAAAA ACATCTTTAG AAGGTATTAA
PCR3.seq CATTCATATG GTCACATTAA TTTTGAAAAA ACATCTTTAG AAGGTATTAA
801 811 821 831 841
Conservation
pgd.S.aureus ACGTGATACT AAAAGATGGA AAGATGAAGT TGAACCAATT GTAGGTAAAA
PCR2.seq ACGTGATACT AAAAGATGGA AAGATGAAGT TGAACCAATT GTAGGTAAAA
PCR3.seq ACGTGATACT AAAAGATGGA AAGATGAAGT TGAACCAATT GTAGGTAAAA
851 861 871 881 891
Conservation
pgd.S.aureus CAGATATGTT TGTATTTCCA CATGGCGCAC AGGATAGACA TACACAAGCG
PCR2.seq CAGATATGTT TGTATTTCCA CATGGCGCAC AGGATAGACA TACACAAGCG
PCR3.seq CAGATATGTT TGTATTTCCA CATGGCGCAC AGGATAGACA TACACAAGCG
90 911 921 931 941
Conservation
pgd.S.aureus TATGATTATT TGGTAGATGA AGCAGAGTTT AAGTTTATTG CAGGTGTCGG
PCR2.seq TGTGATTATT TGGTAGATGA AGCAGAGTTT AAGTTTATTG CAGGTGTCGG
PCR3.seq TATGATTATT TGGTAGATGA AGCAGAGTTT AAGTTTATTG CAGGTGTCGG
951 961 971 981 991
Conservation
pgd.S.aureus TCCAAACAAT TTTACAGATA TATCAGCAAC GAACGTTTAC CAAGATAGGG
PCR2.seq TCCAAACAAT TTTACAGATA TATCAGCAAC GAACGTTTAC CAAGATAGGG
PCR3.seq TCCAAACAAT TTTACAGATA TATCAGCAAC GAACGTTTAC CAAGATAGGG
1001 1011 1021 1031 1041
Conservation
pgd.S.aureus TTGCGATTGA TGGTCTAAAC TTATTTGAAT TTAAATATAA ACTCAAACCG
PCR2.seq TTGCGATTGA TGGTCTAAAC TTATTTGAAT TTAAATATAA ACTCAAACCG
PCR3.seq TTGCGATTGA TGGTCTAAAC TTATTTGAAT TTAAATATAA ACTCAAACCG
1051 1061 1071 1081 1091
Conservation
pgd.S.aureus TTTTTTAATC CTGAAAATGT ATATAGTAAA CAAGATAGAC GTTACTTTAA
PCR2.seq TTTTTTAATC CTGAAAATGT ATATAGTAAA CAAGATAGAC GTTACTTTAA
PCR3.seq TTTTTTAATC CTGAAAATGT ATATAGTAAA CAAGATAGAC GTTACTTTAA
1101 1111 1121
Conservation
pgd.S.aureus AGGGAATCGG GATTATGAAG AATAG--
PCR2.seq AGGGAATCGG GATTATGAAG AACTCGA
PCR3.seq AGGGAATCGG GATTATGAAG AACTCGA